Alliance on Systems Biology

HelmholtzZentrum münchen
German Research Center for Environmental Health

Beyond Boolean Modeling in Systems Biology

Dominik M. Wittmann

CMB — IBIS
Helmholtz Zentrum
München

Zentrum Mathematik
Technische Universität
München

October 2010

TECHNISCHE UNIVERSITÄT MÜNCHEN

Zentrum Mathematik — Lehrstuhl M12 (Biomathematik)

"Beyond Boolean Modeling in Systems Biology"

Dominik M. Wittmann

Vollständiger Abdruck der von der Fakultät für Mathematik der Technischen Universität München zur Erlangung des akademischen Grades eines

Doktors der Naturwissenschaften

genehmigten Dissertation.

Vorsitzender:

Univ.-Prof. Dr. Anusch Taraz

Prüfer der Dissertation:

1. Univ.-Prof. Dr. Dr. Fabian J. Theis
2. Univ.-Prof. Dr. Rupert Lasser
3. Univ.-Prof. Dr. Alexander Bockmayr, Freie Universität Berlin (schriftliche Beurteilung)

Die Dissertation wurde am 7. Oktober 2010 bei der Technischen Universität München eingereicht und durch die Fakultät für Mathematik am 25. März 2011 angenommen.

To my aunt
in Memoriam

Acknowledgements

First and foremost, I would like to thank the many people who have accompanied me over the last three years.

My supervisor Prof. Fabian Theis, for his unwavering optimism, his encouragements and, of course, for his undertaking my introduction into the world of science.

Profs. Rupert Lasser and Hans-Werner Mewes, who willingly agreed to be members of my thesis committee, for their valuable comments and criticisms.

Dr. Nilima Prakash, for her uplifting interest in our collaboration, her imparting as much of her knowledge about neural development to me as I could grasp, and for the patience all this required.

Florian, for many good advices — scientific ones and others —, some of which I should have paid better attention to, for endless discussions about science and related stuff, for coffee that deserves the name, and for many useful comments on this thesis.

Daniel, my fellow mathematician, for keeping me connected to the world of mathematics by organizing our seminars and workshops, for always readily agreeing to discuss math problems with me, and for proof-reading this thesis in as diligent a way as only he is capable of.

The entire CMB group, for some good collaborations and, of course, for all our nice bbqs.

All the people at the IBIS, for a stimulating working atmosphere and many nice chats during lunch or over a cup of coffee.

My "old" friends back in Regensburg, for never tiring of trying to convince me that there is more to life than science.

My parents, for all their unconditional support, which nothing I could write would do justice to.

Abstract

In this thesis, we mathematically investigate generalizations and modifications of Boolean models, as introduced in theoretical biology by Stuart Kauffman. A variable in a Boolean model assumes only two values, zero and one. It develops in discrete time-steps, where its value at a time-point is determined by the values of some of the other variables at the previous time-point according to a Boolean update function. Kauffman, at first, studied large-scale Boolean models, where the dependencies between variables as well as the update functions are chosen randomly. These random Boolean models are generic models of genome-wide regulatory networks. They can exhibit ordered and robust as well as chaotic and perturbation-prone dynamics. Kauffman hypothesized that regulatory networks in living organisms operate at the boundary between both dynamic regimes, which is called the critical boundary.

First, we relax the biologically implausible binary discretization and study random models whose variables take values in discrete, finite sets. The critical boundary of these models is determined analytically. It is an inverse proportionality between the average number of regulators per variable and a parameter measuring the heterogeneity of the update functions. If these update functions are unbiased, i.e. assume each value with equal probability, the heterogeneity is minimal in the Boolean case; it does, however, not necessarily increase with the mean number of discrete states per variable. By biasing the update functions the heterogeneity can be made arbitrarily small, allowing for increasing numbers of regulators per variable along the critical boundary. We conclude by investigating the synchronization of ensembles of random models, which may, for instance, represent cells in an experimental sample.

Second, we study Boolean models that are derived from networks of signed interactions, such as gene regulatory networks, in which a genetic interaction can typically be classified as either activating or inhibiting. The update function of a variable is defined as a logical combination of the variable's activating and inhibiting regulators. In particular, we focus on large-scale Boolean models derived from networks with randomly chosen signed interactions. In these models, we find multiple, intricately shaped critical boundaries. The computation of these boundaries requires us to first study the fraction of variables being one. We can analytically characterize the asymptotic dynamics of this quantity, which in numeric investigations exhibits a rich dynamical behavior including period-doublings leading to chaos. Our results fit in nicely with Kauffman's hypothesis.

Third, a Boolean modeling approach within a systems biology project is presented, which led to novel insights into the regulatory mechanisms underlying brain formation during embryonic development. We use this example to outline a possible extension of Boolean models to continuous dynamical systems.

Zusammenfassung

In dieser Dissertation werden Erweiterungen und Modifikationen von Booleschen Modellen, wie sie ursprünglich von Stuart Kauffman in der theoretischen Biologie eingeführt wurden, mathematisch untersucht. Eine Variable in einem Booleschen Modell kann nur zwei mögliche Zustände annehmen, Null und Eins. Sie entwickelt sich in diskreten Zeitschritten, wobei ihr Wert zu einem Zeitpunkt durch die Zustände einiger der anderen Variablen zum vorhergehenden Zeitpunkt gemäß einer Booleschen Update-Funktion bestimmt wird. Kauffman untersuchte zunächst grosse Boolesche Modelle, in denen die Abhängigkeitsstruktur der Variablen sowie die Update-Funktionen zufällig bestimmt werden. Diese Booleschen Zufallsmodelle sind generische Modelle genomweiter Regulationsnetzwerke. Sie können sowohl geordnetes, robustes als auch chaotisches, störungsanfälliges Verhalten zeigen. Kauffman stellte die Hypothese auf, dass regulatorische Netzwerke in lebenden Organismen an der Grenze der beiden dynamischen Regime operieren, die als kritische Grenze bezeichnet wird.

Zunächst geben wir die biologisch unplausible binäre Diskretisierung auf und untersuchen Zufallsmodelle, deren Variablen Werte aus endlichen, diskreten Mengen annehmen. Die kritische Grenze dieser Modelle wird analytisch bestimmt. Sie ist eine inverse Proportionalität zwischen der mittleren Anzahl der Regulatoren einer Variable und einem Heterogenitätsparameter der Update-Funktionen. Wenn diese Update-Funktionen unverzerrt sind, d.h. jeden Wert mit gleicher Wahrscheinlichkeit annehmen, ist die Heterogenität im Booleschen Fall minimal, nimmt jedoch nicht notwendigerweise mit der mittleren Anzahl der möglichen Zustände einer Variable zu. Durch eine entsprechende Verzerrung der Booleschen Funktionen lässt sich die Heterogenität beliebig verkleinern, was eine wachsende Anzahl an Regulatoren pro Variable entlang der kritischen Grenze erlaubt. Abschließend untersuchen wir die Synchronisation in Ensembles von Zufallsmodellen, die beispielsweise Zellen in einer experimentellen Probe repräsentieren.

Zum zweiten studieren wir Boolesche Modelle, die von Netzwerken mit gefärbten Kanten abgeleitet werden, wie beispielsweise Genregulationsnetzwerken, in denen genetische Interaktionen typischerweise als aktivierend oder inhibierend klassifiziert werden können. Die Update-Funktion einer Variable wird als eine logische Kombination der aktivierenden und inhibierenden Regulatoren dieser Variable definiert. Wir konzentrieren uns vor allem auf große Boolesche Modelle, die von Netzwerken mit zufällig gewählten, gefärbten Kanten abgeleitet wurden. In diesen Modellen finden sich mehrere, nicht-trivial geformte kritische Grenzen. Um sie berechnen zu können, müssen wir zunächst den Anteil der Variablen mit Wert Eins verstehen. Wir charakterisieren das asymptotische Verhalten dieser Größe analytisch; in numerischen Untersuchungen zeigt sie ein reichhaltiges dynamisches Verhalten wie Periodenverdopplungen hin zum Chaos. Unsere Ergebnisse lassen sich gut mit Kauffman's Hypothese in Einklang bringen.

Zum dritten stellen wir einen Booleschen Modellierungsansatz innerhalb eines Systembiologie Projektes vor, der neue Erkenntnisse über die regulatorischen Grundlagen der Gehirnentwicklung in Embryonen brachte. Anhand dieses Beispiels wird eine mögliche Erweiterung von Booleschen Modellen hin zu kontinuierlichen dynamischen Systemen beschrieben.

Contents

List of Figures

List of Tables

LIST OF TABLES

Notation

a	fraction of activating edges, probability for an edge to be activating, $a = 1 - r$
A	attractor of a dynamical system
$\alpha(x)$	Alpha-limit set of x
b	net rate for reproduction and starvation in the logistic equation
$B(A)$	basin of attraction of A
$B_{g,a,K}$	basin of attraction of $L_{g,a,K}$
$\mathfrak{B}_\delta(w)$	δ-neighborhood of w
c	Hill exponent, degree of cooperativity
$d(t)$	Hamming distance of a Kauffman network (order parameter)
$d_{g,a,K}(t)$	Hamming distance of a Kauffman network with generic logic (g, a, K) (order parameter)
D	iteration function for the Hamming distance $d(t)$ of a Kauffman network
$D_{g,a,K}$	iteration function for the Hamming distance $d_{g,a,K}(t)$ of a Kauffman network with generic logic (g, a, K)
δ_{x_1,x_2}	Kronecker symbol
δ_x	Dirac mass on x
E	set of edges of G
$\mathcal{E}^c$	center subspace
$\mathcal{E}^s$	stable subspace
$\mathcal{E}^u$	unstable subspace
f_i	update rule of node i
$\mathbf{f}$	vector of update rules, transfer function, $\mathbf{f} = (f_i)_{i=1}^N$
g	generic logic
G	graph
$\mathcal{G}$	random graph
$\mathcal{G}(m, N)$	Erdös-Rényi graph
$\mathcal{G}(P_{\text{in}})$	configuration model
$\gamma(x)$	orbit of x
γ^{Euler}	Euler-Mascheroni constant, $\gamma^{\text{Euler}} \approx 0.5772$
i	node in G
I	interval
J	Jacobian matrix
K_i	connectivity of node i
$\overline{K}$	mean connectivity of a Kauffman network, mean of P_{in}
$\mathcal{K}$	Kauffman network
$L_{g,a,K}$	attractor of the truth-content $w_{g,a,K}(t)$
$\ell(\zeta, z)$	probability for ζ fields which are randomly filled according to distribution P_S to contain z different entries
M	number of edges in G
$\mathfrak{m}$	mean of $1/S$, $S \sim P_{\text{nos}}$
$\mathfrak{m}_{-1}$	mean of $1/(S-1)$, $S \sim P_{\text{nos}}$
μ	invariant measure
N	number of nodes in G
$\mathcal{N}(i)$	neighbors/predecessors of node i
$\mathcal{N}_t(i)$	t-th generation predecessors of node i, $\mathcal{N}_1(i) = \mathcal{N}(i)$
ν	Lebesgue measure
$\omega(x)$	Omega-limit set of x
p_S	heterogeneity of distribution P_S

$\overline{p}$	heterogeneity of a Kauffman network, $\overline{p} = \sum P_{\text{nos}}(S)\, p_S$
P_{in}	in-degree distribution
P_{nos}	distribution of number of states
P_S	distribution of entries of update rules
$\text{Pre}_t(i)$	predecessors of node i up to the t-th generation, $\text{Pre}_t(i) = (\mathcal{N}_\tau(i) \mid \tau = 0, 1, \ldots, t)$
Φ	evolution function of a dynamical system
r	fraction of inhibiting edges, probability for an edge to be inhibiting, $r = 1 - a$
ρ	density of measure μ with respect to Lebesgue measure ν
S_i	number of states of node i
$\mathbf{S}$	vector of number of states, $\mathbf{S} = (S_i)_{i=1}^N$
Σ_i	range of node i, $\Sigma_i = \{0, 1, \ldots, S_i - 1\}$
t	time
T	time-domain of a dynamical system
u	magnetization bias of a Kauffman network
V	set of nodes of G
$w_{g,a,K}(t)$	truth-content of a Kauffman network with generic logic (g, a, K)
$W_{g,a,K}$	iteration function for the truth-content $w_{g,a,K}(t)$ of a Kauffman network with generic logic (g, a, K)
$\mathcal{W}^s_{loc}$	stable local manifold
$\mathcal{W}^u_{loc}$	unstable local manifold
X	state-space of a dynamical system/Boolean algebra

Glossary of general biological terms

anterior
: in direction of the head

caudal
: towards the spinal cord

dorsal
: towards the back

ectopic
: expressed in an abnormal place

endogenous
: expressed in a normal, unmanipulated fashion as in a wild-type individual

explant
: Here, explant means an isolated part of tissue from an animal harvested in a sterile manner. Cells are kept in their natural environment in the hope to mimic the *in vivo* situation as closely as possible.

gain-of-function experiment
: In a gain-of-function experiment, the translation of a target gene is amplified, either by adding additional copies of that gene on the DNA or by increasing its transcription rate.

gastrulation
: an early phase in embryonic development, during which the morphology of the embryo changes and the three germ layers are formed

***in situ* hybridization**
: an experimental technique that allows localization of a specific DNA or RNA sequence in parts of a tissue (*in situ*). If the tissue is small enough, the sequence can be localized in the entire tissue in a whole mount *in situ* hybridization.

in vitro
: in a controlled environment such as a test tube or Petri dish

in vivo
: in the living organism

loss-of-function experiment
: In a loss-of-function experiment, a target gene is deactivated either by deletion of that gene from the DNA or by inactivation of the protein.

otic vesicle
: the precursor of the membranous labyrinth of the internal ear

posterior
: in direction of the tail

rostral
: towards the forebrain

secreted factor/protein
: Secreted factors are proteins that are secreted from the expressing cells and able to diffuse through the intercellular matrix.

somite
: Somites are a segmented structure in the vertebrate embryo next to the neural tube. Their periodic formation provides a natural time-measure for early embryonic stages. In the mouse embryo, for instance, about one somite is formed every two hours.

ventral
: towards the front

GLOSSARY OF GENERAL BIOLOGICAL TERMS

List of abbreviations

acim
absolutely continuous invariant measure, 21

acip
absolutely continuous invariant probability measure, 21

BM
Boolean model, 40

CNF
conjunctive normal form, 31

DNA
deoxyribonucleic acid, 31

DNF
disjunctive normal form, 31

i.s.L.
in the sense of Lyapunov, 14

IsO
isthmic organizer, 35

KN
Kauffman network, 43

KNGL
Kauffman network with generic logic, 86

KNMB
Kauffman network with magnetization bias, 43

MHB
mid-hindbrain boundary, 35

miRNA
micro RNA, 33

MKN
multistate Kauffman network, 53

MM
multistate model, 51

mRNA
messenger RNA, 33

ncRNA
non-coding RNA, 33

ODE
ordinary differential equation, 144

PDE
partial differential equation, 144

QM
qualitative model, 83

RNA
ribonucleic acid, 33

rRNA
ribosomal RNA, 33

RSP
regular fixed (steady) point, 143

SKN
standard Kauffman network, 43

SSP
singular fixed (steady) point, 143

tRNA
transfer RNA, 33

1

Introduction

If the Lord Almighty had consulted me
before embarking upon Creation,
I should have recommended something simpler.

Alfonso X, King of Castile and Leon

A surprising result from the *Human Genome Project* is, without doubt, that the human genome consists of considerably less genes than previously assumed. While first estimates placed the size of the human genome at around $10^5 - 10^6$ genes, we now know that it consists of around 20000. Even more surprisingly, lower organisms, such as plants, often turn out to possess considerably larger genomes. To put it bluntly, this leads to the question of how the 20000 human genes can contain the blueprint for something as complex as the human brain, when the 40000 rice genes encode no more than little grains.

We now know that it is not the number of genes that is responsible for the complexity of an organism, but its ability to specifically and accurately control the expression of genes. As the expression of a gene is tightly regulated by the products of other genes, a cell's gene expression profile is the emergent property of a complex system of genetic

interactions. Hence, after the giant task of decoding entire genomes, we now face the even bigger challenge of unraveling the regulatory interdependencies between the discovered genes.

This challenge is what Stuart Kauffman's book "Origins of Order: Self-Organization and Selection in Evolution" [Kauffman, 1993] is all about. Kauffman tackles this daunting task in the spirit of *mathematical modeling*. In doing so, he heeds Einstein's advice that "a model should be as simple as possible, but no simpler; as complicated as necessary, but no more." The *Boolean models* of gene regulation that he puts forward are, arguably, one of the simplest kinds of models for complex dynamic systems. In a Boolean model of a gene regulatory network, genes are described by binary variables taking only discrete values 0 or 1. They develop in discrete time-steps. At each time-point, the value of a variable is determined by a so-called *update rule* that deterministically depends upon the values of some of the other variables, the so-called *inputs*, at the previous time-point. The average number of inputs per variable is called the (mean) *connectivity* of the Boolean model. Update rules are often expressed in terms of *Boolean operators*, such as NOT, AND and OR, which gives the name to these models.

In his seminal paper, Kauffman [1969] proposed large-scale random Boolean models — later called *Kauffman networks* — as generic models of gene regulatory networks. Here, the inputs as well as the update rule of a variable are chosen randomly. Kauffman argues that "proto-organisms probably were randomly aggregated nets of chemical reactions." By investigating random Boolean models he wishes to test "the hypothesis that contemporary organisms are also randomly constructed molecular automata."

Despite their simplicity, Boolean models and Kauffman networks already capture salient features of complex dynamic systems and, thus, allow to study their properties within a well-defined, accessible environment. For these reasons, they are popular tools in theoretical biology and especially within the newly emerging field of systems biology.

In theoretical biology, Kauffman networks are discussed under the slogan "Living at the edge of chaos." We will explain in the course of this thesis that, depending on their connectivity, Kauffman networks exhibit three characteristic dynamical behaviors, which we term *frozen* (*ordered*), *critical* and *chaotic*. For low connectivities, they are in the *frozen* or *ordered phase*. Here, their dynamics are dominated by short-periodic oscillations and are robust against external perturbations. As the number

of inputs increases, Kauffman networks undergo a *phase transition* and switch into the *chaotic phase*. Their time-courses no longer show a clear oscillatory behavior and they are highly sensitive to perturbations. The boundary between the frozen and chaotic phase is called the *critical boundary* or *critical connectivity*. Kauffman [1993] argues that properties from the frozen as well as the chaotic phase, *viz* robustness and adaptability, are important for the evolution of living organisms, and that, consequently, their regulatory networks need to be poised at criticality, i.e. "at the edge of chaos." Interestingly, the (mean) connectivities of gene regulatory networks found in lower organisms are all around two, which, as we will see, is precisely the critical connectivity of the random Boolean models introduced by Kauffman.

Besides the study of Kauffman networks, many small- and medium-scale Boolean models of specific biological processes have been manually curated. Such models have been an integrative part of many systems biology research projects over the last years [Saez-Rodriguez et al., 2007, 2009; Samaga et al., 2009; Schlatter et al., 2009; Wittmann et al., 2009a]. They were used to analyze biological processes with the main goal of generating hypothesis and predictions, e.g. about possible regulatory interactions.

Overview of this thesis

Considering the simplicity of Boolean models, it stands to reason to extend and modify them in the hope to bring them closer to biological reality and to further enhance their explanatory power. In this thesis, we study such extensions and modifications.

They are *motivated from a biological point of view*, by a desire to remedy certain inadequacies of Boolean models as models of gene regulatory networks. They are *investigated from a biomathematical point of view*, e.g. by analyzing dynamical systems which describe interesting quantities of modified Kauffman networks. As is typically the case in the theory of Kauffman networks, these quantities will be obtained in *mean-field approximations* and will describe generic properties in ensembles of networks. In this thesis, we will only briefly touch these deep relations between Kauffman networks and concepts from statistical physics. Instead, we will focus on mathematically analyzing the dynamical behavior of the mean-field quantities. Finally, the usefulness of a possible extension of Boolean models to continuous dynamical systems is demonstrated in a systems biology application.

Chapter 2 contains necessary prerequisites from graph theory, dynamic systems theory and Boolean algebra. It also provides a short introduction into the molecular basis of gene regulation and sets the stage for our biological application in chapter 6. Explanations of frequently used basic biological terms can also be found in the glossary on page xix. **Chapter 3** then introduces Boolean models and Kauffman networks. It also provides some background information from statistical physics.

In **chapter 4**, we generalize Boolean Kauffman networks by softening the hard binary discretization and allowing variables to assume values in general discrete, finite sets. These *multistate Kauffman networks* are generic models of gene regulatory networks, in which genes are known to assume more than two functionally different expression levels. We analytically determine the critical connectivity that separates the biologically unfavorable frozen and chaotic phases (Theorem 4.1). This connectivity is inversely proportional to a parameter which measures the heterogeneity of the update rules. If these update rules are unbiased, i.e. assume each value equiprobably, the critical connectivity decreases when we leave the Boolean case and allow for multiple states, albeit it does not necessarily depend on the mean number of discrete states per variable. This decrease might lead to biologically unrealistic situations; we are, however, able to demonstrate that the critical connectivity can be re-increased by sufficiently biasing the update rules. The theory of Boolean Kauffman networks is obtained as a special case of our more general statements. We conclude by investigating the synchronization behavior of multistate Kauffman networks. All analytic results are further corroborated by network simulations.

In **chapter 5** we formally introduce qualitative models of gene regulatory networks as directed graphs with signed edges according to whether a genetic interaction is activating or inhibiting. Qualitative models are what we typically obtain from experiments. They contain less information than a Boolean model, whose update rules also precisely specify the interplay of the various regulators of a gene. We propose to systematically convert qualitative into Boolean models via so-called *generic logics*, which allow combination of activating and inhibiting influences into an update rule.

We investigate Kauffman networks whose update rules are generated by generic logics. Similar to the bias for update rules from chapter 4, we introduce a bias towards activating edges. We begin by studying the *truth-content* of Kauffman networks with generic logics, which is an approximation of the fraction of ones (more precisely, of the

fraction of variables being one). The asymptotic behavior of this quantity is shown to be essentially independent of the initial conditions, and its attractor is characterized (Theorems 5.1, 5.2 and 5.3). We continue with numeric analyses of the truth-content. Especially for small (biologically implausible) fractions of activating edges, the truth-content exhibits a rich dynamical behavior including period-doublings leading to chaos as the connectivity of the network grows. In the biologically plausible case of larger fractions of activating edges and small connectivities, the truth-content has stable stationary dynamics. We define *truth-stable* Kauffman networks with generic logics as networks whose truth-contents exhibit non-chaotic dynamics.

Our results about the truth-content of Kauffman networks with generic logics allow us to derive a criterion for phase transitions in these networks (Theorems 5.5 and 5.6). In numeric analyses we find multiple, intricately shaped critical boundaries, which fit nicely into the theory of "Living at the edge of chaos." Simulations further strengthen the significance of our analytic results.

In **chapter 6** we conclude with a systems biology application. We use this application to outline a possible extension of Boolean models to continuous dynamical systems. The biological process we study is an aspect of brain formation during embryonic development *viz* differentiation of mid- and hindbrain. The differentiation of these two brain regions is mediated *inter alia* by molecular signals emitted from the so-called *isthmic organizer*, in particular, by Fgf8 and Wnt1 proteins. The isthmic organizer is characterized by a well-defined pattern of locally restricted gene expression domains around the boundary between prospective mid- and hindbrain, the *mid-hindbrain boundary*. This pattern is established and maintained by a gene regulatory network that is not yet understood in full detail.

In a first step, we set up a Boolean model of this regulatory network. To this end, we show that a Boolean analysis of the characteristic spatial gene expression patterns at the murine mid-hindbrain boundary reveals key regulatory interactions. Our analysis employs techniques from computational logic for the minimization of Boolean functions. In particular, we predict a maintaining rather than inducing effect of Fgf8 on *Wnt1* expression, an issue that remained unclear from published data. We provide experimental evidence that Fgf8, in fact, only maintains but does not induce *Wnt1*

expression around the murine mid-hindbrain boundary.[1] In combination with previously validated interactions, this finding allows us to construct a Boolean model of the regulatory network at the mid-hindbrain boundary.

We then outline a possible way of transforming Boolean models into continuous dynamical systems with switch-like interactions and briefly discuss the dynamical behavior of these systems, in particular, with respect to fixed points. We apply the transformation to our Boolean model of the mid-hindbrain boundary. Simulations of the resulting continuous system show that it is, indeed, competent to reproduce important biological phenomena, such as refinements and sharpenings of expression patterns, that could not have been captured by the Boolean model.

Main scientific contributions

Here, the main contributions of this thesis are summarized and the respective manuscripts by the author are referenced. Some of these works laid the foundation for collaborations; manuscripts having arisen therefrom are also cited.

Chapter 4

- A general class of multistate Kauffman networks is introduced, and a criterion for phase transitions is derived [Wittmann et al., 2010].

- A dynamical system is presented and analyzed that models ensembles of networks as well as Kauffman networks with fuzzy logics [Wittmann and Theis, 2010a]. It allows, for instance, to investigate the synchronization behavior of these ensembles.

Chapter 5

- The concept of generic logics as a way to link qualitative and Boolean models is introduced and studied [Wittmann and Theis, 2010b].

[1] Collaboration with Nilima Prakash (Institute of Developmental Genetics, Helmholtz Zentrum München)

- The class of Kauffman networks with generic logics is introduced and investigated for critical phenomena. To the best of our knowledge, it is the first class of KNs exhibiting multiple critical connectivities [Wittmann and Theis, 2010b].

Chapter 6

- A method for the analysis of spatial expression patterns is presented [Wittmann et al., 2009a]. Applied to the gene expression profile at the mid-hindbrain boundary several genetic interactions are predicted. Unknown interactions have been experimentally validated.

- The first mathematical model of gene regulation at the mid-hindbrain boundary is presented [Wittmann et al., 2009a]. It is further analyzed by Ansorg et al. [2010] and Breindl et al. [2010].

- A possible transformation of Boolean models into continuous dynamical systems is outlined [Wittmann et al., 2009b], which is also available in our MATLAB modeling toolbox *ODEfy* [Krumsiek et al., 2010].

2

Prerequisites

Was man nicht weiss, das eben brauchte man,
Und was man weiss, kann man nicht brauchen.

Faust, Johann Wolfgang von Goethe

According to Eykhoff [1974], a mathematical model is "a representation of the essential aspects of an existing system (or a system to be constructed) which presents knowledge of that system in usable form." Mathematical models may take many forms. It is probably one of Newton's chief merits to have developed the language of differential equations and *dynamical systems* for the statement of his laws of motion and gravity. In many fields of science, including biomathematics, mathematical models are ever since formulated in this language. Over the last decade, however, a new language has been established, that of *graphs* and *complex networks*. It proved particularly suitable to describe all kinds of complex systems, ranging from the Internet to biological systems, such as gene regulation [Albert and Barabási, 2002].

In this thesis, we speak both languages and are now going to introduce the necessary concepts and techniques from each (sections 2.1 and 2.2). We will also need some

vocabulary from *Boolean algebra* (section 2.3). After these mathematical prerequisites, we familiarize the reader with the basic principles of gene expression and its regulation as well as with our biological application from chapter 6 (section 2.4).

2.1 Prerequisites from graph theory

The study of networks has gained importance in all fields of science which require the analysis of complex relational data. It dates back to the year 1736 when Leonard Euler published his famous paper "Seven Bridges of Königsberg." The mathematical description of vertices and edges introduced by Euler in this publication was the foundation of graph theory, the branch of mathematics that became the framework of complex networks theory. For this reason, we now introduce the basics of this field of mathematics, for details we refer the reader to the "Modern Graph Theory" by Bollobás [1998].

Definition 2.1 (graph)**.** An *undirected (directed) graph* G is an ordered pair of disjoint sets (V, E) such that $V \neq \varnothing$ and E is a set of unordered (ordered) pairs of elements of V. The elements of V are the *nodes* of G, the elements of E are called *edges*.

The numbers of elements in V and E are called the *order* and *size* of G; they are denoted by N and M, respectively. A node is usually referred to by its order i in the set V. In an undirected graph, two nodes $i, i' \in V$ are called *adjacent* (*neighbors*) if $(i, i') \in E$. In this case, the edge (i, i') is said to be *incident* in nodes i and i', or to join the two nodes; the two nodes i and i' are called the *end-nodes* of edge (i, i'). In a directed graph, a node i is called *predecessor* or *input* of a node i' and, conversely, i' is called *successor* or *target* of i if $(i \to i') \in E$.

For some node i in an undirected graph we let $\mathcal{N}(i)$ denote the set of its neighbors; in the case of a directed graph, $\mathcal{N}(i)$ will denote the set of predecessors of i. In the latter case, we inductively define the tuple of the t-th generation predecessors of i, $\mathcal{N}_t(i) := (\mathcal{N}(i') \mid i' \in \mathcal{N}_{t-1}(i))$, $t = 1, 2, \ldots$, where $\mathcal{N}_0(i) = (i)$. (Clearly, $\mathcal{N}_1(i) = \mathcal{N}(i)$.) Finally, we let $\mathrm{Pre}_t(i) = (\mathcal{N}_\tau(i) \mid \tau = 0, 1, \ldots, t)$, $t = 0, 1, \ldots$, denote the tuple of predecessors of i up to the t-th generation.

In an undirected graph, the *degree* (*connectivity*) K_i of a node i is the number of incident edges. In the directed case, one distinguishes between the *in-degree* and *out-degree* of i, which are, of course, defined as the number of inputs and targets of i, respectively. In this thesis, we use the terms degree and connectivity also for directed

graphs and, by convention, refer to the in-degree. A basic topological characterization of a graph G is given by its *degree distribution* $P(K)$, defined as the probability that a node chosen uniformly at random has degree K or, equivalently, as the fraction of nodes in the graph having degree K. In directed graphs we work with the (in-)degree distribution $P_{\text{in}}(K)$.

A *signature* of a graph $G = (V, E)$ is a mapping $\sigma : E \to \{+, -\}$. A graph together with a signature is called *signed graph*. In addition to the purely topological information about interactions in a network provided by an (unsigned) graph, a signed graph also specifies the type of the interactions. For each signature σ of G we denote the *inverted* signature by $\neg\sigma$, i.e. for each edge $e \in E$

$$\neg\sigma(e) = \begin{cases} + & \text{if } \sigma(e) = - \\ - & \text{if } \sigma(e) = + \end{cases} .$$

Random graphs

Starting with the pioneering work of Erdös and Rényi [1959], a new line of research began, focusing on *average properties* of families of graphs. The central object of study in this subfield of graph theory is a *random graph*. Most generally, we can define a random graph as a probability space whose elements are graphs. The probability measure is often defined via a random process which yields graphs as realizations. Such a random process is also called *generative model*. In here, we focus on random graphs with a fixed number of nodes.

An important example for random graphs is the Erdös-Rényi graph, which we present in its version for directed graphs.

Example 2.1 (Erdös-Rényi graph). For $0 \leqslant m \leqslant 1$, let $\mathcal{G}(m, N)$ be the probability space of all 2^{N^2} (directed) graphs on N nodes, where the probability of a graph with M edges is $m^M(1-m)^{N^2-M}$. $\mathcal{G}(m, N)$ is called *Erdös-Rényi graph*. An equivalent definition is given by the following generative model, which yields graphs on N nodes: A graph on N nodes is constructed by including each of the N^2 possible (directed) edges independently with probability m.

Now, suppose we are given some random graph $\mathcal{G}$, and consider the following random experiment. Pick a realization of $\mathcal{G}$ and choose one of its nodes uniformly at random, we call it i. The distribution of the random variable K_i is called the *degree distribution*

of $\mathcal{G}$. If $\mathcal{G} = \mathcal{G}(m, N)$ is an Erdös-Rényi graph, the degree distribution is the binomial distribution

$$P(K_i = K) = \binom{N}{K} m^K (1-m)^{N-K} ,$$

as each of the N nodes is independently chosen to be an input of i with probability m. In the limit of large N, where $mN = M$ constant, this can be approximated by a Poisson distribution

$$P(K_i = K) = \frac{M^K e^{-M}}{K!} .$$

In the undirected case, it is a non-trivial task to define a random graph with a given degree distribution. In the directed case, however, this is easy.

Example 2.2 (configuration model). Let $P_{\text{in}}(K)$, $K = 1, 2, \ldots, K_{\max}$, $K_{\max} \leqslant N$, be a distribution. We let $\mathcal{G}(P_{\text{in}})$ denote the space of all graphs on N nodes whose in-degrees are bounded by $K_{\max}$. We turn $\mathcal{G}(P_{\text{in}})$ into a probability space by defining a generative model that yields realizations in $\mathcal{G}(P_{\text{in}})$: For each node i pick its in-degree K_i randomly according to P_{in} and choose its K_i inputs randomly from among the N nodes with equal probability. This generative model is called *configuration model*.

Often, random graphs are studied in the *thermodynamic limit* of large N. Here, we have the following important lemma, which we generalize from Hilhorst and Nijmeijer [1987].

Lemma 2.1. *Let $K_{\max} \geqslant 1$. There exists a sequence $(t_N)_{N \geqslant K_{\max}}$ such that $t_N \to \infty$ as $N \to \infty$ satisfying the following: For $N \geqslant K_{\max}$ let G be a realization of a random graph $\mathcal{G}(P_{in})$ on N nodes, where P_{in} as in Example 2.2. Then, the probability that for some node i of G equals occur among the $\operatorname{Pre}_t(i)$ for $0 \leqslant t \leqslant t_N$ is on the order of $\mathcal{O}(N^\alpha)$ with $\alpha < 0$. In other words, the probability for the subgraph on $\operatorname{Pre}_t(i)$ to be acyclic as an undirected graph approaches 1 as N grows.*

Proof. Let $N \geqslant K_{\max}$. The following holds for a realization of a random graph $\mathcal{G}(P_{\text{in}})$ on N nodes and some randomly chosen node i: The size of $\operatorname{Pre}_t(i)$ is bounded by

$$|\operatorname{Pre}_t(i)| \leqslant \begin{cases} 1 + K_{\max} + \ldots + K_{\max}^t = \dfrac{K_{\max}^{t+1} - 1}{K_{\max} - 1} , & K_{\max} > 1 \\ t , & K_{\max} = 1 . \end{cases}$$

The probability that equals occur among the $\operatorname{Pre}_t(i)$ is bounded by

$$1 - \prod_{k=1}^{|\operatorname{Pre}_t(i)|} \left(1 - \frac{k}{N}\right) = \frac{1}{2} N^{-1} |\operatorname{Pre}_t(i)| \left(|\operatorname{Pre}_t(i)| - 1\right) + \mathcal{O}\left(N^{-2} |\operatorname{Pre}_t(i)|^{-4}\right) .$$

This is of order $\mathcal{O}(N^\alpha)$ with $\alpha < 0$ if we keep t restricted to $1 \leqslant t \leqslant t_N$, where

$$t_N = \begin{cases} \beta \dfrac{\log(N)}{2\log\left(K_{\max}\right)}\,, & \text{with } \beta < 1\,, \quad \text{if } K_{\max} > 1 \\ N^\beta\,, & \text{with } \beta < \dfrac{1}{2}\,, \quad \text{if } K_{\max} = 1\,. \end{cases}$$

□

One commonly refers to this lemma by claiming that "in the thermodynamic limit we may assume inputs to be independent." We will explain this statement in Remark 4.4.

In the following, unless specified otherwise, a graph will always be directed, and a random graph will always be given by the configuration model from Example 2.2.

2.2 Prerequisites from dynamical systems theory

For the general introduction to dynamical systems in sections 2.2.1–2.2.3 we follow the book by Guckenheimer and Holmes [1990]. For an account of dynamical systems as biomathematical models we refer the reader to the textbooks about mathematical biology by Murray [2002] and De Vries et al. [2006].

2.2.1 General notions from dynamical systems theory

Let us straightaway give the most important definition.

Definition 2.2 (dynamical system)**.** A *dynamical system* is a tuple (T, X, Φ) consisting of a monoid T, a set X, and a function $\Phi : T \times X \to X$ satisfying $\Phi(0, x) = x$ and $\Phi\left(t_2, \Phi\left(t_1, x\right)\right) = \Phi\left(t_1 + t_2, x\right)$. The function Φ is called the *evolution function* of the dynamical system. The set X is called *state-space*.

2.2.1.1 Orbits and invariant sets

Fixing $x \in X$, the function $\Phi_x : T \to X$, $t \mapsto \Phi(t, x)$ is called *flow* through x and its graph $\gamma(x) := \{\Phi_x(t) \mid t \in T\}$ is called *orbit* or *trajectory* of x. A subset $U \subset X$ of the state-space is called *invariant* if for all $x \in U$ it holds $\gamma(x) \subset U$.

Let us now discuss several types of orbits. A point $x \in X$ is called *fixed point* or *equilibrium* if $\Phi(t, x) = x$ for all $t \in T$. In this case, the orbit of x is a singleton, $\gamma(x) = \{x\}$. An orbit $\gamma(x)$ of x is called *periodic* if there exists $\tau \in T$ such that

$\Phi(t,x) = \Phi(t+\tau,x)$ for all $t \in T$. The smallest such τ is called the *period* of $\gamma(x)$. Each point in $\gamma(x)$ is called *τ-periodic point*.

Often, T represents time and one chooses $T = \mathbb{N}_0, \mathbb{Z}, \mathbb{R}_0^+$ or $\mathbb{R}$. If $T = \mathbb{Z}$ or $T = \mathbb{R}$ one distinguishes between *positive* and *negative invariant sets*. A set $U \subset X$ is positive (negative) invariant, if for all $x \in U$ and $t \geqslant 0$ ($t \leqslant 0$) it holds $\Phi(t,x) \in U$.

Of particular interest is the asymptotic behavior of a dynamical system in the limit of large times. We now introduce several notions to characterize this behavior. For this, we let X be a metric space with metric d. This metric then induces a distance function for points $x \in X$ and sets $U \subset X$

$$\operatorname{dist}(x,U) = \inf_{x' \in U} d(x,x') \ .$$

2.2.1.2 Types of stability

We begin with the central concepts of *Lyapunov* and *orbital stability*. An orbit $\gamma(x)$ is called *stable in the sense of Lyapunov* (i.s.L.) if for all $\epsilon > 0$ there is $\delta > 0$ such that

$$d\left(x,x'\right) < \delta \Longrightarrow d\left(\Phi(t,x),\Phi(t,x')\right) < \epsilon \quad \text{for all } t \geqslant 0 \ .$$

Otherwise, $\gamma(x)$ is called *unstable i.s.L.* If $\gamma(x)$ is stable and, moreover, there is $\delta_0 > 0$ such that

$$d\left(x,x'\right) < \delta_0 \Longrightarrow \lim_{t\to\infty} d\left(\Phi(t,x),\Phi(t,x')\right) = 0 \ ,$$

then $\gamma(x)$ is called *asymptotically stable i.s.L.* The orbit $\gamma(x)$ is called *neutrally stable* if it is stable but not asymptotically stable.

If $\gamma(x)$ is a stable orbit i.s.L. the two orbits $\gamma(x)$ and $\gamma(x')$ remain "synchronized" provided x and x' are sufficiently close in the sense of the above definition. Orbital stability is a weaker concept of stability that relaxes the requirement of synchrony. An invariant set $U \subset X$ is called *orbitally stable* if for all $\epsilon > 0$ there exists $\delta > 0$ such that

$$\operatorname{dist}(x,U) < \delta \Longrightarrow \operatorname{dist}\left(\Phi(t,x),U\right) < \epsilon \quad \text{for all } t \geqslant 0 \ .$$

Otherwise, U is called *orbitally unstable*. If U is orbitally stable and, moreover, there is $\delta_0 > 0$ such that

$$\operatorname{dist}(x,U) < \delta_0 \Longrightarrow \lim_{t\to\infty} \operatorname{dist}\left(\Phi(t,x),U\right) = 0$$

then U is called *orbitally asymptotically stable*.

In this thesis, unless specified otherwise, we always work with the concept of Lyapunov stability.

2.2.1.3 ω-limit points and attractors

Another important concept for the characterization of a system's long-time behavior are *ω-limit points*. A point x is called an ω-limit point of some $x_0 \in X$ if there is a sequence of times $(t_q)_{q\geqslant 0}$ such that $t_q \to \infty$ and $\Phi(t_q, x_0) \to x$ as $q \to \infty$. If $T = \mathbb{Z}$ or $T = \mathbb{R}$ we can also define *α-limit points* as limits of sequences $\Phi(t_q, x_0)$ where $t_q \to -\infty$. The sets $\omega(x_0)$ and $\alpha(x_0)$ of all ω-limit points and α-limit points of x_0 are called the *ω-limit set* and *α-limit set* of x_0.

A more global description of the asymptotic dynamics can be given in terms of the *attractors* of a dynamical system. We call a closed, invariant set $A \subset X$ *attracting*, if there is some neighborhood $U \supset A$ of A such that $\Phi(t, x) \in U$ for $t \geqslant 0$ and $\Phi(t, x) \to A$ as $t \to \infty$, for all $x \in U$. A *repelling* set is defined analogously, replacing t by $-t$. The attractors of a dynamical system are its "minimal" or "irreducible" attracting sets. We follow Guckenheimer and Holmes [1990] and make

Definition 2.3 (attractor, preliminary[1])**.** An *attractor* is an attracting set $A \subset X$ that contains a dense orbit.

We already got to know important examples of attracting and repelling sets.

Remark 2.1. Any asymptotically stable fixed point or periodic orbit is an attractor. Any unstable fixed point or periodic orbit is a repelling set.

2.2.1.4 Types of dynamical systems

We now list several types of dynamical systems. In a *real, time-continuous* dynamical system we have $T = \mathbb{R}$, $X = \mathbb{R}^n$. Moreover, we require that for all $x \in X$ the flow $\Phi_x : T \to X$, $t \mapsto \Phi(t, x)$ through x and for all $t \in T$ the function $\Phi_t : X \to X$, $x \mapsto \Phi(t, x)$ are continuous. The set of functions $\{\Phi_t\}_t$ is a group with identity Φ_0 and inverse $\Phi_t^{-1} = \Phi_{-t}$.

Each system of autonomous first order *differential equations*

$$\dot{x} = \varphi(x)\,, \quad x \in \mathbb{R}^n\,,$$

with a vector field $\varphi : \mathbb{R}^n \to \mathbb{R}^n$ induces a time-continuous dynamical system if the pertaining initial value problems

$$\begin{aligned} \dot{x} &= \varphi(x) \\ x(0) &= x_0 \end{aligned} \tag{2.1}$$

[1] In section 2.2.3.1 we will somewhat relax this definition.

have globally unique solutions for all $x_0 \in X$. According to the theorem by *Picard-Lindelöf*, see e.g. Coddington and Levinson [1972], this is, in particular, the case if φ is globally Lipschitz-continuous. The evolution function Φ of the dynamical system is given by the fundamental solution of (2.1). The fixed points of the dynamical system are the zeros of the vector field φ.

The discrete models of gene regulation presented in this thesis give rise to dynamical systems where X is some finite discrete set and $T = \mathbb{N}_0$. We will study mean-field quantities of these models, which are described by dynamical systems with $X = \mathbb{R}^n$ and $T = \mathbb{N}_0$. The first kind of dynamical systems will be introduced in chapter 3. In the remainder of this section, let us speak about dynamical systems with $X = \mathbb{R}^n$ and $T = \mathbb{N}_0$ or $T = \mathbb{Z}$.

2.2.2 Discrete dynamical systems

Let $X = \mathbb{R}^n$ and $T = \mathbb{N}_0$ or $T = \mathbb{Z}$. We consider *time-discrete* dynamical systems defined by a $\mathcal{C}^l$-map $\Psi : \mathbb{R}^n \to \mathbb{R}^n$. If $T = \mathbb{Z}$ we require Ψ to be a diffeomorphism. The evolution function of the dynamical system is given by $\Phi(t, x) = \Psi^t(x)$. If $T = \mathbb{Z}$, we define $\Psi^t = \left(\Psi^{-1}\right)^{-t}$ for $t < 0$. In other words, an orbit $\gamma\left(x(0)\right)$ of this dynamical system is given by the iteration

$$x(t+1) = \Psi\left(x(t)\right) \ . \tag{2.2}$$

2.2.2.1 Linear discrete dynamical systems

Let us begin with the simple case of linear Ψ. Then $x^{(f)} = 0$ is a fixed point of system (2.2).

Proposition 2.1 (stability criteria)**.** *We have the following* stability criteria *for* $x^{(f)}$*.*

- *If* $|\lambda| < 1$ *for all eigenvalues* λ *of* Ψ*, then* $x^{(f)}$ *is asymptotically stable.*
- *If* $|\lambda| \leqslant 1$ *and* λ *semisimple if* $|\lambda| = 1$ *for all eigenvalues* λ *of* Ψ*, then* $x^{(f)}$ *is stable.*
- *Otherwise* $x^{(f)}$ *is unstable.*

To describe the dynamics of (2.2) one often writes $\mathbb{R}^n$ as the direct sum of the so-called *stable*, *unstable* and *center subspaces*, $\mathbb{R}^n = \mathcal{E}^s \oplus \mathcal{E}^u \oplus \mathcal{E}^c$, where

$$\begin{aligned}
\mathcal{E}^s &:= \text{span}\,\{\text{(generalized) eigenvectors } \lambda \text{ of } \Psi \mid |\lambda| < 1\} \\
\mathcal{E}^u &:= \text{span}\,\{\text{(generalized) eigenvectors } \lambda \text{ of } \Psi \mid |\lambda| > 1\} \\
\mathcal{E}^c &:= \text{span}\,\{\text{(generalized) eigenvectors } \lambda \text{ of } \Psi \mid |\lambda| = 1\}\ .
\end{aligned}$$

Observe that, in general, the generalized eigenspaces of Ψ are invariant sets.

2.2.2.2 Non-linear discrete dynamical systems

Now, consider again the case of general Ψ and suppose $x^{(f)}$ is a fixed point of system (2.2). We ask if we can describe the local behavior of system (2.2) around $x^{(f)}$ by the linearized system

$$x(t+1) = Jx(t) \tag{2.3}$$

with $J = \mathrm{D}\Psi|_{x^{(f)}}$. In mathematical terms, we ask if the two systems are *locally conjugate* at $x^{(f)}$, i.e. if there exists a homeomorphism $\mathfrak{h}$ defined in a neighborhood U of $x^{(f)}$ which maps orbits of system (2.2) locally on orbits of system (2.3)

$$\mathfrak{h}\left(\Psi(x)\right) = J\mathfrak{h}(x) \quad \text{for all } x \in U\ .$$

In general, this is not the case. However, we have such a statement if the fixed point $x^{(f)}$ is *hyperbolic*, i.e. if J has no eigenvalues on the unit circle.

Theorem 2.1 (Hartman-Grobman)**.** *If the fixed point $x^{(f)}$ is hyperbolic, the two systems* (2.2) *and* (2.3) *are locally conjugate at $x^{(f)}$ via a homeomorphism $\mathfrak{h}$, which preserves the orientation of orbits.*

As $\mathfrak{h}$ preserves the orientation of orbits, the Hartman-Grobman theorem implies

Corollary 2.1. *In the situation of Theorem 2.1, the type of stability of $x^{(f)}$ (with respect to system* (2.2)*) is equal to the type of stability of $\xi^{(f)} = 0$ with respect to system* (2.3)*.*

In the case of general $x^{(f)}$, we have the following (weaker) stability criterion.

Theorem 2.2 (linear stability analysis)**.** *If any eigenvalue of $J = D\Psi|_{x^{(f)}}$ has absolute value larger than one, the fixed point $x^{(f)}$ of system* (2.2) *is unstable. If all eigenvalues of J have absolute value smaller than one, the fixed point $x^{(f)}$ is asymptotically stable. If the largest eigenvalue modulus is one, the stability of $x^{(f)}$ cannot be determined by a linear analysis alone, but depends on higher-order terms. We also refer to such equilibria as* critical *fixed points.*

Remark 2.2. The study of a τ-periodic orbit $\gamma\left(x^{(p)}\right)$ can be reduced to the analysis of the fixed point $x^{(p)}$ of the map Ψ^τ. This is to say, we simply define J as

$$J = \mathrm{D}\Psi^\tau|_{x^{(p)}} = \prod_{x \in \gamma\left(x^{(p)}\right)} \mathrm{D}\Psi|_x$$

in Theorem 2.2.

If $T = \mathbb{Z}$ (and Ψ is a $\mathcal{C}^l$-diffeomorphism), one also has a (local) generalization of the stable and unstable subspaces to non-linear systems. Let U be a sufficiently small open neighborhood of the fixed point $x^{(f)}$. We define the sets

$$\mathcal{W}^s_{loc}\left(x^{(f)}\right) = \left\{x \in U \;\middle|\; \Psi^t(x) \in U \;\forall\, t \geqslant 0 \text{ and } \lim_{t\to\infty} \Psi^t(x) = x^{(f)}\right\}$$
$$\mathcal{W}^u_{loc}\left(x^{(f)}\right) = \left\{x \in U \;\middle|\; \Psi^t(x) \in U \;\forall\, t \leqslant 0 \text{ and } \lim_{t\to-\infty} \Psi^t(x) = x^{(f)}\right\} .$$

Theorem 2.3 (stable and unstable local manifolds)**.** *The two sets $\mathcal{W}^s_{loc}\left(x^{(f)}\right)$ and $\mathcal{W}^u_{loc}\left(x^{(f)}\right)$ are $\mathcal{C}^l$-manifolds as well as positive and negative invariant sets of system* (2.2)*. They are tangent to the stable and unstable subspaces $\mathcal{E}^s$ and $\mathcal{E}^u$ of system* (2.3) *at $x^{(f)}$, respectively, and can be represented as graphs of functions*

$$\begin{aligned} \mathfrak{w}^s &: U \cap \mathcal{E}^s \;\to\; \mathcal{E}^u \oplus \mathcal{E}^c \qquad \textit{and} \\ \mathfrak{w}^u &: U \cap \mathcal{E}^u \;\to\; \mathcal{E}^s \oplus \mathcal{E}^c \quad . \end{aligned}$$

We call $\mathcal{W}^s_{loc}\left(x^{(f)}\right)$ and $\mathcal{W}^u_{loc}\left(x^{(f)}\right)$ the *stable* and *unstable manifold* of system (2.2) at $x^{(f)}$.

2.2.3 Statistical properties of discrete dynamical systems

There are two general approaches to the study of dynamical systems, we shall call them the geometric and the statistical approach. The goal of the geometric approach, that we have, so far, followed, is to (qualitatively) draw a phase portrait of the dynamical system

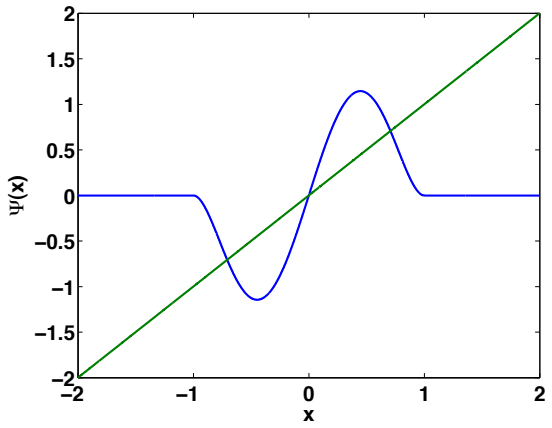

Figure 2.1: Ad Example 2.3. Graph of the map Ψ. The origin is a repellent fixed point and the ω-limit set of Lebesgue-almost all points.

under study. The statistical approach, which we are going to outline in the following, looks for typical properties and behaviors of a system. The distinction between typical and exceptional properties requires the use of a measure. In here, this measure will always be the Lebesgue measure ν. We still consider the time-discrete dynamical system from (2.2).

2.2.3.1 Metric attractors

Let us first re-think Definition 2.3 of an attractor. Collet and Eckman [1980], in adopting the statistical point of view, describe an attractor as "the set of points to which most points evolve." This is to say, an attractor should (at least partially) describe the generic behavior of a dynamical system. The following example taken from Milnor [1985] shows that Definition 2.3 is unable to meet this requirement.

Example 2.3. Consider the dynamical system $T = \mathbb{N}_0$, $X = \mathbb{R}$ and $\Phi(t, x) = \Psi^t(x)$ with

$$\Psi(x) = \begin{cases} 4x\left(1 - x^2\right)^2 , & \text{if } |x| \leqslant 1 \\ 0 , & \text{everywhere else.} \end{cases}$$

By inspection of the graph of Ψ (cf. Figure 2.1) one observes that orbits of Lebesgue-almost all points from the real line ultimately end up in the origin. Exceptions are the two unstable fixed points where the graph intersects with the diagonal. The origin, however, is an unstable fixed point and no attractor according to Definition 2.3.

From now on, we adopt the definition of attractor given by Milnor [1985]. This definition is motivated by the idea that an attractor should represent the generic behavior of a considerable portion of initial conditions. Let us make this a precise mathematical notion. For an invariant set $U \subset X$, we let

$$B(U) := \{x \in X \mid \omega(x) \subset U\}$$

denote the *basin of attraction* of U. In other words, $B(U)$ consists of all points that asymptotically end up in U. An attracting set A is called *globally attracting*, if $X \backslash B(A)$ has measure zero. We now make

Definition 2.4 (metric attractor, Milnor [1985])**.** A *(metric) attractor* (*attractor in the sense of Milnor*) is a (forward) invariant set A satisfying the following.

- The basin of attraction $B(A)$ has positive Lebesgue measure.
- If A' is another (forward) invariant set, which is strictly contained in A, then $B(A) \backslash B(A')$ has positive measure.

If $X \backslash B(A)$ is a measure zero set, we call A a *global* attractor.

Note that an attractor with positive measure need not attract anything outside of itself.

2.2.3.2 Invariant and natural measures

A central concept in the statistical description of dynamical systems is that of a measure describing the long-time distribution of orbits. We call a Borel measure μ *invariant* for Ψ if $\mu\left(\Psi^{-1}(U)\right) = \mu(U)$ for every measurable subset $U \subset X$. An invariant measure μ is a *natural measure* for Ψ if

$$\mu = \lim_{t \to \infty} \frac{1}{t} \sum_{\tau=0}^{t-1} \delta_{\Psi^\tau(x)} \tag{2.4}$$

for all x in a set of positive Lebesgue measure, where $\delta_{\Psi^\tau(x)}$ denotes the *Dirac mass* on $\Psi^\tau(x)$. The limit in (2.4) means convergence of measures in the weak* sense.[1]

If system (2.2) has a periodic attractor, there exists a natural measure for Ψ, *viz* equally weighted point masses on the points of the attractor. In this case, the measure

[1] A sequence of measures μ_t on X is said to *converge weakly** to the measure μ if $\liminf_{t \to \infty} \mu_t(U) \geqslant \mu(U)$ for all open subsets $U \subset X$.

has no density. We shall be particularly interested in the converse case. According to the *Radon-Nikodym theorem*, see e.g. Shilov and Gurevich [1966], a measure μ that is absolutely continuous with respect to the Lebesgue measure ν,[1] has a density ρ with respect to ν, $\mu(U) = \int_U \rho \mathrm{d}\nu$. We write *acim* for an absolutely continuous (with respect to ν) invariant measure and *acip* if the measure is, moreover, a probability measure.

2.2.3.3 Lyapunov exponents

In the geometric approach we introduced the local stability analysis of fixed and periodic points, cf. Theorem 2.2. *Lyapunov exponents* generalize the idea of eigenvalues (of a local linearization) to give *averaged* contraction and expansion rates along a general orbit, i.e. an orbit which need not be a fixed or periodic point. At each point $x(t)$ of a (forward) orbit $(x(t))_{t\geqslant 0}$ these contraction and expansion rates are measured along n orthogonal directions and given by the singular values of the Jacobian $J(t) = \mathrm{D}\Psi^t|_{x(0)}$, i.e. by the eigenvalues of $\left(J(t)J(t)^\top\right)^{1/2}$. The Lyapunov exponents at $x(0)$ are defined as the logarithms of the eigenvalues of the matrix

$$\Lambda := \lim_{t\to\infty} \left(J(t)J(t)^\top\right)^{1/(2t)}, \tag{2.5}$$

provided this limit exists. Given an invariant measure μ for Ψ, the *multiplicative ergodic theorem*, see e.g. Ruelle [1979], guarantees existence of this limit for μ-almost all $x(0)$ if $\mathrm{D}\Psi$ is Hölder continuous.

2.2.4 Maps on the interval

We now describe discrete dynamical systems induced by maps on the interval from a statistical point of view. Hence, we still consider the time-discrete dynamical system from (2.2) but now in the special case where Ψ is an endomorphism of a real interval $I = [\alpha, \beta] \subset \mathbb{R}$. For a comprehensive treatment of this topic, see the books by Collet and Eckman [1980] as well as by De Melo and van Strien [1993] or the review by Thunberg [2001]. In the following, we often refer to attractors, orbits, etc. of system (2.2) as attractors, orbits, etc. of the map Ψ.

[1] This means that $\nu(A) = 0$ implies $\mu(A) = 0$.

2.2.4.1 The logistic equation

A famous representative of this class of dynamical systems is the family of *logistic equations*

$$\Psi_b(x) = bx(1-x) \ ,$$

$0 \leqslant b \leqslant 4$, $I = [0,1]$. It is frequently referred to as an archetypal example of how complex dynamical behavior can arise from simple nonlinear equations. The map was introduced by the biologist Robert May [1976] as a discrete-time demographic model. The $x(t)$ represent populations at years $t = 0, 1, 2, \ldots$. In particular, $x(0)$ represents the initial population at year 0. The parameter b is a positive number, and represents a net rate for reproduction and starvation. The logistic equation captures two effects: First, reproduction with a rate proportional to the size of the current population when the latter is small. Second, starvation with a rate proportional to the "carrying capacity" of the environment less the current population when the latter is large.

Let us begin with the phenomenology of the logistic equation as discussed e.g. by Thunberg [2001]. It is best visualized in the *bifurcation diagram* shown in upper Figures 2.2A and B. Here, the value of $0 \leqslant b \leqslant 4$ is plotted against the attractor A_b of

$$x(t+1) = \Psi_b\left(x(t)\right) \ , \tag{2.6}$$

which is obtained numerically, see figure caption for technical details. We observe what has entered folklore by now as the *period-doubling route to chaos*. For $0 \leqslant b < 3$ system (2.6) has a stable fixed point as unique attractor, zero if $b \leqslant 1$. For $b = 3$ this fixed point becomes *critical* and *bifurcates* into a stable periodic attractor of length two. This is called a *pitchfork bifurcation* or a *period-doubling bifurcation*. At $b = 1 + \sqrt{6}$ a further period-doubling bifurcation occurs as the stable 2-periodic attractor becomes critical and bifurcates into a 4-periodic attractor. This process is repeated leading to 2^q-periodic attractors, $q = 0, 1, 2, \ldots$. The sequence of parameter values $(b_q)_{q \geqslant 0}$ at which the bifurcations occur accumulates at $b_\infty \approx 3.57$ with a geometric rate equal to the *Feigenbaum constant* (≈ 4.669).

The parameter b_∞ is also called the *on-set of chaos*, which we, for now, informally define as an irregular, aperiodic behavior where trajectories show a high sensitivity to initial conditions. Beyond b_∞ we detect windows of periodicity, i.e. intervals $[b'_0, b'_\infty]$,

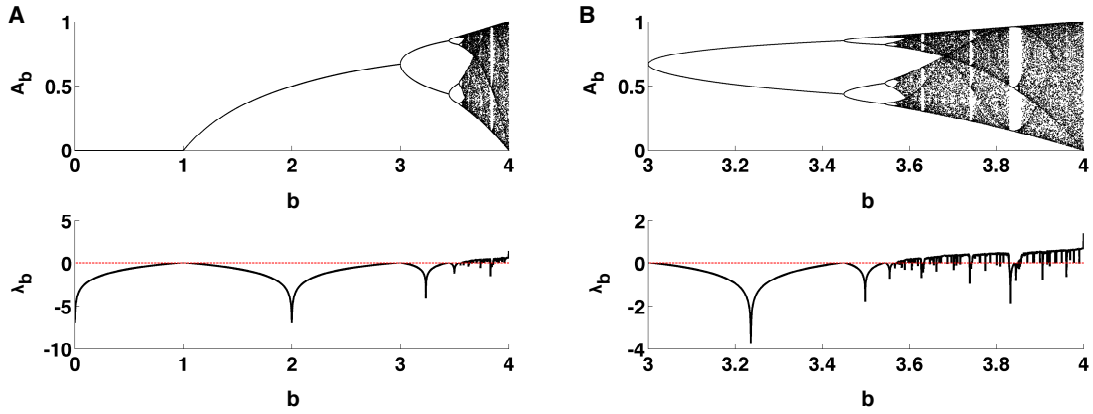

Figure 2.2: The upper figures show the bifurcation diagram of the logistic equation (2.6). The attractor A_b of (2.6) is plotted against **(A)** $0 \leqslant b \leqslant 4$ and **(B)** $3 \leqslant b \leqslant 4$. The attractors were found by iterating (2.6) 10^6 times and plotting the subsequent 10^2 iterations. In the lower figures the corresponding Lyapunov exponents λ_b from (2.7) are plotted against b. They were obtained by averaging over 10^3 iterations (after the burn-in).

where a τ-periodic attractor comes into being as b passes b'_0, and period-doubling bifurcations to $\tau \cdot 2^q$-cycles occur as b reaches certain b'_q. The sequence $\left(b'_q\right)_{q \geqslant 0}$ accumulates again at some finite b'_∞ with an asymptotic geometric rate equal to the Feigenbaum constant. It can be shown [Thunberg, 2001] that there are countably infinitely many of these intervals $[b'_0, b'_\infty]$ and that they are dense in $[0, 4]$. Admittedly, this does not agree with our visual impression from upper Figures 2.2A and B, as here it seems that for b close to 4 no periodic orbits occur any more. This, however, is due to the fact that the system was evaluated at values of b on a grid in $[0, 4]$. For higher resolutions periodic windows would appear in every arbitrarily small interval. Still, although periodicity is predominant in a topological sense, chaotic behavior occurs for a parameter set of positive Lebesgue measure.

2.2.4.2 S-unimodal maps

So far, our description of the logistic equation was rather informal. In particular, we took it for granted that there is only one attractor for each parameter value b. We also did not describe the structure of the attractors other than the stable periodic orbits. Let us now back up the above phenomenological description by rigorous mathematical results. We will do so in a more general context. In fact, the behavior which we just

delineated is not specific to the logistic equation, but the generic behavior of a large class of maps, the so-called *S-unimodal* functions. In chapter 5 we will make use of this theory, which we now outline in the remainder of this section.

Let $I = [\alpha, \beta] \subset \mathbb{R}$ again be an interval. Before defining the class of S-unimodal functions, let us introduce and discuss their crucial properties. A first important property of an S-unimodal function Ψ is that its *Schwarzian derivative*

$$\mathrm{S}\,\Psi = \frac{\Psi'''}{\Psi'} - \frac{3}{2}\left(\frac{\Psi''}{\Psi'}\right)^2 ,$$

where defined, is negative. We recall that the Schwarzian derivative satisfies the following chain rule.

Proposition 2.2 (chain rule of the Schwarzian derivative)**.** *Let $\Theta, \Psi \in \mathcal{C}^3(I)$. Then*

$$\mathrm{S}(\Theta \circ \Psi)(x) = \mathrm{S}\,\Theta\,(\Psi(x)) \cdot \Psi'(x)^2 + \mathrm{S}\,\Psi(x)$$

for $x \in I$.

The importance of a negative Schwarzian derivative for the dynamics of iterations was realized by David Singer [1978], who proved

Theorem 2.4 (Singer [1978])**.** *If γ is a stable periodic orbit of a function $\Psi : I \to I$ with negative Schwarzian derivative, then at least one local extremum of Ψ, i.e. a critical point of Ψ or an endpoint of I, approaches γ under the iteration Ψ.*

Before turning our attention to the intricate dynamics of S-unimodal functions, let us take care of two rather uninteresting cases, that will nonetheless be needed below.

Lemma 2.2. *1. If a continuous function $\Psi : I \to I$ with unique fixed point $x^{(f)}$ is monotonously increasing on at least $\left[\alpha, x^{(f)}\right]$ or at least $\left[x^{(f)}, \beta\right]$, then $x^{(f)}$ is a globally attracting fixed point.*

2. If $\Psi : I \to I$ is a monotonously decreasing $\mathcal{C}^3$ function with negative Schwarzian derivative, then Ψ has a global attractor, which is either a fixed point or a 2-cycle.

Proof. We show the first claim in the case that Ψ is increasing on $\left[\alpha, x^{(f)}\right]$. Observe that $\Psi(x) > x$ for all $x \in \left[\alpha, x^{(f)}\right)$ and $\Psi(x) < x$ for all $x \in \left(x^{(f)}, \beta\right]$. The fixed point attracts $\left[\alpha, x^{(f)}\right]$, as each trajectory starting in this interval is increasing and bounded from above by $x^{(f)}$ and, thus, converges to what has to be $x^{(f)}$. A trajectory starting in $\left(x^{(f)}, \beta\right]$ either stays in this interval or travels into $\left[\alpha, x^{(f)}\right]$. The latter case has

already been taken care of. In the first case, the trajectory is decreasing and bounded from below by $x^{(f)}$ and, thus, converges to what has to be $x^{(f)}$.

Now assume a situation as in the second claim. Observe that Ψ^2 is monotonously increasing. Hence, for $x \in I$ the sequences $\left(\Psi^{2t}(x)\right)_{t\geqslant 0}$ and $\left(\Psi^{2t+1}(x)\right)_{t\geqslant 0}$ are monotonous as well as bounded and thus converge to x^{even} and x^{odd}, respectively. Graphically, the trajectory of x either spirals out and approaches a 2-cycle or spirals in and approaches a 2-cycle or a fixed point. In each case, the ω-limit set $\omega(x) = \left\{x^{\text{even}}, x^{\text{odd}}\right\}$ attracts all points between x and x^{even} and all points between $\Psi(x)$ and x^{odd}. Thus, all attractors of Ψ are either fixed points or periodic attractors of length 2. By Theorem 2.4 there can be at most two such attractors as each of them attracts either of the endpoints of I. The attractor of α attracts all of $[\alpha, \Psi(\alpha)]$. Since $\Psi(\beta) < \Psi(\alpha)$ both endpoints are attracted by the same attractor. □

The second crucial property of S-unimodal functions is that they possess exactly one "hump." This "hump" is a critical point usually assumed to be a maximum. It needs to be *non-degenerate*, i.e. a critical point with non-vanishing second derivative. Sometimes such a point is also called *quadratic* critical point.

Let us now formally define the class of S-unimodal functions.

Definition 2.5 (S-unimodal function)**.** A function $\Psi : I \to I$ is called *S-unimodal* if it satisfies the following.

(S1) Ψ is a $\mathcal{C}^3$ function. The Schwarzian derivative $\mathrm{S}\,\Psi$, where defined, is negative.

(S2) Ψ possesses a unique non-degenerate maximum $x^{(c)} \in (\alpha, \beta)$, $\Psi''\left(x^{(c)}\right) \neq 0$, and $\Psi'(x) \neq 0$ for all $x \neq x^{(c)}$. Ψ is strictly increasing on $\left[\alpha, x^{(c)}\right)$ and strictly decreasing on $\left(x^{(c)}, \beta\right]$.

(S3) $\Psi\left(x^{(c)}\right) = \beta$ and $\Psi^2\left(x^{(c)}\right) = \alpha$.

As already mentioned, the crucial properties are (S1) and (S2). According to Theorem 2.4 they imply that an S-unimodal function possesses at most three stable periodic attractors. One commonly assumes some additional technical condition on the boundaries of I in order to guarantee uniqueness of the attractor. We choose (S3), which is a popular choice (cf. e.g. Thunberg [2001]) but by no means the only possibility.

Remark 2.3. It can easily be seen that any quadratic function has negative Schwarzian derivative. In particular, the maps Ψ_b from the logistic equation (2.6) are S-unimodal functions.

The following Theorem gives a characterization of the possible attractors of S-unimodal maps.

Theorem 2.5 (Blokh and Lyubich [1991])**.** *An S-unimodal function $\Psi : I \to I$ has a unqiue attractor A, such that $\omega(x) = A$ for Lebesgue-almost all $x \in I$. The attractor A is one of the following types:*

1. *an asymptotically stable periodic orbit,*
2. *a Cantor set of measure zero,*
3. *a finite union of intervals with a dense orbit.*

In the first two cases, A is the Omega-limit set of the critical point, $A = \omega\left(x^{(c)}\right)$.

2.2.4.3 Formal definitions of chaos

We already described the "period-doubling route to chaos" of the logistic equation and informally introduced *chaos* as irregular, aperiodic behavior where trajectories show a high sensitivity to initial conditions. Unfortunately, there is no generally accepted formal definition of chaos. One possibility is to define a dynamical system as chaotic if it admits an acip. The following proposition (cf. e.g. Thunberg [2001], Theorem 9) shows that, according to this criterion, chaotic behavior of S-unimodal functions can only take place on interval attractors.

Proposition 2.3. *Let $\Psi : I \to I$ be an S-unimodal map. If Ψ has a periodic attractor, or a Cantor attractor, then Ψ admits a unique natural measure supported on the attractor. If Ψ admits an acip μ, then μ is a natural measure and the attractor A of Ψ is an interval attractor. In both cases, the natural measure describes the distribution for almost all initial conditions.*

Another way to define chaos is via *Lyapunov exponents*. As already explained, they measure the rate of contraction or expansion along an orbit $(x(t))_{t\geqslant 0}$ and are defined as the logarithms of the eigenvalues of matrix Λ from (2.5), provided the defining limit exists. For maps on the interval, this definition simplifies and the Lyapunov exponent at $x(0)$ is given by

$$\lambda\left(x(0)\right) = \lim_{t\to\infty} \frac{1}{t} \sum_{\tau=0}^{t-1} \ln\left|\Psi'\left(x(\tau)\right)\right| \ . \tag{2.7}$$

With respect to the existence of $\lambda\left(x(0)\right)$ and the dependence on $x(0)$ we have the following result.

Proposition 2.4 (Keller [1990]). *The Lyapunov exponent* $\lambda(x(0))$ *from* (2.7) *exists for Lebesgue-almost all* $x(0)$ *if* Ψ *is S-unimodal. In this case,* $\lambda = \lambda(x(0))$ *is identical for almost all* $x(0)$.

This allows us to define the dynamical system induced by Ψ as chaotic if λ is positive (for almost all initial conditions).

We have given two possible formal definitions of chaos. Luckily, one can prove that for S-unimodal maps they are equivalent.

Theorem 2.6 (Keller [1990]). *Let* $\Psi : I \to I$ *be an S-unimodal map. Then* Ψ *admits an acip if and only if the Lyapunov exponent* $\lambda = \lambda(x(0))$ *from* (2.7) *is positive (for Lebesgue-almost all* $x(0) \in I$*). If* λ *is negative, then* Ψ *has a periodic attractor.*

We now come back to the example of the logistic equation from the beginning of this section for a visualization of these results. Lower Figures 2.2A and B show the Lyapunov exponents λ_b of the logistic equation (2.6). We observe $\lambda_b \leqslant 0$ in the periodic windows and $\lambda_b = 0$ at each bifurcation value of b.

A further possible criterion for chaos is the sensitive dependence on initial conditions defined by Guckenheimer [1979].

Definition 2.6 (sensitive dependence, Guckenheimer [1979]). A map Ψ exhibits a *sensitive dependence on initial conditions*, if there is a set $\mathfrak{I} \subset I$ of positive measure and an $\epsilon > 0$ such that for any $x \in \mathfrak{I}$ and any neighborhood U of x, there is $x' \in U$ and a $t_0 \geqslant 0$ with $d\left(\Psi^{t_0}(x), \Psi^{t_0}(x')\right) > \epsilon$.

For general (not necessarily S-unimodal) Ψ, it is often assumed that this kind of sensitive dependence on initial conditions is equivalent to Ψ having positive Lyapunov exponents. In Demir and Koçak [2001] two examples are given showing that this is, in general, wrong. We may have sensitive dependence and negative Lyapunov exponents, as well as positive Lyapunov exponents and no sensitive dependence. For S-unimodal maps Ψ, however, the following result holds.

Theorem 2.7 (Guckenheimer [1979]). *An S-unimodal map* Ψ *with a periodic attractor does not have sensitive dependence on initial conditions. An S-unimodal map* Ψ *with an interval attractor has sensitive dependence on initial conditions.*

Note that the interval attractor in the claim of Theorem 2.7 need not necessarily support an acip. Thus, for an S-unimodal map, sensitive dependence on initial conditions is a weaker requirement than having positive Lyapunov exponent or, equivalently, admitting an acip.

2.2.4.4 Families of S-unimodal maps

We finally turn our attention to parametrized families of S-unimodal maps, such as the family of logistic equations from (2.6). A natural question is how the three possible attractor types from Theorem 2.5 are distributed over the parameter space. The following theorem shows that the second type (Cantor set) appears only for a measure zero set of parameter values.

Theorem 2.8 (Avila et al. [2003][1])**.** *Let $\{\Psi_b\}_{b\in U}$, $U \subset \mathbb{R}$, be an analytic family of S-unimodal functions $\Psi_b : I \to I$. Then, for Lebesgue-almost all parameter values $b \in U$ the map Ψ_b has either a periodic attractor or an interval attractor supporting an acip.*

Remark 2.4. We conclude that in the situation of Theorem 2.8 there is, essentially, a dichotomy: Either an S-unimodal map Ψ_b has a unique stable periodic attractor and no sensitive dependence on initial conditions, or it has an interval attractor with positive Lyapunov exponent supporting an acip and sensitive dependence on initial conditions. We refer to the latter case as chaos.

2.3 Prerequisites from Boolean logic

The modern formalization of mathematical logic was founded by George Boole, a self-educated English mathematician. He introduced his algebraic formalization of logic at first in a minor publication, "The Mathematical Analysis of Logic", which he extended to his more substantial book "The Laws of Thought" [Boole, 1854]. For a modern treatment of the topic, see e.g. the introduction by Givant and Halmos [2009]. Here, a *Boolean algebra* is defined as follows.

Definition 2.7 (Boolean algebra)**.** A *Boolean algebra* is a tuple $(X, \wedge, \vee, \neg, 0, 1)$ consisting of a set X, two binary operations $\wedge$ (AND, *conjunction*) and $\vee$ (OR, *disjunction*), a unary operation $\neg$ (*complement*, *negation*), and two distinct elements 0 and 1, such that the following hold for $x, y, z \in X$.

[1] In Avila et al. [2003] this theorem is proven for the class of quasiquadratic mappings. As discussed ibidem this class contains the S-unimodal functions.

Associativity: $x \vee (y \vee z) = (x \vee y) \vee z$ and $x \wedge (y \wedge z) = (x \wedge y) \wedge z$.

Commutativity: $x \vee y = y \vee x$ and $x \wedge y = y \wedge x$.

Absorption: $x \vee (x \wedge y) = x$ and $x \wedge (x \vee y) = x$.

Distributivity: $x \wedge (y \vee z) = (x \wedge y) \vee (x \wedge z)$.

Complements: $x \vee \neg x = 1$ and $x \wedge \neg x = 0$.

In other words, a Boolean algebra is a complemented distributive lattice.

The two complement-axioms are sometimes also called *"The law of the excluded middle"* and *"The law of noncontradiction."* Together with *"The law of identity"* they make up the classic *Aristotelian laws of thought*. The above irredundant axioms imply

Proposition 2.5 (laws from Boolean algebra)**.** *For elements x, y, z of a Boolean algebra it holds:*

second distributive law: $x \vee (y \wedge z) = (x \vee y) \wedge (x \vee z)$.

Idempotency: $x \wedge x = x$ *and* $x \vee x = x$.

Neutral elements: $x \wedge 1 = x$ *and* $x \vee 0 = x$.

Extremal elements: $x \wedge 0 = 0$ *and* $x \vee 1 = 1$.

Involution: $\neg(\neg x) = x$.

De Morgan's Laws: $\neg(x \wedge y) = \neg x \vee \neg y$ *and* $\neg(x \vee y) = \neg x \wedge \neg y$.

Duality: $\neg 0 = 1$ *and* $\neg 1 = 0$.

In any Boolean algebra the two binary operations $\wedge$ and $\vee$ are dual under the De Morgan's Laws.

Example 2.4. In this thesis, we typically work with the simplest Boolean algebra. It is the generic set with two elements $\{0, 1\}$, and the operators $\wedge$, $\vee$ and $\neg$ are defined as in Table 2.1. We like to refer to the values 0 and 1 as "false" and "true" or "off" and "on." In biological applications we may interpret them, more meaningfully, as "inactive" and "active", or "not expressed" and "expressed."

Table 2.1: Truth-tables of the Boolean operators $\neg$ (negation), $\wedge$ (conjunction), and $\vee$ (disjunction).

$\neg x$	$x=0$	$x=1$
	1	0

$x \wedge y$	$x=0$	$x=1$
$y=0$	0	0
$y=1$	0	1

$x \vee y$	$x=0$	$x=1$
$y=0$	0	1
$y=1$	1	1

The set $\{0,1\}$ together with the operators $\wedge$, $\vee$, and $\neg$ from Table 2.1 is probably the best-known and most widely used, but by no means the only Boolean algebra. The power set of any non-empty set, for instance, forms a Boolean algebra with "intersection" and "union" as the two binary operations $\wedge$ and $\vee$, respectively, and "complement" as the unary operator $\neg$. The 0-element is the empty set and the 1-element is the set itself.

Propositional variables, Boolean functions, and their representations

Let X be the Boolean algebra from Example 2.4. We call a variable x taking values in X a *propositional variable*. A *literal* is a propositional variable or its negation. *Disjunctive* or *conjunctive clauses* are disjunctions or conjunctions of literals.

A K-variate *Boolean function* in the propositional variables $x_1, x_2, \ldots, x_K$ is a function mapping from X^K into X. We say f is monotonously increasing (decreasing) in the k-th input, if

$$f(x_1, \ldots, x_{k-1}, 0, x_{k+1}, \ldots, x_K) \leqslant (\geqslant) f(x_1, \ldots, x_{k-1}, 1, x_{k+1}, \ldots, x_K)$$

for all $x_1, \ldots, x_{k-1}, x_{k+1}, \ldots, x_K \in X$. The function f is called *monotonous* if it is either monotonously increasing or decreasing in every input variable. Note that we specifically exclude the cases where a function is both, monotonously increasing and decreasing, in one of its inputs. This, however, is no severe restriction as the function would be independent of such an input and we could simply cancel it out.

An input x_k of a (not necessarily monotonous) Boolean function f is called *canalyzing* if there exist $\xi_i, \xi_o \in X$ such that $x_k = \xi_i$ implies $f(x_1, x_2, \ldots, x_K) = \xi_o$. This is to say that the other inputs are relevant only if $x_k \neq \xi_i$. A Boolean function f admitting a canalyzing input is called *canalyzing* function [Harris et al., 2002].

The simplest representation of a Boolean function f is its *truth-table*, a table with two columns listing all 2^K possible inputs and the corresponding output values of f. It is often beneficial to rearrange the table, e.g. as a K-dimensional cube. A particular clever way of visualizing truth-tables are *Karnaugh-Veitch maps* [Karnaugh, 1953; Veitch, 1952]; we will demonstrate their use and usefulness in chapter 6.

There is no unique way of expressing f as a propositional formula in its inputs $x_1, x_2, \ldots, x_K$. The expression

$$f(x_1, \ldots, x_K) = \bigvee_{(\xi_1,\ldots,\xi_K) \in X^K | f(\xi_1,\ldots,\xi_K)=1} \left[\left(\bigwedge_{k|\xi_k=1} x_k \right) \wedge \left(\bigwedge_{k|\xi_k=0} \neg x_k \right) \right] \tag{2.8}$$

is called the *full disjunctive normal form* of f. The outer disjunction runs over all *true*-entries of the truth-table of f. In general, any representation of f as a disjunction of conjunctive clauses is called *disjunctive normal form* (DNF). The dual representation as a conjunction of disjunctive clauses is called *conjunctive normal form* (CNF). Here, "dual" means duality under the De Morgan's Laws.

2.4 Prerequisites from molecular biology

Before introducing Kauffman's Boolean models of gene regulation in chapter 3, we wish to briefly discuss their biological background (section 2.4.1); for details we refer the reader to any textbook on molecular biology, e.g. the one by Lodish and Berk [2008]. The reader is also encouraged to consult the glossary on page xix as well as Figure 2.3 for a visualization of the following explanations. In section 2.4.2, we then introduce the biological example that we will be discussing in chapter 6.

2.4.1 Gene expression and its regulation

All information required for the development and functioning of a living organism is stored in its *DNA*, which can be thought of as a long sequence of letters. Almost all cells of the organism contain a complete copy of its DNA. *Genes* are the functional subunits of this DNA.

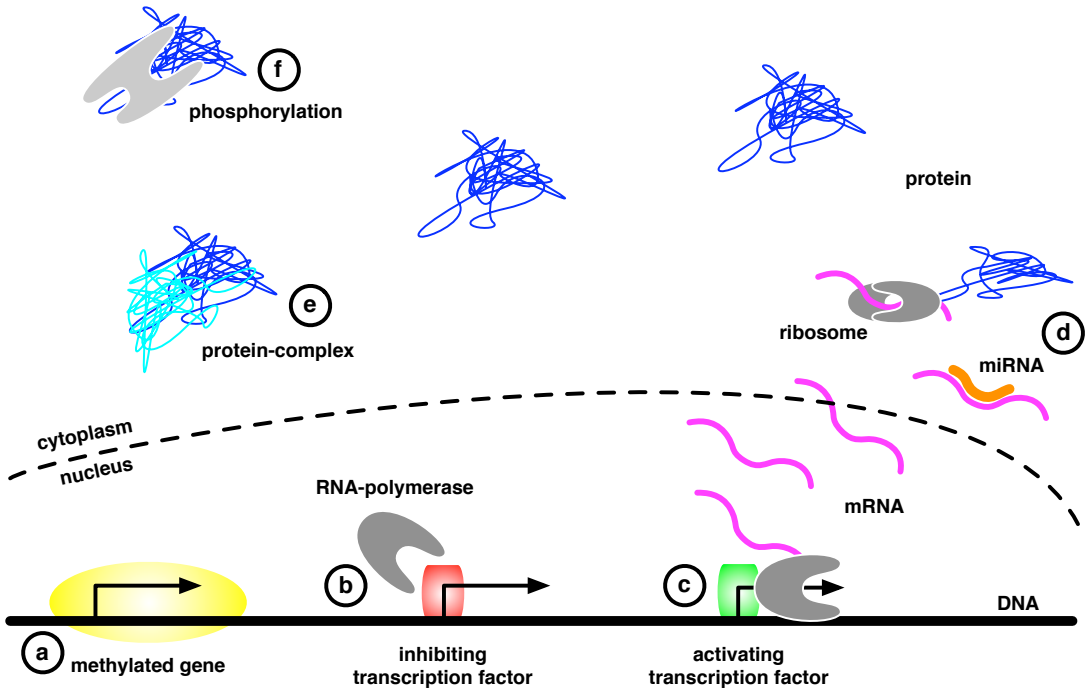

Figure 2.3: Schematic visualization of the process of gene expression. The following regulatory mechanisms are shown: **(a)** A methylation prevents the transcription of a gene. **(b)** An inhibiting transcription factor blocks the promotor of a gene and prevents the RNA-polymerase from attaching. **(c)** An activating transcription factor recruits the RNA-polymerase and promotes the transcription of a gene. **(d)** A miRNA binds to a complementary mRNA and prevents its translation into protein. **(e)** Protein-complex formation. **(f)** Activation of protein by phosphorylation.

2.4.1.1 Gene expression

In principle, the *expression of a gene* works as follows. The piece of DNA encoding for the gene is copied in a process called *transcription* and an *RNA transcript* is assembled by an enzyme called *RNA-polymerase*. In some cases, these RNAs are (after some additional processing) already the final gene products. Examples for this are *ribosomal RNAs* (rRNA), *transfer RNAs* (tRNA) or *non-coding RNAs* (ncRNA) such as *microRNAs* (miRNA); we will discuss these RNA types in the course of this section.

When talking about genes, however, one typically refers to *protein-coding* genes. Here, the RNA transcript is called *messenger RNA* (mRNA) and is used as a blueprint for protein synthesis. This process is carried out by cell organelles called *ribosoms*. These are macromolecules consisting *inter alia* of the already mentioned rRNAs. The *translation* of mRNA into protein occurs according to specific rules, the so-called *genetic code*, which are executed by the tRNAs mentioned above. After synthesis, proteins often require other proteins for being functional. Either, they are active only as part of a *protein-complex*, or they need to be activated by enzymes through modifications such as *phosphorylation*.

We now address two questions:

1. Why does a cell need to control its gene expression?
2. What are the possible regulatory mechanisms controlling the expression of genes and the functionality of their products?

2.4.1.2 The need for control

In order to reproduce, multi-cellular organisms need to regenerate an entire organism from a single fertilized egg cell. During this process, the cells of an embryo need not only divide and grow, but also need to become specified and must differentiate into all cell types of the organism in a precise spatio-temporal order. This *differentiation* of *embryonic stem cells* is possible only because cells can accurately and specifically express genes which determine their cell-fates. We will study an aspect of this process in vertebrates in chapter 6, cf. also section 2.4.2. Similarly, in the adult organism, gene regulation guarantees and mediates the life-long supply of cells from *adult stem cells*.

The *immune system* in higher organisms relies on cells which are able to detect potentially harmful antigens and subsequently re-arrange their gene expression enabling

them to destroy pathogens. More generally, by adapting their gene expression cells and whole organisms can react to all kinds of external influences, such as starvation, physical exercise or exposure to sunlight and the ensuing DNA damage.

2.4.1.3 Regulatory mechanisms

Regulation takes place on every level of the process of gene expression described above. The letters (a)–(f) in the following list of possible regulatory mechanisms indicate the positions in Figure 2.3 where the respective mechanisms are visualized.

- First of all, the location of a gene on the DNA needs to be accessible to the RNA-polymerase. This access can be hindered, for example, by *epigenetic modifications* such as *methylation* of DNA (a).

- The RNA-polymerase initially binds to a region upstream of the actual coding region of a gene called *promotor*. This recruitment and the subsequent transcription of DNA can be hindered (b) as well as enhanced (c) by the binding of so-called *transcription factors* to the promotor. These transcription factors are proteins and as such products of other genes. This regulatory mechanism is called *transcriptional control* and the entirety of all such regulatory dependencies between genes is called the *(transcriptional) gene regulatory network*.

- The above-mentioned miRNAs regulate gene expression *post-transcriptionally*. They bind to mRNA transcripts, promote their degradation and prevent their translation into protein (d). In a broader sense, the interactions between miRNA genes and other genes are also part of the gene regulatory network.

- Protein-complex formations (e) and modifications of proteins by other proteins, such as phosphorylations (f), are called *protein-protein-interactions* and typically not considered part of the gene regulatory network. Still, protein-protein-interactions are as essential for proper cell functioning as (post-)transcriptional control.

2.4.2 Gene regulation during neural development

In chapter 6, we will consider a small-scale example of a specific regulatory process in order to illustrate further possible extensions of Boolean models. Let us now briefly introduce this biological system.

During vertebrate development, the central nervous system arises from a precursor tissue called *neural plate*. Shortly after gastrulation this neural plate is patterned along the anterior-posterior axis into four regions, which continue to develop into *forebrain*, *midbrain*, *hindbrain* and *spinal cord*. This patterning is determined by a well-defined and locally restricted expression of genes as well as by the action of short- and long-range *signaling centers*, also called *secondary organizers* [Echevarria et al., 2003]. These secondary organizers are collections of cells emitting molecular signals which govern the specification of adjacent brain regions.

The development of mid- and hindbrain, for example, is controlled by the activity of such a secondary organizer. It is called the *isthmic organizer* (IsO) and located at the boundary between the prospective mid- and hindbrain, the so-called *mid-hindbrain boundary* (MHB). The two key molecular signals emanating from the IsO are secreted Fgf8 and Wnt1 proteins.

Concomitantly with the patterning along the anterior-posterior axis, the neural plate rolls up and forms the *neural tube*. Before embryonic day 9.0 (E9.0) we prefer to talk about the neural plate, after this point in time we speak of the neural tube. The neural tube is also patterned along the dorsal-ventral axis into four segments called *floor plate*, *basal plate*, *alar plate* and *roof plate*. For a (highly schematic) visualization of the three-dimensional patterning of the neural tube, see Figure 2.4A. The patterning into the four plates is well understood and, for this reason, not treated in this thesis. We only remark that a gene called *Shh*, which is expressed *inter alia* in the floor plate, can be used as an indicator of the ventral direction. This will be of use in chapter 6 for the correct interpretation of Figure 6.3.

The IsO is characterized by the localized expression of several transcription and secreted factors. In here, we focus on the following eight IsO genes: *Otx2*, *Gbx2*, *Fgf8*, *Wnt1*, the *Engrailed* genes *En1* and *En2*, which we subsume under the identifier *En*, as well as the *Pax* genes *Pax2* and *Pax5*, which we subsume under the identifier *Pax*. Our analysis is based on these gene's equilibrium expression pattern at E10.5, which

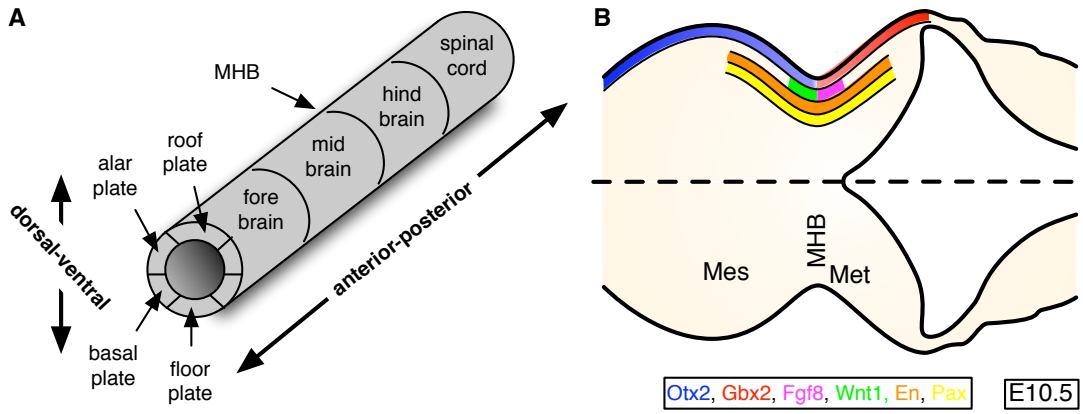

Figure 2.4: **(A)** Patterning of the neural tube (highly schematic) along the anterior-posterior axis into forebrain, midbrain, hindbrain, and spinal cord as well as along the dorsal-ventral axis into floor plate, basal plate, alar plate, and roof plate. **(B)** Dorsal close-up view of the MHB region in the anterior neural tube of an E10.5 mouse embryo, anterior to the left. Colored regions indicate the equilibrium expression domains of the (groups of) IsO genes *Otx2*, *Gbx2*, *Fgf8*, *Wnt1*, *En*, and *Pax*. Abbreviations: Mes, mesencephalon (midbrain); MHB, mid-hindbrain boundary; Met, metencephalon (hindbrain).

is displayed schematically in Figure 2.4B. This expression pattern was derived from various *in situ* hybridization experiments, for a review see e.g. Wurst and Bally-Cuif [2001], in particular, Figure 1c therein.

The initial expression of *Otx2* and *Gbx2* in the anterior and posterior neural plate, respectively, defines the position of the prospective fore-/midbrain (*Otx2*+/*Gbx2*–) and hindbrain/spinal cord (*Otx2*–/*Gbx2*+), respectively [Acampora et al., 1997; Wassarman et al., 1997]. The position of the MHB is set at the expression interface of these two transcription factors [Broccoli et al., 1999; Li et al., 2005; Millet et al., 1999]. Subsequently, expression of *Wnt1* at the rostral border of the MHB in the caudal midbrain, and of *Fgf8* at the caudal border of the MHB in the rostral hindbrain is initiated independently of a requirement of *Otx2* and *Gbx2* for this process [Li and Joyner, 2001; Martinez-Barbera et al., 2001]. Fgf8 plays a pivotal role in IsO patterning activity [Chi et al., 2003; Lee et al., 1997], and Wnt1 regulates midbrain development and is required for the maintenance of the MHB [McMahon et al., 1990; Thomas and Capecchi, 1990].

The *Engrailed* genes *En1* and *En2* are both expressed across the boundary [Davis et al., 1988], yet their expression domains are not fully equivalent. They have been

shown to be targets of *Wnt1* in the midbrain [Danielian and McMahon, 1996] and to regulate the expression of *Fgf8* [Gemel et al., 1999]. Similarly to *Engrailed*, *Pax5* is also expressed across the boundary [Rowitch and McMahon, 1995], whereas expression of *Pax2* is restricted to the caudal part of the isthmic organizer [Bouchard et al., 2000]. Analysis of *Pax2*-deficient embryos [Ye et al., 2001] has suggested an essential role of *Pax2* for the induction of *Fgf8*. In short, it has been demonstrated that by E10.5 these genes have become interdependent and form the core module of a regulatory network that guarantees the stable maintenance of their specific expression patterns [Wurst and Bally-Cuif, 2001].

Although a great deal of experimental effort has been made, this regulatory network is not yet understood in full detail. In chapter 6, we show that a data-based inference of Boolean models yields new insights into gene regulation at the MHB and can be used to design validation experiments.

3

Boolean models and Kauffman networks

To be, Or not to be.

Hamlet, William Shakespeare

This thesis is about models of gene regulatory networks. However, we do not attempt to model all the different levels of control, which we described in section 2.4.1.3, in mechanistic detail. Rather, we consider an abstraction and simplification thereof. In the models we introduce in this chapter, we normally do not distinguish between DNA, RNAs and proteins. Rather, variables may represent any biological entity. Their states are not described by concentrations or actual molecule numbers, but by two abstract categories whose interpretation may vary between different variables. We, therefore, like to speak of generic categories, such as "true" and "false", "on" and "off", or "is" and "is not." Thus, the models describe the complex system of gene regulation in terms of classic Shakespearean choices. These choices are not based on any kinetic or biophysical laws. Instead the state of a variable is determined by an abstract combination

of inputs from some of the other variables.

3.1 Boolean models

In this section, we introduce Boolean models of gene regulation. We will do so from a network perspective. So, let $G = (V, E)$ denote a (directed) graph of order N with nodes $V = \{1, 2, \ldots, N\}$ and edges $(i' \to i) \in E \subset V \times V$. The predecessors (inputs) of a node i are denoted by $i_1 < i_2 < \cdots < i_{K_i}$, where K_i is the node's in-degree. We straightaway make

Definition 3.1 (Boolean model)**.** A *Boolean model* (BM) is a tuple $(G, \mathbf{f})$ consisting of a graph G and a vector of Boolean functions $\mathbf{f} = (f_i)_{i=1}^N$, $f_i : \{0,1\}^{K_i} \to \{0,1\}$. The Boolean function f_i is called *update rule* or *update function* of node i and the vector of update rules $\mathbf{f}$ (as a function from $\{0,1\}^N \to \{0,1\}^N$) is called *transfer function* of the Boolean model.

Remark 3.1. Each BM $(G, \mathbf{f})$ gives rise to a time-discrete dynamical system as follows: To each node i we associate a time-dependent discrete variable $x_i(t) \in \{0,1\}$, $\mathbf{x}(t) = (x_i(t))_{i=1}^N$. The evolution of $\mathbf{x}(t)$ is determined by the iteration

$$\mathbf{x}(t+1) = \mathbf{f}\left(\mathbf{x}(t)\right) \ , \quad t = 0, 1, 2, \ldots \ ,$$

where the i-th component is given by

$$x_i(t+1) = f_i\left(x_{i_1}(t), x_{i_2}(t), \ldots, x_{i_{K_i}}(t)\right) \ . \tag{3.1}$$

In this thesis, we only consider the above synchronous updating, for different update policies, see e.g. Chavez et al. [2005], Fauré et al. [2006] and Greil et al. [2007].

In the following, we will refer to trajectories of the dynamical system from Remark 3.1 as *trajectories of the BM* $(G, \mathbf{f})$.

The state-space of the dynamical system from Remark 3.1 is the discrete, finite set $X = \{0,1\}^N$. We turn it into a metric space by defining the *Hamming distance* d of $\mathbf{x} = (x_i)_{i=1}^N \in X$ and $\mathbf{x}' = (x_i')_{i=1}^N \in X$ as

$$d\left(\mathbf{x}, \mathbf{x}'\right) = \frac{1}{N} \sum_{i=1}^{N} \left(1 - \delta_{x_i, x_i'}\right) \ ,$$

where $\delta_{x_i, x_i'}$ is the *Kronecker* symbol. As measure we simply use the counting measure. Due to the finite state-space we can then easily characterize the ω-limit sets and attractors.

Proposition 3.1. *Consider the dynamical system defined in Remark 3.1. The ω-limit set of each point is either a fixed point or a periodic orbit. The same is true for the attractors of the dynamical system.*

Dynamical systems induced by BMs are, arguably, the simplest kind of dynamical systems one can think of. They are time-discrete and, in addition, restrict their variables to the smallest non-trivial set of values $\{0, 1\}$. Still, they exhibit interesting dynamics as we shall see in the course of this thesis.

The update rules of BMs are often specified in terms of logical expressions. The inputs of an update rule $f_i : \{0,1\}^{K_i} \to \{0,1\}$ are then thought of as propositional variables assuming values in the two-element Boolean algebra from Example 2.4, and the update rule is stated using the operators $\wedge$, $\vee$ and $\neg$ from this structure, cf. Table 2.1. In a biological application, these propositional formulas often allow for the interpretation of an update rule as the (logical) combination of activating and inhibiting regulatory interactions.

3.2 Boolean models of regulatory networks

As already mentioned, the update rules of BMs do obviously not reflect any kinetic or biophysical laws. So, why can one expect the dynamical systems induced by BMs to be acceptable models of the intricate regulatory mechanisms explained in section 2.4.1.3? To answer this question it helps to take a look at the reasons for the complexity of gene regulation.

One reason are *cooperative effects* between transcription factors. Cooperativity exists, if a bound transcription factor protein increases (*positive* cooperativity) or decreases (*negative* cooperativity) the affinity of the promotor for further proteins. The same mechanisms are found in the *allosteric regulation* of enzymes, i.e. the regulation of an enzyme's activity by binding an (activating or inhibiting) effector molecule. The standard kinetic that describes these cooperative biochemical reactions is the *Hill kinetic* [Hill, 1910]. If x denotes the (unit-normalized) concentration of some activating transcription factor, the activity h of the target promotor can be modeled *ceteris paribus* as

$$h(c, x) = \frac{x^c}{x^c + \theta^c} , \tag{3.2}$$

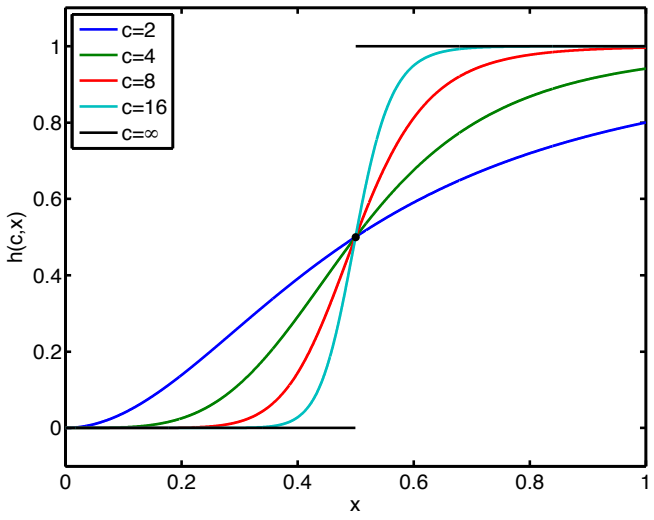

Figure 3.1: Promotor activity $h(c, x)$ from (3.2) in terms of transcription factor concentration x given by a Hill kinetic with various degrees of cooperativity c and threshold $\theta = 0.5$. The black curve shows the step-function idealization.

where c is a measure of the degree of cooperativity and θ is the threshold for half-maximal activation. Figure 3.1 shows the promotor activity h for various degrees of cooperativity c.

The dependence of $h(c, x)$ on x is *switch-like* with a "switch" at $x = \theta$. In general, we call a continuously differentiable, parametrized function $h(c, \bullet) : [0, 1] \to [0, 1]$ switch-like if

- $h(c, \bullet)$ is sigmoidal for large enough c, i.e. $h(c, \bullet)$ is convex upward on an interval $(0, \theta_c]$ and concave upward on an interval $[\theta_c, 1)$, and the sequence θ_c converges, $\theta_c \to \theta^\infty \in (0, 1)$;

- $h(c, \bullet)$ converges point-wise against the *Heaviside step-function* $h(\infty, \bullet)$ with step at $x = \theta^\infty$,

$$h(\infty, x) = \begin{cases} 0 & \text{if } x < \theta^\infty \\ 0.5 & \text{if } x = \theta^\infty \\ 1 & \text{if } x > \theta^\infty \end{cases}.$$

Indeed, for increasing c the function $h(c, x)$ from (3.2) approaches the Heaviside step-function $h(\infty, x)$ with step at $x = \theta$, cf. the black curve in Figure 3.1. This

step-function now takes only two values on $[0,1]\setminus\{\theta\}$, which we can identify with the Boolean algebra $\{0,1\}$. Thus, we may see BMs as idealizations of networks of switch-like interactions [Theis et al., 2010]. Whether or not this approximation is justified, more precisely, whether or not the degree of cooperativity is high enough to justify this approximation, has to be decided anew in each modeling application.

3.3 Kauffman networks

Let us now introduce the random "Kauffman-versions" of BMs.

Definition 3.2 (Kauffman network)**.** A *Kauffman network* (KN) is a probability space whose elements are BMs.

To turn spaces of BMs into probability spaces, one defines generative models yielding BMs as realizations. Common to all these BMs is that they are based on a graph G. In here, this graph will always be a random graph $\mathcal{G}(P_{\text{in}})$ defined by the configuration model from Example 2.2. In order to specify our generative models it, thus, remains to define how the update rules of the BM are realized.

Let us now present the KN originally introduced by Kauffman and a generalization thereof. The *standard Kauffman network* (SKN) with parameters N (order) and K (connectivity) is given by the following random process:

(K1) Create a realization of the random graph $\mathcal{G}(P_{\text{in}})$ with $P_{\text{in}} = \delta_K$.

(K2) For each node i, $i = 1, 2, \ldots, N$, define the update rule f_i by filling the entries of the pertaining truth-table with 0 and 1 with equal probabilities.

A generalization hereof is the *Kauffman network with magnetization bias* (KNMB). Here, we have an additional parameter u (the so-called *magnetization bias*[1]) and replace step (K2) from above by

(K2') For each node i, $i = 1, 2, \ldots, N$, define the update rule f_i by filling the entries of the pertaining truth-table with 0 and 1 with probabilities u and $1-u$, respectively.

In Kauffman [1969] the SKN is introduced. The generalization to KNsMB is due to Bastolla and Parisi [1996]. Also different degree distributions of the random graph have been investigated [Aldana, 2003; Fox and Hill, 2001].

[1]The term magnetization bias originates in an analogy between KNs and networks of atomic spins, which are very small magnets.

3.4 Order parameters and phase transitions of Kauffman networks

When studying KNs, we are not interested in the properties of a particular realization, but we rather search for generic properties in the ensemble of all realizations of a KN. Kauffman [1969], for instance, addresses the following questions.

> *It is a fundamental question whether metabolic stability and epigenesis require the genetic regulatory circuits to be precisely constructed. Has a fortunate evolutionary history selected only nets of highly ordered circuits which alone insure metabolic stability; or are stability and epigenesis, even in nets of randomly interconnected regulatory circuits, to be expected as the probable consequence of as yet unknown mathematical laws? Are living things more akin to precisely programmed automata selected by evolution, or to randomly assembled automata whose characteristic behavior reflects their unorderly construction, no matter how evolution selected the surviving forms?*

Kauffman himself could show by computational experiments that KNs with low connectivities exhibit surprisingly ordered structures and are able to give insights into biological phenomena such as cell replication or lineage differentiation. With increasing connectivities this order seems to disappear.

Soon the close relation between KNs and the concept of a *phase transition* from statistical physics was realized. Originally, this concept denotes the transitions between two or more different *physical phases* of one medium, like ice, water and gas [Kadanoff, 2000]. At the point of phase transition certain properties of this medium change, mostly in a discontinuous fashion, in response to a change of some external condition, such as temperature or pressure. A liquid, for instance, may become gas when heated to the boiling point, leading to a sharp increase in its volume. Phase transitions are typically detected by monitoring an *order parameter*. For phase transitions from solid to liquid or from liquid to gas, for example, this order parameter is the density of the medium.

In a number of studies by Derrida and Pomeau [1986], Derrida and Stauffer [1986] as well as Flyvbjerg [1988], Kauffman's experimental observations were explained by creating an analogy between KNs and physical media undergoing phase transitions. In KNs, the external condition is the connectivity. Several order parameters have been proposed [Derrida and Pomeau, 1986; Flyvbjerg, 1988; Luque and Solé, 1997, 2000],

all yielding the same phase transition criterion. The *Hamming distance* between two initially differing time-courses is, arguably, the most intuitive. The definition of this order parameter is motivated by the hallmark of chaos: a sensitivity to small perturbations. This suggests to detect phase transitions by monitoring how the (Hamming) distance between two nearby configurations evolves over time, i.e. whether it increases or decreases.

We do not review any theoretical details at this point, as we will study a more general version of KNs than KNsMB in chapter 4. In the course of this chapter, we will obtain the theory of SKNs and KNsMB as corollaries to more general statements. In particular, we will see that the order parameter has stationary dynamics, i.e. a globally attracting fixed point, and we will determine the *critical connectivity* at which the phase transition occurs. Below this connectivity the globally attracting equilibrium of the Hamming distance is zero, above the critical connectivity it is strictly positive.

We say a KN is in the *frozen* or *ordered phase* if the Hamming distance has a stationary value of zero, otherwise the KN is said to be in the *chaotic phase*. KNs at the point of phase transition are called *critical*. Some authors prefer the term *regime* over phase. It has been shown that the ordered phase is characterized by small stable attractors, whereas in the chaotic phase long-periodic orbits frequently occur [Aldana et al., 2003]. A more intuitive characterization of these two phases can be given in terms of "damage spreading" (percolation). Assume that a realization of a KN is damaged in one node, i.e. the state of this node is flipped. In the chaotic regime the Hamming distance will increase, i.e. this damage will spread through the network, whereas in the ordered regime the Hamming distance will vanish, i.e. the network is able to "repair" this damage over time.

To visualize this, we generate realizations of SKNs with connectivities $K = 1$, $K = 2$, and $K = 3$, simulate each twice with initial conditions differing by a (normalized) Hamming distance of 0.1, and plot the resulting time-courses in Figure 3.2. We will see in chapter 4 (Remark 4.5) that SKNs with these connectivities are frozen, critical and chaotic. Below the two time-courses their Hamming distance is shown. In the frozen networks this Hamming distance decreases to its equilibrium zero, in the critical and chaotic networks it eventually fluctuates around strictly positive values. In the critical network this value is comparable to the initial distance, whereas in the chaotic network the Hamming distance increases from its initial value.

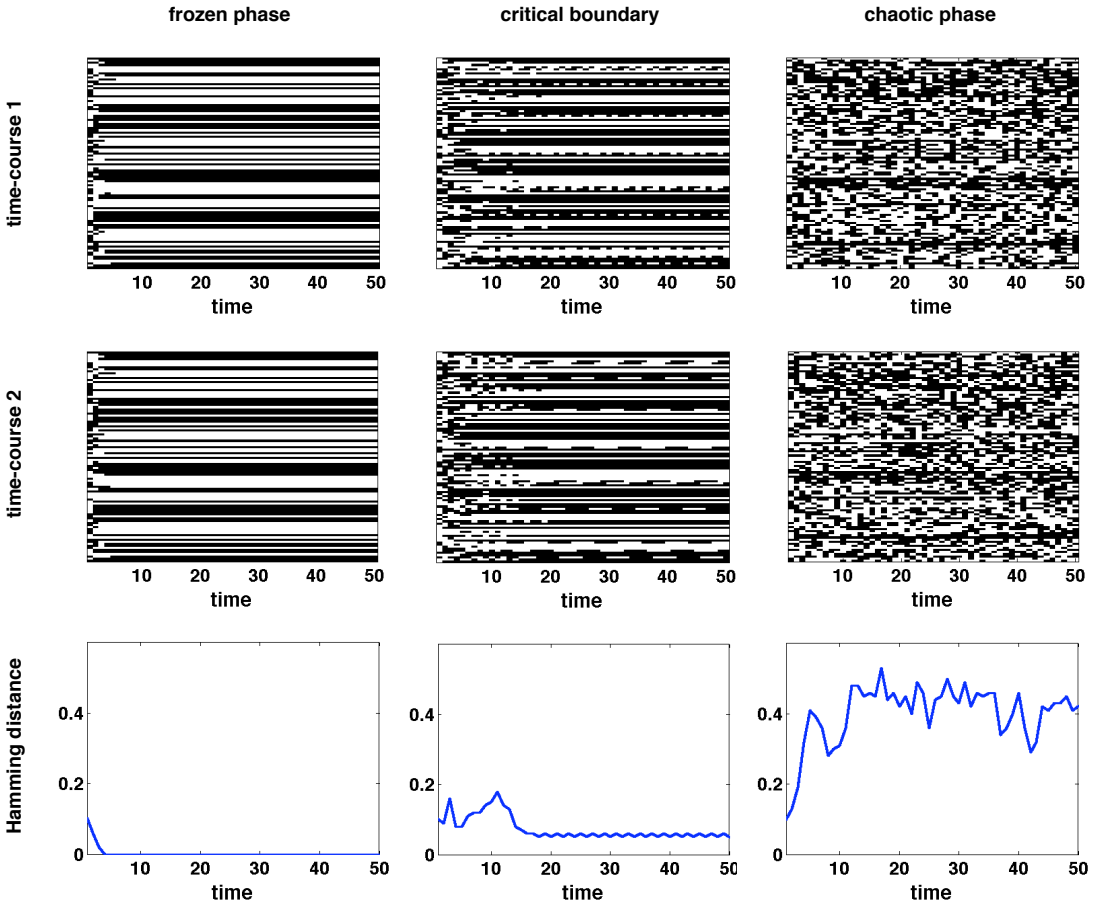

Figure 3.2: Realizations of SKNs with $N = 10^2$ nodes and connectivities $K = 1$, $K = 2$, and $K = 3$ are generated. They fall into the frozen, critical and chaotic phase, cf. Remark 4.5. Each realization is simulated twice for 50 time-steps with initial conditions differing by a (normalized) Hamming distance of 0.1. The resulting time-courses are visualized by representing 0 and 1 as black and white boxes, respectively. Below the two time-courses their Hamming distance is plotted.

The study of KNs has found its way into popular science by the slogan *"Living at the edge of chaos."* Kauffman [1993] hypothesized that regulatory networks in living organisms operate in the frozen regime but close to (at the edge of) the chaotic regime, i.e. near a phase transition. The first part of this hypothesis is well supported by other authors who all claim that robustness is a crucial property of biological systems [Kitano, 2004]. The second part can only be understood in the light of evolution. For natural selection to work, small changes, such as mutations, need to have an effect. Kauffman argues that fully robust networks, which are completely insensitive to small perturbations, do not have the ability to evolve over time by natural selection. Hence, evolvable living organisms operate near a chaotic regime. A nice corroboration of Kauffman's hypothesis is the finding that the (average) connectivity of gene regulatory networks in lower organisms is, indeed, around the critical connectivity of SKNs, see Balleza et al. [2008] and references therein.

4

Multistate Kauffman networks

They fashioned a tomb for thee, O holy and high one
The Cretans, always liars, evil beasts, idle bellies!
But thou art not dead: thou livest and abidest forever,
For in thee we live and move and have our being.

Cretica, Epimenides

The above poem by the Cretan philosopher Epimenides of Knossos is the first version of what is known in logic as the *liar's paradox*. This paradox arises when one interprets Epimenides' statement that all Cretans are liars as a *self-referential* statement. Epimenides, after all, was a Cretan himself. Today, the liar's paradox exists in many forms; in its most simplistic one it headlines the essay "This title is false" by Isalan and Morrison [2009], which they published last year in *Nature*.

They argue that it is self-reference what makes all the difference in genetic regulation. Typical descriptions of regulatory interactions, such as "This gene represses itself." or "Gene A activates gene B. Gene B inhibits gene A.", are, indeed, self-referential. Isalan and Morrison continue to explain that in gene regulation these seemingly paradoxical situations are resolved either in time or space, leading to temporal oscillations

or spatial patterns. In fact, temporal oscillations are found e.g. during cell cycle or in the circadian rhythm, and Alan Turing [1990][1] showed that even from small self-referential motifs such as "Gene A activates gene B. Gene B inhibits gene A." complex spatial patterns may emerge.

There is a third possibility how a self-referential situation can be resolved: By introducing additional truth-values besides the classic "false" and "true", such as "partially true." In a biological context, these truth-values could be interpreted as "medium concentration" or "weakly active." The solution of a self-referential regulation would then be *homeostasis*.

4.1 Motivation and outline

Aesthetic philosophy aside, in many down-to-earth modeling efforts the discretization of continuous biological quantities into binary "on"–"off" categories was found to be insufficient. In fact, it has been demonstrated that genes may well have more than two functionally different expression levels [Setty et al., 2003]. To alleviate this issue, in some modeling applications the Boolean "on"–"off" categories are extended to multiple discrete states, leading to *multistate models* [Fauré et al., 2009; Sánchez and Thieffry, 2001; Thomas, 1991].

Studies of KNs with multiple states, let us call them *multistate Kauffman networks*, are scarce [Solé et al., 2000] and restricted to the biologically implausible case where all nodes have the same number of discrete states. In this chapter, which follows Wittmann et al. [2010] as well as Wittmann and Theis [2010a], we investigate a more general class of multistate KNs with respect to critical phenomena. In particular, contrary to previous studies, the number of discrete states is not fixed for all nodes but follows a distribution. We formally introduce the Hamming distance between two trajectories as an order parameter and show that a transition between a frozen and a chaotic regime takes place in multistate KNs of this class. The critical boundary is analytically determined as a relation between the mean connectivity and a parameter describing the heterogeneity of the update rules, cf. Theorem 4.1.

We study two distributions of update rules in more detail. First, we analyze multistate KNs with unbiased update rules, which generalize the (Boolean) SKNs. We

[1] Reprint of Turing's original publication

find that allowing nodes to assume multiple states lowers the critical connectivity as compared to the Boolean case, the limit being a biologically implausible connectivity of 1, cf. Remark 4.5. Interestingly however, the critical connectivity does not necessarily decrease with the mean number of states per node. Second, we study multistate KNs with biased update rules, which generalize the (Boolean) KNsMB. In section 4.3.4.2, we show that the critical connectivity can be made arbitrarily large by biasing the update rules towards one of the discrete states. In the case of (Boolean) KNsMB, this simply means choosing the magnetization bias either sufficiently large or small. In particular, we can poise multistate KNs with biologically plausible connectivities at criticality (at the edge of chaos). Our analytic results are backed up by simulations.

Subsequently, we extend the analysis of the Hamming distance (between two trajectories) by looking at ensembles of trajectories. This can be motivated from a biological point of view, as in molecular biology experimental data are often average concentrations in cell cultures, which can be thought of as ensembles of trajectories of a multistate model. A dynamical system describing the synchronization behavior of such ensembles is introduced and analyzed. In a low-dimensional example the analytic results are validated by simulations.

4.2 Multistate models and multistate Kauffman networks

Let us now formally introduce our first generalization of BMs and KNs. In this chapter, $G = (V, E)$ again denotes a (directed) graph of order N with nodes $V = \{1, 2, \dots, N\}$ and edges $(i' \to i) \in E \subset V \times V$. The predecessors (inputs) of a node i are denoted by $i_1 < i_2 < \cdots < i_{K_i}$, where K_i is the node's in-degree.

4.2.1 Multistate models

Generalizing Definition 3.1 of BMs we make

Definition 4.1 (multistate model)**.** A *multistate model* (MM) is a triple $(G, \mathbf{S}, \mathbf{f})$ which consists of a graph G, a vector $\mathbf{S} = (S_i)_{i=1}^N$ of numbers of states defining the ranges $\Sigma_i := \{0, 1, \dots, S_i - 1\}$ of nodes $i = 1, 2, \dots, N$, and a vector of discrete functions $\mathbf{f} = (f_i)_{i=1}^N$, $f_i : \prod_{k=1}^{K_i} \Sigma_{i_k} \to \Sigma_i$. The discrete function f_i is called *update rule* or *update function* of node i and the vector of update rules $\mathbf{f}$ (as a function from $\prod_{i=1}^N \Sigma_i \to \prod_{i=1}^N \Sigma_i$) is called *transfer function* of the MM.

Remark 4.1. A BM is the special case of a MM where all $S_i = 2$. Conversely, we can still express an update rule f_i of a MM using the Boolean operators $\wedge$ and $\vee$ from Table 2.1. We do so, by relating the truth-values of the equations "$f_i(x_{i_1}, x_{i_2}, \ldots, x_{i_{K_i}}) = s$", $s \in \Sigma_i$, to the truth-values of the equations "$x_{i_k} = \xi_k$", $k = 1, 2, \ldots K_i$, $\xi_k \in \Sigma_{i_k}$:

$$f_i\left(x_{i_1}, x_{i_2}, \ldots, x_{i_{K_i}}\right) = s \quad \Longleftrightarrow \quad \bigvee_{(\xi_1,\xi_2,\ldots,\xi_{K_i})|f_i(\xi_1,\xi_2,\ldots,\xi_{K_i})=s} \bigwedge_{k=1}^{K_i} (x_{i_k} = \xi_k)$$

This is a generalization of the full DNF of a Boolean function from (2.8). The disjunction on the right-hand side runs over all input combinations of f_i with output value s. For each combination, the inner conjunction is true if and only if the combination agrees with the values of the variables x_{i_k}.

Similarly to BMs, MMs give rise to dynamical systems.

Remark 4.2. Each MM $(G, \mathbf{S}, \mathbf{f})$ gives rise to a time-discrete dynamical system as follows: To each node i we associate a time-dependent discrete variable $x_i(t) \in \Sigma_i$, $\mathbf{x}(t) = (x_i(t))_{i=1}^N$. The evolution of $\mathbf{x}(t)$ is determined by the iteration

$$\mathbf{x}(t+1) = \mathbf{f}\left(\mathbf{x}(t)\right) \ , \quad t = 0, 1, 2, \ldots \ ,$$

where the i-th component is given by

$$x_i(t+1) = f_i\left(x_{i_1}(t), x_{i_2}(t), \ldots, x_{i_{K_i}}(t)\right) \ . \tag{4.1}$$

Again we only consider the above synchronous updating.

In the following, we will refer to trajectories of the dynamical system from Remark 4.2 as *trajectories of the MM* $(G, \mathbf{S}, \mathbf{f})$.

The state-space of the dynamical system from Remark 4.2 is the discrete, finite set $X = \prod_{i=1}^N \Sigma_i$. We proceed as in the Boolean case, i.e. we define the *Hamming distance* d of $\mathbf{x} = (x_i)_{i=1}^N \in X$ and $\mathbf{x}' = (x_i')_{i=1}^N \in X$ as

$$d\left(\mathbf{x}, \mathbf{x}'\right) = \frac{1}{N} \sum_{i=1}^{N} \left(1 - \delta_{x_i, x_i'}\right) \ ,$$

and use the counting measure. Our results about the ω-limit sets and attractors of BMs, cf. Proposition 3.1, generalize to the multistate case.

Proposition 4.1. *Consider the dynamical system defined in Remark 4.2. The ω-limit set of each point is either a fixed point or a periodic orbit. The same is true for the attractors of this dynamical system.*

4.2.2 Multistate Kauffman networks

We now define the random "Kauffman-version" of MMs.

Definition 4.2 (multistate Kauffman network)**.** In general, a *multistate Kauffman network* (MKN) is a probability space whose elements are MMs.

In this thesis, by MKN we always mean the following generative model for MMs on N nodes. It is defined for

- an in-degree distribution $P_{\text{in}}(K)$, $K = 1, 2, \ldots, K_{\max}$,
- a distribution of numbers of states $P_{\text{nos}}(S)$, $S = 2, 3, \ldots, S_{\max}$, and
- distributions $P_S(s)$, $s = 0, 1, \ldots, S-1$, of entries of update rules for all $S = 2, 3, \ldots, S_{\max}$.

Realizations are generated by

(M1) creating a realization of the random graph $\mathcal{G}(P_{\text{in}})$,

(M2) for each node i, $i = 1, 2, \ldots, N$, choosing its number of states S_i randomly from the probability distribution P_{nos},

(M3) for each node i, $i = 1, 2, \ldots, N$, choosing the values of f_i randomly from the probability distribution P_{S_i}.

Note that in (M3) the distribution P_{S_i} does not depend on the node i but only on its number of states S_i.

In the following, we consider, in particular, two examples for the distributions P_S. In section 4.3.3, we treat unbiased update rules sampled from the discrete uniform distributions

$$P_S(s) = \frac{1}{S}\,, \quad s = 0, 1, \ldots, S-1\,. \tag{4.2}$$

In the special case of all $S_i = 2$ and delta-distributed in-degree, the study of the distribution from (4.2) yields the theory of SKNs.

In section 4.3.4, we then study biased update rules sampled from the distributions

$$P_S(s) = \begin{cases} u & s = 0 \\ \dfrac{1-u}{S-1} & s = 1, 2, \ldots, S-1 \end{cases} \tag{4.3}$$

for some $0 < u < 1$. If $S_i = 2$, this simply means that the update function f_i evaluates to 0 with a certain probability $0 < u < 1$ and to 1 with probability $1 - u$. Thus, if all $S_i = 2$ and the in-degree is delta-distributed, the study of the distribution from (4.3) yields the theory of KNsMB.

4.2.3 Parameters of multistate Kauffman networks

Let $\mathcal{K}$ be a MKN. We conclude this section by defining and discussing some effective parameters of $\mathcal{K}$ that will be needed in the following.

- We define the *heterogeneity* p_S of the distributions P_S, $S = 2, 3, \ldots, S_{\max}$, as

$$p_S = \sum_{s=0}^{S-1} P_S(s) \left(1 - P_S(s)\right) \ , \tag{4.4}$$

- the *heterogeneity* $\overline{p}$ of $\mathcal{K}$ as

$$\overline{p} = \sum_{S=2}^{S_{\max}} P_{\text{nos}}(S)\, p_S \ , \tag{4.5}$$

- and the *mean connectivity* $\overline{K}$ of $\mathcal{K}$ as

$$\overline{K} = \sum_{K=1}^{K_{\max}} P_{\text{in}}(K)\, K \ . \tag{4.6}$$

Remark 4.3. From (M3) it follows that the probability for a generated update rule f_i to yield two different values for two different arguments depends only on P_{S_i} (where S_i is the number of states of node i) and is equal to the heterogeneity p_{S_i} of P_{S_i}.

Lemma 4.1. *The heterogeneity p_S becomes maximal if P_S is the discrete uniform distribution from* (4.2)*. In this case, $p_S = (S-1)/S$.*

Proof. The existence of a global maximum follows from the extreme value theorem. Now assume that $\pi_1 = P_S(s_1) \neq \pi_2 = P_S(s_2)$. Then, for $\overline{\pi} = (\pi_1 + \pi_2)/2$ it holds that

$$\begin{aligned} 2\overline{\pi}\left(1 - \overline{\pi}\right) &= \pi_1 + \pi_2 - \frac{\left(\pi_1 + \pi_2\right)^2}{2} \\ &> \pi_1 + \pi_2 - \frac{\left(\pi_1 + \pi_2\right)^2}{2} - \frac{\left(\pi_1 - \pi_2\right)^2}{2} \\ &= \pi_1(1 - \pi_1) + \pi_2(1 - \pi_2) \ . \end{aligned}$$

Hence, the distribution

$$P'_S(s) = \begin{cases} P_S(s) & s \notin \{s_1, s_2\} \\ \overline{\pi} & s \in \{s_1, s_2\} \end{cases}$$

yields a strictly larger value for p_S. In case of uniform P_S one computes

$$p_S = \sum_{s=0}^{S-1} \frac{1}{S} \frac{S-1}{S} = \frac{S-1}{S} \ .$$

□

It follows

Corollary 4.1. *For any choice of P_S, $p_S < 1$ and $\overline{p} < 1$.*

4.3 Dynamic regimes of multistate Kauffman networks

Let again $\mathcal{K}$ be a MKN as defined in section 4.2.2. As outlined in section 3.4 one detects phase transitions by monitoring the evolution of an order parameter, which, in the context of KNs, is often the Hamming distance between two trajectories.

4.3.1 The Hamming distance of a Kauffman network

Before we can formally define our order parameter, we need to state a technical consequence of (M3).

Lemma 4.2. *Let $d_0 \in [0, 1]$ and consider the following random experiment: Generate a realization of $\mathcal{K}$. Choose two configurations $\mathbf{x}(0)$ and $\mathbf{x}'(0)$ whose components differ, $x_i(0) \neq x'_i(0)$, with probability d_0. Iterate the configurations one time-step yielding $\mathbf{x}(1)$ and $\mathbf{x}'(1)$, respectively. We define the random variable $\mathfrak{d}$ as the Hamming distance $d(\mathbf{x}(1), \mathbf{x}'(1))$. Then, it holds*

$$\mathbb{E}(\mathfrak{d}) = \sum_{K=1}^{K_{\max}} P_{in}(K) \sum_{S=2}^{S_{\max}} P_{nos}(S) \left[\left(1 - (1 - d_0)^K \right) p_S \right] \ .$$

In particular, $\mathbb{E}(\mathfrak{d})$ is independent of how the actual values in $\mathbf{x}(0)$ and $\mathbf{x}'(0)$ are chosen, but depends only on the probability d_0 for them to differ.

Proof. Let us introduce identically distributed Bernoulli random variables $\mathfrak{d}_i$, $i = 1, 2, \ldots, N$, defined as 1 if $x_i(1) \neq x'_i(1)$ and as 0 otherwise. It then holds $\mathfrak{d} = (1/N) \sum_{i=1}^{N} \mathfrak{d}_i$, and, consequently,

$$\mathbb{E}(\mathfrak{d}) = \frac{1}{N} \sum_{i'=1}^{N} \mathbb{E}(\mathfrak{d}_{i'}) = \mathbb{E}(\mathfrak{d}_i) \qquad (\star)$$

for any i.

Given K_i and S_i, the conditional expectation $\mathbb{E}(\mathfrak{d}_i \mid K_i, S_i)$ is equal to the probability that

$$f_i\left(x_{i_1}(0), x_{i_2}(0), \ldots, x_{i_{K_i}}(0)\right) \neq f_i\left(x'_{i_1}(0), x'_{i_2}(0), \ldots, x'_{i_{K_i}}(0)\right) . \qquad (\dagger)$$

According to Remark 4.3 the probability for (†) is equal to p_{S_i} given the two arguments $\left(x_{i_1}(0), x_{i_2}(0), \ldots, x_{i_{K_i}}(0)\right)$ and $\left(x'_{i_1}(0), x'_{i_2}(0), \ldots, x'_{i_{K_i}}(0)\right)$ are not identical. The events that inputs differ between both configurations, $x_{i_k}(0) \neq x'_{i_k}(0)$, are independent as in the configuration model the inputs i_k of i are chosen randomly from V. The probability for each of these events is d_0. Thus, the probability for the arguments to differ (in at least one component) is given by $1 - (1 - d_0)^{K_i}$. Hence, the probability for (†) is equal to $\left[1 - (1 - d_0)^{K_i}\right] p_{S_i}$.

Finally, recall that K_i and S_i are chosen according to the distributions $P_{\text{in}}(K)$ and $P_{\text{nos}}(S)$. Thus, averaging over K_i and S_i yields

$$\mathbb{E}(\mathfrak{d}_i) = \sum_{K=1}^{K_{\max}} P_{\text{in}}(K) \sum_{S=2}^{S_{\max}} P_{\text{nos}}(S) \left[\left(1 - (1 - d_0)^K\right) p_S\right] ,$$

and the claim follows from $(\star)$. □

Lemma 4.2 states that the expected Hamming distance between two configurations evolves independently of the actual values in these configurations. In chapter 5, we will introduce a new class of KNs for which this no longer holds: The evolution of the Hamming distance will depend on the actual values in the configurations, more precisely, on the fractions of 1's and 0's. For now, however, Lemma 4.2 allows us to make

Definition 4.3 (Hamming distance of a MKN)**.** The *Hamming distance* of $\mathcal{K}$ is a sequence $(d(t))_{t \geqslant 0}$ which is consistent in the sense of the following random experiment: Pick a realization of $\mathcal{K}$, create two configurations $\mathbf{x}(0)$ and $\mathbf{x}'(0)$ whose components differ with probability $d(t)$, and iterate them one time-step yielding configurations $\mathbf{x}(1)$ and $\mathbf{x}'(1)$. Then, $d(t+1)$ is the expected Hamming distance between $\mathbf{x}(1)$ and $\mathbf{x}'(1)$.

Remark 4.4. We, of course, want the Hamming distance of $\mathcal{K}$ to be a good approximation of the Hamming distance

$$\frac{1}{N}\sum_{i=1}^{N}\left(1-\delta_{x_i(t),x_i'(t)}\right)$$

between two trajectories $\mathbf{x}(t)$ and $\mathbf{x}'(t)$ of a specific realization of $\mathcal{K}$. We will demonstrate that this is, indeed, the case in large networks by simulations in section 4.3.5. From a theoretical point of view, however, the above approximation is *a priori* not justified. The issue is that in the proof of Lemma 4.2 it is crucial that we may assume the inputs i_k of a node i to be independent. At time-points $t \geqslant 1$, however, this assumption is obviously not valid as in a realization of $\mathcal{K}$ the inputs of i might have common predecessors. The reason why we still obtain good approximations in large networks, is given by Lemma 2.1. Here, it was shown that in the thermodynamic limit of large N the probability for common predecessors vanishes.

4.3.2 Analysis of the Hamming distance and detection of a phase transition

The Hamming distance of $\mathcal{K}$ naturally depends on the initial distance $d(0)$. In the following, we take care of this issue by proving that the asymptotic behavior of $d(t)$ is identical for almost all initial conditions. For this we use that, as shown in Lemma 4.2, the Hamming distance $(d(t))_{t\geqslant 0}$ of $\mathcal{K}$ obeys the iteration

$$\begin{aligned} d(t+1) &= D\left(d(t)\right) \\ &:= \sum_{K=1}^{K_{\max}} P_{\text{in}}\left(K\right) \sum_{S=2}^{S_{\max}} P_{\text{nos}}\left(S\right)\left[\left(1-\left(1-d(t)\right)^{K}\right)p_S\right] . \end{aligned} \tag{4.7}$$

Lemma 4.3. *For the dynamical system* (4.7) *three possibilities exist.*

1. *It has a hyperbolic, globally attracting fixed point at* $d^\star = 0$.
2. *The fixed point* $d^\star$ *is still globally attracting, but critical.*
3. *The fixed point* $d^\star$ *is repelling and an additional fixed point* $d^{\star\star} \in (0,1)$ *exists which attracts* $(0,1]$.

Proof. Clearly, $D(0) = 0$, so $d^\star$ is a fixed point. First, suppose that $P_{\text{in}}(1) = 1$. Then $D(d)$ is linear with slope $\overline{p} < 1$ and (4.7) falls into category 1. Now, consider a general

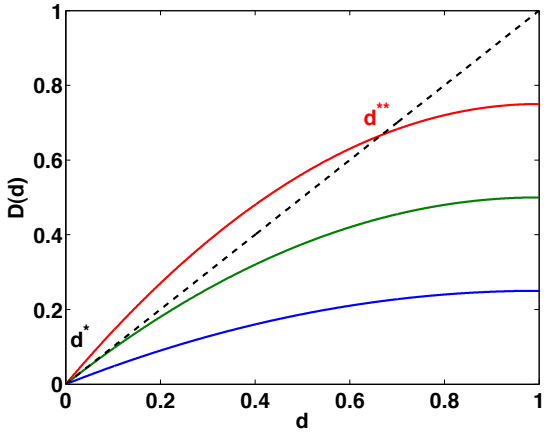

Figure 4.1: Ad proof of Lemma 4.3. Schematic plots of $D(d)$ from (4.7). The blue, green and red curves show the three possible situations listed in Lemma 4.3.

P_{in}. The claim follows from the fact that for $d > 0$ the function $D(d)$ is concave and monotonously increasing. To prove this, it suffices to show these properties for $\left(1-(1-d)^K\right) p_S$ and $K \geqslant 2$, which can easily be done by computing the first and second derivatives, $K(1-d)^{K-1}p_S > 0$ and $-K(K-1)(1-d)^{K-2}p_S < 0$, respectively. Also consult Figure 4.1 for a visualization of the three possible situations listed in the claim. □

If $d^\star$ is attracting we expect trajectories of realizations of $\mathcal{K}$ to re-converge upon perturbations, whereas if $d^\star$ is repelling the trajectories will diverge. This motivates

Definition 4.4 (phases/regimes of MKNs)**.** The *phases* (*regimes*) of $\mathcal{K}$ are defined as follows.

1. If $d^\star$ is hyperbolic and attracting, $\mathcal{K}$ is called *frozen* or *ordered*.
2. If $d^\star$ is critical, $\mathcal{K}$ is called *critical*.
3. If $d^\star$ is repelling, $\mathcal{K}$ is called *chaotic*.

Let us now derive a criterion for the *phase transition* in terms of parameters of $\mathcal{K}$.

Theorem 4.1 (phase transition criterion)**.** *We have the following* phase transition

criterion *in terms of the parameters* $\overline{p}$ *and* $\overline{K}$ *from* (4.5) *and* (4.6).

$$\overline{p}\overline{K} \begin{cases} < 1 & \textit{ordered regime} \\ = 1 & \textit{critical boundary} \\ > 1 & \textit{chaotic regime}\,. \end{cases} \tag{4.8}$$

Proof. Linearizing D from (4.7) about $d^\star$ yields

$$\begin{aligned} \left.\frac{\mathrm{d}D}{\mathrm{d}d}\right|_{d^\star} &= \sum_{K=1}^{K_{\max}} P_{\mathrm{in}}(K) \sum_{S=2}^{S_{\max}} P_{\mathrm{nos}}(S)\, K p_S \\ &= \sum_{K=1}^{K_{\max}} P_{\mathrm{in}}(K)\, K\overline{p} = \overline{p}\overline{K}\,. \end{aligned}$$

The claim follows from Theorem 2.2. □

Corollary 4.2. *MKNs with a mean connectivity* $\overline{K}$ *below (above) the critical connectivity*

$$\overline{K}^{\mathrm{crit}} = \frac{1}{\overline{p}} \tag{4.9}$$

are frozen (chaotic).

A nice intuitive interpretation of Theorem 4.1 is given in terms of "damage spreading." Assume that at time t the state of a realization of a MKN is damaged in one node, i.e. the state of this node is flipped. On average, this node affects $\overline{K}$ other nodes at the next time-step $t+1$. The parameter $\overline{p}$ is the mean probability that a change of input, indeed, leads to a change of output in an update rule. The product $\overline{p}\overline{K}$ thus gives the mean number of damaged (flipped) nodes at time $t+1$. Inductively, we see that in the case $\overline{p}\overline{K} > 1$ damage will spread through the network, whereas in the case $\overline{p}\overline{K} < 1$ the network is able to "repair" damage over time.

We observe that the phase transition depends only on the first moments $\overline{K}$ and $\overline{p}$. Typically, $\overline{K}$ can be easily computed once the underlying network structure is known. The computation of $\overline{p}$ is more involved, as we shall see in the following sections where we compute this quantity for unbiased as well as biased update rules.

4.3.3 Unbiased update rules

Let us first study the multistate counterpart of the SKN. This is to say, we consider the completely unbiased situation where the P_S are the discrete uniform distributions from (4.2). From Lemma 4.1 we know that in this case

$$p_S = \frac{S-1}{S} \,. \tag{4.10}$$

Substituting (4.10) in (4.5) yields

$$\overline{p} = \sum_{S=2}^{S_{\max}} P_{\text{nos}}(S) \frac{S-1}{S} = 1 - \mathfrak{m} \,, \tag{4.11}$$

where

$$\mathfrak{m} = \sum_{S=2}^{S_{\max}} P_{\text{nos}}(S) \frac{1}{S} \,.$$

Remark 4.5. For any P_{nos}, $\mathfrak{m}$ is bounded, $0 < \mathfrak{m} \leqslant 1/2$, where the upper bound is exact iff $P_{\text{nos}}(S) = \delta_{S,2}$, i.e. in the Boolean case. For the critical connectivity from (4.9) together with (4.11)

$$\overline{K}^{\text{crit}} = \frac{1}{1-\mathfrak{m}} \,, \tag{4.12}$$

this implies $1 < \overline{K}^{\text{crit}} \leqslant 2$ and $\overline{K}^{\text{crit}} = 2$ (only) in the Boolean case. Moreover, $\overline{K}^{\text{crit}}$ lowers down to 1 as $\mathfrak{m}$ becomes small. Hence, in the non-Boolean case the critical connectivity of unbiased MKNs is strictly smaller than in the Boolean case.

We visualize this result in two examples.

Examples

We compute $\mathfrak{m}$ in two special cases of P_{nos}.

- First, a delta distribution

  $$P_{\text{nos}}(S) = \delta_{S,\overline{S}} \,, \quad S = 2, 3, \ldots, S_{\max} \,, \tag{4.13}$$

  for a fixed number of states $\overline{S}$ per node. In this case, $\mathfrak{m} = 1/\overline{S}$, and from (4.12) we obtain the criticality condition

  $$\overline{K}^{\text{crit}} = \frac{\overline{S}}{\overline{S}-1} \,, \tag{4.14}$$

  which was already found in Solé et al. [2000]. In the Boolean case, $\overline{S} = 2$, we recover the critical connectivity 2 of the SKN. For an increasing (fixed) number of states $\overline{S}$ the critical connectivity approaches 1.

- Second, a discrete uniform distribution

$$P_{\text{nos}}(S) = \frac{1}{S_{\max} - 1} , \quad S = 2, 3, \ldots, S_{\max} .$$

In this case,

$$\mathfrak{m} = \sum_{S=2}^{S_{\max}} \frac{1}{S_{\max} - 1} \frac{1}{S} = \frac{H_{S_{\max}} - 1}{S_{\max} - 1} ,$$

where $H_{S_{\max}}$ is the $S_{\max}$-th harmonic number, and from (4.12) we obtain the criticality condition

$$\overline{K}^{\text{crit}} = \frac{S_{\max} - 1}{S_{\max} - H_{S_{\max}}} . \tag{4.15}$$

It holds that $\overline{K}^{\text{crit}} \to 1$ as $S_{\max} \to \infty$. A better idea of this convergence is given by the well-known approximation

$$H_{S_{\max}} = \ln(S_{\max}) + \gamma^{\text{Euler}} + \mathcal{O}(S_{\max}^{-1}) ,$$

where γ^{Euler} is the Euler-Mascheroni constant, $\gamma^{\text{Euler}} \approx 0.5772$.

The critical connectivities from (4.14) and (4.15) are plotted in Figure 4.2. We observe that in both examples a growing (fixed) number of states $\overline{S}$ or a growing upper bound $S_{\max}$, respectively, lower the critical connectivity down to 1. At this point, we also refer the reader to section 4.5, where we discuss an example showing that, in general, the critical connectivity does not decrease with the mean of the distribution P_{nos}.

4.3.4 Biased update rules

In the SKN each Booelan update function is drawn randomly from the ensemble of all Boolean functions with equal probability. In subsequent studies, however, it is often assumed that each function evaluates to 0 with a certain probability $0 < u < 1$ and to 1 with probability $1 - u$. (In here, such KNs are called KNsMB.) Biologically speaking, it is assumed that a gene is expressed with probability u. A natural generalization hereof to the multistate case is the distribution

$$P_S(s) = \begin{cases} u & s = 0 \\ \dfrac{1-u}{S-1} & s = 1, 2, \ldots, S-1 \end{cases}$$

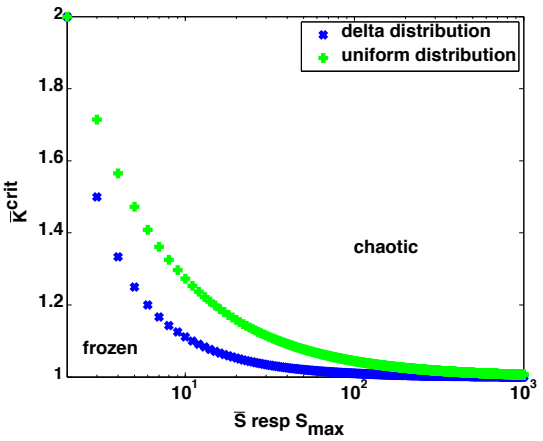

Figure 4.2: The case of unbiased update rules. Critical connectivities $\overline{K}^{\mathrm{crit}}\left(\overline{S}\right)$ from (4.14) (blue "×") and $\overline{K}^{\mathrm{crit}}\left(S_{\max}\right)$ from (4.15) (green "+").

from (4.3) for some $0 < u < 1$. In the Boolean case, it turned out that, even for connectivities above the critical connectivity of the SKN, a KNMB can be kept in the frozen regime by choosing u sufficiently large or small [Bastolla and Parisi, 1996]. Is this still true for MKNs?

To answer this question, let us assume that each P_S is given by (4.3) for some $0 < u < 1$. Then (4.4) becomes

$$p_S^u = 2u(1-u) + (1-u)^2 \frac{S-2}{S-1} \,,$$

and substituting this in (4.5) gives

$$\begin{aligned} \overline{p}^u &= \sum_{S=2}^{S_{\max}} P_{\mathrm{nos}}\left(S\right) \left[2u(1-u) + (1-u)^2 \frac{S-2}{S-1}\right] \\ &= 2u(1-u) + (1-u)^2 \left(1 - \mathfrak{m}_{-1}\right) \,, \end{aligned} \tag{4.16}$$

where

$$\mathfrak{m}_{-1} = \sum_{S=2}^{S_{\max}} P_{\mathrm{nos}}\left(S\right) \frac{1}{S-1} \,.$$

We observe that $0 < \mathfrak{m}_{-1} \leqslant 1$, where the upper bound is exact iff $P_{\mathrm{nos}}\left(S\right) = \delta_{S,2}$, i.e. in the Boolean case.

Substituting (4.16) in (4.8) gives rise to a quadratic equation in u:

$$\overline{K}\left[2u(1-u)+(1-u)^2\left(1-\mathfrak{m}_{-1}\right)\right]\begin{cases}<1 & \text{ordered regime}\\ =1 & \text{critical boundary}\\ >1 & \text{chaotic regime}\end{cases} \tag{4.17}$$

In section 4.3.4.1 this criterion is solved for u^{crit}, the results are summarized in section 4.3.4.2.

4.3.4.1 Computation of critical magnetization biases

Criterion (4.17) is equivalent to

$$-\overline{K}\left(1+\mathfrak{m}_{-1}\right)u^2+2\overline{K}\mathfrak{m}_{-1}u+\overline{K}\left(1-\mathfrak{m}_{-1}\right)-1\begin{cases}<0 & \text{ordered regime}\\ =0 & \text{critical boundary}\\ >0 & \text{chaotic regime .}\end{cases} \tag{4.18}$$

The discriminant of this quadratic equation is given by

$$\mathcal{D}=4\overline{K}\left(\overline{K}-\left(1+\mathfrak{m}_{-1}\right)\right)$$

and

$$\mathcal{D}\begin{cases}<0 & \text{if } \overline{K}<1+\mathfrak{m}_{-1}\\ =0 & \text{if } \overline{K}=1+\mathfrak{m}_{-1}\\ >0 & \text{if } \overline{K}>1+\mathfrak{m}_{-1}\ .\end{cases}$$

From (4.18) it follows that for $\overline{K}<1+\mathfrak{m}_{-1}$ the MKN is always frozen. To see this, note that $-\overline{K}\left(1+\mathfrak{m}_{-1}\right)<0$. For $\overline{K}\geqslant 1+\mathfrak{m}_{-1}$ the quadratic equation from (4.18) has two (possibly coinciding) solutions

$$u^{\text{crit}}_{\frac{1}{2}}\left(\overline{K},\mathfrak{m}_{-1}\right)=\frac{1}{\mathfrak{m}_{-1}+1}\left(\mathfrak{m}_{-1}\mp\sqrt{1-\frac{\mathfrak{m}_{-1}+1}{\overline{K}}}\right)\ .$$

First, observe that for $\mathfrak{m}_{-1}>0$, $u_2^{\text{crit}}<1$ is always a valid solution. Moreover, we have

$$u_1^{\text{crit}}>0\Longleftrightarrow\sqrt{1-\frac{\mathfrak{m}_{-1}+1}{\overline{K}}}<\mathfrak{m}_{-1}\Longleftrightarrow\overline{K}<\frac{1}{1-\mathfrak{m}_{-1}}\ ,$$

where in the case $\mathfrak{m}_{-1}=1$, "$\overline{K}<\infty$" is true for any $\overline{K}$. Since for $\mathfrak{m}_{-1}<1$ it holds that

$$\frac{1}{1-\mathfrak{m}_{-1}}>1+\mathfrak{m}_{-1}\ ,$$

there is always a range for $\overline{K}$, in which (4.18) has two distinct solutions in $(0,1)$. Once more considering that in (4.18) $-\overline{K}\left(1+\mathfrak{m}_{-1}\right)<0$, we obtain in this case

$$-\overline{K}\left(1+\mathfrak{m}_{-1}\right)u^2+2\overline{K}\mathfrak{m}_{-1}u+\overline{K}\left(1-\mathfrak{m}_{-1}\right)-1\begin{cases}<0\ , & u<u_1^{\text{crit}}\text{ or }u>u_2^{\text{crit}}\\ =0\ , & u=u_1^{\text{crit}}\text{ or }u=u_2^{\text{crit}}\\ >0\ , & u_1^{\text{crit}}<u<u_2^{\text{crit}}\ .\end{cases}$$

4.3.4.2 The critical boundary in the case of biased update rules

Summing up, we have the following phase transitions:

(a) For $\overline{\mathbf{K}} < \mathbf{1} + \mathfrak{m}_{-\mathbf{1}}$ the MKN is always frozen.

(b) For $\overline{\mathbf{K}} = \mathbf{1} + \mathfrak{m}_{-\mathbf{1}}$ the MKN is critical if and only if

$$u = u^{\text{crit}}(1 + \mathfrak{m}_{-1}, \mathfrak{m}_{-1}) = \frac{\mathfrak{m}_{-1}}{\mathfrak{m}_{-1} + 1} , \tag{4.19}$$

otherwise it is frozen.

(c) In the **Boolean case, i.e. $\mathfrak{m}_{-\mathbf{1}} = \mathbf{1}$, and for $\overline{\mathbf{K}} > \mathbf{1} + \mathfrak{m}_{-\mathbf{1}} = \mathbf{2}$** the critical boundary is described by

$$u^{\text{crit}}_{\frac{1}{2}}\left(\overline{K}, 1\right) = \frac{1}{2}\left[1 \mp \sqrt{1 - \frac{2}{\overline{K}}}\right] \in (0,1) . \tag{4.20}$$

For

$$u^{\text{crit}}_{1}\left(\overline{K}, 1\right) < u < u^{\text{crit}}_{2}\left(\overline{K}, 1\right)$$

the MKN is chaotic, otherwise it is frozen. This agrees with previous results about Boolean KNs [Bastolla and Parisi, 1996].

(d) For $\mathfrak{m}_{-\mathbf{1}} < \mathbf{1}$ **and** $\mathbf{1}/(\mathbf{1} - \mathfrak{m}_{-\mathbf{1}}) > \overline{\mathbf{K}} > \mathbf{1} + \mathfrak{m}_{-\mathbf{1}}$ the critical boundary is described by

$$u^{\text{crit}}_{\frac{1}{2}}\left(\overline{K}, \mathfrak{m}_{-1}\right) = \frac{1}{\mathfrak{m}_{-1} + 1}\left(\mathfrak{m}_{-1} \mp \sqrt{1 - \frac{\mathfrak{m}_{-1} + 1}{\overline{K}}}\right) \in (0,1) . \tag{4.21}$$

For

$$u^{\text{crit}}_{1}\left(\overline{K}, \mathfrak{m}_{-1}\right) < u < u^{\text{crit}}_{2}\left(\overline{K}, \mathfrak{m}_{-1}\right)$$

the MKN is chaotic, otherwise it is frozen. For $\overline{K} = 1/(1 - \mathfrak{m}_{-1})$, $u^{\text{crit}}_1 = 0$ is not a valid solution for u anymore, as we require $u \in (0,1)$.

(e) For $\mathfrak{m}_{-\mathbf{1}} < 1$ **and** $\overline{\mathbf{K}} \geqslant \mathbf{1}/(\mathbf{1} - \mathfrak{m}_{-\mathbf{1}})$ the critical boundary is described by

$$u^{\text{crit}}\left(\overline{K}, \mathfrak{m}_{-1}\right) = \frac{1}{\mathfrak{m}_{-1} + 1}\left(\mathfrak{m}_{-1} + \sqrt{1 - \frac{\mathfrak{m}_{-1} + 1}{\overline{K}}}\right) \in (0,1) , \tag{4.22}$$

for larger values of u the MKN is frozen, otherwise it is chaotic.

We chose to solve the criticality condition (4.17) for u^{crit} (and not $\overline{K}^{\text{crit}}$), as from this presentation we easily see that for any values of $\overline{K}$ and $\mathfrak{m}_{-1}$ a MKN is kept in its frozen regime by choosing a sufficiently large u. Thus, our motivating question can be answered in the affirmative: Biasing update rules towards one of the discrete states indeed increases the critical connectivity, from a theoretical point of view, even beyond any bound.

In the Boolean case, the critical weights $u_{1/2}^{\text{crit}}$ from (4.20) are, of course, symmetric about 1/2, cf. case (c) in the above classification. In MKNs there still is a range of connectivities where we can freeze a network by choosing either sufficiently large or sufficiently small weights, cf. case (d). For higher connectivities, however, the option of choosing small weights ceases to exist, cf. case (e). Intuitively speaking, even if we set the weight to zero, the heterogeneity among the remaining states would still be too large. Mathematically, this is reflected in the solution u_1^{crit} from (4.21) becoming negative.

Now, suppose P_{nos} is a delta-distribution with a fixed number of states $\overline{S}$. Then, the upper bound $\overline{K} = 1 + \mathfrak{m}_{-1}$ of case (a) in the above classification is precisely the critical connectivity $\overline{K}^{\text{crit}}$ of the unbiased MKN from (4.12). Furthermore, in case (b) the critical value u^{crit} from (4.19) is equal to $1/\overline{S}$. In agreement with Lemma 4.1, we see that, if the connectivity of a MKN with biased update rules is below the critical connectivity $\overline{K}^{\text{crit}}$ (of the unbiased MKN), this MKN will always be frozen, as the heterogeneity is already maximal in the unbiased situation. If its connectivity is equal to $\overline{K}^{\text{crit}}$, it is critical if and only if the bias u is chosen in such a way that the resulting $P_{\overline{S}}$ is uniform. (The MKN then, of course, becomes unbiased.) Above $\overline{K}^{\text{crit}}$, we can freeze any MKN by choosing a sufficiently heavy bias. For a visualization of the above classification and discussion, see Figure 4.3A.

4.3.5 Network simulations

To further visualize our results, we choose six realizations of frozen, critical and chaotic MKNs, cf. Figure 4.3B–K. Each network has $N = 100$ nodes and each node has $\overline{S} = 3$ states, i.e. $\mathfrak{m}_{-1} = 1/2$. We consider two delta-distributed degrees at $\overline{K} = 2$ (shown in B–F) and $\overline{K} = 4$ (shown in G–K). For each connectivity we generate a frozen, critical and chaotic network by sampling the update rules from distribution (4.3). For the frozen networks we set $u = 0.95$, for the critical networks we set $u = u^{\text{crit}}(2, 1/2) \approx 0.8604$

and $u^{\text{crit}}(4, 1/2) = 2/3$ from (4.22), respectively, and for the chaotic networks we set $u = 1/3$. Observe that the latter choice leads to the unbiased distribution from (4.2). Blue, green and red markers in subfigure A show the position of these values of u in the $\overline{K}$-u-plane. The blue markers lie above the critical boundary in the frozen regime, both green markers are located on the critical boundary, and the red markers are in midst the chaotic regime.

Subfigures B and G show $D(d)$ from (4.7) for both connectivities, $\overline{K} = 2$ as well as $\overline{K} = 4$, and the three respective values of u. For the frozen networks (blue curves) $d^\star = 0$ is the only fixed point and it is globally attracting. The fixed point $d^\star$ becomes critical in the critical networks (green curves), and in the chaotic networks (red curves) an additional fixed point $d^{\star\star}$ exists, which is now the global attractor. The additional fixed points lie at $d^{\star\star} \approx 0.498$ in B and at $d^{\star\star} \approx 0.661$ in G.

For each of the six networks, two initial configurations $\mathbf{x}(0)$ and $\mathbf{x}'(0)$ with Hamming distance $d(0) = 0.1$ are chosen and each is iterated for 50 time-steps. Plots of the simulated Hamming distance

$$d(t) = \sum_{i=1}^{N} \left(1 - \delta_{x_i(t), x_i'(t)}\right)$$

between the two trajectories $\mathbf{x}(t)$ and $\mathbf{x}'(t)$ for the six networks are shown in subfigures C ($\overline{K} = 2$) and H ($\overline{K} = 4$). In the frozen networks (blue curves) the Hamming distance quickly reaches its stationary value 0 indicating that both trajectories have re-converged. If we discard the first 20 time-steps, the Hamming distances fluctuate around 0.501 in the chaotic network with connectivity 2 and around 0.663 in the chaotic network with connectivity 4, cf. the red curves and the dashed mean-lines in subfigures C and H, respectively. These means agree well with the values of the "mean-field attractors" $d^{\star\star} \approx 0.498$ and $d^{\star\star} \approx 0.661$, respectively. This is a nice corroboration of our analytical studies.

Subfigures D–F and I–K show the time-course $x_i(t)$, $i = 1, 2, \ldots, 25$, $t = 1, 2, \ldots 50$, for the frozen, critical and chaotic networks with $\overline{K} = 2$ and $\overline{K} = 4$. The three states of a node are represented as black, grey and white boxes. In D and I, both frozen networks quickly reach an equilibrium. While the critical networks in E and J exhibit clear short-periodic oscillations after approximately 10 time-steps, no pattern or periodicity is discernible in the chaotic networks in F and K. We know, of course,

that ultimately also the chaotic networks will fall into a periodic orbit due to the finite size of the state-space, cf. Proposition 4.1. Note that subfigures C–F as well as H–K all have the same X-axis, namely time running from 1 to 50 as indicated in F and K.

4.4 Ensembles of trajectories

The Hamming distance looks at the similarity of two trajectories. More generally, we could ask how a whole *ensemble* of trajectories behaves. A biological motivation for this question is that in molecular biology experimental data are often average concentrations in cell cultures. Mathematically, such a cell culture can be modeled as an ensemble of trajectories of the same MM.

4.4.1 A dynamical system modeling ensembles of trajectories

Let $(G, \mathbf{S}, \mathbf{f})$ be a MM. In order to describe ensembles of trajectories of $(G, \mathbf{S}, \mathbf{f})$ and relative frequencies therein, we consider time-courses of distributions over the Σ_i, $i = 1, 2, \ldots, N$.

Remark 4.6. The MM $(G, \mathbf{S}, \mathbf{f})$ gives rise to a time-discrete dynamical system as follows. To each node i we associate a time-dependent variable

$$\tilde{x}_i(t) = \begin{pmatrix} \tilde{x}_i^0(t) \\ \tilde{x}_i^1(t) \\ \vdots \\ \tilde{x}_i^{S_i-1}(t) \end{pmatrix}, \quad \sum_{s \in \Sigma_i} \tilde{x}_i^s(t) = 1 \,,$$

describing distributions over Σ_i. We let $\tilde{\mathbf{x}}(t) = (\tilde{x}_i(t))_{i=1}^N$. The evolution of $\tilde{\mathbf{x}}(t)$ is governed by the iteration $\tilde{\mathbf{x}}(t+1) = \tilde{\mathbf{f}}\left(\tilde{\mathbf{x}}(t)\right)$, $t = 0, 1, 2, \ldots$, where $\tilde{\mathbf{f}}$ is defined such that

$$\tilde{x}_i^s(t+1) = \sum_{(\xi_1, \xi_2, \ldots, \xi_{K_i}) | f_i(\xi_1, \xi_2, \ldots, \xi_{K_i}) = s} \prod_{k=1}^{K_i} \tilde{x}_{i_k}^{\xi_k}(t) \,, \tag{4.23}$$

$s \in \Sigma_i$, $i = 1, 2, \ldots, N$.

We call trajectories of the dynamical system from Remark 4.6 $\tilde{\mathbf{f}}$-trajectories of $(G, \mathbf{S}, \mathbf{f})$, in order to tell them apart from trajectories of the dynamical system from Remark 4.2.

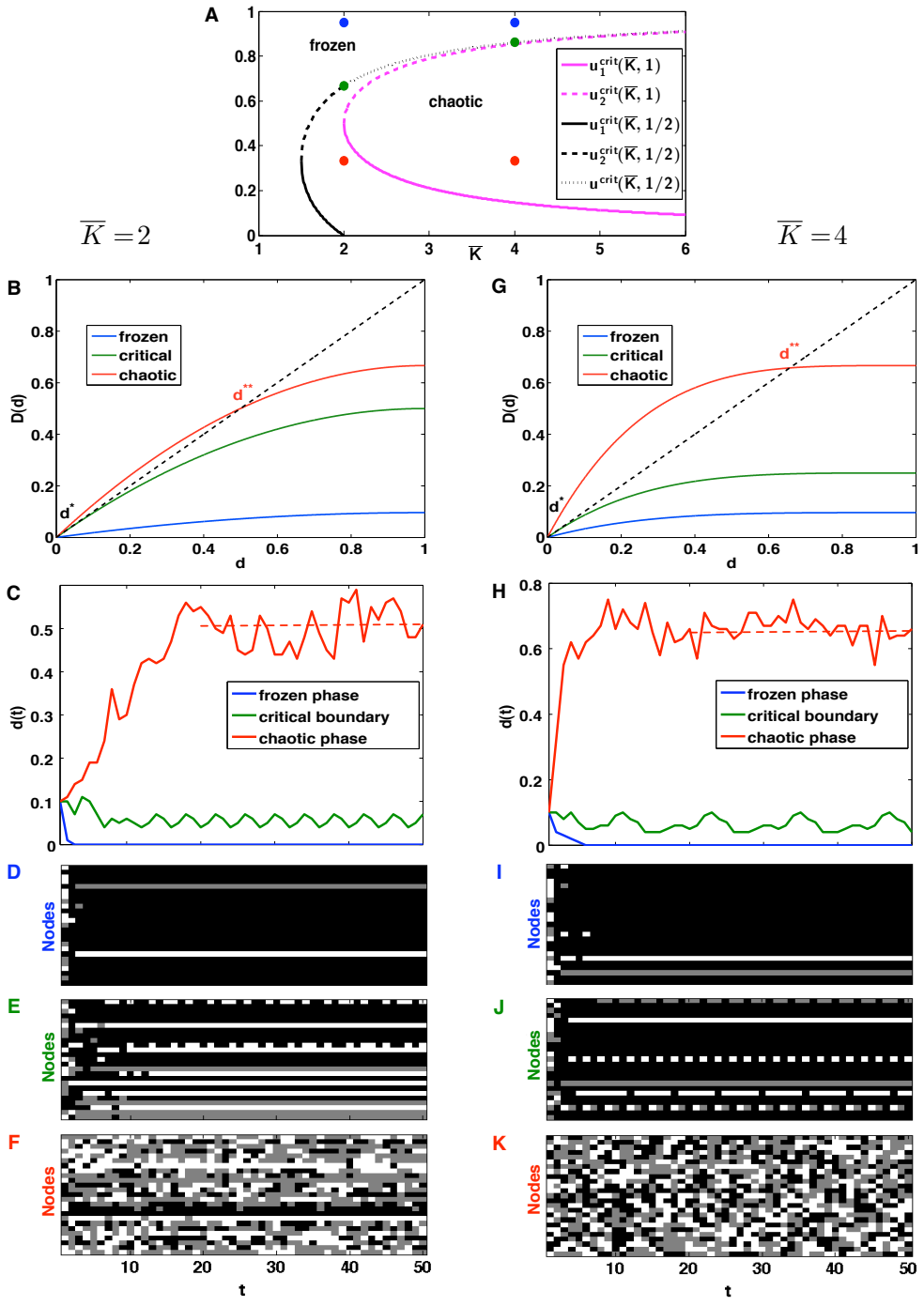

Figure 4.3: **(A)** Critical boundaries $u^{\text{crit}}(\overline{K}, \mathfrak{m}_{-1})$ from section 4.3.4.2. For $\mathfrak{m}_{-1} = 1$ the two branches $u_{1/2}^{\text{crit}}(\overline{K}, 1)$ from (4.20) are shown. For $\mathfrak{m}_{-1} = 1/2$ the critical boundary consists of three parts: $u_{1/2}^{\text{crit}}(\overline{K}, 1/2)$ from (4.21) and $u^{\text{crit}}(\overline{K}, 1/2)$ from (4.22). **(B–K)** Network simulations, cf. section 4.3.5.

Remark 4.7. The right-hand side of (4.23) is the probability for f_i to yield value s given that its inputs i_k are independent and assume values $\xi_k \in \Sigma_{i_k}$ with probabilities given by $\tilde{x}_{i_k}^{\xi_k}(t)$. Now, suppose the MM $(G, \mathbf{S}, \mathbf{f})$ is given as a realization of a MKN with large N. Then, in the N-dependent time-domain $[0, t_N]$ from Lemma 2.1, in which we may assume the inputs of a node to be independent, the dynamical system from Remark 4.6 describes the evolution of probability distributions over the ranges Σ_i of the nodes $i = 1, 2, \ldots, N$. More precisely, if at time t we choose values $x_i(t) \in \Sigma_i$ according to the distributions $\tilde{x}_i(t)$, then $\tilde{x}_i(t+1)$ contains the probabilities for $x_i(t+1) = f_i\left(x_{i_1}(t), x_{i_2}(t), \ldots, x_{i_{K_i}}(t)\right)$ to be equal to the $s \in \Sigma_i$. For this reason, $\tilde{\mathbf{f}}$-trajectories can be approximated by relative frequencies in large ensembles of trajectories of $(G, \mathbf{S}, \mathbf{f})$.

A node i is called *deterministic* at time t, if $\tilde{x}_i^s(t) = 1$ for some $s \in \Sigma_i$. If all nodes are deterministic at t, we call the state $\tilde{\mathbf{x}}(t)$ deterministic. Let Ξ denote the canonical bijection between the states $\mathbf{x}$ of the dynamical system from Remark 4.2 and the deterministic states $\tilde{\mathbf{x}}$ of the dynamical system from Remark 4.6. This is to say that component-wise Ξ maps $x_i \in \Sigma_i$ on the probability distribution

$$\tilde{x}_i^s = \begin{cases} 1\,, & \text{if } s = x_i \\ 0\,, & \text{otherwise} \end{cases}\,, \quad s \in \Sigma_i\,,$$

over Σ_i.

Proposition 4.2. *The function $\tilde{\mathbf{f}}$ maps deterministic states onto deterministic states, and the diagram*

$$\begin{array}{ccc} \prod_{i=1}^N \Sigma_i & \xrightarrow{\Xi} & \Xi\left(\prod_{i=1}^N \Sigma_i\right) \\ \Big\downarrow{\scriptstyle \mathbf{f}} & & \Big\downarrow{\scriptstyle \tilde{\mathbf{f}}} \\ \prod_{i=1}^N \Sigma_i & \xrightarrow{\Xi} & \Xi\left(\prod_{i=1}^N \Sigma_i\right) \end{array}$$

commutes. So $\mathbf{f}$ is compatible with $\tilde{\mathbf{f}}$.

Proof. We fix $\mathbf{x} = (x_i)_{i=1}^N \in \prod_{i=1}^N \Sigma_i$ and let $\tilde{\mathbf{x}} = (\tilde{x}_i)_{i=1}^N$ be its image under Ξ. The function $\tilde{\mathbf{f}}$ maps a component $\tilde{x}_i$ on the distribution

$$\left(\sum_{(\xi_1, \xi_2, \ldots, \xi_{K_i}) \mid f_i(\xi_1, \xi_2, \ldots, \xi_{K_i}) = s} \prod_{k=1}^{K_i} \tilde{x}_{i_k}^{\xi_k} \right)_{s \in \Sigma_i} .$$

The only non-zero contribution to the sum over the $(\xi_1, \xi_2, \ldots, \xi_{K_i})$ is the combination $\xi_k = x_{i_k}$, $k = 1, 2, \ldots, K_i$, which is included if and only if $s = f_i\left(x_{i_1}, x_{i_2}, \ldots, x_{i_{K_i}}\right)$. In this case, $\prod_{k=1}^{K_i} \tilde{x}_{i_k}^{\xi_k} = 1$. Hence, $\tilde{x}_i$ is mapped by $\tilde{\mathbf{f}}$ onto the distribution $(\tilde{y}^s)_{s\in\Sigma_i}$,

$$\tilde{y}^s = \begin{cases} 1\,, & \text{if } s = f_i\left(x_{i_1}, x_{i_2}, \ldots, x_{i_{K_i}}\right) \\ 0\,, & \text{otherwise} \end{cases} \quad , \quad s \in \Sigma_i\,.$$

We, thus, see that the image of $\tilde{\mathbf{x}}$ under $\tilde{\mathbf{f}}$ is deterministic and given by the image of $\mathbf{f}(\mathbf{x})$ under Ξ. □

4.4.2 A generalized Hamming distance

Let $\mathcal{K}$ be a MKN. To avoid drowning the main ideas in too cumbersome formulae, we restrict ourselves to the special case of a MKN with $P_{\text{nos}} = \delta_S$. We begin by stating some technical preliminaries, which will be needed in the following. Let $\ell(\zeta, z)$ denote the probability that ζ fields, which are randomly filled with numbers $0, 1, \ldots, S-1$ according to P_S, contain exactly z different elements. For a vector $(\kappa_\zeta)_{\zeta=1}^S$, we simply write $\ell\left((\kappa_\zeta), z\right)$ instead of $\ell\left(\prod_{\zeta=1}^S \zeta^{\kappa_\zeta}, z\right)$. Concise formulas for the $\ell(\zeta, z)$ are difficult to compute, and one has to resort to exhaustive enumeration. We can, however, prove the following relations.

Lemma 4.4. *1. For any S and P_S we have $\ell(1,1) > \ell(2,2) > \cdots > \ell(S,S)$.*

2. For $S = 3$ and any P_3 we have $\ell(2,2) \leqslant \ell(3,2)$.

3. For any S and P_S we have $\ell(1,1) \geqslant \ell(2,1) \geqslant \cdots \geqslant \ell(S,1)$ with equalities if and only if P_S is a degenerate delta-distribution.

Proof. Claims 1 and 3 are obvious. To prove statement 2, we let $\pi_s := P_3(s)$, $s \in \{0,1,2\}$, and compute

$$\begin{aligned} \ell(2,2) &= 2\left[\pi_0\pi_1 + \pi_0\pi_2 + \pi_1\pi_2\right] \qquad \text{as well as} \\ \ell(3,2) &= 3\left[\pi_0^2\pi_1 + \pi_0^2\pi_2 + \pi_1^2\pi_0 + \pi_1^2\pi_2 + \pi_2^2\pi_0 + \pi_2^2\pi_1\right]\,. \end{aligned}$$

After substituting $\pi_2 = 1 - \pi_0 - \pi_1$, the equation $\ell(2,2) = \ell(3,2)$ has solutions

$$\pi_0^{\left(\frac{1}{2}\right)}(\pi_1) = \frac{-1 + 10\pi_1 - 9\pi_1^2 \mp (3\pi_1 - 1)\sqrt{1 - 10\pi_1 + 9\pi_1^2}}{2\,(9\pi_1 - 1)}\,.$$

On the unit interval, the solutions $\pi_0^{(1/2)}(\pi_1)$ are real for $0 \leqslant \pi_1 < 1/9$, $\pi_1 = 1/3$, and $\pi_1 = 1$. For $0 < \pi_1 < 1/9$, $\pi_0^{(1)}(\pi_1) < 0$ and $\pi_0^{(2)}(\pi_1) > 1$ are invalid solutions (they

need to be probabilities!). Hence, $\ell(2,2) = \ell(3,2)$ has four distinct solutions (π_0, π_1, π_2) in $[0,1]^3$: $(0,0,1)$, $(1,0,0)$, $(1/3,1/3,1/3)$, and $(0,1,0)$. One easily computes that, for instance, $\ell(2,2) = 1/2 < 3/4 = \ell(3,2)$ if $(\pi_0, \pi_1, \pi_2) = (1/2, 1/2, 0)$. This proves $\ell(2,2) \leqslant \ell(3,2)$ on $[0,1]^3$ with equality at the four distinct solutions from above. □

According to Definition 4.3, the Hamming distance $(d(t))_{t\geqslant 0}$ of $\mathcal{K}$ is a sequence of probabilities that for some random realization a node i has two different values in two different trajectories. Now, if we are given a large ensemble of trajectories we can again ask how likely it is that i has at least two different values in the whole ensemble. Since we are dealing with *multistate* KNs we may even ask how likely it is that i assumes exactly z different values in the ensemble, where $z = 1, 2, \ldots, S$. For this reason, we now study the average number of non-zero entries in $\tilde{\mathbf{f}}$-trajectories $\tilde{\mathbf{x}}(t)$. We begin by stating the counterpart of Lemma 4.2.

Lemma 4.5. *Let $\left(Z^\zeta(0)\right)_{\zeta=1}^S$, $\sum_{\zeta=1}^S Z^\zeta(0) = 1$, be a distribution. Consider the following random experiment: Generate a realization of $\mathcal{K}$. Choose a configuration $\tilde{\mathbf{x}}(0)$ in a way such that the probability for a distribution $\tilde{x}_i(0)$ to have (exactly) ζ non-zero entries is given by $Z^\zeta(0)$, $\zeta = 1, 2, \ldots, S$. Iterate $\tilde{\mathbf{x}}(0)$ one time-step under $\tilde{\mathbf{f}}$ yielding configuration $\tilde{\mathbf{x}}(1)$. Then, the probability $Z^z(1)$ that for a randomly chosen node i the distribution $\tilde{x}_i(1)$ has (exactly) z non-zero entries, $z = 1, 2, \ldots, S$, is given by*

$$Z^z(1) = \sum_{K=1}^{K_{\max}} P_{in}(K) \sum_{\kappa_1+\ldots+\kappa_S=K} \binom{K}{\kappa_1, \ldots, \kappa_S} \prod_{\zeta=1}^{S} \left(Z^\zeta(0)\right)^{\kappa_\zeta} \cdot \ell\left((\kappa_\zeta), z\right) .$$

In particular, $Z^z(1)$ is independent of how the actual values in $\tilde{\mathbf{x}}(0)$ are chosen but depends only on the probabilities $Z^\zeta(0)$ for the distributions $\tilde{x}_i(0)$ to have ζ non-zero entries, $\zeta = 1, 2, \ldots, S$.

Proof. Consider a realization of $\mathcal{K}$ and a randomly chosen node i. We describe its inputs by a vector $(\kappa_1, \kappa_2, \ldots, \kappa_S)$ indicating the number of inputs with $1, 2, \ldots, S$ non-zero entries in $\tilde{\mathbf{x}}(0)$. Clearly, $\kappa_1 + \kappa_2 + \ldots + \kappa_S = K_i$. Recall that in the configuration model the inputs i_k of i are chosen randomly from V. Hence, the probability for the configuration $(\kappa_\zeta)_{\zeta=1}^S$ is given by

$$\binom{K_i}{\kappa_1, \ldots, \kappa_S} \prod_{\zeta=1}^{S} \left(Z^\zeta(0)\right)^{\kappa_\zeta} .$$

The number of different tuples $(\xi_1, \xi_2, \ldots, \xi_{K_i})$ satisfying $\prod_{k=1}^{K_i} \tilde{x}_{i_k}^{\xi_k}(0) \neq 0$ in (4.23) is $\prod_{\zeta=1}^S \zeta^{\kappa_\zeta}$. The $\tilde{x}_i^{f_i(\xi_1,\xi_2,\ldots,\xi_{K_i})}(1)$ belonging to these tuples are the different non-zero

entries of $\tilde{x}_i(1)$. The probability that their number is equal to z is $\ell\left((\kappa_\zeta), z\right)$. Averaging over K_i yields the claim. □

Instead of the Hamming distance $(d(t))_{t\geqslant 0}$ of $\mathcal{K}$ we can, therefore, also study a sequence $Z(t) = (Z^z(t))_{z=1}^S \in \mathbb{R}^S$ which is consistent in the sense of Lemma 4.5, i.e. governed by the iteration

$$Z(t+1) = C\left(Z(t)\right) \ , \tag{4.24}$$

where the z-th component $C^z\left(Z(t)\right)$ of the right-hand side is given by

$$\sum_{K=1}^{K_{\max}} P_{\text{in}}(K) \sum_{\kappa_1+\ldots+\kappa_S=K} \binom{K}{\kappa_1,\ldots,\kappa_S} \prod_{\zeta=1}^{S} \left(Z^\zeta(t)\right)^{\kappa_\zeta} \cdot \ell\left((\kappa_\zeta), z\right) \ , \tag{4.25}$$

$z = 1, 2, \ldots, S$.

Remark 4.8. Once more, we argue that, for large N, Lemma 2.1 allows us to assume the inputs of a node to be independent in a realization of $\mathcal{K}$. We can, thus, approximate $Z^z(t)$ by the fraction of nodes with z non-zero entries in a $\tilde{\mathbf{f}}$-trajectory $\tilde{\mathbf{x}}(t)$ of a specific realization of $\mathcal{K}$. By Remark 4.7, we can also approximate $Z^z(t)$ by the fraction of nodes with z different states in a large ($\Omega \gg S$) ensemble of trajectories $\mathbf{x}^q(t)$, $q = 1, 2, \ldots, \Omega$, of a specific realization of $\mathcal{K}$,

$$Z^z(t) \approx \frac{1}{N} \cdot \#\left\{ i \mid (x_i^q(t))_{q=1}^{\Omega} \text{ has } z \text{ different components.} \right\} \ , \tag{4.26}$$

$z = 1, 2, \ldots, S$. We will use this approximation in section 4.4.4.

4.4.3 Synchronization in ensembles of trajectories

Especially when conducting transcriptome-wide measurements, e.g. by microarrays, we want the single cells in our experimental sample to act synchronously, as only then the experimentally observed average concentrations are representative of the single cells. Intuitively, one would expect that for frozen MKNs, an ensemble of trajectories of a realization converges, whereas for chaotic MKNs it diverges. Let us first check, if this can also be analytically seen from system (4.24).

To this end, we investigate the fixed point $Z^\star = (1, 0, \ldots, 0)$ of (4.24). It corresponds to an ensemble of identical trajectories. (That $Z^\star$ is, indeed, a fixed point can be easily seen; note $C^z\left(Z^\star\right) = \ell(1, z)$.) We now show that the stability properties of $Z^\star$ change precisely at the critical boundary of $\mathcal{K}$. The distributions $Z(t)$ live on the affine hyperplane of $\mathbb{R}^S$ defined by $\sum_{z=1}^S Z^z(t) = 1$. In order to take derivatives, we choose as

a global chart the projection on the first $S-1$ coordinates. We remark that the choice of charts, in general, does affect the Jacobian, but not its eigenvalues, as a change of charts merely means a change of basis in the tangent space. Hence, this choice is not crucial for stability analyses.

Let us now compute the Jacobian $J = \mathrm{D}C|_{Z_\star}$ of C at $Z^\star$. First, consider the case of fixed K. In global coordinates we can write:

$$C^z\left(Z^1,\ldots,Z^{S-1}\right) = \sum_{\kappa_1+\ldots+\kappa_S=K} \binom{K}{\kappa_1,\ldots,\kappa_S} \prod_{\zeta=1}^{S-1} \left(Z^\zeta\right)^{\kappa_\zeta} \left(1-\sum_{\zeta=1}^{S-1} Z^\zeta\right)^{\kappa_S} \ell\left(\left(\kappa_\zeta\right),z\right)$$

Differentiating with respect to Z^s yields

$$\frac{\partial C^z}{\partial Z^s} = \sum_{\kappa_1+\ldots+\kappa_S=K} \binom{K}{\kappa_1,\ldots,\kappa_S} \ell\left(\left(\kappa_\zeta\right),z\right) \cdot \prod_{\zeta\neq s,S} \left(Z^\zeta\right)^{\kappa_\zeta} \left[-\left(Z^s\right)^{\kappa_s} \kappa_S \left(1-\sum_{\zeta=1}^{S-1} Z^\zeta\right)^{\kappa_S-1} + \kappa_s \left(Z^s\right)^{\kappa_s-1} \left(1-\sum_{\zeta=1}^{S-1} Z^\zeta\right)^{\kappa_S} \right],$$

where, formally, $0\cdot 0^{-1}=0$. The evaluation of this term at $Z^\star$ is

$$\left.\frac{\partial C^z}{\partial Z^s}\right|_{Z^\star} = K\cdot\ell\left(s,z\right) - K\cdot\ell\left(S,z\right)\ .$$

To see this, note that the only non-zero contributions to the sum over the $(\kappa_1,\ldots,\kappa_S)$ are the combinations $(K,0,\ldots,0,0)$ and $(K-1,0,\ldots,0,1)$ if $s=1$, and the combinations $\kappa_1=K-1,\ldots,\kappa_s=1,\ldots,\kappa_S=0$ and $\kappa_1=K-1,\ldots,\kappa_s=0,\ldots,\kappa_S=1$ if $s\neq 1$.

For general P_{in} it follows

$$\left.\frac{\partial C^z}{\partial Z^s}\right|_{Z^\star} = \sum_{K=1}^{K_{\max}} P_{\mathrm{in}}\left(K\right) K\left[\ell\left(s,z\right)-\ell\left(S,z\right)\right] = \overline{K}\left[\ell\left(s,z\right)-\ell\left(S,z\right)\right]\ ,$$

and we obtain

$$J = \overline{K}\cdot\left[\begin{pmatrix} \ell(1,1) & \ell(2,1) & \cdots & \ell(S-1,1) \\ 0 & \ell(2,2) & \cdots & \ell(S-1,2) \\ \vdots & \vdots & \ddots & \vdots \\ 0 & 0 & \cdots & \ell(S-1,S-1) \end{pmatrix} - \begin{pmatrix} \ell(S,1) & \ell(S,1) & \cdots & \ell(S,1) \\ \ell(S,2) & \ell(S,2) & \cdots & \ell(S,2) \\ \vdots & \vdots & \ddots & \vdots \\ \ell(S,S-1) & \ell(S,S-1) & \cdots & \ell(S,S-1) \end{pmatrix}\right]. \tag{4.27}$$

Lemma 4.6. *The eigenvalues of J are $\overline{K} \cdot \ell\,(s,s)$, $s = 2,3,\ldots,S$.*

Proof. According to (4.27), we write $J = \overline{K}\,(J_1 - J_2)$ with $(S-1)\times(S-1)$ matrices J_1 and J_2. J_2 consists of identical columns $\mathfrak{a}$. We extend J_1 to an $S \times S$ upper triangular matrix J_1' by an S-th row $(0,0,\ldots,\ell(S,S))$ and column $(\ell(S,1),\ell(S,2),\ldots,\ell(S,S))^\top = \left(\mathfrak{a}^\top, \ell(S,S)\right)^\top$. Let $s \in \{2,3,\ldots,S\}$ and $v_s = \left(v_s^\zeta\right)_{\zeta=1}^{S}$ be an eigenvector to the eigenvalue $\ell(s,s)$ of J_1'. As J_1' is a left-stochastic matrix, it follows from $\ell(s,s)v_s = J_1'v_s$ that $\ell(s,s)\sum_{\zeta=1}^{S} v_s^\zeta = \sum_{\zeta=1}^{S} v_s^\zeta$. Thus, $\sum_{\zeta=1}^{S} v_s^\zeta = 0$, since $\ell(s,s) < 1$. As J_2 consists of identical columns $\mathfrak{a}$ this implies $J_2\left(v_s^\zeta\right)_{\zeta=1}^{S-1} = -v_s^S\mathfrak{a}$. It follows

$$\begin{aligned}(J_1 - J_2)\left(v_s^\zeta\right)_{\zeta=1}^{S-1} &= (J_1 \mid \mathfrak{a})\left(v_s^\zeta\right)_{\zeta=1}^{S} - v_s^S\mathfrak{a} - J_2\left(v_s^\zeta\right)_{\zeta=1}^{S-1} \\ &= \ell(s,s)\left(v_s^\zeta\right)_{\zeta=1}^{S-1} - v_s^S\mathfrak{a} + v_s^S\mathfrak{a} \\ &= \ell(s,s)\left(v_s^\zeta\right)_{\zeta=1}^{S-1},\end{aligned}$$

which shows that $\overline{K}\ell(s,s)$ is an eigenvalue of J. □

From Lemma 4.4.1 it follows that the largest eigenvalue is $\overline{K} \cdot \ell\,(2,2)$. Further note that $\ell\,(2,2) = \sum_{s=0}^{S-1} P_S(s)\,(1 - P_S(s)) = p_S = \overline{p}$. The phase transition criterion from Theorem 4.1 together with Theorem 2.2, thus, implies

Theorem 4.2. *The dynamic regimes of MKNs from Definition 4.4 have the following characteristics.*

frozen regime: *$Z^\star$ is a hyperbolic and asymptotically stable fixed point.*

critical boundary: *The fixed point $Z^\star$ is critical.*

chaotic regime: *The fixed point $Z^\star$ is unstable.*

Thus, our intuition about synchronization in ensembles of trajectories agrees with the behavior of system (4.24). Whereas for frozen MKNs we may expect ensembles to synchronize over time, this will not be the case for chaotic MKNs. In other words, we have derived a further characterization of the dynamic regimes from Definition 4.4. We remark that the dynamical system from (4.24) can also be used to study the behavior of KNs with an extension of Boolean logic called fuzzy logic [Wittmann and Theis, 2010a].

4.4.4 Example and simulations

We finish by detailing the behavior of the distributions $Z(t)$ in a specific example, more precisely, in the case $S = 3$. The distribution P_3 will be assumed to be non-degenerate, i.e. $P_3(s) \neq 1$ for all $s \in \{0, 1, 2\}$. We work again in the projection of (4.24) on the first two coordinates. Hence, we are dealing with the planar system

$$\begin{pmatrix} Z^1(t+1) \\ Z^2(t+1) \end{pmatrix} = \begin{pmatrix} C^1\left(Z^1(t), Z^2(t)\right) \\ C^2\left(Z^1(t), Z^2(t)\right) \end{pmatrix} . \tag{4.28}$$

Lemma 4.7. *There exist functions $Z_1^2\left(Z^1\right)$ and $Z_2^2\left(Z^1\right)$ around $Z^\star$, which satisfy $C^1\left(Z^1, Z_1^2\left(Z^1\right)\right) = Z^1$ and $C^2\left(Z^1, Z_2^2\left(Z^1\right)\right) = Z^2$, respectively. Moreover,*

$$\frac{dZ_1^2}{dZ^1}(1) = -\frac{\overline{K}\left[\ell(1,1) - \ell(3,1)\right] - 1}{\overline{K}\left[\ell(2,1) - \ell(3,1)\right]} \qquad \textit{and} \tag{4.29}$$

$$\frac{dZ_2^2}{dZ^1}(1) = -\frac{-\overline{K}\ell(3,2)}{\overline{K}\left[\ell(2,2) - \ell(3,2)\right] - 1} . \tag{4.30}$$

Proof. From (4.27) we read off

$$\left.\frac{\partial\left(C^1\left(Z^1, Z^2\right) - Z^1\right)}{\partial Z^2}\right|_{Z^\star} = \overline{K}\left[\ell(2,1) - \ell(3,1)\right] \qquad \text{and}$$

$$\left.\frac{\partial\left(C^2\left(Z^1, Z^2\right) - Z^2\right)}{\partial Z^2}\right|_{Z^\star} = \overline{K}\left[\ell(2,2) - \ell(3,2)\right] - 1 .$$

By Lemma 4.4.3 and 4.4.2 these derivatives do not vanish. (Recall that we assumed P_3 to be non-degenerate.) The claim follows from the implicit function theorem. □

Lemma 4.8. *It holds $dZ_2^2/dZ^1(1) < 0$. Moreover, the dynamic regimes of MKNs from Definition 4.4 have the following characteristics:*

frozen regime: $\dfrac{dZ_1^2}{dZ^1}(1) > -1 , \quad \dfrac{dZ_2^2}{dZ^1}(1) > -1 .$

critical boundary: $\dfrac{dZ_1^2}{dZ^1}(1) = -1 , \quad \dfrac{dZ_2^2}{dZ^1}(1) = -1 .$

chaotic regime: $\dfrac{dZ_1^2}{dZ^1}(1) < -1 , \quad \dfrac{dZ_2^2}{dZ^1}(1) < -1 .$

Proof. Lemma 4.4.2 implies $\mathrm{d}Z_2^2/\mathrm{d}Z^1(1) < 0$. To determine the relation between nominator and denominator in (4.29) and (4.30) we compute

$$\begin{aligned} & \overline{K}\left[\ell(1,1)-\ell(3,1)\right]-1-\overline{K}\left[\ell(2,1)-\ell(3,1)\right] \\ = \; & \overline{K}\left[\ell(1,1)-\ell(3,1)-\ell(2,1)+\ell(3,1)\right]-1 \\ = \; & \overline{K}\left[1-\ell(2,1)\right]-1 \\ = \; & \overline{K}\ell(2,2)-1 \end{aligned}$$

and

$$\begin{aligned} & -\overline{K}\ell(3,2)-\overline{K}\left[\ell(2,2)-\ell(3,2)\right]+1 \\ = \; & \overline{K}\left[-\ell(3,2)-\ell(2,2)+\ell(3,2)\right]+1 \\ = \; & 1-\overline{K}\ell(2,2) \end{aligned}$$

Recall that $\ell(2,2)=\overline{p}$ as well as the phase transition criterion from Theorem 4.1. To obtain the claim, consider that according to Lemma 4.4.3 and 4.4.2 the denominators in (4.29) and (4.30) are positive and negative, respectively. □

Let us now visualize this for $P_{\mathrm{in}}(K)=\delta_{K,2}$. Here, the C^z from (4.25), $z=1,2$, are quadratic functions, and we can easily solve for

$$Z_1^2\left(Z^1\right)=\frac{-\alpha_5-\alpha_2Z^1+\sqrt{\left(\alpha_5+\alpha_2Z^1\right)^2-4\alpha_3\left(\alpha_6-Z^1+\alpha_4Z^1+\alpha_1\left(Z^1\right)^2\right)}}{2\alpha_3} \tag{4.31}$$

and

$$Z_2^2\left(Z^1\right)=\frac{1-\alpha_{11}-\alpha_8Z^1-\sqrt{\left(-1+\alpha_{11}+\alpha_8Z^1\right)^2-4\alpha_9\left(\alpha_{12}+\alpha_{10}Z^1+\alpha_7\left(Z^1\right)^2\right)}}{2\alpha_9} \tag{4.32}$$

with coefficients α_i from Table 4.1. Figures 4.4A–C show $Z_1^2\left(Z^1\right)$ and $Z_2^2\left(Z^1\right)$ from (4.31) and (4.32), respectively, for the three distributions

$$\begin{aligned} P_3^{(a)}(0)&=\frac{3}{4}\quad, & P_3^{(a)}(1)&=\frac{1}{8}\quad, & P_3^{(a)}(2)&=\frac{1}{8}\quad, \\ P_3^{(b)}(0)&=\frac{2}{3}\quad, & P_3^{(b)}(1)&=\frac{1}{6}\quad, & P_3^{(b)}(2)&=\frac{1}{6}\quad \text{and} \\ P_3^{(c)}(0)&=\frac{1}{2}\quad, & P_3^{(c)}(1)&=\frac{1}{4}\quad, & P_3^{(c)}(2)&=\frac{1}{4}\quad. \end{aligned} \tag{4.33}$$

Table 4.1: Coefficients α_i for Equations (4.31) and (4.32)

$\alpha_1 = \ell(1,1) - 2\ell(3,1) + \ell(9,1)$	$\alpha_2 = 2\ell(2,1) - 2\ell(3,1) - 2\ell(6,1) + 2\ell(9,1)$
$\alpha_3 = \ell(4,1) - 2\ell(6,1) + \ell(9,1)$	$\alpha_4 = 2\ell(3,1) - 2\ell(9,1)$
$\alpha_5 = 2\ell(6,1) - 2\ell(9,1)$	$\alpha_6 = \ell(9,1)$
$\alpha_7 = \ell(1,2) - 2\ell(3,2) + \ell(9,2)$	$\alpha_8 = 2\ell(2,2) - 2\ell(3,2) - 2\ell(6,2) + 2\ell(9,2)$
$\alpha_9 = \ell(4,2) - 2\ell(6,2) + \ell(9,2)$	$\alpha_{10} = 2\ell(3,2) - 2\ell(9,2)$
$\alpha_{11} = 2\ell(6,2) - 2\ell(9,2)$	$\alpha_{12} = \ell(9,2)$

One easily computes $\overline{p}^{(a)}\overline{K} = 13/32{\cdot}2 = 26/32$, $\overline{p}^{(b)}\overline{K} = 1/2{\cdot}2 = 1$, and $\overline{p}^{(c)}\overline{K} = 2/3{\cdot}2 = 4/3$. Thus, according to Theorem 4.1, MKNs with $P_{\text{in}}(K) = \delta_{K,2}$, $P_{\text{nos}}(S) = \delta_{S,3}$, and distributions P_3 as in (4.33) fall into the frozen, critical and chaotic regime. While in the frozen and critical regime (cf. Figures 4.4A and B) $Z^\star$ is the only fixed point, an additional (stable) fixed point $Z^{\star\star}$ emerges in the chaotic regime, cf. Figure 4.4C. (Intersections of $Z_1^2(Z^1)$ and $Z_2^2(Z^1)$ are, of course, fixed points of system (4.28).) Also compare Figures 4.4A–C to Lemma 4.8.

We now further investigate these situations by simulations. For each choice of P_3 from (4.33) (and $P_{\text{in}}(K) = \delta_{K,2}$, $P_{\text{nos}}(S) = \delta_{S,3}$) a realization of the MKN is generated. Figures 4.4D–F show the approximation of $Z(t)$ from (4.26) obtained in ensembles of trajectories of these realizations, see figure caption for technical details. We detect a nice agreement between the coordinates of the (attracting) fixed points in A–C and the equilibrium distributions in D–F. (Refer to the figure caption for numerical details.)

4.5 Discussion

When basing dynamical systems on MMs one needs to make a fundamental decision about how update rules act on variables. Either an update rule *absolutely* determines the value of a variable at the next time-step, or it determines the change of the variable *relative* to its previous state, i.e. whether the variable is assigned the next higher or the next lower state. KNs with multiple states using the latter update policy are called *random-walk networks*. Analyses of these networks revealed a phase transition between a chaotic and an ordered regime similar to the SKN [Ballesteros and Luque, 2005; Luque and Ballesteros, 2004]. In the chaotic regime, variables follow random-walk like trajectories, which gives the name to these networks. In here, we did not consider

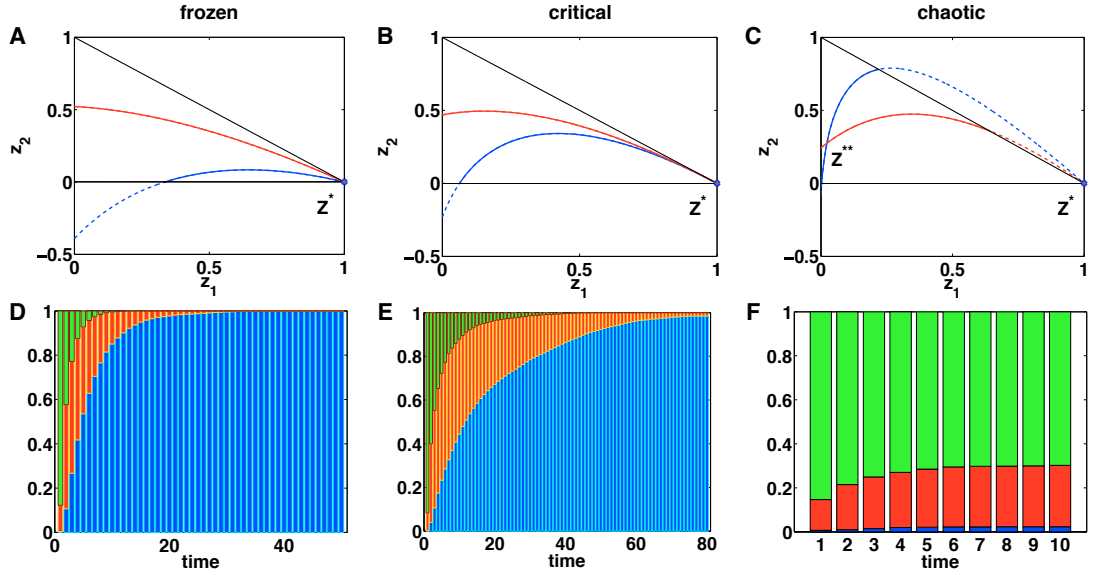

Figure 4.4: The situation of delta-distributed S and K at $S = 3$ and $K = 2$. **(A)**–**(C)** show $Z_1^2\left(Z^1\right)$ (blue) and $Z_2^2\left(Z^1\right)$ (red) from (4.31) and (4.32), respectively, for **(A)** $P_3^{(a)}$, **(B)** $P_3^{(b)}$, and **(C)** $P_3^{(c)}$ from (4.33). The coordinates of the fixed points are $Z^\star = (1, 0)$ and in **(C)** $Z^{\star\star} \approx (0.0226, 0.2747)$. **(D)**–**(F)** show approximations of $Z(t) = (Z^z(t))_{z=1}^3$ according to (4.26). Realizations of MKNs with $N = 10^4$ nodes, $P_{\text{in}}(K) = \delta_{K,2}$, $P_{\text{nos}}(S) = \delta_{S,3}$, and P_3 as in (A)–(C) were generated, and approximations were calculated in ensembles of $\Omega = 10^3$ trajectories. Color legend: $Z^1(t)$: blue, $Z^2(t)$: red, $Z^3(t)$: green. The equilibrium distributions are **(D)** $Z(50) = (0.9993, 0.0007, 0)$, **(E)** $Z(80) = (0.9838, 0.0162, 0)$, and **(F)** $Z(10) = (0.0234, 0.2783, 0.6983)$.

random-walk networks but KNs with multiple states using the first update policy; we referred to them as MKNs.

Previous studies of MKNs by Solé et al. [2000] are restricted to the biologically implausible case in which all nodes have the same number of states. In agreement with our more general results, it has been shown that in the case of unbiased update rules an increasing number of states decreases the critical connectivity down to 1. It is tempting to assume that this stays true (at least in a qualitative sense) when replacing the (fixed) number of states by the mean of a non-degenerate distribution. However, our results demonstrate that, in general, this is wrong. From the critical connectivity in (4.12) we see that the crucial parameter is not the mean number of states, but the mean $\mathfrak{m}$ of the reciprocal number of states.

Generally speaking, the mean of a strictly positive, non-constant random variable $\mathcal{S}$ and the mean of $1/\mathcal{S}$ are related by

$$\mathbb{E}\left(\frac{1}{\mathcal{S}}\right) > \frac{1}{\mathbb{E}\left(\mathcal{S}\right)} ,$$

for a proof see e.g. Kendall et al. [1987]. Furthermore, we can easily come up with a distribution

$$P(\mathcal{S}=2) = \frac{s-1}{s} \qquad \text{and} \qquad P\left(\mathcal{S}=s^2\right) = 1/s$$

for $s \in \mathbb{N}$, such that $\mathbb{E}(\mathcal{S}) \to \infty$ but $\mathbb{E}\left(1/\mathcal{S}\right) \to 1/2$ as $s \to \infty$. Setting $P_{\text{nos}} = P$, the critical connectivity from (4.12) increases up to 2 as $s \to \infty$, although the mean number of states grows beyond any bound.

In this chapter, we investigated a general class of MKNs and demonstrated that they exhibit a phase transition from frozen to chaotic behavior as the connectivity of the network grows. To this end, we formally introduced the Hamming distance between two configurations as an order parameter for MKNs and investigated its dynamical behavior. The critical boundary between the frozen and chaotic phase was determined analytically. In its most general representation (4.9) the critical connectivity is inversely proportional to the heterogeneity $\overline{p}$ from (4.5) of the MKN. This parameter becomes maximal if the update rules are unbiased, i.e. assume each value with equal probability, cf. Lemma 4.1. It is minimal (zero), if the update rules are constant functions.

In particular, we saw that SKNs as introduced by Kauffman [1969] have a critical connectivity of two, cf. Remark 4.5. Below this connectivity they exhibit stable dynamics, whereas above this connectivity their dynamics are unstable and highly sensitive

to perturbations. Bearing this in mind, let us recall the questions which Kauffman [1969] set out to answer, cf. section 3.4. We have now seen that stable dynamics are, indeed, to be expected in nets of randomly interconnected regulatory circuits, provided they are sufficiently sparse. Stability does not require the circuits to be precisely constructed, but only places an upper bound on their connectivity. Kauffman [1993] called this generic stability of sparsely connected KNs "order for free." He argues that regulatory networks in living organisms benefit from this "order for free" as well as from the variability of a nearby chaotic regime.

Our analysis of unbiased MKNs, however, showed that the region in which we get "order for free" shrinks, when we leave the Boolean case and allow for multiple states, cf. Remark 4.5. Yet, we also demonstrated that each MKN can be kept in the ordered regime by putting a sufficiently heavy bias on one of the states, cf. section 4.3.4.2. From a biological point of view, this may indicate that in real genetic networks the update functions have a base level of activation and deviations thereof constitute well-defined exceptions.

At this point, we caution that all our results and their interpretation apply to Kauffman's *idealization* of gene regulatory networks, their significance for the *real* biological systems should, as always, be treated with wariness. Still, there are promising attempts, e.g. by Balleza et al. [2008] and Kauffman et al. [2003], to bridge the gap between the theoretical concept of a KN and real genetic networks.

Finally, we took a look at ensembles of trajectories as an extension to the study of the Hamming distance between two trajectories. We were able to characterize the different regimes of MKNs in terms of the synchronization behavior of such ensembles. In an example, we demonstrated that our analytic computations agree well with simulation results.

5

Kauffman networks with generic logics

You want the truth?
You can't handle the truth!

Jack Nicholson in "A Few Good Men"

The last decades witnessed a series of technological breakthroughs in the life-sciences. We can now monitor the entire gene or protein profile of cells and study epistatic relationships by gain- and loss-of-function experiments. Information about whether or not a gene is expressed in a specific cell type or tissue is readily available, as is information about activating and inhibiting regulatory interactions. Naturally, one always wishes for more accurate and comprehensive data, but compared to what was possible and available some twenty years ago the wealth of information is remarkable. It more and more turns out that, at least from a modeler's point of view, the integration of available information into predictive models is as much a problem as is the possible lack of further important information. In a way, we already have the truth, we just cannot handle it.

In less abstract terms, information about pairwise genetic interactions can typically be obtained experimentally. The question how the various regulatory influences on a gene interact in order to determine its expression, however, is combinatorially complex and often intractable.

5.1 Motivation and outline

Theoretical biologists often distinguish between qualitative and Boolean models of gene regulatory networks. Qualitative models are typically defined as directed signed graphs. The nodes represent genes, the edges positive (activating) and negative (inhibiting) regulatory interactions. Qualitative models may already yield valuable information, e.g. about multistationarity or oscillations [Thomas, 1978]. However, in general they do not allow for time-course simulations as the interplay of a gene's regulators is not specified. This additional information is provided in BMs. Here, each node is assigned an update function, which defines the node's value depending upon the values of the node's regulators at the previous time-point.

The information required for the setup of a qualitative model can be obtained e.g. from gain- or loss-of-function experiments, or on a larger scale from bioinformatics resources. The inference of Boolean update functions from biological data, however, is not as straightforward. Therefore, heuristic modeling approaches for the automated conversion of qualitative into Boolean models have been proposed. The *standardized qualitative dynamical systems* approach, for instance, was successfully used to model *T helper cell differentiation* [Mendoza and Xenarios, 2006]. Several *reverse engineering* approaches also rely on such transformations [Bulashevska and Eils, 2005; Martin et al., 2007]. In our modeling toolbox *ODEfy* [Krumsiek et al., 2010] a unifying framework for all these transformations is established via so-called *generic logics*. These are tuples of Boolean operators that allow to define a node's update rule by linking its activators and inhibitors according to a specific pattern. A complementary approach that cannot be treated within the framework of generic logics are *threshold update rules* as used in Li et al. [2004] or Rohlf and Bornholdt [2002].

In this chapter, which follows Wittmann and Theis [2010b], we study KNs generated by generic logics. We formally introduce this class of KNs in section 5.2. Due to their prominent role in the study of SKNs and KNsMB our main goal is to analyze

phase transitions in these KNs. We already mentioned that a phase transition can be understood as a change of the percolation behavior in realizations of a KN, and that in SKNs or KNsMB this percolation is independent of the actual states of the associated dynamical system, cf. Lemma 4.2. In this chapter, we will see that this is no longer true for realizations of a KN with generic logics.

For this reason, we begin in section 5.3 by studying a quantity which we call the *truth-content* of a KN. It is defined as the probability for a node to be *true* (one). In large KNs the truth-content can be approximated by the fraction of ones in a trajectory $\mathbf{x}(t)$ of a realization. In KNsMB the truth-content has stationary dynamics with an equilibrium given by the magnetization bias. For KNs with generic logics we are able to prove that the dynamics of the truth-content are essentially dynamics of S-unimodal functions as described in sections 2.2.4.1 and 2.2.4.2. In numeric analyses, this truth-content, indeed, exhibits the characteristic, rich dynamical behaviors of these functions including period-doublings leading to chaos. We prove that the truth-content of KNs with generic logics possesses a unique attractor and characterize it, cf. Theorems 5.1, 5.2 and 5.3. This allows us to define *truth-stable* KNs as networks whose truth-contents exhibit non-chaotic dynamics.

In section 5.4, we use the results from the previous section to derive a criterion for phase transitions in KNs with generic logics, cf. Theorems 5.5 and 5.6. Section 5.5 concludes the mathematical part of this chapter by numerical analyses and further confirms the validity of our results by simulations. Finally, in section 5.6, we discuss our results with respect to their biological implications.

5.2 Qualitative models and Kauffman networks with generic logics

In this chapter, $G = (V, E)$ will again denote a (directed) graph of order N with nodes $V = \{1, 2, \ldots, N\}$ and edges $(i' \to i) \in E \subset V \times V$. The predecessors (inputs) of a node i are denoted by $i_1 < i_2 < \cdots < i_{K_i}$, where K_i is the node's in-degree.

Definition 5.1 (qualitative model)**.** A *qualitative model* (QM) is a tuple (G, σ) consisting of a graph G and a signature $\sigma : E \to \{+, -\}$ of G. We call an input i_k of a node i *activating* if $\sigma(i_k \to i) = +$ and *inhibiting* if $\sigma(i_k \to i) = -$.

5.2.1 Mappings between qualitative and Boolean models

Let us now fix the graph G and consider the set $\mathcal{Q}$ of all qualitative and the set $\mathcal{B}$ of all Boolean models on G. Clearly, $\mathcal{B}$ is much larger than $\mathcal{Q}$; more precisely, $\#(\mathcal{Q}) = 2^{\sum_{i=1}^{N} K_i}$ and $\#(\mathcal{B}) = 2^{\sum_{i=1}^{N} 2^{K_i}}$. We study possible mappings between $\mathcal{Q}$ and $\mathcal{B}$. First, we note that there is no canonical projection from $\mathcal{B}$ onto $\mathcal{Q}$. This changes once we restrict $\mathcal{B}$ to the set $\mathcal{M}$ of BMs with monotonous update functions.

Remark 5.1. We have a canonical projection

$$\begin{array}{rccccc} \pi: & \mathcal{M} & \twoheadrightarrow & \mathcal{Q} & & \\ & (f_i)_{i=1}^N & \mapsto & \sigma: \quad E & \to & \{+,-\} \\ & & & (i_k \to i) & \mapsto & \begin{cases} + & \text{if } f_i \text{ mon. inc. in its } k\text{-th input} \\ - & \text{if } f_i \text{ mon. dec. in its } k\text{-th input} \end{cases} \end{array}$$

i.e. we classify an input as activating (inhibiting) if the update rule monotonously increases (decreases) in it.

Conversely, there is no canonical inclusion of $\mathcal{Q}$ in $\mathcal{B}$. In this chapter, we propose *generic logics* in order to define injective mappings from $\mathcal{Q}$ into $\mathcal{B}$.

Definition 5.2 (generic logic)**.** A *generic logic* g is a triple $g = (\oplus, \otimes, \ominus) \in \{\wedge, \vee\}^3$ of Boolean operators from Table 2.1.

There are eight different generic logics; we enumerate them by reading the triple as a binary number, where by convention $\wedge = 0$ and $\vee = 1$, cf. Table 5.1.

Remark 5.2. Let us consider a QM (G, σ) from $\mathcal{Q}$. Via a generic logic $g = (\oplus, \otimes, \ominus)$ we can assign a node i of G the update function

$$\begin{array}{rccc} f_i^g: & \{0,1\}^{K_i} & \to & \{0,1\} \\ & \left(x_{i_1}, x_{i_2}, \ldots, x_{i_{K_i}}\right) & \mapsto & \left(\bigoplus_{k|\sigma(i_k \to i)=+} x_{i_k}\right) \otimes \left(\bigominus_{k|\sigma(i_k \to i)=-} \neg x_{i_k}\right) \end{array} . \tag{5.1}$$

Hence, for each generic logic g we can define a mapping

$$\iota_g : \mathcal{Q} \longrightarrow \mathcal{B}$$

by assigning each node i an update function f_i^g according to (5.1).

Proposition 5.1. *Each Boolean function of the form* (5.1) *is monotonous. Hence, each generic logic g induces a mapping $\iota_g : \mathcal{Q} \to \mathcal{M}$. Each such ι_g is, in general, not onto, but injective and a right-inverse of π, $\pi \circ \iota_g = \mathbb{1}_{\mathcal{Q}}$.*

Table 5.1: Enumeration of all eight generic logics.

Nº	$\oplus$	$\otimes$	$\ominus$
0	$\wedge$	$\wedge$	$\wedge$
1	$\wedge$	$\wedge$	$\vee$

Nº	$\oplus$	$\otimes$	$\ominus$
2	$\wedge$	$\vee$	$\wedge$
3	$\wedge$	$\vee$	$\vee$

Nº	$\oplus$	$\otimes$	$\ominus$
4	$\vee$	$\wedge$	$\wedge$
5	$\vee$	$\wedge$	$\vee$

Nº	$\oplus$	$\otimes$	$\ominus$
6	$\vee$	$\vee$	$\wedge$
7	$\vee$	$\vee$	$\vee$

Proof. The claim follows from the fact that a f_i^g as in (5.1) is monotonously increasing (decreasing) in its k-th input, if i_k is an activating (inhibiting) input of i. Note that this implies, in particular, the injectivity of ι_g as well as $\pi \circ \iota_g = \mathbb{1}_{\mathcal{Q}}$. □

We have the following logical relations between update functions generated by the different generic logics.

Proposition 5.2. *We consider a node of a QM $(G,\sigma) \in \mathcal{Q}$ and the update rules f^g from (5.1) for $g = 0, 1, \ldots, 7$. (For notational simplicity we drop the subscript i.) Then, for propositional variables $x_1, \ldots, x_K \in \{0,1\}$ we have*

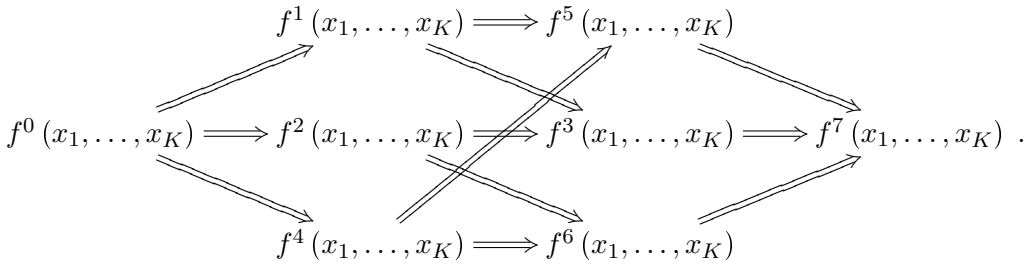

(Arrows indicate logical implication, i.e. $f^0(x_1,\ldots,x_K)$ implies $f^1(x_1,\ldots,x_K)$ etc.)

De Morgan's laws imply the following symmetry properties.

Proposition 5.3. *Let $(G,\sigma) \in \mathcal{Q}$. The update functions f_i^g and $f_i^{\neg,g}$ of the BMs $\iota_g((G,\sigma))$ and $\iota_g((G,\neg\sigma))$, respectively, exhibit the following symmetries:*[1]

1. *For $(g,g') \in \{(0,7),(1,6),(2,5),(3,4)\}$ we have*

$$f_i^g(x_1,\ldots,x_{K_i}) = \neg f_i^{g'}(\neg x_1,\ldots,\neg x_{K_i}) \ ;$$

2. *for $(g,g') \in \{(0,7),(1,3),(2,5),(4,6)\}$ we have*

$$f_i^g(x_1,\ldots,x_{K_i}) = \neg f_i^{\neg,g'}(x_1,\ldots,x_{K_i}) \ ,$$

[1] As defined in section 2.1, $\neg\sigma$ denotes the inverted signature.

where $x_1, \ldots, x_{K_i} \in \{0,1\}$ *are propositional variables.*

Proposition 5.3.1 implies

Corollary 5.1. *Let* (G,σ) *be a QM and consider the BMs* $(G,\mathbf{f}^g) = \iota_g((G,\sigma))$*,* $g = 0,1,\ldots,7$*. For* $(g,g') \in \{(0,7),(1,6),(2,5),(3,4)\}$ *the dynamical systems* $\mathbf{x}(t+1) = \mathbf{f}^g(\mathbf{x}(t))$ *and* $\mathbf{y}(t+1) = \mathbf{f}^{g'}(\mathbf{y}(t))$ *from Remark 3.1 are topologically conjugate via component-wise negation on* $\{0,1\}^N$*.*

5.2.2 Kauffman networks with generic logics

Let us now define the class of KNs which will be the subject of the following investigations. We refer to them as *Kauffman networks with generic logics* (KNGL). Each KNGL is specified by four parameters: the order N, the generic logic g, the connectivity K and an *activation bias* $a \in [0,1]$. As we will always consider the limit of large N we typically omit the parameter N and specify a KNGL by the tuple (g,a,K). Realizations $(G,\mathbf{f})$ of a KNGL (g,a,K) (of order N) are constructed according to the following random process.

(G1) Create a realization of the random graph $\mathcal{G}(P_{\text{in}})$ with $P_{\text{in}} = \delta_K$.

(G2) Define a signature σ of G by setting $\sigma(i_k \to i) = +$ with probability a and $\sigma(i_k \to i) = -$ with probability $r = 1-a$ for each edge $i_k \to i$ of G. We obtain a qualitative model (G,σ).

(G3) Set $(G,\mathbf{f}) = \iota_g((G,\sigma))$.

In other words, G will always be a graph with fixed connectivity K for all nodes. Different generative models for G remain to be investigated, see the outlook in section 7.2.2. Similarly to KNsMB, we introduce a bias a and classify an edge as activating or inhibiting with probabilities a and $r = 1-a$, respectively.

Remark 5.3. Note that for $K = 1$, KNsGL are critical KNs where only "copy" and "invert" are used as update rules. These KNs are well understood and we refer the interested reader to Drossel [2005].

In the following, $g \in \{0,1,\ldots,7\}$ always denotes the generic logic, $0 \leqslant a \leqslant 1$ the bias towards activations, and $K \in \mathbb{N}$ the connectivity of a KNGL. We point out once more that K is the fixed connectivity of a regular graph and cannot be interpreted as a mean connectivity.

5.3 The truth-content of a Kauffman network with generic logic

As explained above, we first turn our attention to a quantity we call the truth-content of a KN. We introduce this concept for general KNs and only later restrict ourselves to KNsGL. So, at first let $\mathcal{K}$ be a general KN.

Definition 5.3 (truth-content of a KN)**.** The *truth-content* of $\mathcal{K}$ is a sequence $(w(t))_{t\geqslant 0}$ which is consistent in the sense of the following random experiment: Pick a realization of $\mathcal{K}$, create a configuration $\mathbf{x}(0)$ whose components are 1 with probability $w(t)$, and iterate it one time-step yielding configuration $\mathbf{x}(1)$. Then, $w(t+1)$ is the probability for a component of $\mathbf{x}(1)$ to be 1.

Remark 5.4. Lemma 2.1 allows us to approximate the truth-content of $\mathcal{K}$ by the fraction of ones

$$w(t) \approx \frac{1}{N}\sum_{i=1}^{N} x_i(t) \tag{5.2}$$

in a trajectory $\mathbf{x}(t)$ of a specific realization of $\mathcal{K}$ provided N is sufficiently large. We further illustrate this by simulations in section 5.5.3.

The truth-content of a KN with magnetization bias u exhibits a rather uninteresting dynamical behavior.

Remark 5.5. In a KN with magnetization bias u we have $w(t) = u$ for all $t > 0$.

The proof that KNs with canalyzing update rules are always frozen, cf. Kauffman et al. [2004], also involves computing the truth-content. However, also for this particular choice of update rules $w(t)$ has stationary equilibrium dynamics. Let us now see how $w(t)$ behaves in KNsGL and whether a more interesting dynamical behavior can be observed. We let $\mathcal{K} = (g, a, K)$ be a KNGL and denote its truth-content by $(w_{g,a,K}(t))_{t\geqslant 0}$. If no ambiguity exists, we simply write $w_g(t)$ instead of $w_{g,a,K}(t)$.

First, we take care of the issue that the truth-content $w_g(t)$ of $\mathcal{K}$ depends on the initial condition $w_g(0)$. To this end, we prove that the asymptotic behavior of $w_g(t)$ is identical for almost all initial conditions. We consider this a result in its own right. Moreover, it will allow us to derive a criterion for phase transitions in section 5.4. We proceed as follows. In section 5.3.1 we describe the truth-content $w_g(t)$ of $\mathcal{K}$ by an iteration. Section 5.3.2 then lists some useful properties of the iteration functions.

Together with the theory of S-unimodal maps as outlined in section 2.2.4.2, these pre-considerations will allow the derivation of our main result in section 5.3.3. Finally, section 5.3.4 establishes the concept of truth-stability.

5.3.1 Iterations for the truth-content

In this section, we derive functions $W_{g,a,K} = W_g$ such that the truth-content $w_g(t)$ of $\mathcal{K}$ satisfies the iteration

$$w_g(t+1) = W_g\left(w_g(t)\right) \ . \tag{5.3}$$

The following two corollaries implied by Proposition 5.3 will considerably simplify our computations.

Corollary 5.2. *The $W_{g,a,K}$ from (5.3) exhibit the following symmetries.*

1. *For $(g,g') \in \{(0,7),(1,6),(2,5),(3,4)\}$ we have $W_{g,a,K}(w) = 1 - W_{g',a,K}(1-w)$.*
2. *For $(g,g') \in \{(0,7),(1,3),(2,5),(4,6)\}$ we have $W_{g,a,K}(w) = 1 - W_{g',r,K}(w)$.*

Corollary 5.3. *For $(g,g') \in \{(0,7),(1,6),(2,5),(3,4)\}$ the two dynamical systems $w_g(t+1) = W_g\left(w_g(t)\right)$ and $w_{g'}(t+1) = W_{g'}\left(w_{g'}(t)\right)$ are topologically conjugate via the involution $w \mapsto 1-w$.*

Now, given $w_g(t)$, let us consider the random experiment from Definition 5.3 and take a look at a prototypic node i. In $\mathbf{x}(0)$ each of the K inputs of i is 1 with probability $w_g(t)$ and 0 with probability $1 - w_g(t)$, as the configuration model chooses these inputs randomly from V. According to (G2), the influence of an input on i is activating with probability a and inhibiting with probability r. Hence, the probability for α inputs of i to be activating and $K-\alpha$ inputs to be inhibiting is given by $\binom{K}{\alpha} a^\alpha r^{K-\alpha}$. In this situation and

- using $g = 0$, the probability for $x_i(1)$ to be 1 is given by $w_0(t)^\alpha (1 - w_0(t))^{K-\alpha}$ as the α activators need to be 1 and the $K-\alpha$ inhibitors need to be 0 in $\mathbf{x}(0)$. Summing over all possible activator-inhibitor-combinations yields

$$\begin{aligned} W_0\left(w_0(t)\right) &= \sum_{\alpha=0}^{K} \binom{K}{\alpha} a^\alpha r^{K-\alpha} w_0(t)^\alpha \left(1 - w_0(t)\right)^{K-\alpha} \\ &= \left(a w_0(t) + r\left(1 - w_0(t)\right)\right)^K \ . \end{aligned} \tag{5.4}$$

- using $g = 1$, the probability for $x_i(1)$ to be 1 is given by

$$\begin{cases} w_1(t)^\alpha \left(1 - w_1(t)^{K-\alpha}\right) , & \text{if } \alpha < K \\ w_1(t)^K , & \text{if } \alpha = K , \end{cases}$$

as the α activators need to be 1 and, if existing, at least one of the $K-\alpha$ inhibitors needs to be 0 in $\mathbf{x}(0)$. Summing over all possible activator-inhibitor-combinations yields

$$\begin{aligned} W_1\left(w_1(t)\right) &= \sum_{\alpha=0}^{K-1} \binom{K}{\alpha} a^\alpha r^{K-\alpha} w_1(t)^\alpha \left(1 - w_1(t)^{K-\alpha}\right) + a^K w_1(t)^K \\ &= \left(a w_1(t) + r\right)^K - \left(1 - a^K\right) w_1(t)^K . \end{aligned} \tag{5.5}$$

- using $g = 2$, the probability for $x_i(1)$ to be 1 is given by

$$\begin{cases} \left(1 - w_2(t)\right)^K , & \text{if } \alpha = 0 \\ w_2(t)^\alpha + \left(1 - w_2(t)\right)^{K-\alpha} - w_2(t)^\alpha \left(1 - w_2(t)\right)^{K-\alpha} , & \text{if } 0 < \alpha < K \\ w_2(t)^K , & \text{if } \alpha = K . \end{cases}$$

These are the probabilities that all activators are 1 or all inhibitors are 0 in $\mathbf{x}(0)$. If i has both, activators and inhibitors, we need to correct by the probability that all activators are 1 and all inhibitors are 0. Summing over all possible activator-inhibitor-combinations yields

$$\begin{aligned} W_2\left(w_2(t)\right) = &\left(a w_2(t) + r\right)^K + \left(a + r\left(1 - w_2(t)\right)\right)^K - \left(a w_2(t) + r\left(1 - w_2(t)\right)\right)^K \\ &- r^K \left(1 - \left(1 - w_2(t)\right)^K\right) - a^K \left(1 - w_2(t)^K\right) . \end{aligned} \tag{5.6}$$

The remaining W_g follow from Corollary 5.2.

$$W_{3,a,K}\left(w_3(t)\right) = 1 - W_{1,r,K}\left(w_3(t)\right) \tag{5.7}$$

$$W_{4,a,K}\left(w_4(t)\right) = 1 - W_{3,a,K}\left(1 - w_4(t)\right) \tag{5.8}$$

$$W_{5,a,K}\left(w_5(t)\right) = 1 - W_{2,a,K}\left(1 - w_5(t)\right) \tag{5.9}$$

$$W_{6,a,K}\left(w_6(t)\right) = 1 - W_{1,a,K}\left(1 - w_6(t)\right) \tag{5.10}$$

$$W_{7,a,K}\left(w_7(t)\right) = 1 - W_{0,a,K}\left(1 - w_7(t)\right) \tag{5.11}$$

The W_g, $g = 0, 1, \ldots, 7$, are plotted in Figure 5.1.

In the remainder of this section we will study the time-discrete dynamical system (5.3) with W_g from (5.4)–(5.11).

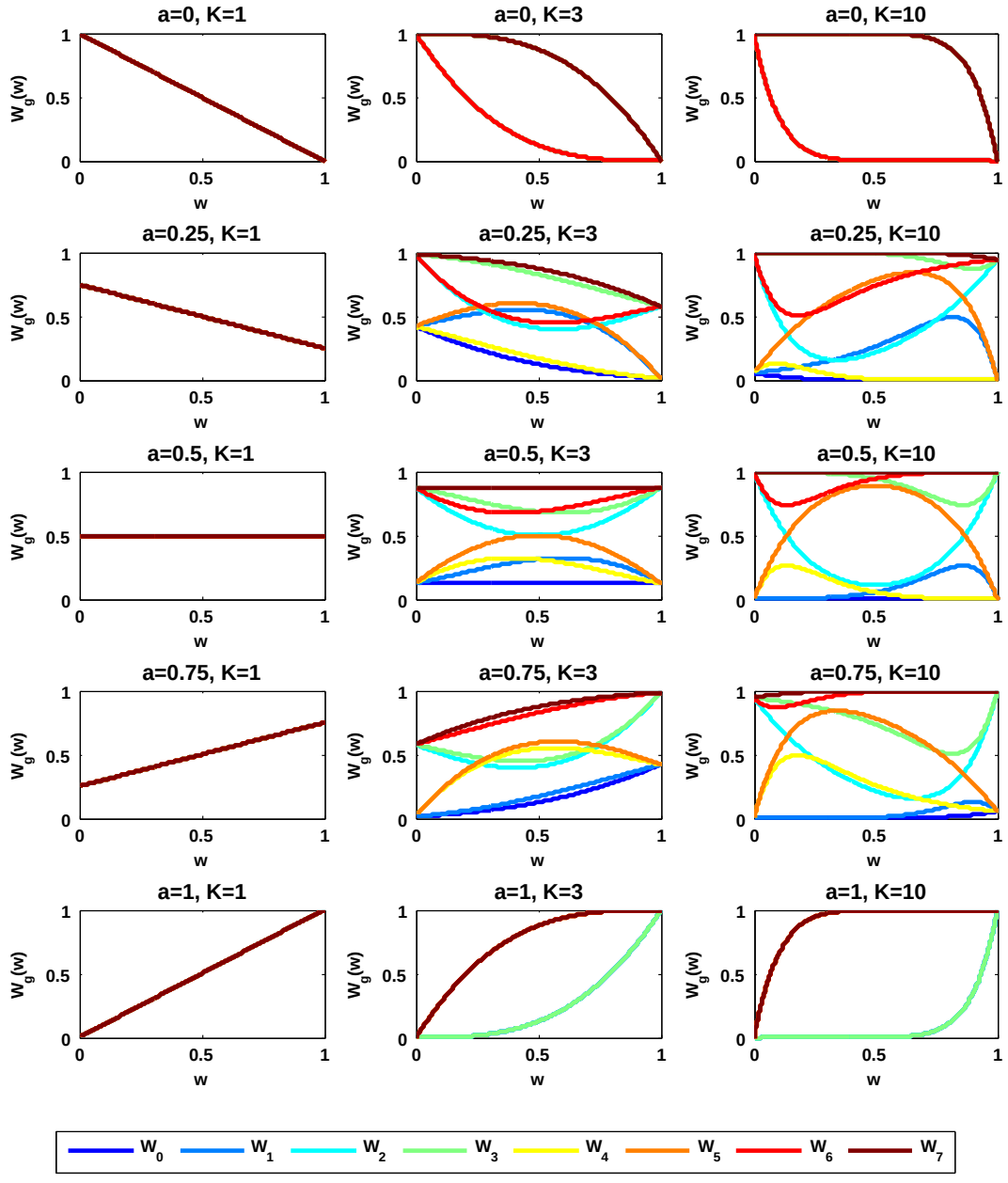

Figure 5.1: $W_{g,a,K}(w)$, $g = 0, 1, \ldots, 7$, from (5.4)–(5.11) for $a = 0, 0.25, 0.5, 0.75, 1$ and $K = 1, 3, 10$.

5.3.2 Properties of the iteration functions

Let us first collect some properties of the W_g, which will be needed below.

5.3.2.1 Lower and upper bounds

We begin by stating two results about lower and upper bounds of the W_g. First of all, Proposition 5.2 implies

Proposition 5.4. *For $w \in [0,1]$, $0 \leqslant a \leqslant 1$, and $K \geqslant 1$ we have the following ordering*

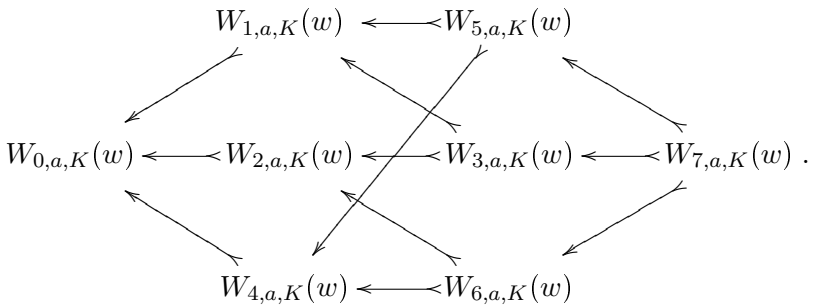

($\prec\!\!\longleftarrow$ edges indicate "less or equal"-relationships, i.e. $W_{0,a,K}(w) \leqslant W_{1,a,K}(w)$ etc.)

For the sake of completeness let us also mention the following (possibly rather loose) bounds.

Proposition 5.5. *For $w \in [0,1]$, $0 \leqslant a \leqslant 1$, and $K \geqslant 1$ we have*

1. $\min(a,r)^K \leqslant W_{0,a,K}(w) \leqslant \max(a,r)^K$.
2. $\min(a,r)^K \leqslant W_{1,a,K}(w) \leqslant \max(a,r)$.
3. $0 \leqslant W_{2,a,K}(w) \leqslant 1$.
4. $\min(a,r) \leqslant W_{3,a,K}(w) \leqslant 1 - \min(a,r)^K$.
5. $\min(a,r)^K \leqslant W_{4,a,K}(w) \leqslant \max(a,r)$.
6. $0 \leqslant W_{5,a,K}(w) \leqslant 1$.
7. $\min(a,r) \leqslant W_{6,a,K}(w) \leqslant 1 - \min(a,r)^K$.
8. $1 - \max(a,r)^K \leqslant W_{7,a,K}(w) \leqslant 1 - \min(a,r)^K$.

Proof. Claim 1 is obvious as $W_0(w)$ is monotonous. If $a > r$ ($a < r$), $W_0(w)$ increases (decreases) from r^K to a^K. The lower bound in claim 2 follows from part 1 and Proposition 5.4. For the upper bound we reason

$$\begin{aligned} W_{1,a,K}(w) &\leqslant aw^K + r - w^K + (aw)^K \\ &\leqslant \begin{cases} w^K(a-1+a) + r = w^K(a-r) + r \leqslant r\,, & \text{if } a \leqslant r \\ rw^K + a - w^K + (aw)^K \leqslant w^K(r-1+a) + a = a\,, & \text{if } a > r\,. \end{cases} \end{aligned}$$

The remainder of the claim follows from Corollary 5.2. □

5.3.2.2 Extreme and asymptotic cases

This section takes care of all extreme and asymptotic cases. Trivial computations show

Proposition 5.6. *The following hold.*

1. *For $g \in \{0,1,4,5\}$ we have $W_g(0) = r^K$ and $W_g(1) = a^K$. For $g \in \{2,3,6,7\}$ we have $W_g(0) = 1 - a^K$ and $W_g(1) = 1 - r^K$.*

2. *Let $a = 1$. For $g \in \{0,1,2,3\}$ we have $W_{g,1,K}(w) = w^K$. For $g \in \{4,5,6,7\}$ we have $W_{g,1,K}(w) = 1 - (1-w)^K$.*

3. *Let $a = 0$. For $g \in \{0,2,4,6\}$ we have $W_{g,0,K}(w) = (1-w)^K$. For $g \in \{1,3,5,7\}$ we have $W_{g,0,K}(w) = 1 - w^K$.*

4. *Let $K = 1$. For all $g \in \{0,1,\ldots,7\}$ we have $W_{g,a,1}(w) = aw + r(1-w)$.*

5. *Let $0 < w < 1$ and $0 < a < 1$. For $g \in \{0,1,2,4\}$ we have $W_{g,a,K}(w) \to 0$ as $K \to \infty$. For $g \in \{3,5,6,7\}$ we have $W_{g,a,K}(w) \to 1$ as $K \to \infty$.*

Proposition 5.6 has an intuitive explanation:

- In 1. the decisive characteristic is the operator $\otimes$ that links the group of activators and inhibitors. In the case $\otimes = \wedge$, *viz* $g = 0,1,4,5$, the only chance for a node to be switched on if $w = 0$ ($w = 1$) is that all its inputs are inhibitors (activators). Conversely, in the case $\otimes = \vee$, *viz* $g = 2,3,6,7$, the only chance for a node to be switched on if $w = 0$ ($w = 1$) is that not all its inputs are activators (inhibitors).

- In 2. the decisive characteristic is the operator $\oplus$ that links the activators. In the case $\oplus = \wedge$, *viz* $g = 0,1,2,3$, if the fraction of activators increases, the probability

for a node to be switched on approaches the probability that all its inputs are on. Conversely, in the case $\oplus = \vee$, *viz* $g = 4, 5, 6, 7$, if the fraction of activators increases, the probability for a node to be switched on approaches the probability that any of its inputs is on.

- In 3. the decisive characteristic is the operator $\ominus$ that links the inhibitors. In the case $\ominus = \wedge$, *viz* $g = 0, 2, 4, 6$, if the fraction of activators decreases, the probability for a node to be switched on approaches the probability that all its inputs are off. Conversely, in the case $\ominus = \vee$, *viz* $g = 1, 3, 5, 7$, if the fraction of activators decreases, the probability for a node to be switched on approaches the probability that any of its inputs is off.

- In 5. the decisive characteristic is the number of $\vee$'s in g. First, note that, unless $a = 0$ or $a = 1$, the number of both, activators and inhibitors, increases with K. Now, if there are less than two $\vee$'s in g, *viz* $g = 0, 1, 2, 4$, all activators need to be on and/or all inhibitors need to be off for a node to be switched on. Clearly, the probability for this tends to zero as the connectivity increases unless $w = 0$ or $w = 1$. Conversely, if there are more than one $\vee$'s in g, *viz* $g = 3, 5, 6, 7$, it suffices that any activator is on and/or any inhibitor is off for a node to be switched on. Clearly, the probability for this tends to one as the number of inputs increases unless $w = 0$ or $w = 1$.

5.3.2.3 The general shape of the iteration functions

In between the extreme cases from Proposition 5.6 the shapes of the W_g are characterized by

Proposition 5.7. *Let* $K \geqslant 2$ *and* $0 < a < 1$.

1. W_0 *is convex on* $[0, 1]$ *and increasing (decreasing) if* $a > r$ $(a < r)$.

2. W_7 *is concave on* $[0, 1]$ *and increasing (decreasing) if* $a < r$ $(a > r)$.

3. W_2 *is convex on* $[0, 1]$ *and has exactly one critical point* $w_2^{(c)}$, *which is non-degenerate and coincides with the global minimum.*

4. W_5 *is concave on* $[0, 1]$ *and has exactly one critical point* $w_5^{(c)}$, *which is non-degenerate and coincides with the global maximum.*

5. *Let $g \in \{1,3,4,6\}$. W_g has at most one critical point $w_g^{(c)}$ and at most one inflection point $w_g^{(i)}$. If existing, $w_g^{(c)}$ is non-degenerate. If no inflection point exists, also no critical point can exist. In the case that both exist, $w_g^{(i)} < w_g^{(c)}$ if $g \in \{1,3\}$, and $w_g^{(i)} > w_g^{(c)}$ if $g \in \{4,6\}$.*

6. *We can subdivide $[0,1]$ into three intervals $I_1^1 = \left[0, w_1^{(i)}\right]$, $I_1^2 = \left[w_1^{(i)}, w_1^{(c)}\right]$, $I_1^3 = \left[w_1^{(c)}, 1\right]$ such that W_1 is convex-increasing on I_1^1, concave-increasing on I_1^2, and concave-decreasing on I_1^3. If there is no critical (inflection) point in $[0,1]$ then $I_1^3 = \varnothing$ ($I_1^2 = I_1^3 = \varnothing$).*

7. *We can subdivide $[0,1]$ into three intervals $I_3^1 = \left[0, w_3^{(i)}\right]$, $I_3^2 = \left[w_3^{(i)}, w_3^{(c)}\right]$, $I_3^3 = \left[w_3^{(c)}, 1\right]$ such that W_3 is concave-decreasing on I_3^1, convex-decreasing on I_3^2, and convex-increasing on I_3^3. If there is no critical (inflection) point in $[0,1]$ then $I_3^3 = \varnothing$ ($I_3^2 = I_3^3 = \varnothing$).*

8. *We can subdivide $[0,1]$ into three intervals $I_4^1 = \left[0, w_4^{(c)}\right]$, $I_4^2 = \left[w_4^{(c)}, w_4^{(i)}\right]$, $I_4^3 = \left[w_4^{(i)}, 1\right]$ such that W_4 is concave-increasing on I_4^1, concave-decreasing on I_4^2, and convex-decreasing on I_4^3. If there is no critical (inflection) point in $[0,1]$ then $I_4^1 = \varnothing$ ($I_4^1 = I_4^2 = \varnothing$).*

9. *We can subdivide $[0,1]$ into three intervals $I_6^1 = \left[0, w_6^{(c)}\right]$, $I_6^2 = \left[w_6^{(c)}, w_6^{(i)}\right]$, $I_6^3 = \left[w_6^{(i)}, 1\right]$ such that W_6 is convex-decreasing on I_6^1, convex-increasing on I_6^2, and concave-increasing on I_6^3. If there is no critical (inflection) point in $[0,1]$ then $I_6^1 = \varnothing$ ($I_6^1 = I_6^2 = \varnothing$).*

Proof. The case $g = 0$ is obvious. The characterization of the shape of W_1 can be obtained as follows: If $K = 2$ there is obviously at most one critical point and no inflection point. In the case $K \geqslant 3$ the zeros of the first and second derivatives of W_1 are simple and given by

$$w_1^{(c)} = \frac{r}{v_1^{(c)} - a} \quad \text{and} \quad w_1^{(i)} = \frac{r}{v_1^{(i)} - a} \,,$$

where

$$\left(v_1^{(c)}\right)^{K-1} = \frac{1-a^K}{a} \quad \text{and} \quad \left(v_1^{(i)}\right)^{K-2} = \frac{1-a^K}{a^2} \,.$$

This implies that there is at most one critical and one inflection point of W_1 in $[0,1]$ as possible negative solutions for $v_1^{(c/i)}$ lead to values $w_1^{(c/i)} < 0$. One easily verifies that $W_1'(0) = Kar^{K-1} > 0$ and $W_1''(0) = K(K-1)a^2r^{K-2} > 0$. Now, suppose a

critical point $w_1^{(c)} \in (0,1)$ exists. It follows that $w_1^{(c)}$ is a local maximum, which implies $W_1''\left(w_1^{(c)}\right) < 0$. Thus, there has to be an inflection point $0 < w_1^{(i)} < w_1^{(c)}$. If there is no critical point in $(0,1)$ the function W_1 is increasing on $[0,1]$ and $I_1^3 = \varnothing$. If, moreover, there is no inflection point either, the function W_1 is also convex on $[0,1]$ and $I_1^2 = \varnothing$.

In the case $g = 2$ one can check that

$$\begin{aligned} W_2''(w) =& K(K-1)\Big[a^2\left(aw+r\right)^{K-2} + r^2\left(a + r(1-w)\right)^{K-2} - \\ & (a-r)^2\left(aw + r(1-w)\right)^{K-2} + r^K(1-w)^{K-2} + a^K w^{K-2}\Big] \end{aligned}$$

is positive for $0 < w < 1$. (We have $a^2(aw+r)^{K-2} > (a-r)^2\left(aw + r(1-w)\right)^{K-2}$ for $a \geqslant 0.5$, and $r^2(a + r(1-w))^{K-2} > (a-r)^2\left(aw + r(1-w)\right)^{K-2}$ for $a < 0.5$.) Hence, W_2 is convex on $[0,1]$. The claim follows from $W_2'(0) = -Kr < 0$ and $W_2'(1) = Ka > 0$.

The shapes of W_3, W_4, W_5, W_6 and W_7 can be obtained from Corollary 5.2. □

Corollary 5.4. *Let $0 < a < 1$ and $K \geqslant 1$. For each $g \in \{0, 1, \ldots, 7\}$, W_g has exactly one fixed point.*

Proof. For $K = 1$, see Proposition 5.6.4. For $K \geqslant 2$ the claim follows from Propositions 5.6.1 and 5.7. A little work remains to be done in the case $g = 1$ (and $g = 6$) as functions with a shape as W_1 could have multiple fixed points. However, we can rule out this possibility as W_1 and W_1' are bounded from above by $H(w) = (aw + r)^K$ and $H'(w)$, respectively. The function H is convex and increasing and has fixed points $0 < w_h < 1$ and 1. The fixed point w_h is attracting and $H'(w_h) < 1$. Any fixed point of W_1 lies in the interval $(0, w_h)$, and, thus, the derivative of W_1 in a fixed point $w_1^{(f)}$ satisfies $W_1'\left(w_1^{(f)}\right) < H'\left(w_1^{(f)}\right) < H'(w_h) < 1$ as H is convex. Hence, W_1 cannot have more than one fixed point as in this case in at least one fixed point the derivative would have to be greater than 1 (the diagonal would be crossed from below). □

5.3.2.4 The limit of large connectivities

In this section, we investigate the limit of large K in more detail. This is of particular importance to our numerical analyses in section 5.5, as here we will, of course, only be able to portray the dynamic behavior up to some finite K. We begin by studying the existence of critical points of W_g, $g \in \{1, 3, 4, 6\}$. Recall that, in general, we can only limit the number of critical points but not guarantee existence, cf. Proposition 5.7.5.

Proposition 5.8. *Let $g \in \{1, 3, 4, 6\}$ and $0 < a < 1$. For sufficiently large K, W_g has a critical point $w_g^{(c)}$ and an inflection point $w_g^{(i)}$ in $(0,1)$. For $g \in \{1, 3\}$ we have*

$w_g^{(c/i)} \to 1$ *from below as* $K \to \infty$. *For* $g \in \{4,6\}$ *we have* $w_g^{(c/i)} \to 0$ *from above as* $K \to \infty$.

Proof. By virtue of Corollary 5.2 we can restrict ourselves to the case $g = 1$. In this case the critical point $w_1^{(c)}$ and the inflection point $w_1^{(i)}$ were already computed in the proof of Proposition 5.7. The radicand in the expression $v_1^{(c)} = \sqrt[K-1]{(1-a^K)/a}$ is bounded and for sufficiently large K greater than one. Hence, $\lim_{K\to\infty} v_1^{(c)} = 1$ from above. It follows $\lim_{K\to\infty} w_1^{(c)} = 1$ from below. Analogously one proves $\lim_{K\to\infty} w_1^{(i)} = 1$ from below. □

Now, let $0 < a < 1$ and K be sufficiently large in the sense of Proposition 5.8. In the cases $g \in \{1,4,5\}$, we denote the maximum of W_g by $m_{g,a,K} = W_g\left(w_g^{(c)}\right)$. In the cases $g \in \{2,3,6\}$, we denote the minimum of W_g by $m_{g,a,K} = W_g\left(w_g^{(c)}\right)$. Let $M_{g,a} = \lim_{K\to\infty} m_{g,a,K}$.

Proposition 5.9. *We have*

1. *for* $g \in \{1,3\}$*:* $\lim_{a\to 0} M_{g,a} = 1$ *and* $\lim_{a\to 1} M_{g,a} = 0$.
2. *for* $g = 2$ *and* $0 < a < 1$*:* $M_{2,a} = 0$.
3. *for* $g \in \{4,6\}$*:* $\lim_{a\to 0} M_{g,a} = 0$ *and* $\lim_{a\to 1} M_{g,a} = 1$.
4. *for* $g = 5$ *and* $0 < a < 1$*:* $M_{5,a} = 1$.

Proof. By virtue of Corollary 5.2 we can restrict ourselves to $g \in \{1,2\}$. We take care of the case $g = 2$ first. Let $0 < w < 1$. We know from Proposition 5.7.3 that $W_2(w) \geqslant m_{2,a,K}$ and from Proposition 5.6.5 that $W_2(w) \to 0$ as $K \to \infty$. This implies $M_{2,a} = 0$. If $g = 1$, we compute $m_{g,a,K}$ (using e.g. $w_g^{(c)}$ from the proof of Proposition 5.7) and validate the claim numerically. □

We denote the range of W_g by

$$R_{g,a,K} := \left[\min_{[0,1]}\left(W_g(w)\right), \max_{[0,1]}\left(W_g(w)\right)\right].$$

Proposition 5.10. *Let* $0 < a < 1$. *We have*

1. *for* $g = 0$*:* $R_{0,a,K} \to \{0\}$ *as* $K \to \infty$.
2. *for* $g \in \{1,4\}$*:* $R_{g,a,K} \to [0, M_{g,a}]$ *as* $K \to \infty$.

3. *for* $g \in \{2,5\}$*:* $R_{g,a,K} \to [0,1]$ *as* $K \to \infty$*.*

4. *for* $g \in \{3,6\}$*:* $R_{g,a,K} \to [M_{g,a},1]$ *as* $K \to \infty$*.*

5. *for* $g = 7$*:* $R_{7,a,K} \to \{1\}$ *as* $K \to \infty$*.*

Proof. If $g \in \{0,7\}$, one boundary of $R_{g,a,K}$ is given by $W_g(0)$ and the other one by $W_g(1)$. In the case $g = 0$ ($g = 7$) these converge to 0 (1), cf. Proposition 5.6.1. Now, consider $g \in \{1,2,\ldots,6\}$. Note that for large enough K in each of these cases one boundary of $R_{g,a,K}$ is given by either $W_g(0)$ or $W_g(1)$ and the other one by $m_{g,a,K}$. The first converges to either 0 or 1 as $K \to \infty$ (cf. Proposition 5.6.1) the latter to $M_{g,a}$. □

The following remark summarizes our results.

Remark 5.6. In the cases $g \in \{0,7\}$ we have $W_0 \to 0$ and $W_7 \to 1$ as $K \to \infty$ with respect to the maximum norm, which, of course, implies point-wise convergence. For $g \in \{1,4\}$ ($g \in \{3,6\}$) the convergence $W_g \to 0$ (1) is only point-wise. In fact, W_g converges to zero (one) by pushing its bump towards either boundary of $[0,1]$. In other words, the range $R_{g,a,K}$ does not degenerate in the limit of large K but converges to a non-trivial interval of length $M_{g,a}$ $(1 - M_{g,a})$. Similarly, in the case $g = 2$ ($g = 5$) the convergence $W_g \to 0$ (1) is also only point-wise. The graph of W_2, for instance, is "pushed towards the path $(0,1) \to (0,0) \to (1,0) \to (1,1)$." We can somewhat sloppily describe the shape of W_g for large K as follows, see also Figure 5.2.

1. W_0 is an essentially flat line approaching 0 as $K \to \infty$.

2. W_1 is an essentially flat line approaching 0 as $K \to \infty$ except for a narrow peak at the right end of $[0,1]$. Its height decreases as $a \to 1$ and increases as $a \to 0$. The peak does not intersect with the diagonal.

3. W_2 has an almost rectangular shape and "interpolates" the points $(0,1)$, $(0,0)$, $(1,0)$ and $(1,1)$.

4. W_3 is an essentially flat line approaching 1 as $K \to \infty$ except for a narrow peak at the right end of $[0,1]$. Its height decreases as $a \to 0$ and increases as $a \to 1$.

5. W_4 is an essentially flat line approaching 0 as $K \to \infty$ except for a narrow peak at the left end of $[0,1]$. Its height decreases as $a \to 0$ and increases as $a \to 1$.

6. W_5 has an almost rectangular shape and "interpolates" the points $(0,0)$, $(0,1)$, $(1,1)$ and $(1,0)$.

7. W_6 is an essentially flat line approaching 1 as $K \to \infty$ except for a narrow peak at the left end of $[0,1]$. Its height decreases as $a \to 1$ and increases as $a \to 0$. The peak does not intersect with the diagonal.

8. W_7 is an essentially flat line approaching 1 as $K \to \infty$.

5.3.3 Attractors of the truth-content and their basins of attraction

In this section, we use the technical prerequisites developed and outlined in sections 2.2.4 and 5.3.2 to describe the dynamics of (5.3). In particular, we prove the existence of a unique attractor and characterize it. We take care of the cases $a \in \{0,1\}$, $K = 1$, and $K \to \infty$ first.

Theorem 5.1. *The discrete dynamical system* (5.3) *exhibits the following asymptotic behavior.*

1. *Let $K \geqslant 2$. For $g \in \{0,1,2,3\}$ and sufficiently large a,* (5.3) *has a unique asymptotically stable fixed point $w_g^{(f)}$ in a neighborhood of* 0 *and $w_g^{(f)} \to 0$ as $a \to 1$. If $a = 1$ there is an additional unstable fixed point at* 1.

   For $g \in \{4,5,6,7\}$ and sufficiently large a, (5.3) *has a unique asymptotically stable fixed point $w_g^{(f)}$ in a neighborhood of* 1 *and $w_g^{(f)} \to 1$ as $a \to 1$. If $a = 1$ there is an additional unstable fixed point at* 0.

2. *Let $K \geqslant 2$. For all $g \in \{0,1,\ldots,7\}$ and sufficiently small a,* (5.3) *has a unique asymptotically stable periodic orbit of length* 2 *which approaches the cycle $\overline{0,1}$ as $a \to 0$.*

3. *If $K = 1$ and $0 < a < 1$,* (5.3) *has a unique asymptotically stable fixed point $w_g^{(f)} = 0.5$ for all $g \in \{0,1,\ldots,7\}$.*

4. *If $K = 1$ and $a = 1$ each point is a neutrally stable fixed point.*

5. *If $K = 1$ and $a = 0$ every orbit $\{w, 1-w\}$ is neutrally stable.*

6. *Let $0 < a < 1$. For $g \in \{0,1\}$ and sufficiently large K,* (5.3) *has a unique asymptotically stable fixed point $w_g^{(f)}$ near* 0 *and $w_g^{(f)} \to 0$ as $K \to \infty$.*

   For $g = 3$ and $t > 0$ we have $\lim_{a\to 0} \lim_{K\to\infty} w_{3,a,K}(t) = 1$. For $g = 4$ and $t > 0$ we have $\lim_{a\to 0} \lim_{K\to\infty} w_{4,a,K}(t) = 0$.

   For $g \in \{6,7\}$ and sufficiently large K, (5.3) *has a unique asymptotically stable fixed point $w_g^{(f)}$ near* 1 *and $w_g^{(f)} \to 1$ as $K \to \infty$.*

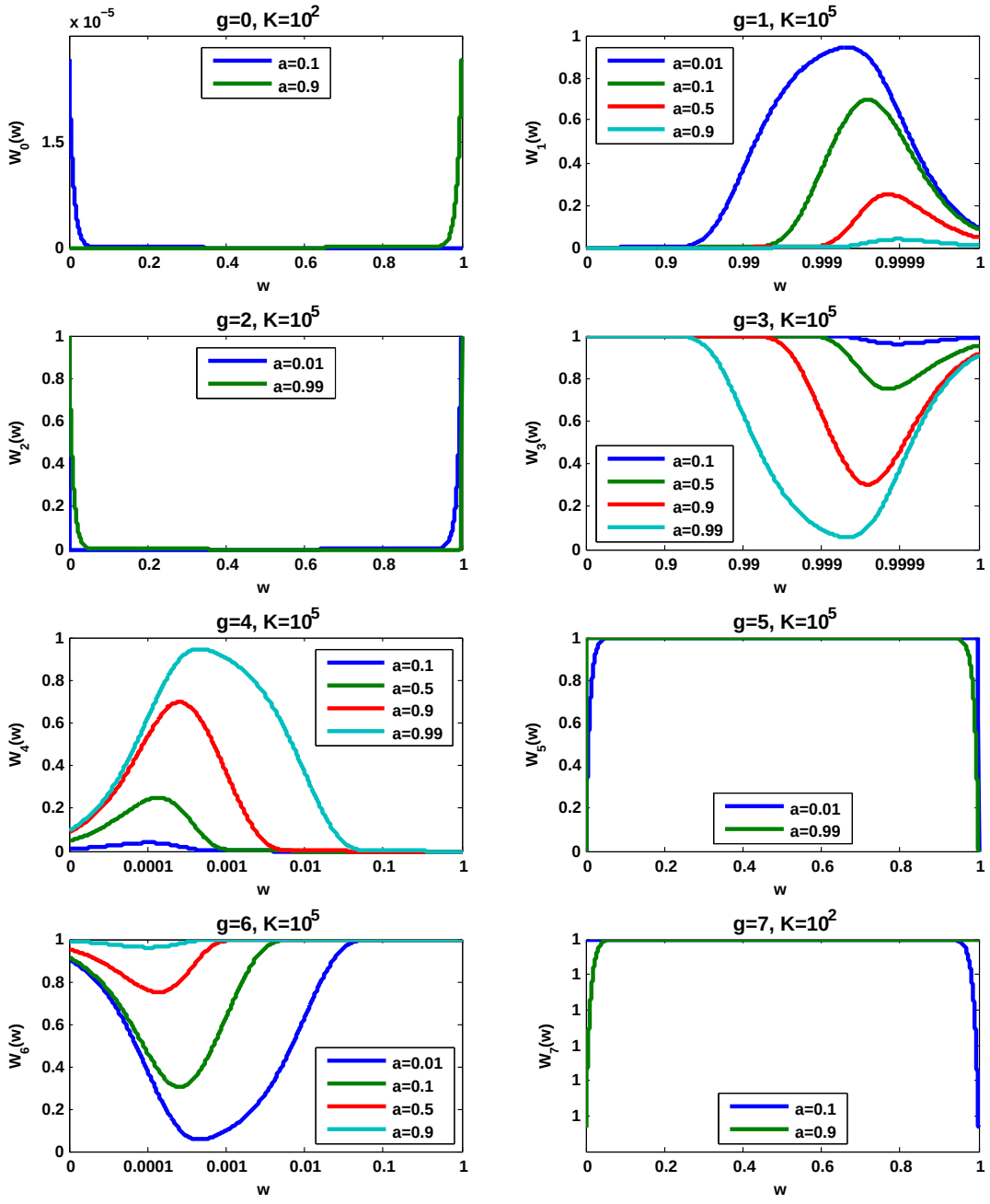

Figure 5.2: $W_{g,a,K}(w)$, $g = 0, 1, \ldots, 7$, from (5.4)–(5.11) for large K.

All asymptotically stable fixed points or periodic orbits are global attractors.

Proof. Claims 1 and 2 are obvious from Proposition 5.6.2 and 5.6.3 if $a = 1$ or $a = 0$, respectively. Since the existence of asymptotically stable periodic orbits is an open property and since $W_{g,a,K}$ depends analytically on a, this extends to neighborhoods of $a = 1$ and $a = 0$, respectively. Claims 3–5 follow from Proposition 5.6.4. Claim 6 follows from Remark 5.6. □

Now, let $K \geqslant 2$. We begin by proving

Lemma 5.1. *Let $K \geqslant 2$. For $g \in \{0, 7\}$ we have $\mathrm{S}\, W_{g,a,K} < 0$ (where defined) if $a \neq 0.5$, and $\mathrm{S}\, W_{g,a,K} = 0$ (where defined) if $a = 0.5$. For $g \in \{1, 2, \ldots, 6\}$ we have $\mathrm{S}\, W_g < 0$ (where defined).*

Proof. By the chain rule from Proposition 2.2 and the symmetry properties from Corollary 5.2 it suffices to consider $g \in \{0, 1, 2\}$. If $K = 2$, W_g is a quadratic polynomial unless $g = 0$ and $a = 0.5$ in which case W_g is constant. Thus, the Schwarzian derivative is negative or zero, respectively. Now suppose $K \geqslant 3$. The case $g = 0$ follows from

$$W_0'(w)W_0'''(w) - \frac{3}{2}W_0''(w)^2 = -\frac{1}{2}K^2(K-1)(a-r)^4\left(aw + r(1-w)\right)^{2K-4}(K+1)\,.$$

If $g \in \{1, 2\}$ we have

$$W_g'(w)W_g'''(w) - \frac{3}{2}W_g''(w)^2 = \frac{3}{2}K^2(K-1)^2\left[\frac{K-2}{(3/2)(K-1)}H(w,1)H(w,3) - H(w,2)^2\right]\,, \qquad (\star)$$

where

$$H(w,\alpha) = \begin{cases} \left(a^K - 1\right)w^{K-\alpha} + a^\alpha(aw+r)^{K-\alpha}\,, & \text{if } g = 1 \\ \\ a^\alpha(aw+r)^{K-\alpha} + (-1)^\alpha r^\alpha\left(a + r(1-w)\right)^{K-\alpha} - \\ (a-r)^\alpha\left(aw + r(1-w)\right)^{K-\alpha} + \\ (-1)^\alpha r^K(1-w)^{K-\alpha} + a^K w^{K-\alpha}\,, & \text{if } g = 2\,, \end{cases}$$

$\alpha = 1, 2, 3$. We denote the summands in the above expressions of the $H(w,\alpha)$ by $v_q(w,\alpha)$, $q = 1, 2$ if $g = 1$ and $q = 1, 2, 3, 4, 5$ if $g = 2$.

As $(3/2)K^2(K-1)^2 > 0$, we only need to take care of the bracketed expression in $(\star)$. If $H(w,1)H(w,3) \leqslant 0$ it immediately follows that $(\star) < 0$. Otherwise, the

bracketed expression in $(\star)$ is strictly smaller than $H(w,1)H(w,3) - H(w,2)^2$. This can be further simplified to

$$\begin{aligned} &H(w,1)H(w,3) - H(w,2)^2 = \\ &\sum_{q,q'} \left[v_q(w,1)v_{q'}(w,3) - v_q(w,2)v_{q'}(w,2) \right] = \\ &\sum_{q \neq q'} \left[v_q(w,1)v_{q'}(w,3) - v_q(w,2)v_{q'}(w,2) \right] , \end{aligned} \tag{$\dagger$}$$

as $v_q(w,1)v_q(w,3) - v_q(w,2)^2 = 0$ for $q = 1,2$ if $g = 1$ and $q = 1,2,3,4,5$ if $g = 2$. One now proves the claim by showing that the expression in $(\dagger)$ is non-positive. In the case $g = 1$, one can, for instance, compute

$$\begin{aligned} (\dagger) = &\left(a^K - 1\right) w^{K-1} a^3 (aw + r)^{K-3} + \left(a^K - 1\right) w^{K-3} a (aw + r)^{K-1} - \\ &2 \left(a^K - 1\right) w^{K-2} a^2 (aw + r)^{K-2} \\ = &a \left(a^K - 1\right) w^{K-3} (aw + r)^{K-3} \left[a^2 w^2 + (aw + r)^2 - 2aw(aw + r) \right] \\ = &a \left(a^K - 1\right) w^{K-3} (aw + r)^{K-3} r^2 \leqslant 0 . \end{aligned}$$

□

Now, suppose $g \in \{0, 7\}$. The simple forms of W_0 and W_7 allow us to analytically describe (or, at least, narrow down) the asymptotic behavior of (5.3).

Theorem 5.2. *Let $K \geqslant 2$, $0 \leqslant a \leqslant 1$, and $g \in \{0, 7\}$. Iteration (5.3) has a unique global periodic attractor A. For $a \geqslant 0.5$ the attractor A is an asymptotically stable fixed point. In particular, $A = \left\{0.5^K\right\}$ if $a = 0.5$. For each $0 < a < 0.5$ there exists $K_0 = K_0(a)$ such that for any $K > K_0$ the attractor A is an asymptotically stable fixed point. Otherwise it is either an asymptotically stable fixed point or periodic orbit of length 2.*

Proof. By virtue of Corollary 5.3 we restrict ourselves to $g = 0$. Let us first consider the case $a \geqslant 0.5$. Here, W_0 is monotonously increasing, and the claim follows from Lemma 2.2.1. If $a = 0.5$, we have $W_0(w) = 0.5^K$.

Now, let $0 < a < 0.5$. Here, W_0 is monotonously decreasing, and the claim follows from Lemma 2.2.2 together with Lemma 5.1. To show existence of $K_0(a)$ we reason as follows. It holds

$$\begin{aligned} \left(W_0^2\right)''(w) = &\left(K(a - r)\right)^2 \left(r + (a - r)W_0(w)\right)^{K-2} (K - 1) \left(r + (a - r)w\right)^{K-2} (a - r) \\ &\left[r + (a - r)(K + 1)W_0(w)\right] . \end{aligned}$$

The sign of this derivative is determined by $r + (a-r)(K+1)W_0(w)$. As a function of $W_0(w)$, this expression has a unique zero at

$$W_0(w) = -\frac{r}{(a-r)(K+1)} \; . \qquad (\star)$$

For sufficiently large $K > K_0(a)$ we have $W_0(w) \leqslant r^K < -r/((a-r)(K+1))$ and $(\star)$ is not satisfied for any $0 \leqslant w \leqslant 1$. Thus, W_0^2 is concave on $[0,1]$. Moreover, note that W_0 is decreasing, and, consequently, W_0^2 is increasing. Hence W_0^2 has exactly one stable fixed point.

The case $a = 0$ was already taken care of in Theorem 5.1.2. □

Let us now consider the remaining cases $g \in \{1, 2, \ldots, 6\}$. Due to the more complicated expressions of W_g we can only obtain weaker results than in Theorem 5.2.

Theorem 5.3. *Let $K \geqslant 2$, $0 \leqslant a \leqslant 1$, and $g \in \{1, 2, \ldots, 6\}$. The iteration* (5.3) *has a unique global attractor, which is one of the following types:*

1. *an asymptotically stable periodic orbit,*
2. *a Cantor set of measure zero,*
3. *a finite union of intervals with a dense orbit.*

Proof. By virtue of Corollary 5.3 we restrict ourselves to $g \in \{1, 4, 5\}$. Recall the shape of these W_g as described in Proposition 5.7. We already remarked that they have exactly one fixed point, cf. Corollary 5.4. We denote the maximizing argument of W_g by $w_g^{\max}$, i.e. $w_g^{\max} = w_g^{(c)}$ is the critical point or $w_g^{\max}$ is a boundary point of $[0,1]$.

Case (a): If the maximum $W_g^{\max} = W_g\left(w_g^{\max}\right)$ of W_g lies below or on the diagonal, i.e. $W_g^{\max} \leqslant w_g^{\max}$, the iteration has a unique stable fixed point with full basin of attraction. This follows from Lemma 2.2.1 as W_g is increasing above the diagonal. The two shapes of W_g for which this occurs are shown schematically in Figures 5.3A, B.

The delicate point is what happens if the maximum is located above the diagonal, i.e. $W_g^{\max} > w_g^{\max}$. The three shapes of W_g for which this occurs are shown schematically in Figures 5.3C–E. We subdivide $[0,1]$ into three intervals $I_1 = \left[0, W_g\left(W_g^{\max}\right)\right]$, $I_2 = \left[W_g\left(W_g^{\max}\right), W_g^{\max}\right]$, and $I_3 = \left[W_g^{\max}, 1\right]$. Trajectories of points in I_1 ultimately land in I_2; points in I_3 are mapped into I_1 and thus later into I_2. Moreover, $W_g(I_2) \subset I_2$. Hence, we can restrict W_g to I_2.[1]

[1] I_2 is the so-called dynamical core of W_g.

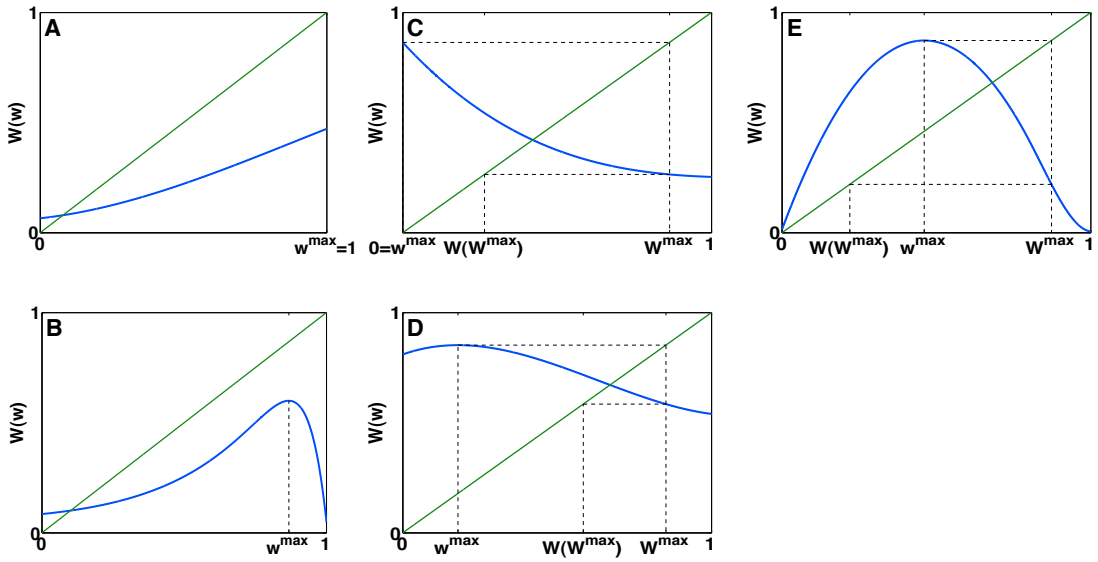

Figure 5.3: Ad proof of Theorem 5.3. Schematic plots of W_g. For the sake of presentation the subscript g has been dropped.

Case (b): First, suppose that $W_g\left(W_g^{\max}\right) \geqslant w_g^{\max}$. The two shapes of W_g for which this occurs are shown schematically in Figures 5.3C, D. By Lemmas 2.2.2 and 5.1 the restriction $W_g|_{I_2}$ has a global periodic attractor of length 1 or 2.

Case (c): Now suppose that $W_g\left(W_g^{\max}\right) < w_g^{\max}$. The shape of W_g for which this occurs is shown schematically in Figure 5.3E. In this case $w_g^{\max} = w_g^{(c)}$ is a critical point and the restriction $W_g|_{I_2}$ is S-unimodal, cf. Lemma 5.1. The statement follows from Theorem 2.5. □

Remark 5.7. According to Theorems 5.1, 5.2 and 5.3, the dynamical system (5.3) has a unique attractor for all KNsGL (g, a, K) unless $(a, K) = (0, 1)$ or $(a, K) = (1, 1)$. We denote this attractor by $L_{g,a,K}$ and formally set $L_{g,a,1} = [0, 1]$ if $a = 0$ or $a = 1$. The above-mentioned theorems also show that the basin of attraction $B_{g,a,K}$ of $L_{g,a,K}$ has full Lebesgue measure in $[0, 1]$. Again, we formally set $B_{g,a,1} = [0, 1]$ if $a = 0$ or $a = 1$. As usual, we drop the subscripts a and K if no ambiguity exists.

5.3.4 Truth-stability

Building on our results from the last section, we now define a property of KNsGL which we call *truth-stability*. We begin by taking a look at the Lyapunov exponent (cf. section 2.2.3.3) of the truth-content of a KNGL.

Proposition 5.11. *Let $g \in \{0,1,\ldots,7\}$, $0 \leqslant a \leqslant 1$, and $K \geqslant 1$. For Lebesgue-almost all $w_g(0) \in [0,1]$ the Lyapunov exponent*

$$\lambda_g = \lambda_{g,a,K} = \lim_{t\to\infty} \frac{1}{t} \sum_{\tau=0}^{t-1} \ln \left| W_g'\left(w_g(\tau)\right)\right| , \tag{5.12}$$

exists.[1] *In this case, it is identical for almost all $w_g(0) \in [0,1]$. Moreover,*

1. $\lambda_g > 0 \iff$ *W_g admits an acip.*
2. $\lambda_g < 0 \implies$ *L_g is a periodic attractor.*

Proof. By virtue of Corollary 5.2.1 we restrict ourselves to $g \in \{0,1,4,5\}$. If $K = 1$ and $a \in \{0,1\}$ we have $\lambda_{g,a,1} = 0$, and the dynamical system (5.3) possesses neutrally stable orbits, cf. Theorem 5.1.4 and 5.1.5. Now, let $(a,K) \neq (0,1)$ and $(a,K) \neq (1,1)$. If L_g is a periodic attractor, λ_g exists for all $w_g(0) \in B_g$, more precisely,

$$\lambda_g = \frac{1}{|L_g|} \sum_{w\in L_g} \ln \left| W_g'(w)\right| .$$

As L_g is stable it follows that $\lambda_g \leqslant 0$. It is also evident that a periodic attractor L_g cannot support an acip.

Thus, it remains to prove the claims for $g \in \{1,4,5\}$, if the shape of W_g is as described in case (c) from the proof of Theorem 5.3, (cf. Figure 5.3E), as in all other cases L_g is a periodic attractor. By the reasoning from the proof of Theorem 5.3 we see that in this case all trajectories are trajectories of S-unimodal functions, possibly after discarding finitely many iteration-steps. The claims follow from Proposition 2.4 and Theorem 2.6. □

With respect to sensitive dependence on initial conditions (cf. Definition 2.6) of the truth-content we have the following result.

Proposition 5.12. *Let $g \in \{0,1,\ldots,7\}$, $0 \leqslant a \leqslant 1$, and $K \geqslant 1$. If the map W_g has a periodic attractor, it does not have sensitive dependence on initial conditions. In the case it has an interval attractor, it has sensitive dependence on initial conditions.*

Proof. We denote the euclidean distance by 'dist' and the δ-neighborhood of some point w by $\mathfrak{B}_\delta(w)$. First, suppose W_g has a (global) periodic attractor as well as sensitive dependence on initial conditions. Then, there exist $\epsilon > 0$ and a point

[1] Here, we include the possibility that $\lambda_g = -\infty$.

$w^{(0)} \in B_g$ such that for any neighborhood U of $w^{(0)}$ there is $w \in U$ and $t \geqslant 0$ with $\operatorname{dist}\left(W_g^t(w^{(0)}), W_g^t(w)\right) > \epsilon$. Let $w^{(p)}$ be a periodic point of W_g. As $w^{(p)}$ is stable there is $\delta > 0$ such that $\operatorname{dist}\left(W_g^t(w'), W_g^t(w'')\right) < \epsilon$ for all $w', w'' \in \mathfrak{B}_\delta\left(w^{(p)}\right)$ and all $t \geqslant 0$. As $w^{(0)} \in B_g$ there is t_0 such that $W_g^{t_0}(w^{(0)}) \in \mathfrak{B}_\delta\left(w^{(p)}\right)$. From the continuity of W_g it follows that there is $\delta_0 > 0$ such that for all $w \in \mathfrak{B}_{\delta_0}(w^{(0)})$ we have $\operatorname{dist}\left(W_g^t(w^{(0)}), W_g^t(w)\right) < \epsilon$ for $0 \leqslant t \leqslant t_0$ and $W_g^{t_0}(w) \in \mathfrak{B}_\delta\left(w^{(p)}\right)$. This implies $\operatorname{dist}\left(W_g^t(w^{(0)}), W_g^t(w)\right) < \epsilon$ for all $w \in \mathfrak{B}_{\delta_0}(w^{(0)})$ and all $t \geqslant 0$ — a contradiction to the sensitive dependence on initial conditions.

In the proof of Theorem 5.3 we saw that, if W_g has an interval attractor, it has to be as shown in Figure 5.3E, as otherwise a periodic attractor would exist. We also saw that in this case the non-transient dynamics of W_g are dynamics of an S-unimodal function. The claim follows from Theorem 2.7. □

Now, recall that in parametrized families of S-unimodal functions there is a dichotomy except for a measure zero set of parameters, cf. Remark 2.4. The following Theorem shows that this implies also a dichotomy for KNsGL.

Theorem 5.4. *Let $g \in \{0, 1, \ldots, 7\}$. Except for a measure zero set of parameters (a, K) the dynamical system (5.3) has either a global periodic attractor and no sensitive dependence on initial conditions or an interval attractor with positive Lyapunov exponent supporting an acip and sensitive dependence on initial conditions.*

Proof. Again, we denote neighborhoods of points by $\mathfrak{B}_\cdot(\cdot)$. As the Lebesgue measure is countably additive, it suffices to prove the theorem for fixed K. Let $\mathcal{A}$ denote the set of parameters a such that (5.3) has neither a periodic attractor nor an interval attractor supporting an acip. We show that $\mathcal{A}$ is a Lebesgue measure zero set, $\nu(\mathcal{A}) = 0$. To this end, suppose that the converse is true. Then Lebesgue's density theorem, see e.g. Wheeden and Zygmund [1977], implies the existence of a point $a_0 \in \mathcal{A}$ such that $\nu\left(\mathfrak{B}_\epsilon(a_0) \cap \mathcal{A}\right) > 0$ for all $\epsilon > 0$. Since $a_0 \in \mathcal{A}$ the shape of $W_{g,a_0,K}$ has to be as shown in Figure 5.3E as otherwise $W_{g,a_0,K}$ would have a periodic attractor, cf. the reasoning in the proof of Theorem 5.3. $W_{g,a,K}$ depends analytically on a, and, consequently, there exists an interval $\mathcal{A}^I = \mathfrak{B}_{\epsilon_0}(a_0)$ containing a_0 such that $W_{g,a,K}$ has a shape as shown in Figure 5.3E for all $a \in \mathcal{A}^I$. Hence, the non-transient dynamics of the family $\left(W_{g,a,K}\right)_{a \in \mathcal{A}^I}$ are the dynamics of S-unimodal functions, cf. case (c) in the proof of Theorem 5.3. Theorem 2.8 implies $\nu\left(\mathcal{A} \cap \mathcal{A}^I\right) = 0$ which is a contradiction. The claim follows from Propositions 5.11 and 5.12. □

Theorem 5.4 motivates

Definition 5.4 (truth-stable)**.** A KNGL (g, a, K) is called *truth-stable* if $L_{g,a,K}$ is a periodic attractor.

In truth-stable networks the truth-content $w_g(t)$ has non-chaotic dynamics. Theorems 5.1 and 5.2 imply

Corollary 5.5. *We have the following sufficient conditions for the truth-stability of a KNGL* (g, a, K)*.*

1. $K = 1$ *and* $0 < a < 1$*.*
2. $K \geqslant 2$ *and* a *sufficiently small or sufficiently large.*
3. $g \in \{0, 7\}$*,* $(a, K) \neq (0, 1)$*, and* $(a, K) \neq (1, 1)$*.*

The truth-stability in the remaining cases is investigated numerically in section 5.5.

5.4 Dynamic regimes of Kauffman networks with generic logics

In truth-stable KNsGL the truth-content $w_g(t)$ is a stable quantity, i.e. upon perturbations this quantity will converge back to its unique attractor. In realizations we, therefore, expect the fraction of ones in a trajectory to re-converge upon perturbations. This, however, does not necessarily imply that also the trajectory itself will re-converge (in the Boolean state-space). This property is exactly what distinguishes frozen from chaotic KNs. In frozen KNs flips of single bits will not propagate through the network but will be eradicated over time. For this reason, we will also call frozen (chaotic) KNsGL *bit-stable* (*bit-unstable*) in the following.

Let us now investigate how truth-stable KNsGL behave with respect to possible phase transitions. In this section, we analytically determine their critical boundary using again the Hamming distance between two trajectories as an order parameter. Throughout this section, $\mathcal{K} = (g, a, K)$ will always be a truth-stable KNGL with truth-content $(w_g(t))_{t \geqslant 0}$.

5.4.1 The Hamming distance of a Kauffman network with generic logic

We use again the Hamming distance between two trajectories as an order parameter to detect phase transitions in KNsGL. In chapter 4 we saw that in KNsMB the behavior of this Hamming distance is controlled by the mean connectivity $\overline{K}$ as well as by the heterogeneity $\overline{p}$ of the KN, cf. Theorem 4.1. According to Remark 4.3, the heterogeneity is the probability for a generated update rule f_i to yield two different values for two different arguments. In KNsMB this probability depends only on the magnetization bias. In KNsGL, however, it depends also on whether the inputs are 0 or 1: Suppose, for instance, that an update rule was generated using $g = 0\hat{=}(\wedge, \wedge, \wedge)$ and that one of its inputs is flipped. Now, this will only have an effect on the output if all further inputs are 1 in the case they are activators and 0 in the case they are inhibitors. This explains why we went to such great lengths to understand the truth-content of KNsGL in the previous section. We modify Definition 4.3 accordingly and obtain

Definition 5.5 (order parameter for KNsGL)**.** The *Hamming distance* of $\mathcal{K}$ is a sequence $(d_{g,a,K}(t))_{t\geqslant 0}$ which is consistent in the sense of the following random experiment: Pick a realization of $\mathcal{K}$. Create two configurations $\mathbf{x}(0)$ and $\mathbf{x}'(0)$ whose components differ with probability $d_{g,a,K}(t)$ and whose identical components are 1 with probability $w_g(t)$. Iterate $\mathbf{x}(0)$ and $\mathbf{x}'(0)$ one time-step yielding configurations $\mathbf{x}(1)$ and $\mathbf{x}'(1)$. Then, $d_{g,a,K}(t+1)$ is the expected Hamming distance between $\mathbf{x}(1)$ and $\mathbf{x}'(1)$. If no ambiguity exists, we simply write $d_g(t)$ instead of $d_{g,a,K}(t)$.

Remark 5.8. Two clarifications are in order.

1. As argued in Remark 4.4, Lemma 2.1 allows us to approximate the Hamming distance of $\mathcal{K}$ by the Hamming distance

$$\frac{1}{N}\sum_{i=1}^{N}\left(1-\delta_{x_i(t),x_i'(t)}\right)$$

between two trajectories $\mathbf{x}(t)$ and $\mathbf{x}'(t)$ of a specific realization of $\mathcal{K}$ provided N is sufficiently large. We will demonstrate this by simulations in section 5.5.3.

2. Apart from the initial distance $d_{g,a,K}(0)$, the Hamming distance also depends on the initial truth-content $w_{g,a,K}(0)$ of $\mathcal{K}$. This seems a problem, as in 1. the initial fractions of ones in the trajectories $\mathbf{x}(t)$ and $\mathbf{x}'(t)$ might differ. However, we know from Remark 5.7 that the asymptotic behavior of $w_g(t)$ is (almost)

independent of the initial condition. Moreover, we will investigate the evolution of small perturbations and may therefore assume the fractions of ones in $\mathbf{x}(t)$ and $\mathbf{x}'(t)$ to be almost identical, even from the beginning on.

5.4.2 Iterations for the Hamming distance

We now derive functions $D_{g,a,K} = D_g$ such that the Hamming distance $(d_g(t))_{t\geqslant 0}$ of $\mathcal{K}$ satisfies the iteration $d_g(t+1) = D_g\left(d_g(t), w_g(t)\right)$. Given $d_g(t)$ and $w_g(t)$, let us consider the random experiment from Definition 5.5. We proceed as in the proof of Lemma 4.2. Let the random variable $\mathfrak{d}$ be defined as the Hamming distance $d\left(\mathbf{x}(1), \mathbf{x}'(1)\right)$ and the identically distributed Bernoulli random variables $\mathfrak{d}_i$, $i = 1, 2, \ldots, N$, as 1 if $x_i(1) \neq x'_i(1)$ and as 0 otherwise. It then holds $\mathfrak{d} = (1/N)\sum_{i=1}^{N} \mathfrak{d}_i$, and, consequently,

$$d_g(t+1) = \mathbb{E}\left(\mathfrak{d}\right) = \frac{1}{N}\sum_{i'=1}^{N} \mathbb{E}\left(\mathfrak{d}_{i'}\right) = \mathbb{E}\left(\mathfrak{d}_i\right) \tag{5.13}$$

for any i.

Fixing some node i with $K_i = K$ inputs, the mean $\mathbb{E}\left(\mathfrak{d}_i\right)$ is equal to the probability for

$$f_i^g\left(x_{i_1}(0), x_{i_2}(0), \ldots, x_{i_K}(0)\right) \neq f_i^g\left(x'_{i_1}(0), x'_{i_2}(0), \ldots, x'_{i_K}(0)\right)$$

with f_i^g from (5.1). The edges $i_k \to i$ are independently classified as activating and inhibiting with probabilities a and r, respectively, the inputs are independently chosen to differ, $x_{i_k}(0) \neq x'_{i_k}(0)$, with probability $d_g(t)$, and the identical inputs are 1 with probability $w_g(t)$. In this situation, the probability that k of the K inputs differ is equal to $\binom{K}{k} d_g(t)^k \left(1 - d_g(t)\right)^{K-k}$, and we let

$$p_g^{(k)}\left(w_g(t)\right) = p_{g,a,K}^{(k)}\left(w_g(t)\right) \tag{5.14}$$

be the probability that the update rule f_i^g non-trivially depends on these k inputs. We may, thus, write

$$\mathbb{E}\left(\mathfrak{d}_i\right) = \sum_{k=0}^{K} \binom{K}{k} d_g(t)^k \left(1 - d_g(t)\right)^{K-k} p_g^{(k)}\left(w_g(t)\right) \ ,$$

where, formally, $p_g^{(0)}\left(w_g(t)\right) = 0$. Hence, according to (5.13) the Hamming distance $(d_g(t))_{t\geqslant 0}$ of $\mathcal{K}$ obeys the iteration

$$d_g(t+1) = D_g\left(d_g(t), w_g(t)\right) = \sum_{k=0}^{K} \binom{K}{k} d_g(t)^k \left(1 - d_g(t)\right)^{K-k} p_g^{(k)}\left(w_g(t)\right) \ .$$

The tricky part is the computation of the $p_g^{(k)}(w)$, especially for $k > 1$. Here, however, we can make use of the following corollary implied by Proposition 5.3.

Corollary 5.6. *The $p_{g,a,K}^{(k)}(w)$ from (5.14) satisfy the following symmetry properties.*

1. *For $(g, g') \in \{(0,7), (1,6), (2,5), (3,4)\}$ we have $p_{g,a,K}^{(k)}(w) = p_{g',a,K}^{(k)}(1-w)$.*
2. *For $(g, g') \in \{(0,7), (1,3), (2,5), (4,6)\}$ we have $p_{g,a,K}^{(k)}(w) = p_{g',r,K}^{(k)}(w)$.*

Moreover, we will soon see that for our purposes it suffices to know $p_g^{(1)}(w)$.

5.4.3 Analysis of the Hamming distance and detection of a phase transition

Let us now consider the iteration

$$\begin{pmatrix} w_g(t+1) \\ d_g(t+1) \end{pmatrix} = \begin{pmatrix} W_g(w_g(t)) \\ D_g(d_g(t), w_g(t)) \end{pmatrix}. \tag{5.15}$$

As $p_g^{(0)}(w_g) = 0$ independently of w_g, the set $\{(w_g, d_g) \mid d_g = d^\star = 0\}$ is an invariant set of (5.15). This is intuitive, as the realizations of KNs give rise to fully deterministic dynamical systems, and trajectories that agree at some point in time will also agree at all future time-points. The first component $w_g(t)$ of (5.15) is independent of the second, and its behavior was analyzed in section 5.3. It was shown that it possesses a unique attractor $L_{g,a,K}$, which in the case of a truth-stable network is a stable periodic orbit.

Recall that we distinguished the dynamic regimes of MKNs according to the stability of the fixed point $d^\star$ of iteration (4.7). In the case of KNsGL, we distinguish between frozen and chaotic regimes by looking at the stability of the orbit $D^\star = L_{g,a,K} \times \{d^\star\}$. If $D^\star$ is asymptotically stable, we expect trajectories of realizations of the KNGL to re-converge upon small perturbations, whereas if $D^\star$ is unstable they will diverge. This motivates

Definition 5.6 (phases/regimes of KNsGL)**.** We say that the KNGL (g, a, K) is frozen/critical/chaotic if the orbit $D^\star$ is asymptotically stable/critical/unstable.

We now determine the stability of $D^\star$. First of all, we observe that the Jacobian of (5.15) in $(w_g, d^\star)$ is triangular with eigenvalues $W_g'(w_g)$ and $(\partial/\partial d) D_g(d, w)|_{(d^\star, w_g)} = K p_g(w_g)$, where $p_g(w_g) := p_g^{(1)}(w_g)$.

Interestingly, it suffices to consider the dependencies $p_g(w)$ of update rules on single inputs. Let us now compute them. We consider a prototypic update function f_i^g from (5.1) with $K_i = K$ inputs, $K-1$ of which are fixed, w.l.o.g. $x_{i_2}, x_{i_3}, \ldots, x_{i_K}$, and study its dependence on x_{i_1}. The edges $i_k \to i$ are independently classified as activating and inhibiting with probabilities a and r, respectively; the $K-1$ identical inputs are 1 with probability w and 0 with probability $1-w$.

The probability for α of the $K-1$ fixed inputs of f_i^g to be activating and $K-1-\alpha$ inputs to be inhibiting is given by $\binom{K-1}{\alpha} a^\alpha r^{K-1-\alpha}$. In this situation and

- using $g=0$, the probability for f_i^0 to depend on x_{i_1} is given by $w^\alpha (1-w)^{K-1-\alpha}$, as already one inactive activator or one active inhibitor will determine the value of f_i^0 irrespective of x_{i_1}. Summing over all possible activator-inhibitor-combinations of the $K-1$ fixed inputs yields

$$p_0(w) = (aw + r(1-w))^{K-1} \ . \tag{5.16}$$

- using $g=1$, the probability for f_i^1 to depend on x_{i_1} is given by

$$\begin{array}{ll} w^\alpha \left(1 - w^{K-1-\alpha}\right) \ , & \text{if } i_1 \text{ is activating and } \alpha < K-1 \\ w^{K-1} \ , & \text{if } i_1 \text{ is activating and } \alpha = K-1 \\ w^{K-1} \ , & \text{if } i_1 \text{ is inhibiting.} \end{array}$$

  In the case that i_1 is activating, all other activators need to be 1, and, if existing, at least one of the inhibitors needs to be 0 for the value of f_i^1 to depend on x_{i_1}. In the case that i_1 is inhibiting, f_i^1 will depend on x_{i_1}, if all activators and inhibitors are 1. Summing over all possible activator-inhibitor-combinations of the K inputs yields

$$p_1(w) = a\left[(aw+r)^{K-1} - \left(1 - a^{K-1}\right) w^{K-1}\right] + r w^{K-1} \ . \tag{5.17}$$

- using $g=2$, the probability for f_i^2 to depend on x_{i_1} is given by

$$\begin{array}{ll} w^\alpha \left(1 - (1-w)^{K-1-\alpha}\right) \ , & \text{if } i_1 \text{ is activating and } \alpha < K-1 \\ w^{K-1} \ , & \text{if } i_1 \text{ is activating and } \alpha = K-1 \\ (1-w)^{K-1} \ , & \text{if } i_1 \text{ is inhibiting and } \alpha = 0 \\ (1-w^\alpha)(1-w)^{K-1-\alpha} \ , & \text{if } i_1 \text{ is inhibiting and } \alpha > 0 \ . \end{array}$$

  In the case that i_1 is activating, all other activators need to be 1, and, if existing, at least one of the inhibitors needs to be 1 for the value of f_i^2 to depend on x_{i_1}. In

the case that i_1 is inhibiting, f_i^2 will depend on x_{i_1}, if all inhibitors are 0 and, if existing, at least one activator is 0. Summing over all possible activator-inhibitor-combinations of the K inputs yields

$$p_2(w) = a\left[(aw+r)^{K-1} - (aw+r(1-w))^{K-1} + (aw)^{K-1}\right] + r\left[(a+r(1-w))^{K-1} - (aw+r(1-w))^{K-1} + (r(1-w))^{K-1}\right]. \tag{5.18}$$

Using Corollary 5.6

$$p_{3,a,K}(w) = p_{1,r,K}(w) \tag{5.19}$$

$$p_{4,a,K}(w) = p_{3,a,K}(1-w) \tag{5.20}$$

$$p_{5,a,K}(w) = p_{2,a,K}(1-w) \tag{5.21}$$

$$p_{6,a,K}(w) = p_{1,a,K}(1-w) \tag{5.22}$$

$$p_{7,a,K}(w) = p_{0,a,K}(1-w)\ . \tag{5.23}$$

Recall that the Jacobian of (5.15) in $(w_g, d^\star)$ has eigenvalues $W_g'(w_g)$ and $Kp_g(w_g)$. In our stability analysis of $D^\star$ we proceed by showing

Lemma 5.2. *For all $w \in (0,1)$ we have $Kp_g(w) \geqslant \left|W_g'(w)\right|$ with equality iff $a = 0$ or $a = 1$.*

Proof. By virtue of Corollaries 5.2 and 5.6 we can restrict ourselves to $g \in \{0,1,2\}$. If $g = 0$ we compute

$$Kp_0(w) - \left|W_0'(w)\right| = K\left(aw + r(1-w)\right)^{K-1}\left(1 - |a-r|\right) \geqslant 0$$

with equality iff $a = 0$ or $a = 1$.

In the case $g = 1$, we have

$$Kp_1(w) - \left|W_1'(w)\right| \left\{ \begin{array}{ll} = 2Krw^{K-1}\,, & \text{if } W_1'(w) \geqslant 0 \\ \geqslant Kw^{K-1}\left(a + 2a^K\right)\,, & \text{if } W_1'(w) < 0 \end{array} \right\} \geqslant 0$$

with equality iff $a = 0$ or $a = 1$. (Note that $a = 0$ implies $W_1'(w) \leqslant 0$, while $a = 1$ implies $W_1'(w) \geqslant 0$.)

Finally, for $g = 2$ it holds

$$Kp_2(w) - \left|W_2'(w)\right| = \begin{cases} 2Kr\left[(a+r(1-w))^{K-1} - (aw+r(1-w))^{K-1} + (r(1-w))^{K-1}\right], & W_2'(w) \geqslant 0 \\ 2Ka\left[(aw+r)^{K-1} - (aw+r(1-w))^{K-1} + (aw)^{K-1}\right], & W_2'(w) < 0\,. \end{cases}$$

If $a \in (0,1)$, these expressions are positive as $(a + r(1-w))^{K-1} > (aw + r(1-w))^{K-1}$ (in the case $W_2'(w) \geqslant 0$) and $(aw+r)^{K-1} > (aw + r(1-w))^{K-1}$ (in the case $W_2'(w) < 0$). □

Thus, the maximal eigenvalue of the Jacobian of (5.15) in $(w_g, d^\star)$ is $Kp_g(w_g)$. Theorem 2.2 together with Remark 2.2 yields

Theorem 5.5 (phase transition criterion)**.** *The dynamic regimes of a KNGL (g,a,K) are determined by*

$$\Lambda_g = \Lambda_{g,a,K} = \prod_{w \in L_{g,a,K}} Kp_{g,a,K}(w) \tag{5.24}$$

via

$$\Lambda_g \begin{cases} < 1 & \textit{frozen regime, bit-stability} \\ = 1 & \textit{critical boundary} \\ > 1 & \textit{chaotic regime, bit-unstability.} \end{cases}$$

Again, we can interpret Λ_g from (5.24) in terms of "damage spreading." It is the mean number of flipped nodes triggered by the flip of a single node after one circulation of the truth-content.

In the extreme and asymptotic cases from Theorem 5.1 we have

Theorem 5.6. *The following hold.*

1. *Let $1 < K$ and $g \in \{0,1,\ldots,7\}$. For either a sufficiently close to 0 or sufficiently close to 1 the KNGL (g,a,K) is bit-stable.*
2. *For $K = 1$, any $0 \leqslant a \leqslant 1$ and any $g \in \{0,1,\ldots,7\}$ the KNGL (g,a,K) is critical. (See also Remark 5.3.)*
3. *For $g \in \{0,1,6,7\}$, any $0 < a < 1$ and sufficiently large K, the KNGL (g,a,K) is bit-stable.*

Proof. We show claim 1 exemplarily for $g = 0$ and sufficiently small a. Let $a = 0$. From Theorem 5.1.2 we know that $L_{0,0,K} = \{0,1\}$. Moreover, $p_{0,0,K}(w) = (1-w)^{K-1}$. Thus,

$$\Lambda_{0,0,K} = \left(K1^{K-1}\right) \cdot \left(K0^{K-1}\right) = 0\,.$$

Since $\Lambda_{0,a,K}$ depends continuously on a, the claim for sufficiently small a follows. Claim 2 is obvious, but the limit of large K warrants a little attention. We know from

Theorem 5.1.6 that for $g \in \{0,1\}$ ($g \in \{6,7\}$) the attractor $L_{g,a,K}$ becomes a fixed point $w_g^{(f)}$ approaching 0 (1) as K increases. Hence, for sufficiently large K we have $\Lambda_{g,a,K} = K p_{g,a,K}\left(w_g^{(f)}\right)$. By virtue of Corollary 5.6 we restrict ourselves to $g \in \{0,1\}$. In these cases it follows from (5.16) and (5.17) that $\Lambda_{g,a,K} \to 0$ as K increases. (Note that $p_{g,a,K}\left(w_g^{(f)}\right) \to 0$ exponentially.) □

The behavior in between these extrema will be investigated numerically in the following section.

Remark 5.9. Theorem 5.6.3 shows that for high connectivities KNs with generic logics $0, 1, 6$ and 7 become frozen. This is somewhat counterintuitive, as from the theory of MKNs we would expect a phase transition from order to chaos as the connectivity increases, cf. Corollary 4.2.

5.5 Numeric results and network simulations

After the analytic investigations in the previous sections, we now present results from numeric studies. We focus, in particular, on the behavior of KNsGL (g, a, K) for biologically reasonable values of a and K. Finally, we show that our analytic results from the previous sections agree with simulations of realizations of KNsGL. As justified in Corollary 5.1 we will restrict ourselves to $g \in \{0,1,2,3\}$ throughout this section. For aesthetic reasons, we allow $K \in \mathbb{R}$, $K \geqslant 1$, in our numeric studies.

5.5.1 Biologically reasonable parameters

The transcriptional gene regulatory networks of lower organisms, such as *E. coli* or *yeast* have been identified to a large extent [Keseler et al., 2008; Lee et al., 2002]. The average connectivity[1] in these networks is typically small, $K \approx 2-3$, which, interestingly, agrees well with the critical connectivity of SKNs. With few exceptions all interactions in these networks could be classified as either activating or inhibiting. (The exceptions are transcription factors whose regulatory function can be altered by the binding of so-called co-factors.) One observes a clear bias towards activating

[1] We may, of course, always compute the average connectivity of some given graph. The question is, however, whether this quantity is a meaningful characteristic. In scale-free networks [Albert and Barabási, 2002], whose degrees are power-law distributed, this is, for instance, typically not the case. We comment on this issue in section 7.2.2.

interactions. In Alon [2006], a rough estimate of $60\% - 80\%$ activating interactions in gene regulatory networks is given.

In higher organisms, our knowledge about epistatic relationships is hopelessly incomplete, but available data also suggest a bias towards activations. Also, it has been speculated that biological networks, in general, are sparse, i.e. the mean connectivity is low [Leclerc, 2008]. We will consider $a \approx 0.7$ and $K \approx 2 - 3$ biologically reasonable parameters.

5.5.2 Numerical investigation of truth- and bit-stability

For $g \in \{1, 2, \ldots, 6\}$, the dynamics of (5.3) are essentially dynamics of S-unimodal functions. Thus, we may expect a transition to chaos of $w_g(t)$ via period-doublings, similar to the behavior of the logistic equation described in section 2.2.4.1.

5.5.2.1 A global view of the parameter space

In a first attempt to get a rough overview of the behavior of (5.3) we search for stable periodic orbits of (5.3) for values of a and K on a fine grid in $[0, 1] \times [1, 30]$. The results are shown in Figure 5.4. Figure 5.4A nicely confirms our analytic results from Theorem 5.2 about KNs with generic logics 0 and 7. As expected, we detect period-doublings with increasing K for $g \in \{1, 2, 3\}$. In the case $g = 1$, we have period-doublings for small values of a, cf. Figure 5.4B and the magnification in Figure 5.4E. In the cases $g = 2$ and $g = 3$ we seem to have period-doublings for all values of a, cf. Figures 5.4C and D.

Still, according to section 5.5.1 the values of a and K at which this mathematically interesting behavior occurs are biologically not plausible. Instead, we observe that a unique asymptotically stable fixed point exists for any generic logic and biologically reasonable values of a and K.

Phase transitions are marked by green lines in Figure 5.4. Strikingly, we find that for fixed a KNsGL possess several critical connectivities at which a phase transition occurs, see, in particular, the magnification in Figure 5.4F. (Recall that KNsMB possess a single critical connectivity for each magnetization bias u, cf. Corollary 4.2.) Qualitatively, the phase transitions for $g = 0$ and $g = 1$ as well as for $g = 2$ and $g = 3$ are similar. Theorem 5.6 agrees well with our numerical findings. For each generic logic, KNs are critical if

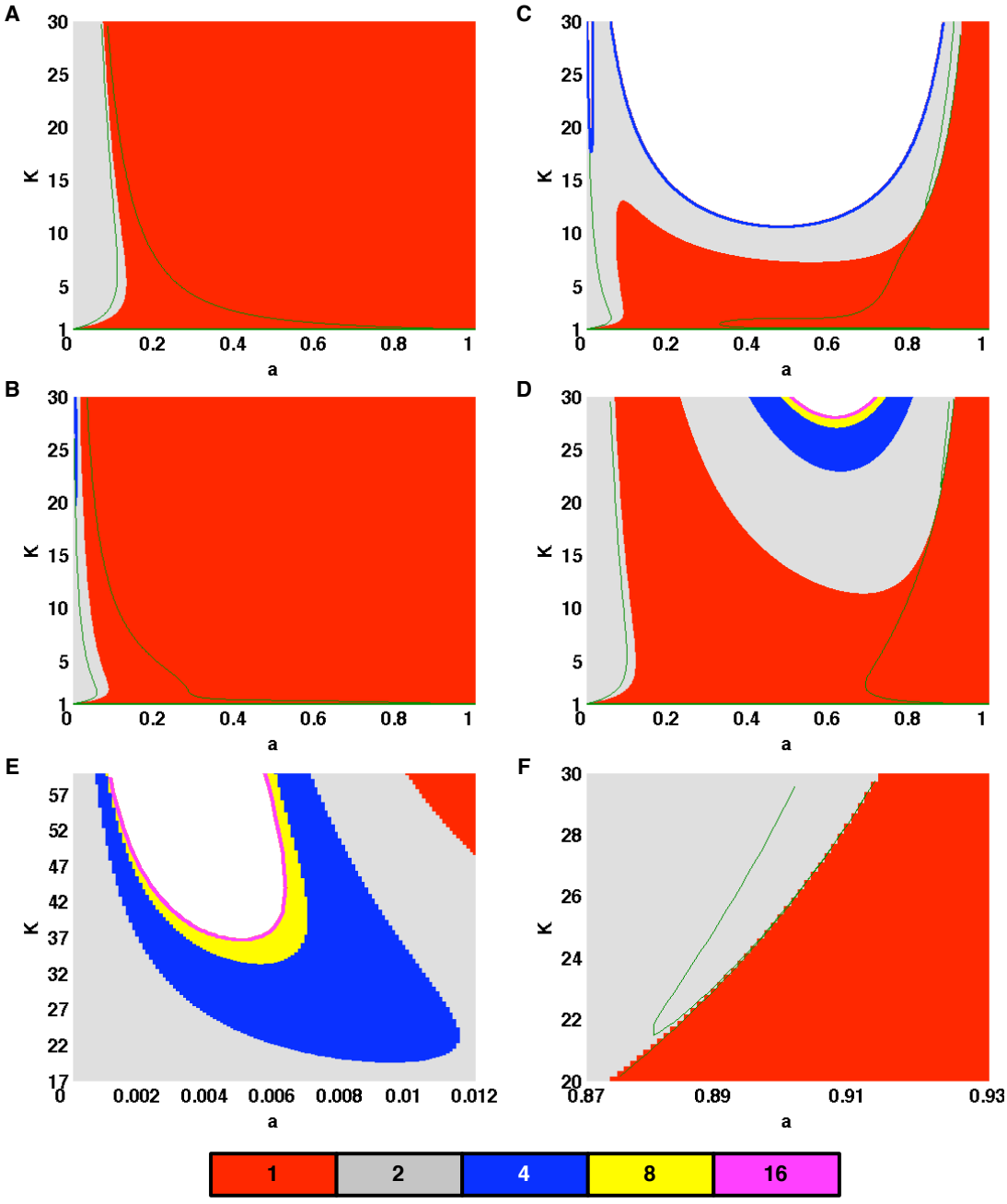

Figure 5.4: Stable periodic orbits of (5.3) were detected for **(A)** $g = 0$, **(B)** $g = 1$, **(C)** $g = 2$, **(D)** $g = 3$, and values of a and K on a fine grid in $[0, 1] \times [1, 30]$. For $g \in \{0, 1, 3\}$ periodic orbits could be reliably detected up to length 16, for $g = 2$ up to length 4. In the a-K-plane the regions corresponding to different attractor-lengths are color-coded. Green lines indicate phase transitions, i.e. points where Λ_g from (5.24) crosses 1. In any case, the $K = 1$-line is a critical boundary where Λ_g crosses 1 from below as K grows. **(E)** and **(F)** show magnifications of (B) and (D), respectively.

$K = 1$ and become frozen as $a \to 0$ or $a \to 1$. In the cases $g \in \{0, 1\}$, cf. Figures 5.4A and B, KNsGL become frozen as K grows for any $0 < a < 1$.

5.5.2.2 Dynamics for selected parameter values

We now select the most interesting values of a for each $g \in \{0, 1, 2, 3\}$ from both, a mathematical as well as biological point of view, and analyze the behavior of (5.3) in more detail.

Unbiased networks: Let us begin with the case $a = 0.5$, that corresponds to the standard (unbiased) KNs. For $g \in \{0, 1\}$, (5.3) has an asymptotically stable fixed point which approaches zero as $K \to \infty$, cf. Figures 5.5A and B. This agrees with Theorems 5.1.6 and 5.2. For $g \in \{2, 3\}$, we observe a "period doubling route to chaos" as described in section 2.2.4.1, cf. Figures 5.5C and D.

Biologically reasonable networks: The behavior in the biologically reasonable case $a = 0.7$ does not differ qualitatively from the case $a = 0.5$, cf. Figure 5.6.

Networks with a bias towards inhibitions: The mathematically most interesting behavior is observed for small a, cf. Figures 5.7 and 5.8. In Theorem 5.1.6 we remarked that for $g \in \{0, 1\}$ the truth-content has stationary dynamics for sufficiently large K with an equilibrium approaching zero. In agreement with this theoretical result, we observe in Figure 5.7A that for $g = 0$ and $a = 0.1$ the stable fixed point first bifurcates into a stable 2-cycle and ultimately becomes stable again near zero. In the case $g = 1$ and $a = 0.006$ we also detect an attractive fixed point near zero for large K, cf. Figure 5.7B. For smaller K, however, the behavior for $g = 1$ is much more intricate than for $g = 0$. Here we observe a "chaotic bubble" that opens with a sequence of period-doublings and closes with a sequence of period-halvings, cf. the magnifications in Figures 5.7C and D.

The cases $g = 2$ ($a = 0.01$) and $g = 3$ ($a = 0.1$) are also interesting. The behavior for small K is shown in Figures 5.8B and D. With growing K, KNs with generic logic 2 exhibit period-doublings as described in section 2.2.4.1, and the diameter of the attractor decreases. KNs with $g = 3$ have a stable fixed point or a stable periodic attractor of length 2 for smaller K. As can be seen in Figures 5.8A and C these behaviors change as K increases. In the case $g = 2$ the diameter of the

attractor starts re-increasing up to 1. For $g = 3$ the change is even more abrupt when for large K period-doublings set in.

The bifurcation diagrams for $g = 3$ and increasing a, cf. Figures 5.8C, 5.5D and 5.6D, nicely confirm Theorem 5.1.6. Although $w_3(t)$ exhibits chaotic dynamics, for large K the sequence becomes restricted to an interval with upper bound 1, whose length decreases with a. Hence, for small a, we have essentially $w_3(t) \approx 1$ despite the chaotic dynamics.

5.5.3 Network simulations

We now further validate our results from section 5.3 by comparing the truth-contents of KNsGL to the fractions of ones in trajectories of realizations. To this end, we generate realizations of KNsGL with $g = 0/a = 0.1$, $g = 1/a = 0.006$, $g = 2/a = 0.5$ and $g = 3/a = 0.5$. Figure 5.9 shows the attractors of the fraction of ones in trajectories of these realizations (see figure caption for technical details). Comparing Figure 5.9 to the bifurcation diagrams of the truth-content shown in Figures 5.7A, C, 5.5C, D we observe an almost perfect agreement.

In a next step, we validate also the critical boundaries obtained by studying the Hamming distance of KNsGL in section 5.4. To this end, realizations of KNsGL with connectivities $K = 1, 2, \ldots, 30$, and activation biases $a = 0.001, 0.002, \ldots, 0.999$ are generated for $g = 0, 1, 2, 3$. Two different configurations with (normalized) Hamming distance 10^{-3} are each iterated and their Hamming distance after 50 time-steps is plotted in Figure 5.10. Comparing the results to the critical boundaries shown in Figure 5.4 we observe a good agreement in the cases $g = 1$ and $g = 2$. For $g = 0$ and $g = 3$ there is a good agreement up to a connectivity of around 10, above the agreement is rather poor.

A possible explanation for this is that the assumption of independent inputs is not valid for high connectivities, cf. Lemma 2.1. However, we would not know why this is critical only in the cases $g = 0$ and $g = 3$. Therefore, we deem another explanation more likely. It is suggested by the fact that the agreement is worst for small a and large K. Let us choose representatives for this region of the parameter space, say $a = 0.1$ and $K = 20$. Then for $w_g \in L_{g,0.1,20}$, $g = 0, 1, 2, 3$, we have $w_0 = 0.049$, $w_1 = 0.181$, $0.087 < w_2 < 0.218$, and $w_3 = 0.932$. Hence, while there is still variability in $w_1(t)$

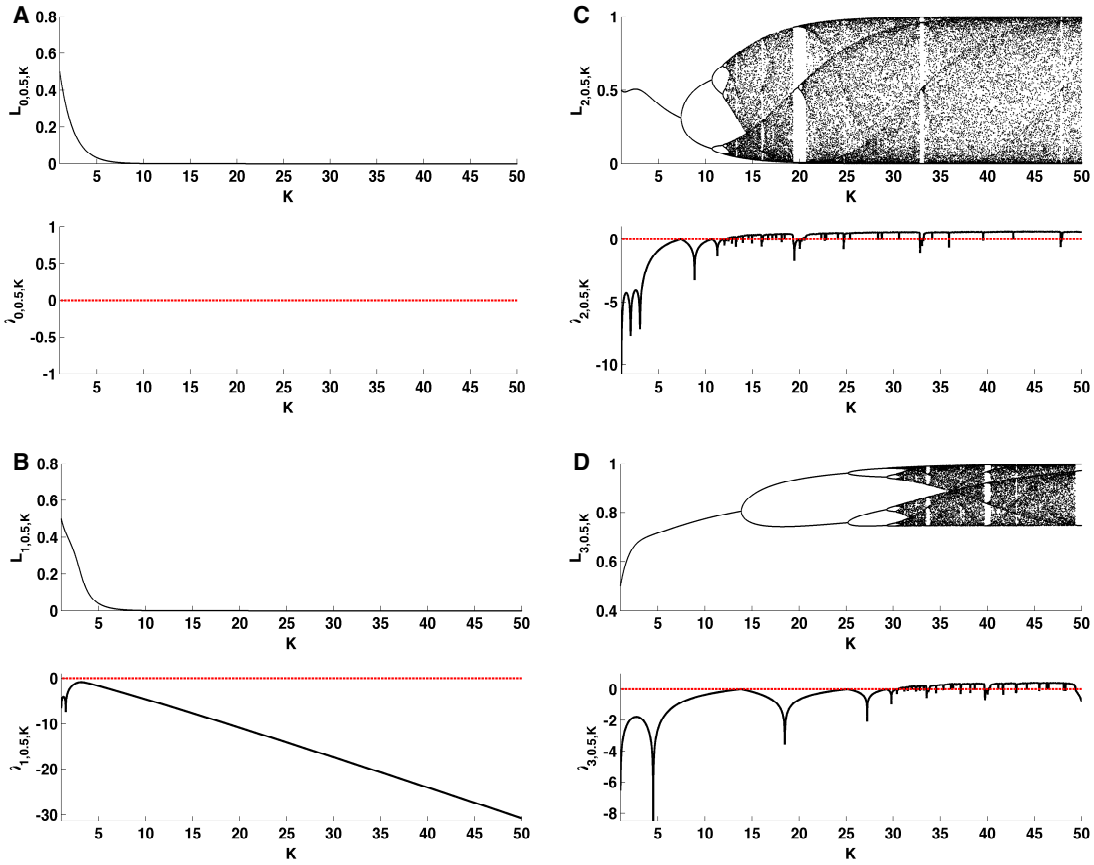

Figure 5.5: Bifurcation diagrams of (5.3) for **(A)** $g = 0$, **(B)** $g = 1$, **(C)** $g = 2$, **(D)** $g = 3$, $a = 0.5$, and $K = 1, 1.01, 1.02, \ldots, 50$. In each subfigure the upper part shows the attractor $L_{g,0.5,K}$ for increasing K. The attractor was found by iterating (5.3) 10^6 times and plotting the subsequent 10^2 iterations. The lower part of each subfigure shows the Lyapunov exponent $\lambda_{g,0.5,K}$ from (5.12). It was obtained as the average over 10^3 iterations (after the burn-in). Note that in (A) $\lambda_{0,0.5,K} = -\infty$.

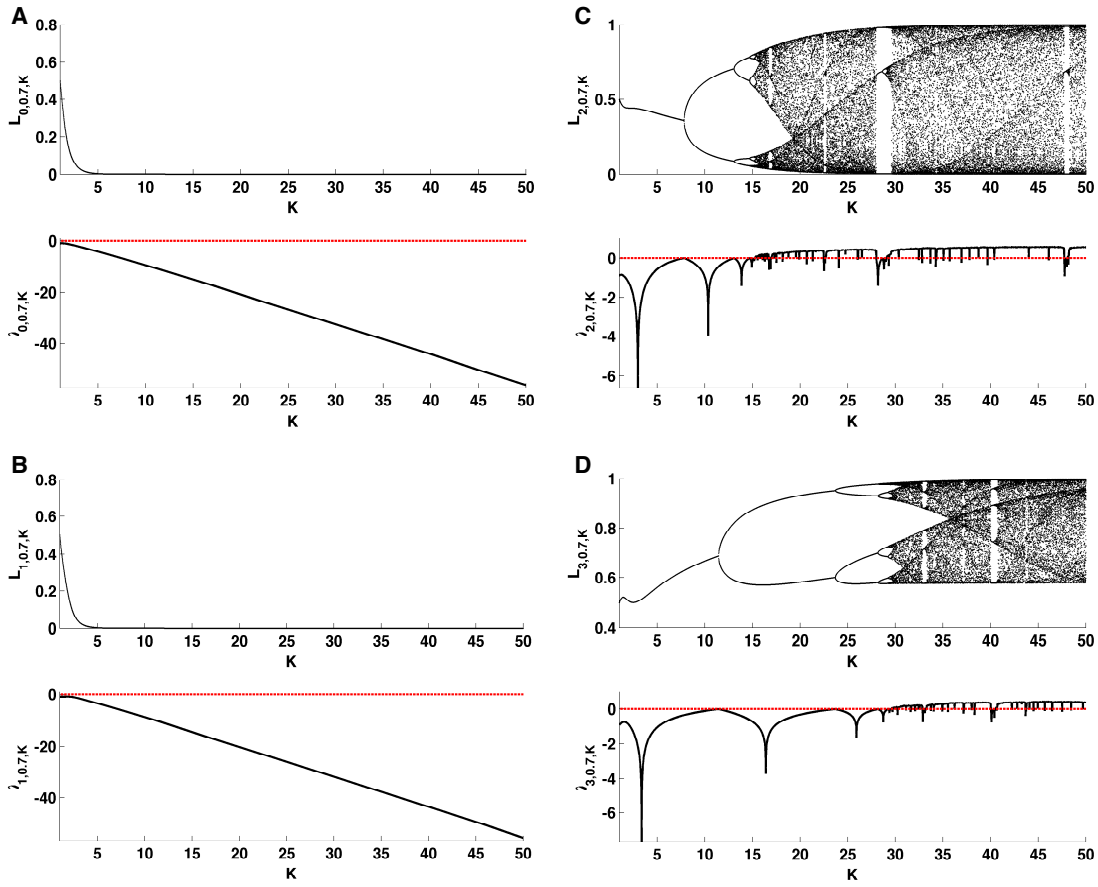

Figure 5.6: Bifurcation diagrams of (5.3) for **(A)** $g = 0$, **(B)** $g = 1$, **(C)** $g = 2$, **(D)** $g = 3$, $a = 0.7$, and $K = 1, 1.01, 1.02, \ldots, 50$. In each subfigure the upper part shows the attractor $L_{g,0.7,K}$ for increasing K. The lower part shows the Lyapunov exponent $\lambda_{g,0.7,K}$ from (5.12). Technicalities as in Figure 5.5.

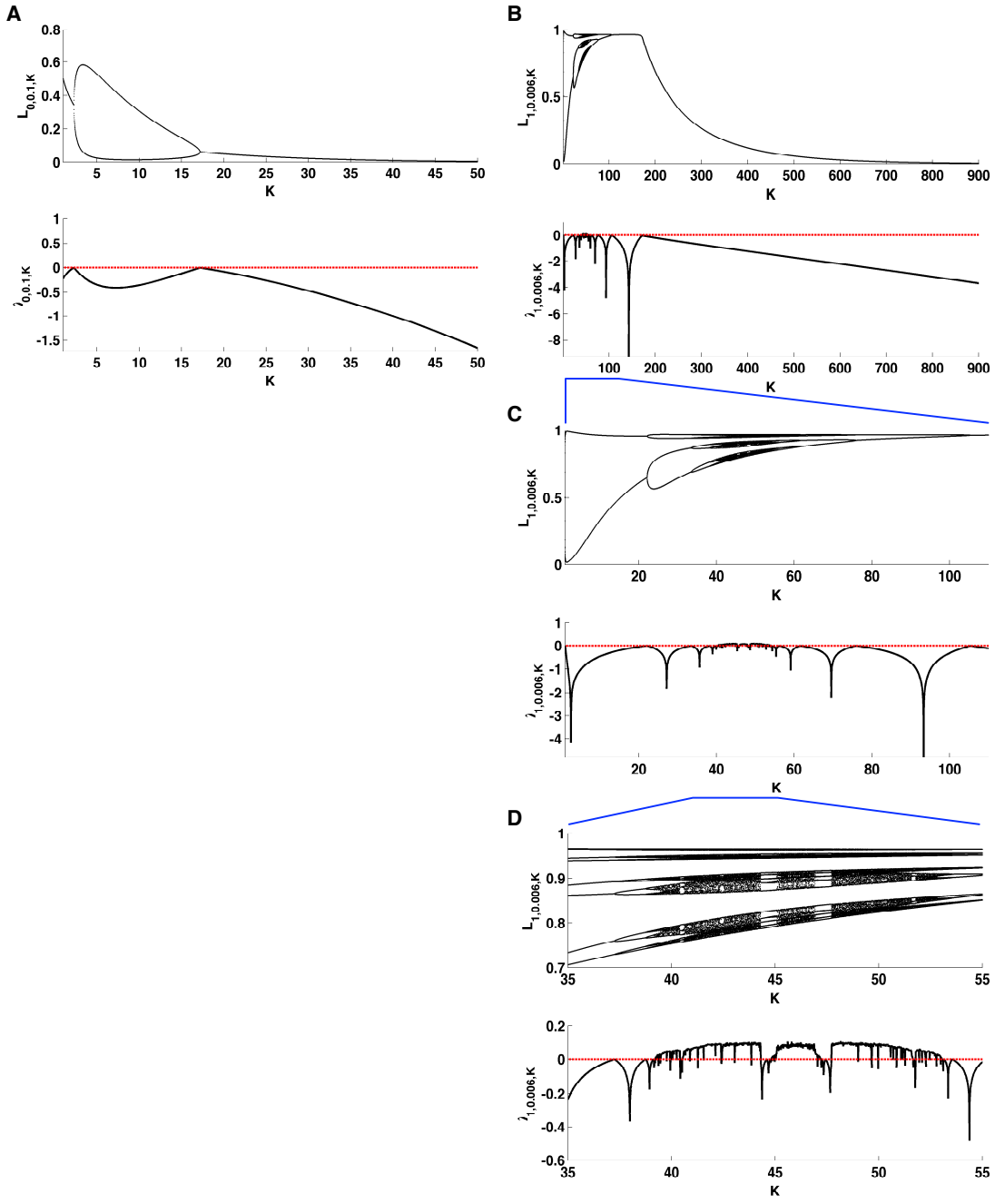

Figure 5.7: Bifurcation diagrams of (5.3) for $g \in \{0, 1\}$, small a, and $K \geqslant 1$ in .01-steps. In each subfigure the upper part shows the attractor $L_{g,a,K}$ for increasing K. The lower part shows the Lyapunov exponent $\lambda_{g,a,K}$ from (5.12). **(A)** $g = 0$, $a = 0.1$, and $K \leqslant 50$. **(B)** $g = 1$, $a = 0.006$, and $K \leqslant 900$. **(C)** Magnification of (B). **(D)** Magnification of (C). Technicalities as in Figure 5.5.

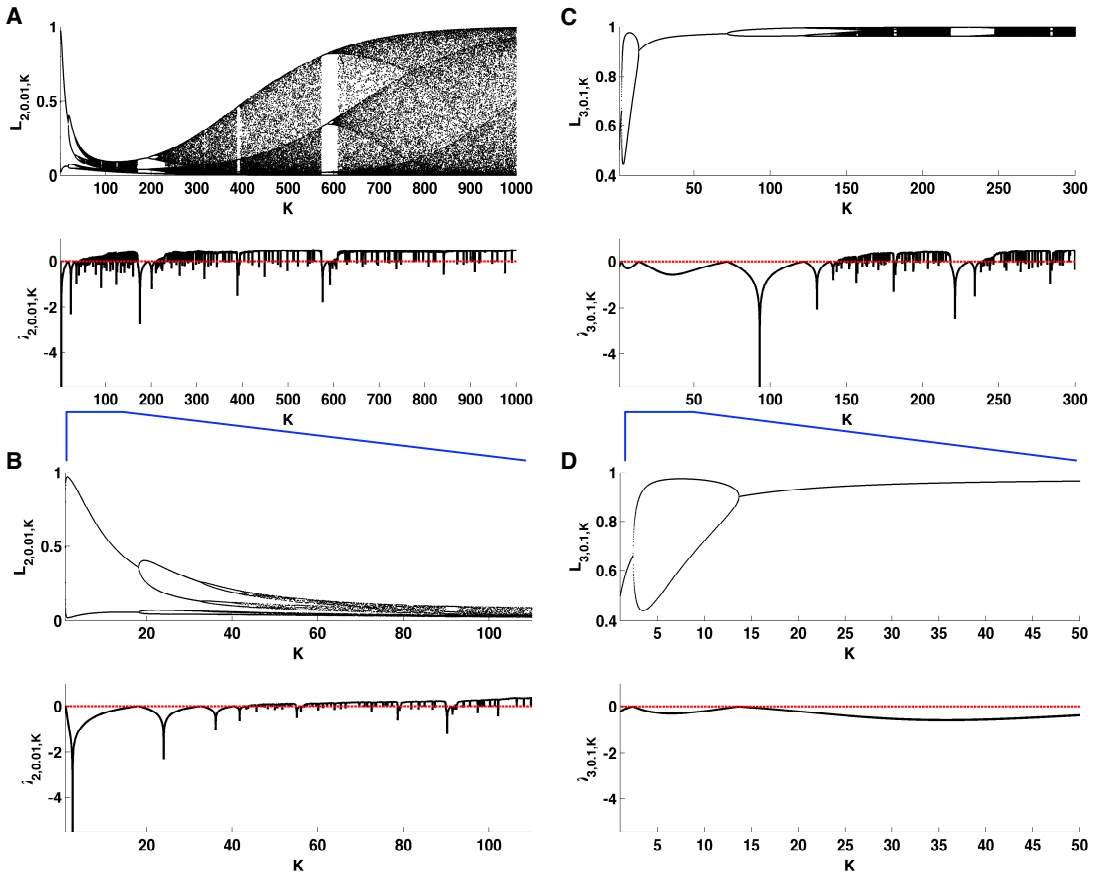

Figure 5.8: Bifurcation diagrams of (5.3) for $g \in \{2, 3\}$, small a, and $K \geqslant 1$ in .01-steps. In each subfigure the upper part shows the attractor $L_{g,a,K}$ for increasing K. The lower part shows the Lyapunov exponent $\lambda_{g,a,K}$ from (5.12). **(A)** $g = 2$, $a = 0.01$, and $K \leqslant 1000$. **(B)** Magnification of (A). **(C)** $g = 3$, $a = 0.1$, and $K \leqslant 300$. **(D)** Magnification of (C). Technicalities as in Figure 5.5.

and $w_2(t)$, the values of $w_0(t)$ and $w_3(t)$ are pushed towards 0 and 1, respectively. This implies that trajectories of realizations of KNsGL with these parameters are almost identical to $(0, 0, \ldots, 0)$ and $(1, 1, \ldots, 1)$, respectively, and, thus, likely to coincide due to finite size effects.

5.6 Discussion

Accepting Kauffman's hypothesis about "Living at the edge of chaos", cf. section 3.4, which generic logic g from Table 5.1 is most reasonable from a biological point of view? Let us take a look at Figure 5.4 and the region of biologically meaningful parameter values $a \approx 0.7$ and $K \approx 2 - 3$. For $g \in \{0, 1\}$ KNsGL are frozen for these parameter values but quite far away from a critical boundary. However, for $g \in \{2, 3\}$ a critical boundary crosses right through this region of the a-K-plane. In particular, for $g = 3$ we find a "frozen headland" in midst of the chaotic regime stretching out to $a \approx 0.7$. Also in the simulation results shown in Figure 5.10D we detect a rather big region of critical networks around $a \approx 0.7$ and $2 \leqslant K \leqslant 3$.

Interestingly, $g = 3$ (more precisely, its symmetric counterpart $g = 4$) has been considered biologically meaningful by several authors. This case corresponds to the standardized qualitative dynamical systems approach [Mendoza and Xenarios, 2006]. It has also been successfully employed in the analysis of immunology microarray datasets [Martin et al., 2007]. Biologically speaking, in all these studies it is assumed that a gene is expressed if any of its activators and none of its inhibitors is active. In other words, the regulating activators and inhibitors are assumed to be functionally equivalent or acting in an additive fashion.

Starting point of our investigations in this chapter were what we called qualitative and Boolean models of gene regulatory networks. A QM is the language of biology, it is a graphical representation of biological knowledge. A BM on the other hand gives rise to a dynamical system, which is something mathematicians like to talk about. We then introduced the concept of generic logics and showed that they induce a mapping from qualitative to Boolean models.

Since the study of BMs in theoretical biology originated in the study of KNs, we deemed it appropriate to investigate KNs obtained by applying generic logics to QMs. We began by studying the truth-content of these networks, i.e. the mean-field fraction of

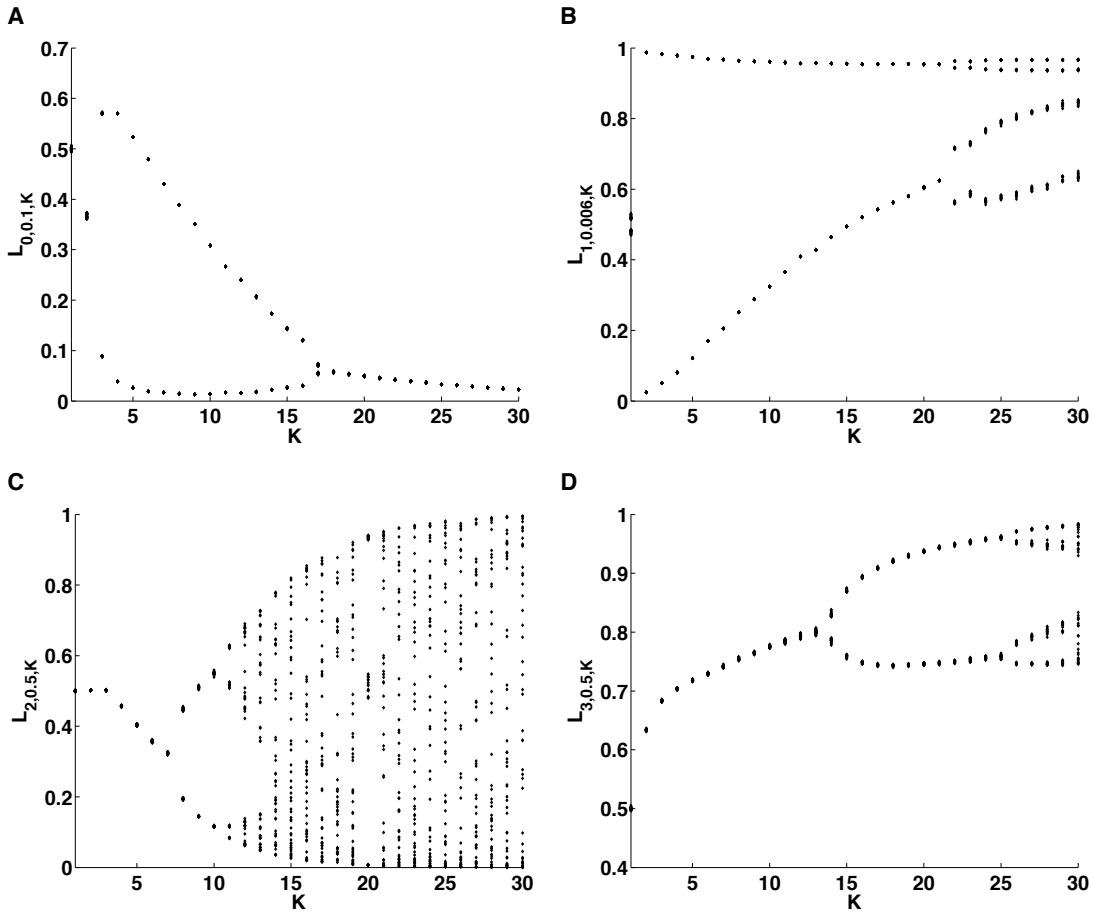

Figure 5.9: Realizations of KNsGL with $N = 10^5$ nodes and connectivities $K = 1, 2, \ldots, 30$ were generated for **(A)** $g = 0$, $a = 0.1$, **(B)** $g = 1$, $a = 0.006$, **(C)** $g = 2$, $a = 0.5$, and **(D)** $g = 3$, $a = 0.5$. After a burn-in of 1000 time-steps, the value of $w_g(t)$ was approximated according to (5.2) in 100 iterations and plotted.

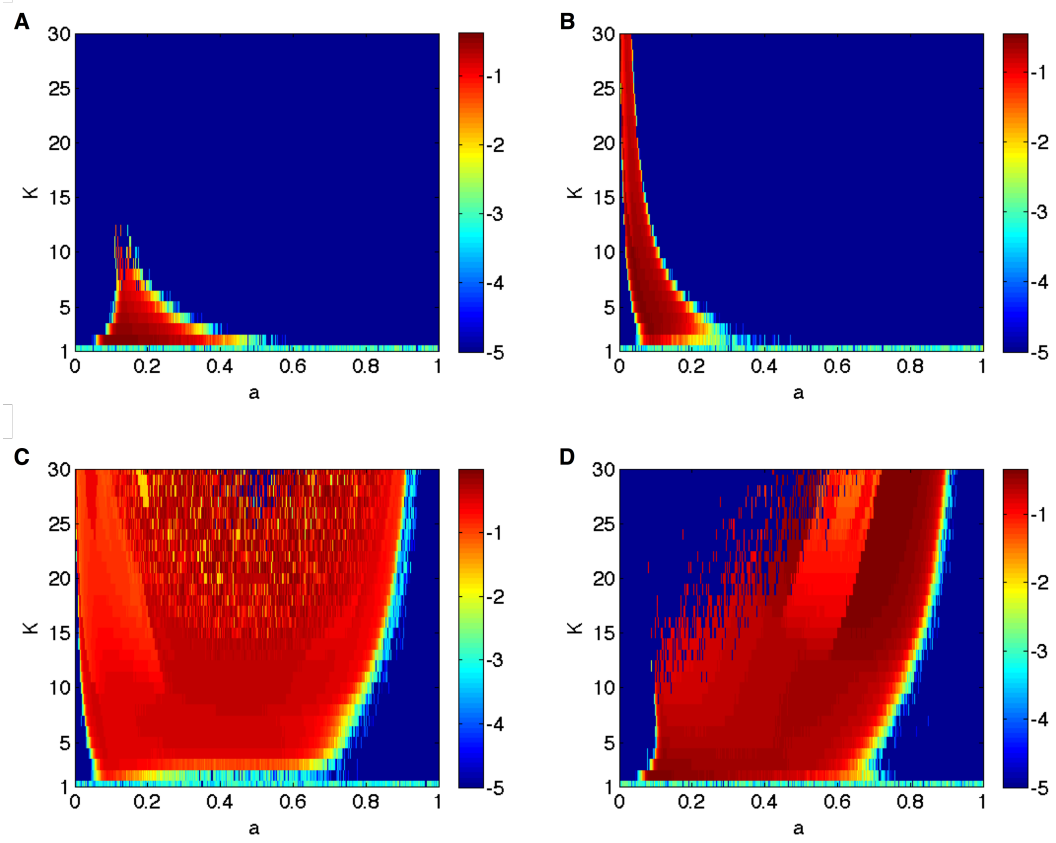

Figure 5.10: Realizations of KNsGL with $N = 10^5$ nodes, connectivities $K = 1, 2, \ldots, 30$, and fraction of activating edges $a = 0.001, 0.002, \ldots, 0.999$ were generated for **(A)** $g = 0$, **(B)** $g = 1$, **(C)** $g = 2$, and **(D)** $g = 3$. Two different configurations with (normalized) Hamming distance 10^{-3} were each iterated, and the 10-logarithm of their Hamming distance after 50 time-steps was plotted.

ones, and analytically characterized the attractor of this quantity. For parameter values selected from both, a mathematical as well as a biological point of view, we numerically computed the bifurcation diagrams of the truth-content. These investigations revealed a rich dynamical behavior including period-doublings leading to chaos as the network connectivity increases. In a next step, we defined a criterion for phase transitions. We found that in contrast to KNsMB, KNsGL possess multiple, intricately shaped critical boundaries. Simulations further strengthened the significance of our results.

Our findings are also interesting from a biological point of view. First of all, we observed that with biologically reasonable fractions of activators a and network connectivities K the truth-content has stationary dynamics for all generic logics. Oscillations of the truth-content — biologically speaking, of the total gene expression — would be economically disadvantageous for cells, especially in the case of large amplitudes, as massive amounts of mRNA and protein would have to be assembled and degraded during each cycle. Moreover, we found that KNs with the biologically plausible generic logics $g = 3$ and $g = 4$ are near criticality for realistic fractions of activators a and network connectivities K.

6

Discrete and continuous models of the mid-hindbrain boundary

Prediction is very difficult,
especially about the future.

Niels Bohr

There are many notions of what "*systems biology*" is. A popular one was conceived of by Hiroaki Kitano [2002]. For him, systems biology is characterized by a hypothesis-driven "*research cycle*" iterating between computational modeling and wet-lab experiments. The overall goal of the computational modeling part is the generation of *predictions* such as potential genetic interactions, which can then be experimentally validated or falsified. Especially when available data are scarce and of qualitative nature, BMs can be beneficially employed to this purpose, as we shall see in the course of this chapter.

Using BMs to model specific biological processes, however, one quickly discovers that not all biological phenomena can be equally well reproduced by these models.

BMs are typically well suited to capture differentiation processes, where the common modeling assumption is that attractors of the dynamical system induced by the BM correspond to different cell types, lineages or tissues. This will also be our "working hypothesis" in the following, when we model the differentiation of mid- and hindbrain. BMs as defined herein are, however, less suitable to capture quantitative effects in a precise temporal order due to the unrealistic time-discrete synchronous updating in the associated dynamical systems. These effects fall into the realm of (time-)continuous dynamical systems.

6.1 Motivation and outline

In this chapter, which follows Wittmann et al. [2009a] and Wittmann et al. [2009b], we venture a glimpse at a possible way of transforming BMs into real time-continuous dynamical systems. We review some results about fixed points in discrete and continuous dynamical systems based on the same BM. In general, however, the dynamics of both systems may differ vastly, and any such transformation should primarily be regarded as a heuristic modeling approach. We validate this approach in section 6.3 from a biological point of view, by applying it to a BM of a specific biological process — differentiation of mid- and hindbrain during vertebrate development —, which we already introduced in section 2.4.2. To be precise, the BM will be a model of the regulatory network between the IsO genes *Otx2*, *Gbx2*, *Fgf8*, *Wnt1*, *En*, and *Pax*. Its key functionality will be the stable maintenance of these's genes expression patterns around the MHB at E10.5 as shown in Figure 2.4B.

We develop the BM in section 6.2. To this end, we describe a methodology for the inference of regulatory interactions by systematic logical analyses of spatial gene expression patterns. As our information about gene expression at the MHB is of purely qualitative nature, it is only natural to base this analysis on BMs. For the determination of the update rules our methodology employs techniques that were originally devised to optimize logic circuits in order to facilitate their hardware implementation.

Applied to the wild-type gene expression pattern at the MHB (cf. Figure 2.4B) our method predicts several genetic interactions, which well agree with published data. In this context, an unclarified experimental issue is the reported ectopic induction of *Wnt1* by Fgf8 in gain-of-function experiments performed *in vitro* and *in vivo* [Adams et al.,

2000; Bally-Cuif and Wassef, 1994; Liu and Joyner, 2001; Liu et al., 1999]. As *Fgf8* expression in the anterior neural plate initiates several hours after *Wnt1*, and as *Wnt1* is expressed in a very broad domain at the time most experimental manipulations took place [Crossley and Martin, 1995; McMahon et al., 1992], the ectopic maintenance of *Wnt1* expression by Fgf8 might have been mis-interpreted as an ectopic activation. Our analysis, indeed, predicts that *Fgf8* and *Wnt1* signaling are dependent on each other for stable maintenance, but Fgf8 is not sufficient to ectopically induce *Wnt1* expression. We validate this prediction experimentally by performing a time-course analysis of *Wnt1* expression after implantation of Fgf8-*coated beads* into mouse anterior neural plate/tube explants.[1] Thus, our analysis clarifies epistatic relationships at the MHB, especially between the two key patterning molecules Fgf8 and Wnt1. In a subsequent step, the results of our analysis combined with published data allow construction of a BM that is able to explain the stable maintenance of the characteristic gene expression patterns at the MHB.

These expression patterns are the result of a refinement and sharpening of initially blurred expression domains. A natural question is if our model is able to reproduce this process in a correct spatio-temporal order. The coarse-grained state-space and the unrealistic time-discrete synchronous updating of dynamical systems induced by BMs, however, prevent us from addressing this question. As an outlook we, therefore, present a possible way of transforming BMs into real time-continuous dynamical systems (section 6.3). We apply this transformation to our BM of the MHB. Simulations of the resulting continuous system show that it is, indeed, competent to reproduce the observed refinement and sharpening of expression domains under wild-type as well as several loss-of-function conditions.

6.2 Inference of a Boolean model of the mid-hindbrain boundary

In this section, we describe a way of inferring BMs from spatial gene expression patterns. Our primary object is to obtain new biological insights into gene regulation at the MHB. We will, therefore, extensively discuss the results of our Boolean modeling approach

[1] Collaboration with Nilima Prakash (Institute of Developmental Genetics, Helmholtz Zentrum München)

with respect to their biological plausibility and relevance. For this reason, this section will be more biological in tone than the other parts of this thesis. The reader may, however, skip this entire section. All one needs to know in order to be able to follow the remainder of this chapter is the BM from (6.3). We begin by the necessary pre-processing of available data.

6.2.1 Data pre-processing

We subdivide the expression patterns of the IsO genes *Otx2*, *Gbx2*, *Fgf8*, *Wnt1*, *En*, and *Pax* at E10.5 into six compartments I-VI, cf. the dashed lines in Figures 6.1A and 6.1B. As is typically the case with Boolean analyses, this pre-processing of biological data is to a certain extent artificial and an over-simplification of biological reality. It is, however, necessary as it allows us to represent the expression patterns as Boolean matrices (see Figure 6.1C), which constitute the data basis for our analysis.

The morphological entity of the MHB is located between compartments III and IV. Other than that, this partitioning is based on the expression patterns of the IsO genes and not on morphological properties. Compartments I-III correspond to the prospective midbrain (*Otx2*+/*Gbx2*–) and IV-VI to the prospective hindbrain (*Otx2*–/*Gbx2*+). The boundary compartments III and IV are characterized by the expression of *Wnt1* and *Fgf8*, respectively. We assume that the secreted Wnt1 and Fgf8 proteins are still present in compartments II and V due to passive or active diffusion [Scholpp and Brand, 2004; Strigini and Cohen, 2000], whereas compartments I and VI are devoid of these secreted factors as they are farthest away from the MHB. So, all in all, the six compartments are characterized as follows.

(I) Only *Otx2* is expressed.

(II) *Otx2*, *En*, and *Pax* are expressed. Secreted Wnt1 protein is present.

(III) *Otx2*, *En*, *Pax*, and *Wnt1* are expressed. Secreted Wnt1 and Fgf8 proteins are present.

(IV) *Gbx2*, *En*, *Pax*, and *Fgf8* are expressed. Secreted Wnt1 and Fgf8 proteins are present.

(V) *Gbx2*, *En*, and *Pax* are expressed. Secreted Fgf8 protein is present.

(VI) Only *Gbx2* is expressed.

The crucial point is that this expression pattern is stably maintained by a regulatory network between the IsO genes. In the following section we demonstrate that key genetic interactions of this network can be obtained already by analyzing only this spatial information.

6.2.2 The inverse problem

So far, information about genetic interactions at the MHB has been obtained mainly from the analyses of gene expression patterns (by *in situ* hybridization) and epistatic relationships between these genes in gain-of-function and loss-of-function mutant mice. The task of elucidating gene regulation at the MHB, therefore, leads to the theoretical challenge of inferring as much information as possible about the structure of multicellular regulatory networks from their spatial expression patterns. To this end, we now describe a methodology for the inference of regulatory interactions by systematic logical analyses of spatial gene expression patterns.

These analyses are based on a Boolean model $(G, \mathbf{f})$. In case of the MHB example, we set G equal to the fully connected directed graph (without self-loops) on six nodes, which represent (in this order) the (groups of) genes *Otx2*, *Gbx2*, *Fgf8*, *Wnt1*, *En*, and *Pax*. For the sake of clarity, we will use *otx*, *gbx*, *fgf*, *wnt*, *en*, and *pax* as node indices. The left-hand table in Figure 6.1C shows a Boolean representation of these gene's expression patterns around the MHB. The right-hand table displays protein expression also taking into account diffusion of secreted Fgf8 and Wnt1 protein into regions adjacent to their mRNA expression domains. We denote the columns of the left-hand table by $\mathbf{x}_I, \mathbf{x}_{II}, \mathbf{x}_{III}, \mathbf{x}_{IV}, \mathbf{x}_V, \mathbf{x}_{VI}$, and the columns of the right-hand table by $\mathbf{x}'_I, \mathbf{x}'_{II}, \mathbf{x}'_{III}, \mathbf{x}'_{IV}, \mathbf{x}'_V, \mathbf{x}'_{VI}$. We already remarked that the stable maintenance of these patterns is a key function of the regulatory network between the IsO genes. In mathematical terms, the conditions that need to be satisfied by the transfer function $\mathbf{f}$ are

$$\mathbf{x}_j = \mathbf{f}\left(\mathbf{x}'_j\right) \ , \quad j = I, II, \ldots, VI \ . \tag{6.1}$$

Conditions (6.1) partially define the update rules f_i, $i = otx, gbx, fgf, wnt, en, pax$. Naturally, there are many ways of extending them to their full domain, which is why we need to impose further constraints. This is best done in terms of the Boolean

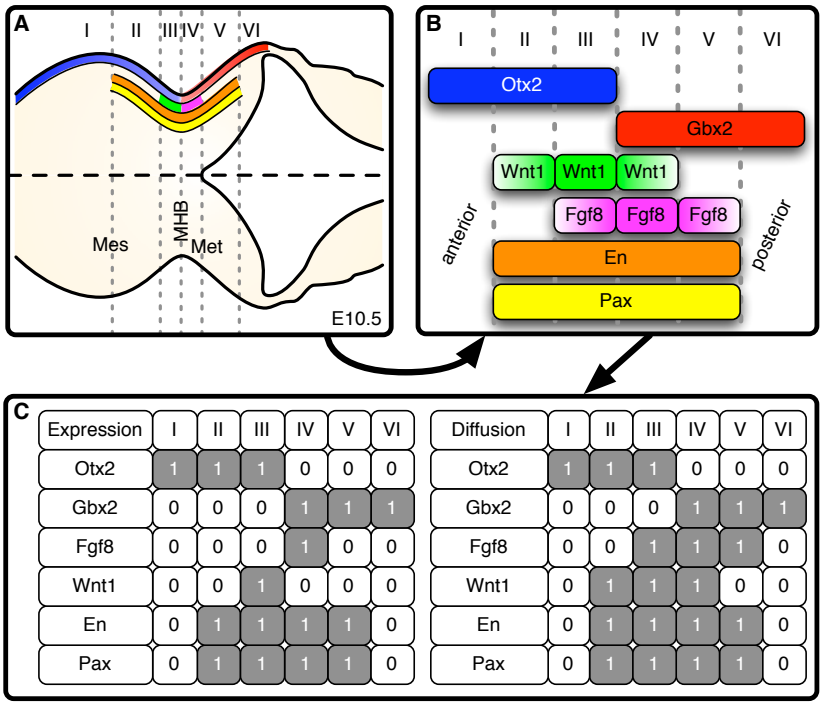

Expression	I	II	III	IV	V	VI
Otx2	1	1	1	0	0	0
Gbx2	0	0	0	1	1	1
Fgf8	0	0	0	1	0	0
Wnt1	0	0	1	0	0	0
En	0	1	1	1	1	0
Pax	0	1	1	1	1	0

Diffusion	I	II	III	IV	V	VI
Otx2	1	1	1	0	0	0
Gbx2	0	0	0	1	1	1
Fgf8	0	0	1	1	1	0
Wnt1	0	1	1	1	0	0
En	0	1	1	1	1	0
Pax	0	1	1	1	1	0

Figure 6.1: Equilibrium expression domains of *Otx2* (blue), *Gbx2* (red), *Fgf8* (magenta), *Wnt1* (green), *En* (orange), and *Pax* (yellow) as well as diffusion of Fgf8 and Wnt1 (color gradients) around the MHB at E10.5. **(A)** Dorsal close-up view of the MHB region in the anterior neural tube of an E10.5 mouse embryo, anterior to the left. The expression pattern of the IsO genes can be subdivided into the six compartments I-VI. **(B)** Schematic representation of compartments I-VI. The MHB is located between compartments III and IV. **(C)** Representation of compartments I-VI as Boolean matrices. The $(i, j)^{th}$ entry indicates if species i is present (1) in compartment j or not (0). The left-hand matrix (labeled "Expression") represents the gene expression pattern. The right-hand matrix (labeled "Diffusion") displays protein expression also taking into account diffusion of secreted Fgf8 and Wnt1 protein. Abbreviations: Mes, mesencephalon (midbrain); MHB, mid-hindbrain boundary; Met, metencephalon (hindbrain).

expressions describing the update rules. A possible regularization would, for instance, be the restriction to a certain class of Boolean functions such as canalyzing functions,[1] or functions generated by one of the generic logics introduced in chapter 5. Which regularization proves most effective has to be figured out anew in each application. In the example of the MHB, a suitable choice was to extend the partially defined update rules under the regularization that the resulting f_i be minimal with respect to the length of the shortest representing Boolean expression in DNF. This analysis is based on the assumption that the thus obtained minimal BM reflects the core module of the real network.

6.2.3 Minimization of Boolean functions

Standard ways of finding minimal Boolean expressions for (partially filled) truth-tables are either *Karnaugh-Veitch maps* [Karnaugh, 1953; Veitch, 1952] or the *Quine-McCluskey algorithm* [McCluskey and Bartee, 1962; Quine, 1952] — two functionally equivalent approaches. Karnaugh-Veitch maps are a clever graphical representation of truth-tables. They transform the problem of finding minimal Boolean expressions into the problem of finding a maximal-size covering of either the *true*- or the *false*-entries. For small functions (typically no more than five inputs) the latter problem can be easily solved by inspection. For larger functions the Quine-McCluskey algorithm can be used instead, whose tabular form is less illustrative but easier to implement. However, also the Quine-McCluskey algorithm has a limited range of applicability, as it tries to solve a problem which has been shown to be NP-complete, cf. the *Cook-Levine Theorem* about the *Boolean satisfiability problem* [Cook, 1971]. Therefore, in the case of large systems, heuristic methods like the *Espresso algorithm* [Brayton, 1984; Rudell and Sangiovanni-Vincentelli, 1987] may be more suitable.

Here we outline how minimal Boolean expressions for partially defined update rules can be found by using Karnaugh-Veitch maps. Each of our Boolean update functions f_i, $i = otx, gbx, fgf, wnt, en, pax$, can be represented as a truth-table with $2^5 = 32$ entries. Conditions (6.1) allow to specify at most six entries in each truth-table. The remaining entries are indetermined "*don't cares*." These truth-tables are now represented as Karnaugh-Veitch maps, see Figure 6.2. Actually, these maps are three-dimensional

[1] A possible justification for this restriction is that in lower organisms most genes have one canalyzing regulator [Harris et al., 2002].

cubes but for better presentability the cube was sliced up and the two layers put next to each other. Moreover, the green as well as the blue sides are identified, so each "slice" is actually a torus. By inspection, we now determine a covering of the *true*-entries by rectangular boxes of size $1, 2, 4, 8, 16$ or 32 such that the following hold.

- No *false*-entry is contained in any of the boxes.
- All *true*-entries are contained in at least one box.
- The boxes have maximal size.
- The number of boxes is minimal.

Note that there may be multiple coverings satisfying these conditions. In Figure 6.2 all suitable coverings are shown. From each box in these coverings a conjunctive clause is built, where variables appearing both, negated and non-negated within the box, are omitted. These conjunctive clauses are linked by disjunction and give a minimal DNF of the Boolean expression. We illustrate this using

$$\begin{array}{rccc} f_{fgf} & : & \{0,1\}^5 & \longrightarrow & \{0,1\} \\ & & (x_{otx}, x_{gbx}, x_{wnt}, x_{en}, x_{pax}) & \longmapsto & f_{fgf}(x_{otx}, x_{gbx}, x_{wnt}, x_{en}, x_{pax}) \end{array}$$

as a showcase. Two coverings satisfying the above conditions could be found, each consisting of only one box, cf. the dashed and solid red boxes in Figure 6.2B. Let us choose the first (dashed lines). Here the only variables that do not appear both, negated as well as non-negated, are x_{otx} (which appears only as $\neg x_{otx}$) and x_{wnt} (which appears only as x_{wnt}). Consequently, the conjunction term for this box is $\neg x_{otx} \wedge x_{wnt}$. Similarly, minimal expressions for the remaining update rules can be found from the maps in Figure 6.2, and we obtain:

$$\begin{array}{lcll} f_{otx}(x_{gbx}, x_{fgf}, x_{wnt}, x_{en}, x_{pax}) & = & \neg x_{gbx} & \\ f_{gbx}(x_{otx}, x_{fgf}, x_{wnt}, x_{en}, x_{pax}) & = & \neg x_{otx} & \\ f_{fgf}(x_{otx}, x_{gbx}, x_{wnt}, x_{en}, x_{pax}) & = & x_{wnt} \quad \wedge & \left\{ \begin{array}{c} x_{gbx} \\ \neg x_{otx} \end{array} \right\} \\ f_{wnt}(x_{otx}, x_{gbx}, x_{fgf}, x_{en}, x_{pax}) & = & x_{fgf} \quad \wedge & \left\{ \begin{array}{c} x_{otx} \\ \neg x_{gbx} \end{array} \right\} \\ f_{en}(x_{otx}, x_{gbx}, x_{fgf}, x_{wnt}, x_{pax}) & = & x_{pax} & \\ f_{pax}(x_{otx}, x_{gbx}, x_{fgf}, x_{wnt}, x_{en}) & = & x_{en} \quad . & \end{array} \tag{6.2}$$

In the case of *Fgf8* and *Wnt1* two equally minimal expressions could be found, indicated by the factors in curly brackets, one of which has to be included.

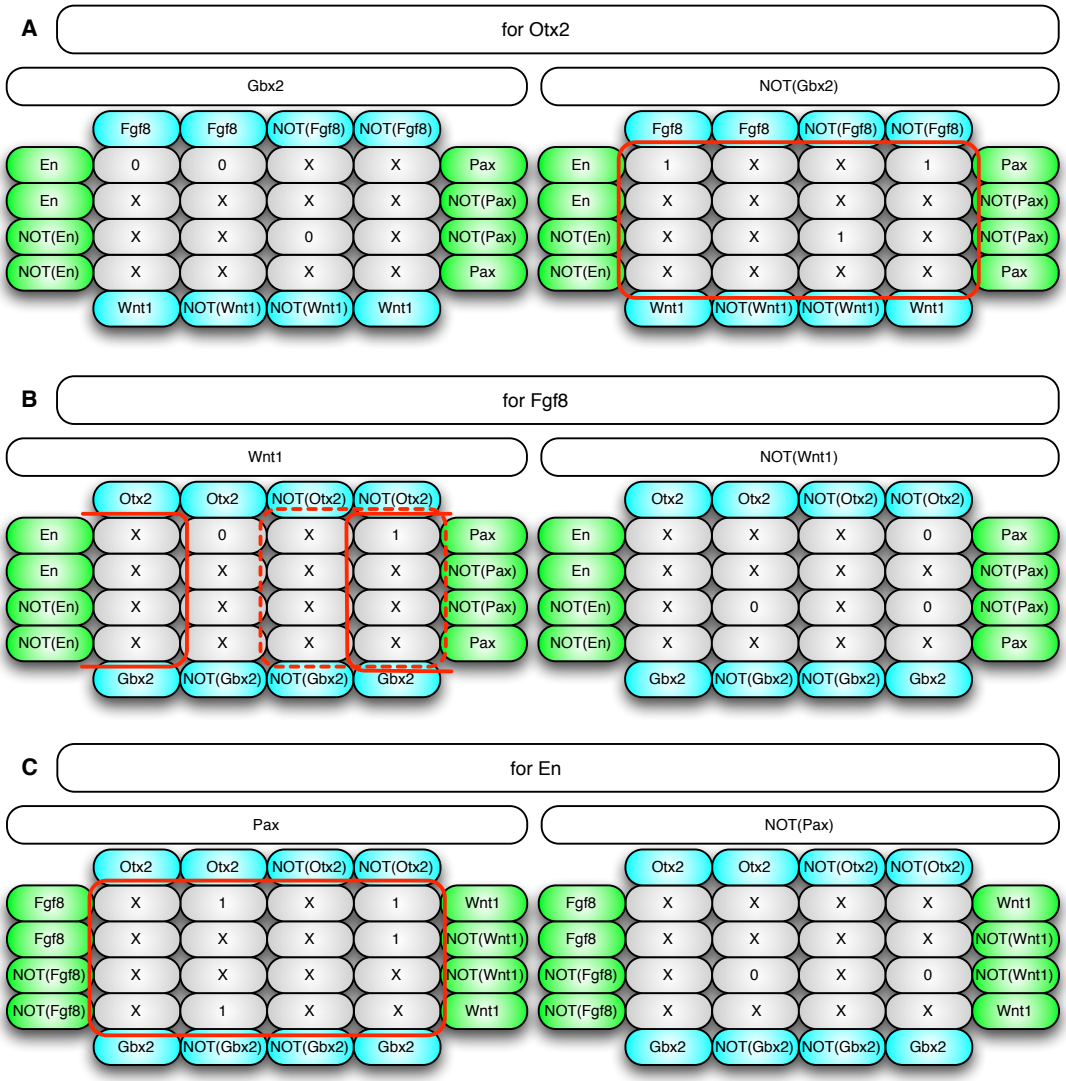

Figure 6.2: Karnaugh-Veitch maps for the update rules of **(A)** *Otx2*, **(B)** *Fgf8*, and **(C)** *En*. 0: *false*, 1: *true*, X: "don't cares." In each map the blue and green sides are identified. Red boxes indicate the maximal coverings. Similar maps for *Gbx2*, *Wnt1*, and *Pax* can be obtained by flipping *Gbx2* and *Otx2* in (A), *Fgf8* and *Wnt1* in (B), and *En* and *Pax* in (C), respectively.

6.2.4 Predictions and experimental validation

The minimal update rules from (6.2) show that, in addition to the mutual inhibition of *Otx2* and *Gbx2*, these two transcription factors have antagonistic effects on *Fgf8* and *Wnt1* expression. This agrees well with experimental results showing that opposing interactions between *Otx2* and *Gbx2* are required for the positioning and refinement of the MHB [Li and Joyner, 2001; Simeone, 2000]. Furthermore, a mutual positive regulation between *En* and *Pax* was predicted which is well supported by experimental results from Song et al. [2000], Liu and Joyner [2001] as well as Bouchard et al. [2005]. Finally, our analysis revealed that *Fgf8* and *Wnt1* require each other for their stable maintenance, but are not sufficient to induce each other's expression, as the respective update rules contain at least one additional factor. The early loss of *Fgf8* expression in $Wnt1^{-/-}$ mutants by nine-somites [Lee et al., 1997] indeed suggests that Wnt1 is directly required for the maintenance of *Fgf8* expression [Prakash and Wurst, 2004]. We subsequently set out to validate also the prediction that Fgf8 is, in turn, necessary for the maintenance but not sufficient for the induction of *Wnt1* expression.

To find out if Fgf8 only maintains or *de novo* induces *Wnt1* expression *in vivo*, we performed a time-course analysis of *Wnt1* expression after implantation of Fgf8-*coated beads* into mouse anterior neural plate (E8.0-E8.5) or tube (E9.0-E9.5) explants,[1] cf. Figure 6.3. In E8.0-E8.5 anterior neural plate explants (Figure 6.3A), *Wnt1* expression retracted from its originally broad expression domain in the prospective midbrain (control side of explant incubated for 6 h) and was confined to the dorsal side of the midbrain and to the rostral border of the MHB in the control side of explants incubated for 18 and 24 h. Fgf8-coated beads implanted within or close to the endogenous *Wnt1* expression domain in the midbrain (*Otx2*+/*Gbx2*– territory, not shown) maintained *Wnt1* expression within but not outside of this domain over 24 h (compare with contralateral control side of the explants). Notably, Fgf8-coated beads placed outside the endogenous *Wnt1* expression domain in the rostral hindbrain (*Otx2*–/*Gbx2*+ territory, not shown) or forebrain (*Otx2*+/*Gbx2*– territory) did not induce ectopic *Wnt1* transcription at any time-point analyzed, as predicted by our logical analysis.

[1] Explant cultures of anterior neural plates/tubes (open-book preparations) from wild-type (C57BL/6) mouse embryos were essentially prepared as reported by Echevarría et al. [2001]. Bead preparation is described in Prakash et al. [2006]. Explants were fixed in fresh 4% paraformaldehyde for 4 hours at 4 °C and whole mount *in situ* hybridization was carried out using standard procedures.

When these experiments were performed with E9.0-E9.5 anterior neural tube explants incubated for 24 h (as in Liu et al. [1999] or Liu and Joyner [2001]) (Figure 6.3B), ectopic expression of *Wnt1* was only observed around Fgf8-coated beads that were implanted 24 h before close to the endogenous *Wnt1* domain in the midbrain. This result shows that the ectopic *Wnt1* expression observed by Liu et al. [1999] or Liu and Joyner [2001] is due to the maintenance but not *de novo* induction of *Wnt1* transcription by Fgf8. Therefore, it is in agreement with our predicted update rule (6.2) for *Wnt1*, which implies that *Wnt1* expression requires Fgf8 for stable maintenance, but that Fgf8 is not sufficient to induce *Wnt1* ectopically.

6.2.5 A Boolean model of the mid-hindbrain boundary

Our minimal BM from (6.2) was derived solely from the wild-type expression patterns shown in Figure 6.1. We now complement this by a careful literature mining for further experimentally validated interactions. Thus, we extend the minimal BM to a literature-based BM comprising *Otx2*, *Gbx2*, *Fgf8*, *Wnt1*, *En*, and *Pax*. The new update rules read:

$$\begin{array}{lcl} f_{otx}(x_{gbx}, x_{fgf}, x_{wnt}, x_{en}, x_{pax}) & = & \neg x_{gbx} \\ f_{gbx}(x_{otx}, x_{fgf}, x_{wnt}, x_{en}, x_{pax}) & = & \neg x_{otx} \\ f_{fgf}(x_{otx}, x_{gbx}, x_{wnt}, x_{en}, x_{pax}) & = & x_{wnt} \wedge x_{gbx} \wedge \neg x_{otx} \wedge x_{en} \wedge x_{pax} \\ f_{wnt}(x_{otx}, x_{gbx}, x_{fgf}, x_{en}, x_{pax}) & = & x_{fgf} \wedge x_{otx} \wedge \neg x_{gbx} \\ f_{en}(x_{otx}, x_{gbx}, x_{fgf}, x_{wnt}, x_{pax}) & = & (x_{fgf} \vee x_{wnt}) \wedge x_{pax} \\ f_{pax}(x_{otx}, x_{gbx}, x_{fgf}, x_{wnt}, x_{en}) & = & x_{en}\,. \end{array} \tag{6.3}$$

The model is visualized in Figure 6.4. The figure caption contains primary research references for all included interactions.

It can easily be checked that the transfer function $\mathbf{f}$ of the BM (6.3) satisfies conditions (6.1), and is, thus, able to stably maintain the expression patterns of the IsO genes at E10.5. As already mentioned, these patterns are the result of a refinement and sharpening of initially blurred expression domains at E8.5, cf. Figure 6.5A. In the following section, we ask if our model is able to reproduce also this process in a correct spatio-temporal order.

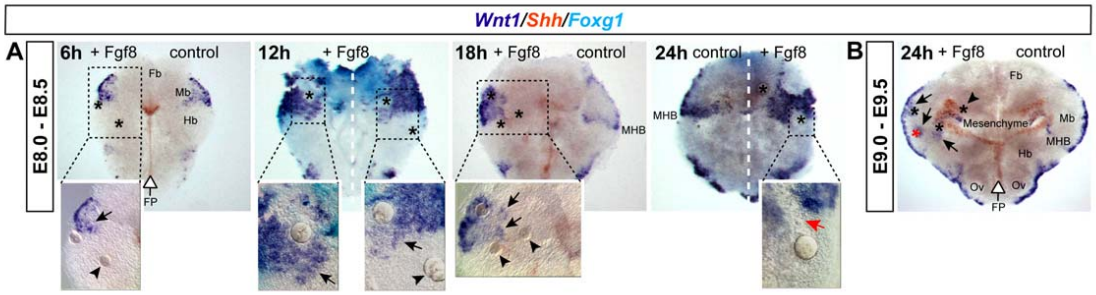

Figure 6.3: *Wnt1* expression is maintained in the midbrain and at the MHB by Fgf8-coated beads. **(A)** E8.0-E8.5 (4-6 somites) mouse anterior neural plate explants were incubated for 6, 12, 18 and 24 hours (h) after implantation of Fgf8-coated beads (asterisks) and prior to fixation and detection of *Wnt1* (dark blue), *Shh* (red) and *Foxg1* (a forebrain marker; light blue) expression by whole mount *in situ* hybridization. High magnifications of the boxed areas in the overviews are shown below. Repression of endogenous *Wnt1* (red arrow) around an Fgf8-bead located in the presumptive rostral hindbrain close to the MHB is apparent in the 24 h explant. **(B)** E9.0-E9.5 (20-25 somites) mouse anterior neural tube explant incubated for 24 h after implantation of Fgf8-coated beads (asterisks) and prior to fixation and detection of *Wnt1* (dark blue) and *Shh* (red) expression. The ectopic *Wnt1* expression around the Fgf8-coated bead marked by a red asterisk might have been maintained during the 24 h incubation period. *Shh* expression in the floor plate (open arrow) or a white broken line indicate the position of the ventral midline of the neural plate/tube in the explants. Beads were implanted unilaterally except for the 12 h explant. The contralateral side served as control. The control side shows the *Wnt1* expression pattern under "normal" (unmanipulated) conditions, the Fgf8-treated side shows the changes in *Wnt1* expression after bead implantation. Ectopic *Wnt1* expression around Fgf8-coated beads is indicated by black arrows. Beads that did not induce ectopic *Wnt1* expression are indicated by black arrowheads. Abbreviations: Fb, forebrain; FP, floor plate; Hb, hindbrain; Mb, midbrain; MHB, mid-hindbrain boundary; Ov, otic vesicle.

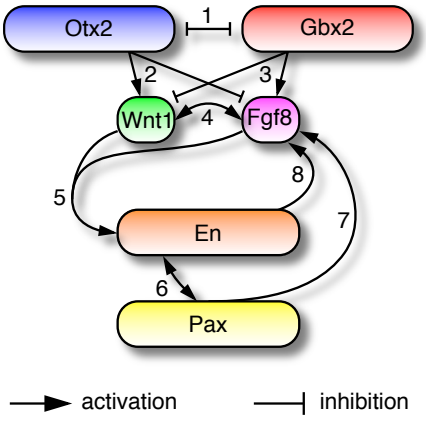

Figure 6.4: Regulatory network at the MHB obtained from literature data. It includes the following interactions: *(1)* The mutual repression of *Otx2* and *Gbx2* [Broccoli et al., 1999; Millet et al., 1999]. *(2)* The positive regulation of *Wnt1* and the negative regulation of *Fgf8* by *Otx2* [Acampora et al., 1997; Broccoli et al., 1999; Rhinn et al., 1999]. *(3)* The positive regulation of *Fgf8* and the negative regulation of *Wnt1* by *Gbx2* [Liu and Joyner, 2001; Millet et al., 1999; Wassarman et al., 1997]. *(4)* The maintenance of *Fgf8* by Wnt1 [Lee et al., 1997] and, vice versa, the maintenance of *Wnt1* by Fgf8 as demonstrated herein and by Chi et al. [2003]. *(5)* The synergy between Fgf8 and Wnt1 in the maintenance of *En* [Crossley and Martin, 1995; Danielian and McMahon, 1996; Liu et al., 1999; McMahon et al., 1992]. This synergy is modeled by a disjunction. *(6)* The mutual activation of *En* and *Pax* [Bouchard et al., 2005; Liu and Joyner, 2001; Song et al., 2000]. *(7)* The induction of *Fgf8* by *Pax* [Favor et al., 1996; Ye et al., 2001]. *(8)* The positive regulation of *Fgf8* by *En* [Gemel et al., 1999].

6.3 Boolean models and continuous dynamical systems: a proof-of-principle

To answer the question posed at the end of the previous section, we now present a possible way of transforming BMs into real time-continuous dynamical systems (section 6.3.1). In section 6.3.2 we apply the transformation to our BM from (6.3). Section 6.3.3 concludes with simulation results from the resulting continuous model of the MHB.

6.3.1 The general approach

Consider a BM $(G, \mathbf{f})$ of a regulatory network, e.g. the one from (6.3). In Remark 3.1 we explained that this BM gives rise to a time-discrete dynamical system in a canonical way. Does it also give rise to a continuous dynamical system on $\mathbb{R}^N$, which can still be expected to be a meaningful model of the underlying regulatory network? To answer this question, we recall where the BM "comes from." In section 3.2 we saw that BMs are idealizations of networks of switch-like interactions. Each of these interactions can, for instance, be modeled by the sigmoidal Hill kinetic h from (3.2), which can be thought of as the promotor activity function of a gene depending on the concentration of a single activating transcription factor.

Now, let $\overline{x}_i \in [0,1]$, $i = 1, 2, \ldots, N$, be real variables and choose a prototypic update rule f_i from $\mathbf{f}$. We think of f_i as a function on the vertices of the K_i-dimensional hypercube $[0,1]^{K_i}$ and ask how a possible K_i-variate promotor activity function $\overline{f}_i$ defined on the entire cube $[0,1]^{K_i}$ (including its interior) could look like such that it would be approximated by f_i in a Boolean modeling attempt. A suitable candidate is

$$\overline{f}_i\left(\overline{x}_{i_1}, \ldots, \overline{x}_{i_{K_i}}\right) = \sum_{(\xi_1,\ldots,\xi_{K_i})\in\{0,1\}^{K_i} | f_i(\xi_1,\ldots,\xi_{K_i})=1} \prod_{k=1}^{K_i} \left[\xi_k h_{i,k}\left(c_{i,k}, \overline{x}_{i_k}\right) + \left(1-\xi_k\right)\left(1 - h_{i,k}\left(c_{i,k}, \overline{x}_{i_k}\right)\right)\right] , \tag{6.4}$$

where $h_{i,k}\left(c_{i,k}, \bullet\right) : [0,1] \to [0,1]$ are parametrized switch-like functions as defined in section 3.2 [Plahte et al., 1998; Wittmann et al., 2009b]. The function $\overline{f}_i$ is the (unique) *multilinear interpolation* of f_i (as a function on the vertices of the hypercube $[0,1]^{K_i}$) coupled with the $h_{i,k}$, cf. Figure 6.6.

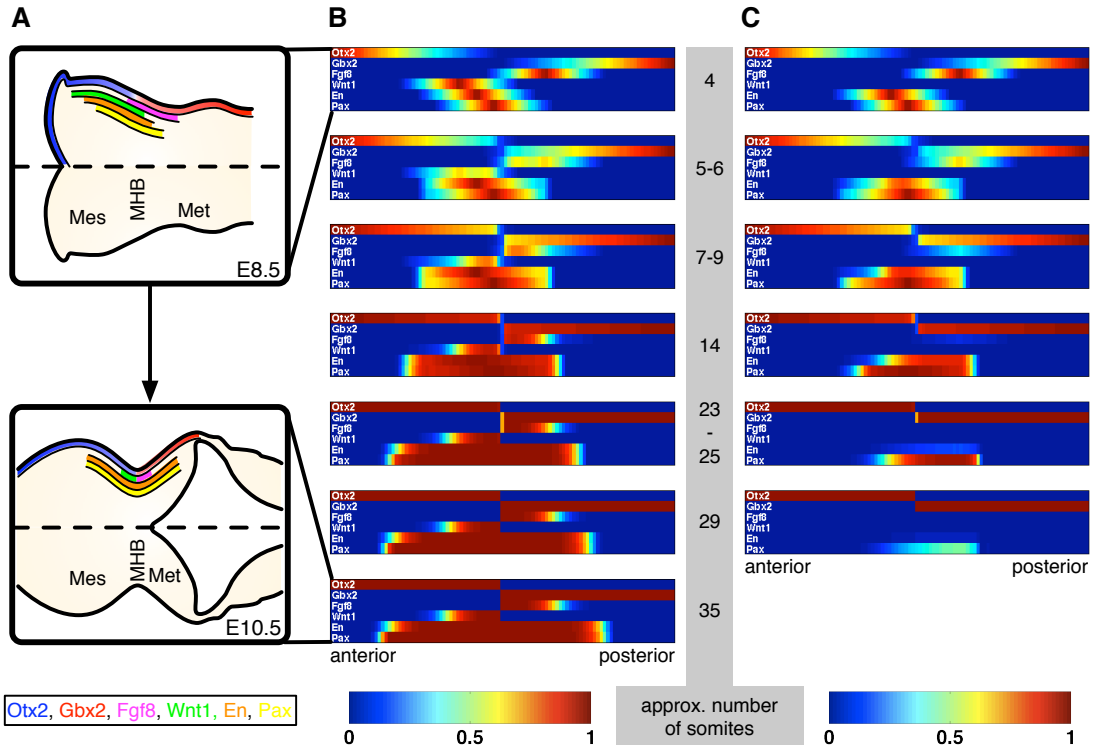

Figure 6.5: Time-courses of the IsO genes under wild-type and loss-of-function conditions. **(A)** Expression pattern of the IsO genes at E8.5 (upper figure) and at E10.5 (lower figure). The initially blurred expression domains are refined and a sharp boundary is established. **(B)**, **(C)** Simulations of the continuous MHB model. Initial conditions are chosen to resemble the expression pattern at E8.5, cf. upper Figure (A). Model simulations are shown at time-points $t = 0, 8, 20, 50, 100, 125$, and (only in (B)) 155. This corresponds to a linear relationship between the model's time-scale and the somitogenesis clock, where approximately 1 somite is formed per every 5 time-units. **(B)** Simulated gene expression domains under wild-type conditions. The refinement and sharpening of the expression domains is clearly visible. Finally, an expression pattern similar to lower Figure (A) is established. **(C)** Simulation of a $Wnt1^{-/-}$ mutant. The expression of *Fgf8*, *En*, and *Pax* is lost over time. In particular, the expression of *Fgf8* and *En* agrees well with the time-courses described in McMahon et al. [1992] and Lee et al. [1997], cf. Table 6.1. Abbreviations: Mes, mesencephalon (midbrain); MHB, mid-hindbrain boundary; Met, metencephalon (hindbrain).

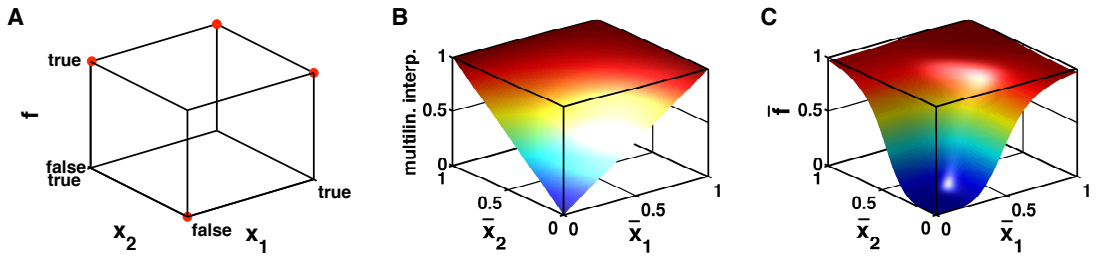

Figure 6.6: **(A)** A two-variate Boolean function f, **(B)** its multilinear interpolation, and **(C)** the corresponding function $\overline{f}\,(\overline{x}_1, \overline{x}_2)$ from (6.4). The sigmoidal functions h_1 and h_2 were chosen to be Hill kinetics from (3.2) with degree of cooperativity $c = 5$ and thresholds $\theta = 0.5$.

According to our definition of switch-like functions, the functions $h_{i,k}$ approach Heaviside step-functions $h_{i,k}(\infty, \bullet)$ with steps at $\theta^{\infty}_{i,k}$ as the $c_{i,k}$ grow. The function $\overline{f}_i$, thus, converges against a function $\overline{f}^{\infty}_i$ which satisfies

$$\overline{f}^{\infty}_i\left(\overline{x}_{i_1}, \ldots, \overline{x}_{i_{K_i}}\right) = f_i\left(\overline{x}_{i_1} > \theta^{\infty}_{i,1}, \ldots, \overline{x}_{i_{K_i}} > \theta^{\infty}_{i,K_i}\right)$$

unless one of the $\overline{x}_{i_k}$ is located on its threshold $\theta^{\infty}_{i,k}$, in which case $\overline{f}^{\infty}_i$ evaluates to 0.5. Hence, except for the measure zero set of hyperplanes $\overline{x}_{i_k} = \theta^{\infty}_{i,k}$ the limiting function $\overline{f}^{\infty}_i$ is a piecewise constant function whose values are fully determined by the Boolean function f_i.

We now define a function $\overline{f}_i$ for each node $i = 1, 2, \ldots, N$ according to (6.4) by choosing switch-like functions $h_{i,k}\,(c_{i,k}, \bullet)$. We collect the $\overline{f}_i$ into a function $\overline{\mathbf{f}} : [0,1]^N \to [0,1]^N$. In analogy to the discrete dynamical system in $\mathbf{x}(t) = (x_i(t))_{i=1}^N \in \{0,1\}^N$ from Remark 3.1 given by the difference equations

$$\Delta x_i(t) = f_i\left(x_{i_1}(t), x_{i_2}(t), \ldots, x_{i_{K_i}}(t)\right) - x_i(t)\ , \quad i = 1, 2, \ldots, N\ , \tag{6.5}$$

we define a continuous dynamical system in $\overline{\mathbf{x}}(t) = (\overline{x}_i(t))_{i=1}^N \in [0,1]^N$ via the differential equations

$$\frac{\mathrm{d}}{\mathrm{d}t}\overline{x}_i(t) = \overline{f}_i\left(\overline{x}_{i_1}(t), \overline{x}_{i_2}(t), \ldots, \overline{x}_{i_{K_i}}(t)\right) - \overline{x}_i(t)\ , \quad i = 1, 2, \ldots, N\ . \tag{6.6}$$

The dynamics of (6.6) are best understood in the limit of all $c_{i,k} \to \infty$, in which the differential equations (6.6) become *piecewise linear* differential equations. In theoretical biology, these equations were first studied by Glass and Kauffman [1973]. A

mathematically rigorous treatment within the framework of differential inclusions can be found in de Jong et al. [2004]. Fixed points of systems of piecewise linear differential equations were investigated by El Snoussi and Thomas [1993] as well as by Mestl et al. [1995]. In general, there are two classes of fixed points: *regular fixed (steady) points* (RSP) and *singular fixed (steady) points* (SSP). In a SSP at least one variable $\overline{x}_i$ lies on a threshold, whereas in RSPs all variables are located beside their thresholds. RSPs are always (asymptotically) stable and in 1-1-relation with fixed points of system (6.5). SSPs may but need not be stable. They do not correspond to fixed points of system (6.5). An algorithmic approach to detecting RSPs and SSPs in systems of piecewise linear differential equations has been presented in de Jong and Page [2008].

Generalizations of the above results to the case of sufficiently large but finite $c_{i,k}$ via the implicit function theorem exist. With respect to RSPs, the following statement was proven in Wittmann et al. [2009b].

Proposition 6.1. *Consider the two dynamical systems from* (6.5) *and* (6.6)*, and suppose the switch-like functions* $h_{i,k}(c_{i,k}, \bullet)$ *in the* $\overline{f}_i$ *from* (6.4) *are given by Hill kinetics from* (3.2)*. Let* $\mathbf{x}^{(f)} \in \{0,1\}^N$ *be a fixed point of* (6.5)*. Then, for sufficiently large* $c_{i,k}$ *there exists an asymptotically stable fixed point* $\overline{\mathbf{x}}^{(f)}(c_{i,k}) \in [0,1]^N$ *of* (6.6) *in a neighborhood of* $\mathbf{x}^{(f)}$ *and*

$$\lim_{\min c_{i,k} \to \infty} \overline{\mathbf{x}}^{(f)}(c_{i,k}) = \mathbf{x}^{(f)} \ .$$

The case of SSPs is more involved and taken care of in Plahte et al. [1998]. In general, it is difficult to give explicit lower bounds for the $c_{i,k}$, such that the approximation of sigmoidal functions by step-functions is valid from a dynamical point of view. Even more critical is, of course, the transition from the time-discrete system (6.5) to the time-continuous system (6.6). To see this, it suffices to recall the intricate dynamical behavior of the (discrete time) logistic equation from section 2.2.4.1, and to consider that according to the Poincaré-Bendixson theorem, see e.g. Guckenheimer and Holmes [1990], any one-dimensional *continuous* dynamical system has either stationary or periodic behavior. Nonetheless, small-scale [Omholt et al., 1998] as well as large-scale [Wittmann et al., 2009b] examples exhibit evidence that biologically meaningful, continuous models may arise from the above modeling approach. In the following, we provide further such evidence.

6.3.2 A continuous model of the mid-hindbrain boundary

In this section, we derive a continuous dynamical system from the BM in (6.3). The model's variables $\overline{x}_i(j,t)$, $i = \mathit{otx}, \mathit{gbx}, \mathit{fgf}, \mathit{wnt}, \mathit{en}, \mathit{pax}$, depend on time and the now continuous spatial variable $j \in [0,1]$, which is to say we model the neural tube as a one-dimensional interval.

With *Otx2*, *Gbx2*, *En*, and *Pax* we do not differentiate between mRNA and protein. In the case of *Fgf8* and *Wnt1*, however, we need to introduce two additional variables $\overline{x}^{\text{ext}}_{\mathit{fgf}}(j,t)$ and $\overline{x}^{\text{ext}}_{\mathit{wnt}}(j,t)$ in order to account for the diffusion of secreted Fgf8 and Wnt1 protein. They are governed by the *reaction-diffusion equations*

$$\frac{\partial}{\partial t}\overline{x}_i^{\text{ext}}(j,t) = \alpha_i \overline{x}_i(j,t) - \beta_i \overline{x}_i^{\text{ext}}(j,t) + \gamma_i \frac{\partial^2}{\partial j^2}\overline{x}_i^{\text{ext}}(j,t) \;, \quad i = \mathit{fgf}, \mathit{wnt}\,, \tag{6.7}$$

with translation rates α_i, degradation rates β_i, and diffusion rates γ_i, $i = \mathit{fgf}, \mathit{wnt}$. In here, we use the parameter values from Wittmann et al. [2009a] and Ansorg et al. [2010], $\alpha_i = \gamma_i = 1$ and $\beta_i = 0.8$.

For $i = \mathit{otx}, \mathit{gbx}, \mathit{fgf}, \mathit{wnt}, \mathit{en}, \mathit{pax}$, we define functions $\overline{f}_i$ according to (6.4) choosing all $h_{i,k}$ equal to a Hill kinetic from (3.2) with degree of cooperativity $c = 5$ and threshold $\theta = 0.1$. The equations

$$\begin{aligned}
\frac{\partial}{\partial t}\overline{x}_{\mathit{otx}}(j,t) &= \overline{f}_{\mathit{otx}}\left(\overline{x}_{\mathit{gbx}}(j,t), \overline{x}^{\text{ext}}_{\mathit{fgf}}(j,t), \overline{x}^{\text{ext}}_{\mathit{wnt}}(j,t), \overline{x}_{\mathit{en}}(j,t), \overline{x}_{\mathit{pax}}(j,t)\right) - \overline{x}_{\mathit{otx}}(j,t) \\
\frac{\partial}{\partial t}\overline{x}_{\mathit{gbx}}(j,t) &= \overline{f}_{\mathit{gbx}}\left(\overline{x}_{\mathit{otx}}(j,t), \overline{x}^{\text{ext}}_{\mathit{fgf}}(j,t), \overline{x}^{\text{ext}}_{\mathit{wnt}}(j,t), \overline{x}_{\mathit{en}}(j,t), \overline{x}_{\mathit{pax}}(j,t)\right) - \overline{x}_{\mathit{gbx}}(j,t) \\
\frac{\partial}{\partial t}\overline{x}_{\mathit{fgf}}(j,t) &= \overline{f}_{\mathit{fgf}}\left(\overline{x}_{\mathit{otx}}(j,t), \overline{x}_{\mathit{gbx}}(j,t), \overline{x}^{\text{ext}}_{\mathit{wnt}}(j,t), \overline{x}_{\mathit{en}}(j,t), \overline{x}_{\mathit{pax}}(j,t)\right) - \overline{x}_{\mathit{fgf}}(j,t) \\
\frac{\partial}{\partial t}\overline{x}_{\mathit{wnt}}(j,t) &= \overline{f}_{\mathit{wnt}}\left(\overline{x}_{\mathit{otx}}(j,t), \overline{x}_{\mathit{gbx}}(j,t), \overline{x}^{\text{ext}}_{\mathit{fgf}}(j,t), \overline{x}_{\mathit{en}}(j,t), \overline{x}_{\mathit{pax}}(j,t)\right) - \overline{x}_{\mathit{wnt}}(j,t) \\
\frac{\partial}{\partial t}\overline{x}_{\mathit{en}}(j,t) &= \overline{f}_{\mathit{en}}\left(\overline{x}_{\mathit{otx}}(j,t), \overline{x}_{\mathit{gbx}}(j,t), \overline{x}^{\text{ext}}_{\mathit{fgf}}(j,t), \overline{x}^{\text{ext}}_{\mathit{wnt}}(j,t), \overline{x}_{\mathit{pax}}(j,t)\right) - \overline{x}_{\mathit{en}}(j,t) \\
\frac{\partial}{\partial t}\overline{x}_{\mathit{pax}}(j,t) &= \overline{f}_{\mathit{pax}}\left(\overline{x}_{\mathit{otx}}(j,t), \overline{x}_{\mathit{gbx}}(j,t), \overline{x}^{\text{ext}}_{\mathit{fgf}}(j,t), \overline{x}^{\text{ext}}_{\mathit{wnt}}(j,t), \overline{x}_{\mathit{en}}(j,t)\right) - \overline{x}_{\mathit{pax}}(j,t)
\end{aligned} \tag{6.8}$$

then describe the regulatory network at the MHB at a single spatial position $j \in [0,1]$. Equations (6.7) together with (6.8) constitute a system of partial (PDE) and ordinary (ODE) differential equations.

In the following simulations, initial conditions at $t = 0$ are chosen to mimic the fuzzy expression patterns at E8.5, cf. upper Figure 6.5A. They are obtained by specifying

the boundaries as well as the maximum of the expression profile of each gene and interpolating these points by cubic splines. In detail, the points are:

***Otx2*:** $\overline{x}_{otx}(0,0) = 1$, $\overline{x}_{otx}(0.5,0) = 0$, $\overline{x}_{otx}(1,0) = 0$

***Gbx2*:** $\overline{x}_{gbx}(0,0) = 0$, $\overline{x}_{gbx}(0.5,0) = 0$, $\overline{x}_{gbx}(1,0) = 1$

***Fgf8*:** $\overline{x}_{fgf}(0,0) = 0$, $\overline{x}_{fgf}(0.45,0) = 0$, $\overline{x}_{fgf}(0.625,0) = 1$, $\overline{x}_{fgf}(0.8,0) = 0$, $\overline{x}_{fgf}(1,0) = 0$

Fgf8: $\overline{x}^{\text{ext}}_{fgf}(0,0) = 0$, $\overline{x}^{\text{ext}}_{fgf}(0.45,0) = 0$, $\overline{x}^{\text{ext}}_{fgf}(0.625,0) = 1$, $\overline{x}^{\text{ext}}_{fgf}(0.8,0) = 0$, $\overline{x}^{\text{ext}}_{fgf}(1,0) = 0$

***Wnt1*:** $\overline{x}_{wnt}(0,0) = 0$, $\overline{x}_{wnt}(0.2,0) = 0$, $\overline{x}_{wnt}(0.375,0) = 1$, $\overline{x}_{wnt}(0.55,0) = 0$, $\overline{x}_{wnt}(1,0) = 0$

Wnt1: $\overline{x}^{\text{ext}}_{wnt}(0,0) = 0$, $\overline{x}^{\text{ext}}_{wnt}(0.2,0) = 0$, $\overline{x}^{\text{ext}}_{wnt}(0.375,0) = 1$, $\overline{x}^{\text{ext}}_{wnt}(0.55,0) = 0$, $\overline{x}^{\text{ext}}_{wnt}(1,0) = 0$

***En*:** $\overline{x}_{en}(0,0) = 0$, $\overline{x}_{en}(0.25,0) = 0$, $\overline{x}_{en}(0.425,0) = 1$, $\overline{x}_{en}(0.6,0) = 0$, $\overline{x}_{en}(1,0) = 0$

***Pax*:** $\overline{x}_{pax}(0,0) = 0$, $\overline{x}_{pax}(0.3,0) = 0$, $\overline{x}_{pax}(0.475,0) = 1$, $\overline{x}_{pax}(0.65,0) = 0$, $\overline{x}_{pax}(1,0) = 0$

For the simulation of a $Wnt1^{-/-}$ mutant, the above initial conditions are used, but the initial values $\overline{x}_{wnt}(j,0)$ and $\overline{x}^{\text{ext}}_{wnt}(j,0)$, $j \in [0,1]$, are set to zero. Also the promotor activity function $\overline{f}_{wnt}$ and the translation rate α_{wnt} of Wnt1-protein are set to zero.

For the reaction-diffusion equations (6.7) homogenous Dirichlet boundary conditions are chosen. In the following, we simply refer to this initial value boundary problem as "continuous MHB model."

6.3.3 Numeric solution

Let us conclude by showing simulations of the continuous MHB model. Equations (6.7) together with (6.8) constitute a system of ODEs and PDEs. For the numeric integration of this system we used the MATLAB solver `pdepe`, which implements the *method of lines*, see e.g. Schiesser and Griffiths [2009]. In general, the method of lines reduces a system of PDEs to a (much larger) system of ODEs, which is then solved using standard ODE solvers. In our case, this standard solver was the stiff MATLAB solver `ode15s`. On a one-dimensional interval I, the method of lines uses spatial difference operators to approximate the spatial differential operators at grid points $j_q \in I$. For this spatial discretization of Equations (6.7) we did not use an equidistant grid but one that is condensed around $j = 0.5$ (MHB) in order to account for arising discontinuities in the limit of large times. For each grid point j_q and each variable we obtained an ODE (in

Table 6.1: Time-course of *Fgf8* and *En* expression at the MHB in $Wnt1^{-/-}$ mutants.

4 somites	*En* and *Fgf8* expression indistinguishable from wild-type
5-6 somites	Reduction of the *En* domain in the midbrain by loss of anteriormost *En* expression, *Fgf8* expression indistinguishable from wild-type
7-9 somites	*En* expression restricted to hindbrain, *Fgf8* expression markedly reduced
14 somites	*En* still expressed in hindbrain, *Fgf8* expression completely abolished
23-25 somites	*En* expression reduced to a small domain in the hindbrain
29 somites	*En* expression completely abolished

time). The solutions of these ODEs give an approximate solution to the continuous MHB model.

The blurred expression domains of the IsO genes at E8.5 as well as their sharp expression domains and the clearly demarcated boundary at E10.5 are shown in upper and lower Figure 6.5A, respectively. Simulations of the continuous MHB model show that it is able to reproduce this development (see Figure 6.5B). Starting from initial conditions chosen to resemble the expression domains at E8.5 the model establishes the characteristic expression pattern at E10.5. This demonstrates that our continuous MHB model — although not accounting for their initial induction — also explains the refinement and sharpening of gene expression patterns at the MHB.

A further key feature of the IsO genes studied here is their tight and indispensable interaction for the maintenance of their own expression and of the MHB, as revealed by the analysis of loss-of-function mouse mutants for these genes [Wurst and Bally-Cuif, 2001; Ye et al., 2001]. Simulations show that our continuous MHB model is able to reproduce these experiments. We discuss $Wnt1^{-/-}$ mutants as a showcase. From McMahon et al. [1992] together with Lee et al. [1997] a time-course of *Fgf8* and *En* expression in these mutants can be reconstructed; it is shown in Table 6.1. A simulation demonstrates that the continuous MHB model is able to reproduce this phenotype even in a correct spatio-temporal order (see Figure 6.5C). A comparison of the model simulation with the time-course from Table 6.1 indicates a linear relationship between the model's time-scale and the somitogenesis clock, where approximately 1 somite is formed per every 5 time-units.

6.4 Discussion

We demonstrated that similar to temporal expression patterns, also spatial expression patterns can be used to gain information about the structure of regulatory networks. In particular, we showed that the characteristic expression patterns of key IsO genes reveal a maintaining effect of Fgf8 on *Wnt1* expression — a prediction we also validated experimentally. The presented method allows to harness qualitative experimental results like snapshots of expression patterns for model construction in systems biology. This is exemplified by our BM of gene regulation at the MHB.

Gene regulation is a highly non-linear process due to the cooperative binding exhibited by many macromolecules such as DNA. Here, cooperativity means that the macromolecule's affinity for its ligand changes with the amount of ligand already bound. Mathematically, gene regulatory networks can, therefore, be thought of as complex systems with switch-like interactions. Below a certain threshold a regulator has no or little influence on its target, while above this threshold the effect of the regulator on its target saturates rapidly to a constant level. BMs and the dynamical system from Remark 3.1 idealize this "switching behavior" and completely ignore the transition between the "low influence" and "saturated influence" states. This may be a severe simplification, but has the advantage that no information about regulatory mechanisms and kinetic parameters is needed.

If, in addition to a BM, this information is provided, a continuous dynamical system of switch-like interactions, such as (6.6) with activation functions $\overline{f}_i$ from (6.4), can be set up. The dynamic behavior of this system, of course, greatly depends on the precise nature of the additional mechanistic and kinetic information. For this reason, general mathematical results about the relation between the discrete and possible continuous dynamical systems based on the same BM are hard to obtain. They are, however, available in the limit where switch-like interactions become Heaviside step-functions and the continuous system becomes a system of piecewise linear differential equations. The dynamics of these systems can be characterized in terms of the underlying BM once the switching thresholds are fixed [de Jong et al., 2004].

Systems of piecewise linear differential equations are still simplistic idealizations of gene regulatory mechanisms, and one would wish for systems incorporating realistic

kinetics such as the Hill kinetic from (3.2). We used our BM of the MHB for a proof-of-principle, that — given these realistic kinetics — one may, indeed, obtain a meaningful continuous dynamical system from a BM, whose explanatory power is increased as compared to the discrete dynamical system from Remark 3.1. Taken together, the simulations of our continuous MHB model show that it captures certain salient features of mid-hindbrain differentiation that could not have been analyzed with a BM alone.

7

Conclusions and Outlook

Now this is not the end.
It is not even the beginning of the end.
But it is, perhaps, the end of the beginning.

Winston Churchill

Arguably, there are two avenues of research in mathematical modeling of biological systems, and in both Boolean models are frequently used. The first focuses on small- and medium-scale models of specific biological processes. Such models are used to analyze these processes, with the main goal of obtaining new biological insights. The second direction is the study of generic properties, especially in the context of regulatory networks. Kauffman's contributions fall into this category. Predominantly done by physicists, works in this direction often study mean-field quantities and properties of ensembles of large-scale models.

7.1 Boolean modeling in systems biology

The first line of research has gained particular importance in the newly emerging field of systems biology. In systems biology, experimentalists and theoreticians make a concerted effort to unravel the functionality of complex biological systems in a holistic fashion [Kitano, 2002]. Especially in the context of gene regulation, Boolean models are frequently employed by the theoreticians involved in a systems biology project [Saez-Rodriguez et al., 2007, 2009; Samaga et al., 2009; Schlatter et al., 2009; Wittmann et al., 2009a].

In this thesis, we discussed one such project. We presented a method to glean information about genetic interactions from spatial gene expression profiles. The key idea is to use available data to partially define the update rules of a Boolean model, and to extend them under regularization constraints. In here, this constraint was minimality of the resulting Boolean expressions. Using this method, we set up a Boolean model of the gene regulatory network at the mid-hindbrain boundary. Along the way, a newly predicted genetic interaction was experimentally validated.

7.1.1 Possible extensions of the model of the mid-hindbrain boundary

From a biological point of view, our model of the mid-hindbrain boundary can be extended in several ways. Further investigations of the two key patterning molecules Fgf8 and Wnt1, for instance, will require inclusion of known modulators of the *Fgf8* signaling pathway such as the *Fgf* inhibitors *Sprouty* [Chambers et al., 2000; Minowada et al., 1999], *Sef* [Fürthauer et al., 2002] or *Mkp3* [Echevarria et al., 2005; Li et al., 2007]. In the present model these regulators at the signal transduction level are not considered. Being widely coexpressed with *Fgf8*, they are assumed to fine-tune *Fgf8* expression itself and the expression of *Fgf8* target genes by negative feedback modulations. This exquisite regulation of *Fgf8* agrees well with results demonstrating a concentration-dependent effect of *Fgf8* signaling [Liu et al., 1999; Sato et al., 2001]. Inclusion of these fine-tuning mechanisms will, therefore, require a detailed kinetic model of *Fgf8* signaling at the mid-hindbrain boundary. To this end, existing kinetic models of the *Fgf* pathway, e.g. the one by Yamada et al. [2004], could be adapted.

Fgf8 and *Wnt1*, however, are not the only important regulators of mid-hindbrain development. Further crucial genes, that we are considering for inclusion in our model,

are *Lmx1b* [Guo et al., 2007, 2008; Matsunaga et al., 2002] and *Grg4* [Puelles et al., 2004; Sugiyama et al., 2000]. They are of particular importance for possible extensions of our model which aim at including related processes, such as the specification of cell populations in the patterning field. The mid-hindbrain boundary not only controls patterning of the mid- and rostral hindbrain, but also controls the location and size of several neuronal populations [Brodski et al., 2003]. One could envision hybrid-models integrating pattern formation and spatial differentiation with fate decisions of single cells.

At some point, we will also have to abandon our simplifying assumptions with respect to *En1* and *En2* as well as *Pax2* and *Pax5*, and consider a more refined picture of *Engrailed* and *Pax* expression patterns and interactions. Such extensions will be particularly interesting in spatially higher-dimensional models that take into account the dorsal-ventral patterning of the neural plate/tube as well. A critical issue in these higher-dimensional models is the topological alteration at around E9.0 when the neural plate becomes the neural tube, as for non-symmetric initial conditions discontinuities arise at the junction where the two edges of the neural plate fuse together. We are planning on modeling this situation as a free moving boundary problem.

7.1.2 Inverse problems under sparsity constraints

From a theoretical point of view, predicting genetic interactions by solving inverse problems under sparsity constraints seems a promising and interesting idea that merits further research efforts. Especially for larger numbers of genes, however, additional constraints might be beneficial. One could, for example, look for minimal canalyzing update rules or minimal update rules generated by one of the generic logics. This will require adaption of either the Quine-McCluskey algorithm or of one of the heuristic minimizers. As always, the lack of suitable testing data sets is an issue, and probably one will have to resort to synthetic toy data for performance evaluations.

7.2 Random Boolean models

As mentioned above, a major contribution to the second line of research is the work by Stuart Kauffman. In his seminal paper, Kauffman [1969] proposes large-scale random Boolean models — in here, we called them Kauffman networks — as generic models

of gene regulatory networks. Kauffman [1993] hypothesized that regulatory networks in evolvable, living organisms can only operate in a frozen regime but close to (at the edge of) a chaotic regime.

We began by defining a general class of Kauffman networks. In particular, we relaxed the binary Boolean classification and considered general discrete, finite sets. The cardinalities of these sets followed a general distribution, as did the in-degrees and the entries of the update rules. We investigated these Kauffman networks with respect to critical phenomena. Our results are a generalization of the well-known case of random Boolean models as introduced by Kauffman. We could also generalize the finding by Bastolla and Parisi [1996] that any Kauffman network can be kept in its frozen regime by sufficiently biasing the update rules.

We then introduced the concept of generic logics, which allows to build Boolean models from networks of signed interactions by logically linking the activating and inhibiting regulators of a node according to a specific pattern. The class of Kauffman networks whose realizations are obtained using generic logics was studied. We, first, analyzed the truth-content of these networks, which is a mean-field approximation of the fraction of ones. Analytic and numeric investigations showed that this quantity exhibits a rich dynamical behavior including period-doublings leading to chaos. In a next step, we found that, surprisingly, Kauffman networks with generic logics possess multiple, intricately shaped critical boundaries. In particular, for a biologically plausible generic logic the region of biologically reasonable network parameters is enclosed by a critical boundary. Hence, these parameters need not even be particularly fine-tuned in order for the network to be near criticality but may vary over quite some range. This finding fits in nicely with Kauffman's hypothesis.

7.2.1 Structure matters

Update rules in the original Kauffman network are random functions without any structural properties, such as monotonicity or canalyzing inputs. The same is true for the update rules of the multistate Kauffman networks studied herein. The regulators of a gene, however, exert their regulatory influences by mechanistic processes, such as the binding of transcription factors to promotor regions of the DNA, and these mechanistic processes should give the activation function of a gene certain structural properties. A simple abstraction hereof are qualitative models, in which biochemical mechanisms are

reflected in the classification of interactions as either activating or inhibiting. We investigated Kauffman networks with structured update rules that are derived from such qualitative models. Our results show that this additional structure greatly influences the dynamics of these networks.

The reader might find it interesting to compare this discussion to Balleza et al. [2008]. In this study, Boolean dynamics are implemented on the gene regulatory networks of *S. cerevisiae*, *E. coli*, and *B. subtilis*. The update rules are constructed as (unstructured) random functions evaluating to 1 with a probability equal to the average fraction of expressed genes in hundreds of microarray experiments. While such approaches certainly increase the biological plausibility and relevance of Kauffman networks as models of gene regulation, it might still be necessary to also take into account structural information, e.g. about activating and inhibiting regulatory interactions.

7.2.2 Topology and dynamics

Another issue is that topological properties, such as degree distributions, also play a pivotal role in the study of complex networks. For this reason, it is somewhat unsatisfactory that in standard Kauffman networks this degree distribution is taken to be a simple delta distribution. In this thesis, we studied Kauffman networks with (unstructured update rules and) general degree distributions on finite supports similar to Fox and Hill [2001] or Aldana [2003]. In agreement with these studies, we found, however, that the phase transition of such Kauffman networks completely ignores all topological properties but the mean connectivity.

We have first results demonstrating that this is not the case with Kauffman networks generated by generic logics. If we base these Kauffman networks on an Erdös-Rényi graph from Example 2.1, for instance, their in-degrees are Poisson distributed, cf. section 2.1. We could already show that also in this case the truth-content is governed by an iteration function with negative Schwarzian derivative. This awakens hopes that we will be able to treat this case similarly to our proceeding inhere. In preliminary numeric analyses the truth-content, indeed, appears to possess a unique attractor. These analyses, however, also reveal that the critical boundaries in the case of an Erdös-Rényi graph differ qualitatively from the ones shown in Figure 5.4.

A comprehensive discussion of Kauffman networks with generic logics on different topologies is an interesting subject for future work. On the one hand, it would, of course,

be intriguing to use real-world networks, such as the transcriptional gene regulatory networks from *E. coli* or *yeast* [Keseler et al., 2008; Lee et al., 2002]. On the other hand, for more systematic analyses, lattices and random graphs, such as the Erdös-Rényi graph from Example 2.1, small-world networks generated according to Watts and Strogatz [1998], or scale-free networks obtained via preferential attachment [Barabási and Albert, 1999], might be better suited.

7.2.3 The state-space of Kauffman networks with generic logics

Furthermore, the structure of the Boolean state-space of Kauffman networks with generic logics needs to be analyzed in detail. Similarly to Samuelsson and Troein [2003], one could attempt to compute the average number and length of attractors in these networks. For truth-stable networks, it will be particularly interesting to see how the lengths of attractors (in the Boolean state-space) are related to the length of the attractor of the truth-content. Intuitively, one would expect the former to be multiples of the latter.

Index

References

D. Acampora, V. Avantaggiato, F. Tuorto, and A. Simeone. Genetic control of brain morphogenesis through Otx gene dosage requirement. *Development*, 124(18):3639–3650, 1997. 36, 139

K. A. Adams, J. M. Maida, J. A. Golden, and R. D. Riddle. The transcription factor Lmx1b maintains Wnt1 expression within the isthmic organizer. *Development*, 127(9): 1857–1867, 2000. 128

R. Albert and A. Barabási. Statistical mechanics of complex networks. *Rev Mod Phys*, 74(1):47–97, 2002. 9, 113

M. Aldana. Boolean dynamics of networks with scale-free topology. *Physica D*, 185(1):45–66, 2003. 43, 153

M. Aldana, S. Coppersmith, and L. P. Kadanoff. Boolean dynamics with random couplings. In *Perspectives and Problems in Nonlinear Science: A Celebratory Volume in Honor of Lawrence Sirovich*, pages 23–89. Springer Verlag, 2003. 45

U. Alon. *An Introduction to Systems Biology: Design Principles of Biological Circuits*. CRC Press, 2006. 114

M. Ansorg, F. Blöchl, W. zu Castell, F. J. Theis, and D. M. Wittmann. Gene regulation at the mid-hindbrain boundary: Study of a mathematical model in the stationary limit. *International Journal of Biomathematics and Biostatistics*, in press, 2010. 7, 144

A. Avila, M. Lyubich, and W. De Melo. Regular or stochastic dynamics in real analytic families of unimodal maps. *Invent Math*, 154(3):451–550, 2003. 28

F. Ballesteros and B. Luque. Order-disorder phase transition in random-walk networks. *Phys Rev E*, 71(3):31104, 2005. 77

E. Balleza, E. R. Alvarez-Buylla, A. Chaos, S. A. Kauffman, I. Shmulevich, and M. Aldana. Critical dynamics in genetic regulatory networks: examples from four kingdoms. *PLoS One*, 3(6):e2456, 2008. 47, 80, 153

L. Bally-Cuif and M. Wassef. Ectopic induction and reorganization of Wnt-1 expression in quail/chick chimeras. *Development*, 120(12):3379–3394, 1994. 129

A. Barabási and R. Albert. Emergence of scaling in random networks. *Science*, 286(5439):509–512, 1999. 154

U. Bastolla and G. Parisi. Closing probabilities in the Kauffman model: an annealed computation. *Physica D*, 98(1): 1–25, 1996. 43, 62, 64, 152

A. M. Blokh and M. Y. Lyubich. Measurable dynamics of S-unimodal maps of the interval. In *Annales scientifiques de l'Ecole normale supérieure*, volume 24, pages 545–573. Elsevier, 1991. 26

B. Bollobás. *Modern graph theory*. Springer Verlag, 1998. 10

G. Boole. *An investigation of the laws of thought: on which are founded the mathematical theories of logic and probabilities*. Walton and Maberly, 1854. 28

M. Bouchard, P. Pfeffer, and M. Busslinger. Functional equivalence of the transcription factors Pax2 and Pax5 in mouse development. *Development*, 127(17):3703–3713, 2000. 37

M. Bouchard, D. Grote, S. E. Craven, Q. Sun, P. Steinlein, and M. Busslinger. Identification of Pax2-regulated genes by expression profiling of the mid-hindbrain organizer region. *Development*, 132(11):2633–2643, 2005. 136, 139

R. Brayton. *Logic minimization algorithms for VLSI synthesis*. Springer Verlag, 1984. 133

C. Breindl, S. Waldherr, D. M. Wittmann, F. J. Theis, and F. Allgöwer. Steady state robustness of qualitative gene regulation networks. *Int J Robust Nonlinear Control*, under review, 2010. 7

V. Broccoli, E. Boncinelli, and W. Wurst. The caudal limit of Otx2 expression positions the isthmic organizer. *Nature*, 401(6749):164–168, 1999. 36, 139

C. Brodski, D. Weisenhorn, M. Signore, I. Sillaber, M. Oesterheld, V. Broccoli, D. Acampora, A. Simeone, and W. Wurst. Location and size of dopaminergic and serotonergic cell populations are controlled by the position of the midbrain-hindbrain organizer. *J Neurosci*, 23(10): 4199–4207, 2003. 151

S. Bulashevska and R. Eils. Inferring genetic regulatory logic from expression data. *Bioinformatics*, 21(11):2706–2713, 2005. 82

D. Chambers, A. Medhurst, F. Walsh, J. Price, and I. Mason. Differential Display of Genes Expressed at the Midbrain–Hindbrain Junction Identifies sprouty2: An FGF8-Inducible Member of a Family of Intracellular FGF Antagonists. *Mol Cell Neurosci*, 15(1):22–35, 2000. 150

M. Chavez, R. Albert, and E. Sontag. Robustness and fragility of boolean models for genetic regulatory networks. *J Theor Biol*, 235(3):431–449, 2005. 40

C. Chi, S. Martinez, W. Wurst, and G. Martin. The isthmic organizer signal FGF8 is required for cell survival in the prospective midbrain and cerebellum. *Development*, 130 (12):2633–2644, 2003. 36, 139

E. Coddington and N. Levinson. *Theory of ordinary differential equations*. Tata McGraw-Hill, 1972. 16

P. Collet and J. P. Eckman. *Iterated maps on the interval as dynamical systems*. Birkhäuser, 1980. 19, 21

S. Cook. The complexity of theorem-proving procedures. In *Proceedings of the third annual ACM symposium on Theory of computing*, pages 151–158. ACM New York, NY, USA, 1971. 133

REFERENCES

P. Crossley and G. Martin. The mouse Fgf8 gene encodes a family of polypeptides and is expressed in regions that direct outgrowth and patterning in the developing embryo. *Development*, 121(2):439–451, 1995. 129, 139

P. Danielian and A. McMahon. Engrailed-1 as a target of the Wnt-1 signalling pathway in vertebrate midbrain development. *Nature*, 383(6598):332–334, 1996. 37, 139

C. A. Davis, S. E. Noble-Topham, J. Rossant, and A. L. Joyner. Expression of the homeo box-containing gene en-2 delineates a specific region of the developing mouse brain. *Genes Dev*, 2(3):361–371, 1988. 36

H. de Jong and M. Page. Search for Steady States of Piecewise-Linear Differential Equation Models of Genetic Regulatory Networks. *IEEE/ACM Trans Comput Biol Bioinf*, 5(2):208–222, 2008. 143

H. de Jong, J. Gouzé, C. Hernandez, M. Page, T. Sari, and J. Geiselmann. Qualitative simulation of genetic regulatory networks using piecewise-linear models. *Bull Math Biol*, 66(2):301–340, 2004. 143, 147

W. De Melo and S. van Strien. *One-dimensional dynamics*. Springer Verlag, 1993. 21

G. De Vries, T. Hillen, M. Lewis, B. Schönfisch, and J. Müller. *A course in mathematical biology: quantitative modeling with mathematical and computational methods*. Society for Industrial Mathematics, 2006. 13

B. Demir and S. Koçak. A note on positive Lyapunov exponent and sensitive dependence on initial conditions. *Chaos Soliton Fract*, 12(11):2119–2121, 2001. 27

B. Derrida and Y. Pomeau. Random networks of automata: a simple annealed approximation. *Europhys Lett*, 1(2):45–49, 1986. 44

B. Derrida and D. Stauffer. Phase transitions in two dimensional Kauffman cellular automata. *Europhys Lett*, 2(10): 739–745, 1986. 44

B. Drossel. Number of attractors in random Boolean networks. *Phys Rev E*, 72(1):16110–16114, 2005. 86

D. Echevarría, C. Vieira, and S. Martinez. Mammalian neural tube grafting experiments: an in vitro system for mouse experimental embryology. *Int J Dev Biol*, 45(8):895–902, 2001. 136

D. Echevarria, C. Vieira, L. Gimeno, and S. Martinez. Neuroepithelial secondary organizers and cell fate specification in the developing brain. *Brain Res Rev*, 43(2):179–191, 2003. 35

D. Echevarria, S. Martinez, S. Marques, V. Lucas-Teixeira, and J. Belo. Mkp3 is a negative feedback modulator of Fgf8 signaling in the mammalian isthmic organizer. *Dev Biol*, 277(1):114–128, 2005. 150

H. El Snoussi and R. Thomas. Logical identification of all steady states: The concept of feedback loop characteristic states. *Bull Math Biol*, 55(5):973–991, 1993. 143

P. Erdös and A. Rényi. On random graphs I. *Publ. Math. Debrecen*, 6:290–297, 1959. 11

P. Eykhoff. *System identification: parameter and state estimation*. Wiley New York, 1974. 9

A. Fauré, A. Naldi, C. Chaouiya, and D. Thieffry. Dynamical analysis of a generic boolean model for the control of the mammalian cell cycle. *Bioinformatics*, 22(14):124–131, 2006. 40

A. Fauré, A. Naldi, F. Lopez, C. Chaouiya, A. Ciliberto, and D. Thieffry. Modular logical modelling of the budding yeast cell cycle. *Mol BioSyst*, 5(12):1787–1796, 2009. 50

J. Favor, R. Sandulache, A. Neuhauser-Klaus, W. Pretsch, B. Chatterjee, E. Senft, W. Wurst, V. Blanquet, P. Grimes, R. Sporle, et al. The mouse Pax2(1Neu) mutation is identical to a human PAX2 mutation in a family with renal-coloboma syndrome and results in developmental defects of the brain, ear, eye, and kidney. *Proc Natl Acad Sci U S A*, 93(24):13870–13875, 1996. 139

H. Flyvbjerg. An order parameter for networks of automata. *J Phys A: Math Gen*, 21(19):L955–L960, 1988. 44

J. Fox and C. Hill. From topology to dynamics in biochemical networks. *Chaos*, 11(4):809–815, 2001. 43, 153

M. Fürthauer, W. Lin, S. Ang, B. Thisse, and C. Thisse. Sef is a feedback-induced antagonist of Ras/MAPK-mediated FGF signalling. *Nat Cell Biol*, 4(2):170–174, 2002. 150

J. Gemel, C. Jacobsen, and C. MacArthur. Fibroblast Growth Factor-8 Expression Is Regulated by Intronic Engrailed and Pbx1-binding Sites. *J Biol Chem*, 274(9):6020–6026, 1999. 37, 139

S. Givant and P. Halmos. *Introduction to Boolean algebras*. Springer Verlag, 2009. 28

L. Glass and S. A. Kauffman. The logical analysis of continuous, non-linear biochemical control networks. *J Theor Biol*, 39(1):103–129, 1973. 142

F. Greil, B. Drossel, and J. Sattler. Critical kauffman networks under deterministic asynchronous update. *New J Phys*, 9:373, 2007. 40

J. Guckenheimer. Sensitive dependence to initial conditions for one dimensional maps. *Commun Math Phys*, 70(2):133–160, 1979. 27

J. Guckenheimer and P. Holmes. *Nonlinear oscillations, dynamical systems, and bifurcations of vector fields*. Springer Verlag, 1990. 13, 15, 143

C. Guo, H.-Y. Qiu, Y. Huang, H. Chen, R.-Q. Yang, S.-D. Chen, R. L. Johnson, Z.-F. Chen, and Y.-Q. Ding. Lmx1b is essential for Fgf8 and Wnt1 expression in the isthmic organizer during tectum and cerebellum development in mice. *Development*, 134(2):317–325, 2007. 151

C. Guo, H.-Y. Qiu, M. Shi, Y. Huang, R. L. Johnson, M. Rubinstein, S.-D. Chen, and Y.-Q. Ding. Lmx1b-controlled isthmic organizer is essential for development of midbrain dopaminergic neurons. *J Neurosci*, 28(52):14097–14106, 2008. 151

S. Harris, B. Sawhill, A. Wuensche, and S. A. Kauffman. A model of transcriptional regulatory networks based on biases in the observed regulation rules. *Complexity*, 7(4): 23–40, 2002. 30, 133

REFERENCES

H. J. Hilhorst and M. Nijmeijer. On the approach of the stationary state in Kauffman's random Boolean network. *J Phys*, 48(2):185–191, 1987. 12

A. Hill. The possible effects of the aggregation of the molecules of haemoglobin on its dissociation curves. *J Physiol*, 40:4–7, 1910. 41

M. Isalan and M. Morrison. This title is false. *Nature*, 458 (7241):969, 2009. 49

L. Kadanoff. *Statistical physics: statics, dynamics and renormalization*. World Scientific, 2000. 44

M. Karnaugh. The map method for synthesis of combinational logic circuits. *Trans Am Inst Electr Eng*, 72(9):593–599, 1953. 31, 133

S. A. Kauffman. Metabolic stability and epigenesis in randomly constructed genetic nets. *J Theor Biol*, 22(3):437–467, 1969. 2, 43, 44, 79, 80, 151

S. A. Kauffman. *The origins of order: Self organization and selection in evolution*. Oxford University Press, USA, 1993. 2, 3, 47, 80, 152

S. A. Kauffman, C. Peterson, B. Samuelsson, and C. Troein. Random Boolean network models and the yeast transcriptional network. *Proc Natl Acad Sci U S A*, 100(25):14796–14799, 2003. 80

S. A. Kauffman, C. Peterson, B. Samuelsson, and C. Troein. Genetic networks with canalyzing Boolean rules are always stable. *Proc Natl Acad Sci U S A*, 101(49):17102–17107, 2004. 87

G. Keller. Exponents, attractors and Hopf decompositions for interval maps. *Ergod Theor Dyn Syst*, 10(4):717–744, 1990. 27

M. Kendall, A. Stuart, and J. Ord. *Kendall's advanced theory of statistics*. Oxford University Press, USA, 1987. 79

I. M. Keseler, C. Bonavides-Martinez, J. Collado-Vides, S. Gama-Castro, R. P. Gunsalus, D. Aaron Johnson, M. Krummenacker, L. M. Nolan, S. Paley, I. T. Paulsen, et al. EcoCyc: a comprehensive view of Escherichia coli biology. *Nucleic acids res*, 37:D464–D470, 2008. 113, 154

H. Kitano. Systems Biology: A Brief Overview. *Science*, 295 (5560):1662–1664, 2002. 127, 150

H. Kitano. Biological robustness. *Nat Rev Genet*, 5(11):826–837, 11 2004. 47

J. Krumsiek, S. Poelsterl, D. M. Wittmann, and F. J. Theis. Odefy - from discrete to continuous models. *BMC Bioinf*, 11:233, 2010. 7, 82

R. D. Leclerc. Survival of the sparsest: robust gene networks are parsimonious. *Mol Syst Biol*, 4:213, 2008. 114

S. Lee, P. Danielian, B. Fritzsch, and A. McMahon. Evidence that FGF8 signalling from the midbrain-hindbrain junction regulates growth and polarity in the developing midbrain. *Development*, 124(5):959–969, 1997. 36, 136, 139, 141, 146

T. I. Lee, N. J. Rinaldi, F. Robert, D. T. Odom, Z. Bar-Joseph, G. K. Gerber, N. M. Hannett, C. T. Harbison, C. M. Thompson, I. Simon, et al. Transcriptional regulatory networks in Saccharomyces cerevisiae. *Science*, 298 (5594):799–804, 2002. 113, 154

C. Li, D. Scott, E. Hatch, X. Tian, and S. Mansour. Dusp6 (Mkp3) is a negative feedback regulator of FGF-stimulated ERK signaling during mouse development. *Development*, 134(1):167–176, 2007. 150

F. Li, T. Long, Y. Lu, Q. Quyang, and C. Tang. The yeast cell-cycle network is robustly designed. *Proc Natl Acad Sci U S A*, 101(14):4781–4786, 2004. 82

J. Y. Li and A. L. Joyner. Otx2 and gbx2 are required for refinement and not induction of mid hindbrain gene expression. *Development*, 128(24):4979–4991, 2001. 36, 136

J. Y. H. Li, Z. Lao, and A. L. Joyner. New regulatory interactions and cellular responses in the isthmic organizer region revealed by altering gbx2 expression. *Development*, 132(8):1971–1981, 2005. 36

A. Liu and A. Joyner. EN and GBX2 play essential roles downstream of FGF8 in patterning the mouse mid/hindbrain region. *Development*, 128(2):181–191, 2001. 129, 136, 137, 139

A. Liu, K. Losos, and A. L. Joyner. FGF8 can activate Gbx2 and transform regions of the rostral mouse brain into a hindbrain fate. *Development*, 126(21):4827–4838, 1999. 129, 137, 139, 150

H. Lodish and A. Berk. *Molecular cell biology*. WH Freeman, 2008. 31

B. Luque and F. Ballesteros. Random walk networks. *Physica A*, 342(1-2):207–213, 2004. 77

B. Luque and R. Solé. Phase transitions in random networks: Simple analytic determination of critical points. *Phys Rev E*, 55(1):257–260, 1997. 44

B. Luque and R. Solé. Lyapunov exponents in random Boolean networks. *Physica A*, 284(1–4):33–45, 2000. 44

S. Martin, Z. Zhang, A. Martino, and J.-L. Faulon. Boolean dynamics of genetic regulatory networks inferred from microarray time series data. *Bioinformatics*, 23(7):866–874, 2007. 82, 122

J. Martinez-Barbera, M. Signore, P. Boyl, E. Puelles, D. Acampora, R. Gogoi, F. Schubert, A. Lumsden, and A. Simeone. Regionalisation of anterior neuroectoderm and its competence in responding to forebrain and midbrain inducing activities depend on mutual antagonism between OTX2 and GBX2. *Development*, 128(23):4789–4800, 2001. 36

E. Matsunaga, T. Katahira, and H. Nakamura. Role of lmx1b and wnt1 in mesencephalon and metencephalon development. *Development*, 129(22):5296–5277, 2002. 151

R. May. Simple mathematical models with very complicated dynamics. *Nature*, 261(5560):459–467, 1976. 22

E. McCluskey and T. Bartee. *A survey of switching circuit theory*. McGraw-Hill, 1962. 133

REFERENCES

A. McMahon, A. Bradley, K. Thomas, M. Capecchi, P. Danielian, Y. Echelard, G. Vassileva, and A. McMahon. The Wnt-1 (int-1) proto-oncogene is required for development of a large region of the mouse brain. *Cell*, 62(6): 1073–1085, 1990. 36

A. McMahon, A. Joyner, A. Bradley, and J. McMahon. The midbrain-hindbrain phenotype of Wnt-1-/Wnt-1-mice results from stepwise deletion of engrailed-expressing cells by 9.5 days postcoitum. *Cell*, 69(4):581–595, 1992. 129, 139, 141, 146

L. Mendoza and I. Xenarios. A method for the generation of standardized qualitative dynamical systems of regulatory networks. *Theor Biol Med Model*, 3:13, 2006. 82, 122

T. Mestl, E. Plahte, and S. W. Omholt. A mathematical framework for describing and analysing gene regulatory networks. *J Theor Biol*, 176(2):291–300, 1995. 143

S. Millet, K. Campbell, D. J. Epstein, K. Losos, E. Harris, and A. L. Joyner. A role for gbx2 in repression of otx2 and positioning the mid/hindbrain organizer. *Nature*, 401 (6749):161–164, 1999. 36, 139

J. Milnor. On the concept of attractor. *Commun Math Phys*, 99(2):177–195, 1985. 19, 20

G. Minowada, L. A. Jarvis, C. L. Chi, A. Neubuser, X. Sun, N. Hacohen, M. A. Krasnow, and G. R. Martin. Vertebrate sprouty genes are induced by fgf signaling and can cause chondrodysplasia when overexpressed. *Development*, 126(20):4465–4475, 1999. 150

J. Murray. *Mathematical biology: an introduction*. Springer Verlag, 2002. 13

S. W. Omholt, X. Kefang, Ø. Andersen, and E. Plahte. Description and analysis of switchlike regulatory networks exemplified by a model of cellular iron homeostasis. *J Theor Biol*, 195(3):339–350, 1998. 143

E. Plahte, T. Mestl, and S. W. Omholt. A methodological basis for description and analysis of systems with complex switch-like interactions. *J Math Biol*, 36(4):321–348, 1998. 140, 143

N. Prakash and W. Wurst. Specification of midbrain territory. *Cell Tissue Res*, 318(1):5–14, 2004. 136

N. Prakash, C. Brodski, T. Naserke, E. Puelles, R. Gogoi, A. Hall, M. Panhuysen, D. Echevarria, L. Sussel, D. Weisenhorn, S. Martinez, E. Arenas, A. Simeone, and W. Wurst. A Wnt1-regulated genetic network controls the identity and fate of midbrain-dopaminergic progenitors in vivo. *Development*, 133(1):89–98, 2006. 136

E. Puelles, A. Annino, F. Tuorto, A. Usiello, D. Acampora, T. Czerny, C. Brodski, S. Ang, W. Wurst, and A. Simeone. Otx2 regulates the extent, identity and fate of neuronal progenitor domains in the ventral midbrain. *Development*, 131(9):2037–2048, 2004. 151

W. Quine. The problem of simplifying truth functions. *Am Math Mon*, 59(8):521–531, 1952. 133

M. Rhinn, A. Dierich, M. Le Meur, and S. Ang. Cell autonomous and non-cell autonomous functions of Otx2 in patterning the rostral brain. *Development*, 126(19):4295–4304, 1999. 139

T. Rohlf and S. Bornholdt. Criticality in random threshold networks: annealed approximation and beyond. *Physica A*, 310(1–2):245–259, 2002. 82

D. Rowitch and A. McMahon. Pax-2 expression in the murine neural plate precedes and encompasses the expression domains of Wnt-1 and En-1. *Mech Dev*, 52(1):3–8, 1995. 37

R. Rudell and A. Sangiovanni-Vincentelli. Multiple-valued minimization for PLA optimization. *IEEE Trans Comput Aided Des Integr Circuits Syst*, 6(5):727–750, 1987. 133

D. Ruelle. Sensitive dependence on initial condition and turbulent behavior of dynamical systems. *Ann N.Y. Acad Sci*, 316(1):408–416, 1979. 21

J. Saez-Rodriguez, L. Simeoni, J. A. Lindquist, R. Hemenway, U. Bommhardt, B. Arndt, U.-U. Haus, R. Weismantel, E. D. Gilles, S. Klamt, and B. Schraven. A logical model provides insights into t cell receptor signaling. *PLoS Comput Biol*, 3(8):e163, 2007. 3, 150

J. Saez-Rodriguez, L. G. Alexopoulos, J. Epperlein, R. Samaga, D. A. Lauffenburger, S. Klamt, and P. K. Sorger. Discrete logic modelling as a means to link protein signalling networks with functional analysis of mammalian signal transduction. *Mol Syst Biol*, 5:331, 2009. 3, 150

R. Samaga, J. Saez-Rodriguez, L. G. Alexopoulos, P. K. Sorger, and S. Klamt. The logic of egfr/erbb signaling: theoretical properties and analysis of high-throughput data. *PLoS Comput Biol*, 5(8):e1000438, 2009. 3, 150

B. Samuelsson and C. Troein. Superpolynomial Growth in the Number of Attractors in Kauffman Networks. *Phys Rev Lett*, 90(9):98701–98704, 2003. 154

L. Sánchez and D. Thieffry. A logical analysis of the Drosophila gap-gene system. *J Theor Biol*, 211(2):115–141, 2001. 50

T. Sato, I. Araki, and H. Nakamura. Inductive signal and tissue responsiveness defining the tectum and the cerebellum. *Development*, 128(13):2461–2469, 2001. 150

W. Schiesser and G. Griffiths. *A compendium of partial differential equation models: method of lines analysis with MATLAB*. Cambridge University Press New York, NY, USA, 2009. 145

R. Schlatter, K. Schmich, I. Avalos Vizcarra, P. Scheurich, T. Sauter, C. Borner, M. Ederer, I. Merfort, and O. Sawodny. On/off and beyond–a boolean model of apoptosis. *PLoS Comput Biol*, 5(12):e1000595, 2009. 3, 150

S. Scholpp and M. Brand. Endocytosis controls spreading and effective signaling range of fgf8 protein. *Curr Biol*, 14(20): 1834–1841, 2004. 130

Y. Setty, A. E. Mayo, M. G. Surette, and U. Alon. Detailed map of a cis-regulatory input function. *Proc Natl Acad Sci U S A*, 100(13):7702–7707, 2003. 50

G. Shilov and B. Gurevich. *Integral, measure and derivative: a unified approach*. Prentice-Hall, 1966. 21

A. Simeone. Positioning the isthmic organizer: where otx2 and gbx2 meet. *Trends Genet*, 16(6):237–240, 2000. 136

D. Singer. Stable orbits and bifurcation of maps of the interval. *SIAM J Appl Math*, 35(2):260–267, 1978. 24

R. V. Solé, B. Luque, and S. A. Kauffman. Phase transitions in random networks with multiple states. Working Papers 00-02-011, Santa Fe Institute, 2000. URL `http://ideas.repec.org/p/wop/safiwp/00-02-011.html`. 50, 60, 79

D. Song, G. Chalepakis, P. Gruss, and A. Joyner. Two Pax2/5/8-binding sites in Engrailed2 are required for proper initiation of endogenous mid-hindbrain expression. *Mech Dev*, 90(2):155–165, 2000. 136, 139

M. Strigini and S. M. Cohen. Wingless gradient formation in the drosophila wing. *Curr Biol*, 10(6):293–300, 2000. 130

S. Sugiyama, J. Funahashi, and H. Nakamura. Antagonizing Activity of Chick Grg4 against Tectum-Organizing Activity. *Dev Biol*, 221(1):168–180, 2000. 151

F. J. Theis, S. Bohl, and U. Klingmüller. Theoretical analysis of time-to-peak responses in biological reaction networks. *Bull Math Biol*, epub ahead of print:1–26, 2010. URL `http://dx.doi.org/10.1007/s11538-010-9548-x`. 43

K. Thomas and M. Capecchi. Targeted disruption of the murine int-1 proto-oncogene resulting in severe abnormalities in midbrain and cerebellar development. *Nature*, 346 (6287):847–850, 1990. 36

R. Thomas. Logical analysis of systems comprising feedback loops. *J Theor Biol*, 73(4):631–656, 1978. 82

R. Thomas. Regulatory networks seen as asynchronous automata: A logical description. *J Theor Biol*, 153(1):1–23, 1991. 50

H. Thunberg. Periodicity versus chaos in one-dimensional dynamics. *SIAM rev*, 43(1):3–30, 2001. 21, 22, 23, 25, 26

A. Turing. The chemical basis of morphogenesis. *Bull Math Biol*, 52(1):153–197, 1990. 50

E. Veitch. A chart method for simplifying truth functions. In *Proceedings of the 1952 ACM national meeting (Pittsburgh)*, pages 127–133. ACM New York, NY, USA, 1952. 31, 133

K. Wassarman, M. Lewandoski, K. Campbell, A. Joyner, J. Rubenstein, S. Martinez, and G. Martin. Specification of the anterior hindbrain and establishment of a normal mid/hindbrain organizer is dependent on Gbx2 gene function. *Development*, 124(15):2923–2934, 1997. 36, 139

D. Watts and S. Strogatz. Collective dynamics of 'small-world' networks. *Nature*, 393(6684):440–442, 1998. 154

R. Wheeden and A. Zygmund. *Measure and integral: an introduction to real analysis*. CRC Press, 1977. 105

D. M. Wittmann and F. J. Theis. Dynamic regimes of random fuzzy logic networks. *New J Phys*, under review, 2010a. 6, 50, 74

D. M. Wittmann and F. J. Theis. Truth-content and phase transitions of random boolean networks with generic logics. *SIAM J Appl Dyn Syst*, under review, 2010b. 6, 7, 82

D. M. Wittmann, F. Blöchl, D. Trümbach, W. Wurst, N. Prakash, and F. J. Theis. Spatial analysis of expression patterns predicts genetic interactions at the mid-hindbrain boundary. *PLoS Comput Biol*, 5(11):e1000569, 2009a. 3, 7, 128, 144, 150

D. M. Wittmann, J. Krumsiek, J. Saez-Rodriguez, D. A. Lauffenburger, S. Klamt, and F. J. Theis. Transforming Boolean Models to Continuous Models: Methodology and Application to T-Cell Receptor Signaling. *BMC Syst Biol*, 3:98, 2009b. 7, 128, 140, 143

D. M. Wittmann, C. Marr, and F. J. Theis. Biologically meaningful update rules increase the critical connectivity of generalized kauffman networks. *J Theor Biol*, 266(3): 436–448, 2010. 6, 50

W. Wurst and L. Bally-Cuif. Neural plate patterning: Upstream and downstream of the isthmic organizer. *Nat Rev Neurosci*, 2(2):99–108, 2001. 36, 37, 146

S. Yamada, T. Taketomi, and A. Yoshimura. Model analysis of difference between EGF pathway and FGF pathway. *Biochem Biophys Res Commun*, 314(4):1113–1120, 2004. 150

W. Ye, M. Bouchard, D. Stone, and A. Rosenthal. Distinct regulators control the expression of the mid-hindbrain organizer signal fgf8. *Nat Neurosci*, 4(12):1175–1181, 2001. 37, 139, 146